





This is to certify that the

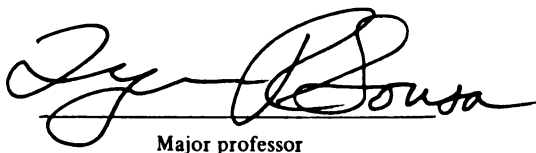
thesis entitled

Investigation of the Perturbation of the Excited State  
Processes of Naphthalene Crown Ether Derivatives by  
Complexation of the Cations of Alkali Metal Chlorides,  
Barium Bromide, and Silver Triflate; Investigation of  
the External Heavy Atom Perturbation . . . . .  
presented by

James M. Larson

has been accepted towards fulfillment  
of the requirements for

Ph.D. degree in Chemistry

  
Major professor

Date Dec 4, 1978



OVERDUE FINES ARE 25¢ PER DAY  
PER ITEM

Return to book drop to remove  
this checkout from your record.

--	--

INVESTIGATION OF THE PERTURBATION OF THE EXCITED STATE PROCESSES  
OF NAPHTHALENE CROWN ETHER DERIVATIVES BY COMPLEXATION OF THE  
CATIONS OF ALKALI METAL CHLORIDES, BARIUM BROMIDE, AND  
SILVER TRIFLATE; INVESTIGATION OF THE EXTERNAL HEAVY  
ATOM PERTURBATION OF THE EXCITED STATE PROCESSES OF NAPHTHALENE  
CROWN ETHER DERIVATIVES BY ETHYL BROMIDE AND BY MEANS OF  
COMPLEXED HALOALKYAMMONIUM CATIONS

By

James M. Larson

A DISSERTATION

Submitted to

Michigan State University

in partial fulfillment of the requirements

for the degree of

DOCTOR OF PHILOSOPHY

Department of Chemistry

1979



## ABSTRACT

INVESTIGATION OF THE PERTURBATION OF THE EXCITED STATE PROCESSES  
OF NAPHTHALENE CROWN ETHER DERIVATIVES BY COMPLEXATION OF THE  
CATIONS OF ALKALI METAL CHLORIDES, BARIUM BROMIDE, AND  
SILVER TRIFLATE; INVESTIGATION OF THE EXTERNAL HEAVY  
ATOM PERTURBATION OF THE EXCITED STATE PROCESSES OF NAPHTHALENE  
CROWN ETHER DERIVATIVES BY ETHYL BROMIDE AND BY MEANS OF  
COMPLEXED HALOALKYAMMONIUM CATIONS

By

James M. Larson

The excited state behavior of naphthalene, naphthalene crown ether derivatives 2,3-naphtho-20-crown-6, 1,8-naphtho-21-crown-6, and 1,5-naphtho-22-crown-6; 2,3-, 1,8-, and 1,5-bis(methoxymethyl) and dimethyl naphthalene derivatives; and alkali metal chloride, barium bromide, silver triflate, ammonium, and haloalkylammonium chloride complexes of the above named naphthalene crown ether derivatives was investigated in alcohol glasses at 77 K. Ultraviolet absorption, fluorescence, and phosphorescence spectra were determined at 77 K. Fluorescence and phosphorescence quantum yields (relative to naphthalene) and lifetimes were also measured.

The dissertation considers complexation as a tool to study a phenomenon - naphthalene's excited state behavior - by characterizing

the phenomenon in terms of the way in which it is perturbed by a variety of complexed species (perturbers). The approach is to consider changes in rate constants of excited state processes as a function of perturber and of crown by which it is complexed.

The relative advantages and disadvantages of the proposed perturbational method are compared to those of other perturbational methods which have been used to study excited states. The major advantage of the proposed method is that it allows the investigation of effects of perturbers which aren't chemically affixed to the chromophore yet whose orientation relative to the chromophore is reasonably well defined. A complicating feature of the proposed method is the perturbation due to chemically affixing the complexing agent to the chromophore. Methylene groups were interposed between the oxygens of the crown ether and the naphthalene nucleus to electrically insulate the chromophore from the oxygen atoms. The perturbation due to attachment of the complexing agent is considered by comparing 2,3-, 1,8-, and 1,5-dimethyl and bis-(methoxymethyl) substituent and complexed perturber induced changes in spectra and rate constants to those induced by complexation of metal cations. It is concluded that changes in rate constants due to complexed metal cation perturbers are different from those due to substituents and are characteristic of the properties of the metal cation and of where and how it is held by the crown ether complexer relative to the chromophore.

Perturbation of excited state behavior by complexed haloalkyl-ammonium chloride salts is considered, and, from a comparison to

perturbation by alkylammonium chloride salts, it is concluded that the perturbation due to complexation of the ammonium group can be "separated" from those due to perturbation by the alkyl halide function. The results provide new information on the external heavy atom effect. The relative susceptibilities of rate constants for excited state processes to perturbation by complexed haloalkylammonium salts are different for each crown.

Changes in quantum yields and triplet lifetimes for naphthalene, naphthalene crown ether derivatives, and various alkali metal complexes of these crowns due to perturbation by ethyl bromide containing glass (20% by volume) were also determined.

The major conclusions of the investigation are: 1) there is a directional dependence for external excited state perturbation (from results of ethyl bromide and haloalkylammonium salt perturbation); 2) there is either a strong distance and/or directional dependence (from metal cation perturbation); 3) the positive charge of cationic perturbers in itself induces little change in the rates of excited state processes of naphthalene derivatives; 4) the external heavy atom effect due to alkyl halides does not require the mediation of charge transfer states; 5) the effects of two external perturbers are not additive and that the perturbation due to one external perturber (e.g., ethyl bromide) decreases as the perturbation due to a complexed cation increases; and 6) there is no general order for the susceptibility of rate constants for excited state processes; the relative susceptibility is found to depend upon both the perturber and where it is held relative to the chromophore.

## DEDICATION

I dedicate this dissertation to my parents, family, and friends, for their economic and moral support; and to my teachers, both from The College of St. Thomas and Michigan State University, for their encouragement and for their excellence in teaching. I would especially like to remember here my research director, Dr. Lynn R. Sousa, for his patience, encouragement, warmth as a human being, and his excellence in directing my development as a scientist. Also, I would like to remember Dr. William D. Larson (College of St. Thomas) for removing the terrors of introductory chemistry through his excellence in teaching and his kindly manner, Dr. Richard J. Connell, Dr. Thomas D. Sullivan, and Rev. Vincent E. Rush (College of St. Thomas, Department of Philosophy) for their excellence in teaching and for providing me with a general intellectual orientation and help in training my mind to think; and to Dr. Hubert R. Walczak, for his excellence in the teaching of mathematics.

I would like to remember here the members of the Lynn R. Sousa group, with whom I have had the privilege of associating both as friends and colleagues:

Houston S. Brown  
Joseph G. Bucher, III  
John E. Emswiler  
Mark R. Johnson  
Sandra Klassen  
Jerry L. Meinzer

Also, I would like to remember here Barb A. Duhl-Emswiler and Kim S. Chamberlin colleagues who have become dear to me as friends.

## ACKNOWLEDGMENTS

It would not have been possible to obtain the large quantity of data contained in this dissertation without the help of many people. I am deeply indebted to my colleague Houston S. Brown for the many useful computer programs which he wrote and especially for his work in computer interfacing the Hitachi/Perkin-Elmer spectrophotofluorometer used. The large number of precisely determined quantum yields reported herein would not have been possible without the use of a computer interfaced instrument. I am also indebted to Dr. Lynn R. Sousa, my research director, John E. Emswiler, Mark R. Johnson, Joseph G. Bucher, III, and Sandra Klassen for their help in manually digitizing spectra before the computer interface was available. I would like to thank Dr. Peter J. Wagner for use of his Hitachi/Perkin-Elmer spectrophotofluorometer, without which the high quality corrected emission spectra, precise spectroscopic energies, and accurate quantum yields would not have been possible. Also, I would like to thank Dr. Wagner for use of his Aminco-Bowman spectrophotofluorometer, which was used for the early experimental work and used throughout for phosphorescence lifetime determinations. I thank Dr. Michael Thomas, a post-doctoral with Dr. Wagner at the time, for technical assistance in the early part of the project in the determination of quantum yields and lifetimes and for many useful theoretical discussions. Dr. Thomas modified the Aminco-Bowman spectrophotofluorometer with a solenoid operated shutter, which greatly facilitated phosphorescence lifetime determinations. I would like to thank Dr. Ashraf El-Bayoumi for use

of his single photon counting apparatus and David B. Carr for technical assistance in obtaining fluorescence lifetimes. I am very grateful to Dr. Lynn R. Sousa for his help with fluorescence lifetime determinations, digitization and computer analysis of both phosphorescence and fluorescence lifetimes, and help with synthesis of the crown ether derivatives. I consider it an honor and privilege to have had the opportunity to have worked on this project for him. I am also indebted to him for his help in pushing through the difficult theoretical problems which arose in interpretation of the results.

I also would like to thank Dr. Donald G. Farnum for making his group meetings open to members of other groups. His group meetings provided an excellent opportunity for discussion of topics in organic chemistry and for practice in problem solving. I consider myself to have been privilege to observe the Farnum mind at work on solving a problem.

Finally, I would like to thank the National Science Foundation, the Petroleum Research Fund, and Michigan State University for financial support of this work.

## TABLE OF CONTENTS

Chapter	Page
LIST OF TABLES. . . . .	.vii
LIST OF FIGURES . . . . .	xiv
INTRODUCTION. . . . .	1
General Methodology. . . . .	1
Excited State Processes. . . . .	2
Perturbational Methods . . . . .	6
Proposed Perturbational Methods. . . . .	13
Proposed Experiments . . . . .	20
Background of Heavy Atom Effects . . . . .	24
RESULTS . . . . .	40
Synthesis. . . . .	40
Ultraviolet Absorption Spectra . . . . .	41
Low Temperature (77 K) Fluorescence and Phosphorescence Spectra. . . . .	85
Spectroscopic Energies.. . . .	139
Fluorescence and Phosphorescence Quantum Yields at 77 K . . . . .	148
Fluorescence and Phosphorescence Lifetimes at 77 K. . . . .	184
Tests for Anion Effects on Emission Properties at 77 K . . . . .	198
DISCUSSION. . . . .	199
Preamble . . . . .	199
Preliminaries. . . . .	200
Validity of the Perturbational Method Used . . . . .	203
Conclusions for Validity of Studying Excited State Perturbation <u>via</u> Complexed Perturbers . . . . .	241

Chapter	Page
Validity of Method Used for Study of Perturbation Due to Alkyl Halides <u>via</u> Complexed Haloalkylammonium Chloride Salts. . . . .	242
Method for Consideration of Perturbation by Ethyl Bromide Containing Glass. . . . .	252
Directional Dependence of External Heavy Atom Effect. . . . .	256
Distance Dependence of External Heavy Atom Effect. . . . .	259
Effects of the Positive Charge of the Perturber Necessity of Charge Transfer States for the External Heavy Atom Effect. . . . .	263
Effectiveness of External Perturba- tion as a Function of Perturbation Already Present. . . . .	269
Relative Susceptibility of Rate Constants for Excited State Processes. . . . .	271
EXPERIMENTAL. . . . .	276
General Procedures . . . . .	276
77 K UV Spectra. . . . .	276
Reagent Purity . . . . .	280
Preparation of Samples for Emission Spectroscopy and Quantum Yield Determination. . . . .	286
Emission Spectra . . . . .	287
Spectral Energy Levels . . . . .	288
Quantum Yields . . . . .	289
Titrations Monitored by Following Relative Integrated Emission Intensity . . . . .	294
Complexation Competition Studies . . . . .	299
Variables Affecting Quantum Yield and Integrated Intensity Determinations. . . . .	300
Fluorescence and Phosphorescence Lifetimes. . . . .	305
Synthesis. . . . .	315
REFERENCES. . . . .	324



# LIST OF TABLES

Table		Page
1	Absorption and Emission Frequencies and Changes in Energy Level Separations (all in $\text{cm}^{-1}$ ) for 2,3-, 1,8-, and 1,5-Disubstituted Naphthalenes in Alcohol Glasses at 77 K . . . . .	.140
2	Absorption and Emission Frequencies and Changes in Energy Level Separations (Relative to Free Crown 1) for Alkali Metal Chloride, Barium Bromide, and Silver Triflate Complexes of 2,3-Naphtho-20-Crown-6 (1) at 77 K in Alcohol Glass. All Numbers in $\text{cm}^{-1}$ . . . . .	.141
3	Absorption and Emission Frequencies and Changes in Energy Level Separations (Relative to Free Crown 2) for Alkali Metal Chloride, Barium Bromide, and Silver Triflate Complexes of 1,8-Naphtho-21-Crown-6 (2) in Alcohol Glass at 77 K. All Numbers in $\text{cm}^{-1}$ . . . . .	.142
4	Absorption and Emission Frequencies and Changes in Energy Level Separations (Relative to Free Crown 3) for Alkali Metal Chloride, Barium Bromide, and Silver Triflate Complexes of 1,5-Naphtho-22-Crown-6 (3) at 77 K in Alcohol Glass. All Numbers in $\text{cm}^{-1}$ . . . . .	.143
5	Absorption and Emission Frequencies and Changes in Energy Level Separations (Relative to Free Crown 1) for Alkyl and Haloalkylammonium Chloride Complexes of 2,3-Naphtho-20-Crown-6 (1) at 77 K in Alcohol Glass. All Numbers in $\text{cm}^{-1}$ . . . . .	.144
6	Absorption and Emission Frequencies and Changes in Energy Level Separations (Relative to Free Crown 2) for Alkyl and Haloalkylammonium Chloride Complexes of 1,8-Naphtho-21-Crown-6 (2) at 77 K	

	in Alcohol Glass. All Numbers in $\text{cm}^{-1}$ . . . . .	.145
7	Absorption and Emission Frequencies and Changes in Energy Level Separations (Relative to Free Crown 3) for Alkyl and Haloalkylammonium Chloride Complexes of 1,5-Naphtho-22-Crown-6 (3) at 77 K in Alcohol Glass. All Numbers in $\text{cm}^{-1}$ . . . . .	.146
8	Emission Quantum Yields ( $\phi_f$ and $\phi_p$ ) and Lifetimes ( $\tau_f$ and $\tau_p$ ) for Naphthalene and 2,3-, 1,8-, and 1,5-Disubstituted Naphthalenes in Alcohol Glass at 77 K. . . . .	.150
9	Titrations of 2,3-Naphtho-20-Crown-6 (1) with Ammonium and Alkylammonium Chloride Salts in Un- cracked 95% Ethanol Glass at 77 K Followed by Monitoring Relative Fluorescence Peak intensities. . .	.161
10	Titration of $2.00 \times 10^{-4}$ M 1,8-Naphtho-21-Crown- 6 (2) with Ammonium and Alkyl Ammonium Chlorides in Uncracked 95% Ethanol Glass at 77 K Followed by Monitoring Relative Phosphorescence Peak In- tensities. . . . .	.162
11	Titration of 1,5-Naphtho-22-Crown-6 (3) with Ammonium and <u>n</u> -Propylammonium Chlorides in Un- cracked 95% Ethanol Glass at 77 K Followed by Monitoring Relative Integrated Fluorescence Intensities. . . . .	.163
12	Titration of 2,3-Naphtho-20-Crown-6 (1) with Halo- alkylammonium Chlorides in Uncracked 95% Ethanol Glass at 77 K Followed by Monitoring Relative Fluorescence Intensities . . . . .	.164
13	Titration of 1,8-Naphtho-21-Crown-6 (2) with Halo- alkylammonium Chlorides in Uncracked 95% Ethanol Glass at 77 K Followed by Monitoring Relative Integrate Emission Intensities . . . . .	.165

14	Titration of 1,5-Naphtho-22-Crown-6 ( $\lambda$ ) with Halo-alkylammonium Chlorides in Uncracked 95% Ethanol Glass at 77 K Followed by Monitoring Relative Integrated Fluorescence Intensity. . . . .	.166
15	Titration of 2,3-Naphtho-20-Crown-6 ( $\lambda$ ) with Barium Bromide and Silver Triflate in Uncracked 95% Ethanol Glass at 77 K Followed by Monitoring Relative Integrated Fluorescence Intensities . . . . .	.167
16	Titration of 1,8-Naphtho-21-Crown-6 ( $\lambda$ ) with Silver Triflate in Uncracked 95% Ethanol Glass at 77 K Followed by Monitoring Relative Integrated Phosphorescence Intensity. . . . .	.168
17	Titration of 1,5-Naphtho-22-Crown-6 ( $\lambda$ ) with Barium Bromide and Silver Triflate in Uncracked 95% Ethanol Glass at 77 K Followed by Monitoring Relative Integrated Emission Intensities . . . . .	.169
18	Competition for $1.00 \times 10^{-4} \text{ M}$ 1,8-Naphtho-21-Crown-6 ( $\lambda$ ) in Uncracked 95% Ethanol Glass at 77 K by Sodium and Rubidium Chlorides Followed by Monitoring Arbitrary Relative Integrated Intensity. . . . .	.171
19	Competition for $1.00 \times 10^{-4} \text{ M}$ 1,8-Naphtho-21-Crown-6 ( $\lambda$ ) in Uncracked 95% Ethanol Glass at 77 K by Barium Bromide and Rubidium Chloride Followed by Monitoring Arbitrary Relative Integrated Intensity. . . . .	.173
20	Emission Quantum Yields ( $\phi_f$ and $\phi_p$ ) and Lifetimes ( $\tau_f$ and $\tau_p$ ) for 2,3-Naphtho-20-Crown-6 ( $\lambda$ ) and Alkali Metal Chloride, Barium Bromide, and Silver Triflate Complexes of Crown $\lambda$ in Alcohol Glass at 77 K. . . . .	.175
21	Emission Quantum Yields ( $\phi_f$ and $\phi_p$ ) and Lifetimes ( $\tau_f$ and $\tau_p$ ) for 1,8-Naphtho-21-Crown-6 ( $\lambda$ ) and	

	Alkali Metal Chloride, Barium Bromide, and Silver Triflate Complexes of Crown $\mathcal{L}$ in Alcohol Glass at 77 K. . . . .	.176
22	Emission Quantum Yields ( $\phi_f$ and $\phi_p$ ) and Lifetimes ( $\tau_f$ and $\tau_p$ ) for 1,5-Naphtho-22-Crown-6 and Alkali Metal Chloride, Barium Bromide, and Silver Tri- flate Complexes of Crown $\mathcal{L}$ in Alcohol Glass at 77 K . . . . .	.177
23	Emission Quantum Yields ( $\phi_f$ and $\phi_p$ ) and Lifetimes ( $\tau_f$ and $\tau_p$ ) for 2,3-Naphtho-20-Crown-6 ( $\mathcal{L}$ ) and Ammonium and Alkylammonium Chloride Complexes of Crown $\mathcal{L}$ in Alcohol Glass at 77 K . . . . .	.178
24	Emission Quantum Yields ( $\phi_f$ and $\phi_p$ ) and Lifetimes ( $\tau_f$ and $\tau_p$ ) for 1,8-Naphtho-21-Crown-6 ( $\mathcal{L}$ ) and Ammonium and Alkylammonium Chloride Complexes of Crown $\mathcal{L}$ in Alcohol Glass at 77 K . . . . .	.179
25	Emission Quantum Yields ( $\phi_f$ and $\phi_p$ ) and Lifetimes ( $\tau_f$ and $\tau_p$ ) for 1,5-Naphtho-22-Crown-6 ( $\mathcal{L}$ ) and Ammonium and <u>n</u> -Propylammonium Complexes of Crown $\mathcal{L}$ in 95% Ethanol Glass at 77 K . . . . .	.180
26	Emission Quantum Yields ( $\phi_f$ and $\phi_p$ ) for 2,3- Naphtho-20-Crown-6 ( $\mathcal{L}$ ) and Haloalkylammonium Chloride Complexes of Crown $\mathcal{L}$ in Uncracked 95% Ethanol Glass at 77 K. . . . .	.181
27	Emission Quantum Yields ( $\phi_f$ and $\phi_p$ ) for 1,8- Naphtho-21-Crown-6 ( $\mathcal{L}$ ) and Haloalkylammonium Chloride Complexes of Crown $\mathcal{L}$ in Uncracked 95% Ethanol Glass at 77 K. . . . .	.182
28	Emission Quantum Yields ( $\phi_f$ and $\phi_p$ ) for 1,5- Naphtho-22-Crown-6 ( $\mathcal{L}$ ) and Haloalkylammonium Chloride Complexes of Crown $\mathcal{L}$ in Uncracked 95% Ethanol Glass at 77 K. . . . .	.183

29	Emission Quantum Yields ( $\phi_f$ and $\phi_p$ ) for Naphthalene, 2,3-Naphtho-20-Crown-6 (1), 1,8-Naphtho-21-Crown-6 (2), 1,5-Naphtho-22-Crown-6 (3), and Alkali Metal Complexes of Crowns, 1, 2, and 3 in Uncracked Ethyl Bromide-Ethanol-Methanol (4:1:1, v/v) Glass and in Ethanol-Methanol (4:1, v/v) Glass at 77 K. Numbers in Parentheses are for Results in Ethanol-Methanol (4:1, v/v) Glass at 77 K . . . . .	.185
30	Fluorescent Lifetimes (Double and Single Exponential Analysis) for Bromoalkylammonium Chloride Complexes of 2,3-Naphtho-20-crown-6 (1) and 1,8-Naphtho-21-Crown-6 (2) in 95% Ethanol-Methanol (4:1, v/v) Glass at 77 K . . . . .	.187
31	Triplet Lifetimes (Double and Single Exponential Analysis) for Haloalkylammonium Chloride Complexes of 2,3-Naphtho-20-Crown-6 (1), 1,8-Naphtho-21-Crown-6 (2), and 1,5-Naphtho-22-Crown-6 (3) in Uncracked 95% Ethanol Glass at 77 K. . . . .	.188
32	Triplet Lifetimes (Single and Double Exponential Analysis) for Naphthalene, 2,3-Naphtho-20-Crown-6, 1,8-Naphtho-21-Crown-6 (2), 1,5-Naphtho-22-Crown-6 (3), and Alkali Metal Chloride Complexes of Crowns 1, 2, and 3 in Uncracked Ethyl Bromide-Ethanol-Methanol (1:4:1, v/v) Glass at 77 K. . . . .	.190
33	Estimates for Rate Constants of Excited State Processes of Naphthalene and 2,3-, 1,8-, and 1,5-Disubstitutednaphthalenes in Alcohol Glass at 77 K . . . . .	.215
34	Estimates for Rate Constants of Excited State Processes for 2,3-Naphtho-20-Crown-6 (1) and Alkali Metal Chloride, Barium Bromide, and Silver Triflate Complexes of Crown 1 in Alcohol Glass at 77 K. . . . .	.216

35	Estimates for Rate Constants of Excited State Processes for 1,8-Naphtho-21-Crown-6 ( $\mathcal{2}$ ) and Alkali Metal Chloride, Barium Bromide, and Silver Triflate Complexes of Crown $\mathcal{2}$ in Alcohol Glass at 77 K. . . . .	.217
36	Estimates for Rate Constants of Excited State Processes for 1,5-Naphtho-22-Crown-6 ( $\mathcal{3}$ ) and Alkali Metal Chloride, Barium Bromide, and Silver Triflate Complexes of Crown $\mathcal{3}$ in Alcohol Glass at 77 K. . . . .	.218
37	Estimates for Rate Constants of Excited State Processes of 2,3-Naphtho-22-Crown-6 ( $\mathcal{1}$ ) and Ammonium, Alkylammonium, and Haloalkylammonium Chloride Complexes of Crown $\mathcal{1}$ in Alcohol Glass at 77 K. . . . .	.244
38	Estimates for Rate Constants of Excited State Processes of 1,8-Naphtho-21-Crown-6 ( $\mathcal{2}$ ) and Ammonium, Alkylammonium, and Haloalkylammonium Chloride Complexes of Crown $\mathcal{2}$ in Alcohol Glass at 77 K. . . . .	.245
39	Estimates for Rate Constants of Excited State Processes of 1,5-Naphtho-22-Crown-6 ( $\mathcal{3}$ ) and Ammonium, Alkylammonium, and Haloalkylammonium Chloride Complexes of Crown $\mathcal{3}$ in Alcohol Glass at 77 K. . . . .	.246
40	Estimates for Ratios of Fluorescence ( $\phi_{f,o}$ ) and Phosphorescence ( $\phi_{p,o}$ ) Quantum Yields and Phosphorescence Lifetimes ( $\tau_{p,o}$ ) in Alcohol Glass to the Corresponding Quantum Yields ( $\phi_{f,EtBr}$ and $\phi_{p,EtBr}$ ) and Lifetimes ( $\tau_{p,EtBr}$ ) in Ethyl Bromide-Ethanol-Methanol (1:4:1, v/v) Glass at 77 K. . . . .	.255

41	Relative Susceptibility of Rate Constants of Excited State Processes of 2,3-Naphtho-20-Crown-6 (1), 1,8-Naphtho-21-Crown-6 (2), and 1,5-Naphtho- 22-Crown-6 (3) to Perturbation by Complexed Alkali Metal, Barium and Silver Cations in Alcohol Glass at 77 K. . . . .	.272
42	Relative Susceptibility of Rate Constants of Excited State Processes of 2,3-Naphtho-20-Crown-6 (1), 1,8-Naphtho-21-Crown-6 (2), and 1,5-Naphtho- 22-Crown-6 (3) to Perturbation by Complexed Alkyl and Haloalkylammonium Cations in Alcohol Glass at 77 K. . . . .	.273
43	Comparison of Room Temperature UV Absorption Spectra of 2,3-Naphtho-20-Crown-6 (1) in Square Cells and in Round Dewar . . . . .	.278
44	Wavelengths (nm) at which Quantum Yield Comparisons Relative to Naphthalene Were Made and Number of Determinations Made for Disubstituted Naphtha- lenes. . . . .	.292
45	Wavelengths at Which Quantum Yield Comparisons Relative to Free Crowns Were Made. . . . .	.293

# LIST OF FIGURES

Figure		Page
1	77 K UV spectra of 2,3-disubstitutednaphthalenes in 95% ethanol-methanol (4:1, v/v) glass. See figure legend. Intensities are given in terms of relative absorbancies (see text for explanation). Relative absorbancies for shorter wavelength regions are given by the scale on the left; for longer wavelength region, by scale on the right. Concentrations (at room temperature) were $4.00 \times 10^{-4}$ <u>M</u> for longer wavelength region and $1.20 \times 10^{-4}$ <u>M</u> for shorter wavelength region (except for naphthalene, $1.00 \times 10^{-4}$ <u>M</u> ). The scales have been adjusted so that the absorbancies of both sections, after multiplication if necessary by the factors given in the figure legend are those of a $8.00 \times 10^{-5}$ <u>M</u> solution. Curve A, 2,3-naphtho-20-crown-6 ( <u>1</u> ); curve B, 2,3-bis-(methoxymethyl)naphthalene ( <u>4</u> ); curve C, 2,3-dimethylnaphthalene ( <u>5</u> ); curve D, naphthalene ( <u>10</u> ). . . . .	43
2	77 K UV spectra of 1,8-disubstitutednaphthalenes in 95% ethanol-methanol (4:1, v/v) glass. Intensities are given in terms of relative absorbancies (see text for explanation). Relative absorbancies for shorter wavelength region are given by the scale on the left; for longer wavelength region, by the scale on the right. Concentrations (at room temperature) were $4.00 \times 10^{-4}$ <u>M</u> for longer wavelength region and $8.00 \times 10^{-5}$ <u>M</u> for shorter wavelength	



- region (except for naphthalene,  $1.00 \times 10^{-4}$  M). The scales have been adjusted so that the absorbancies of both sections, after multiplication if necessary by the factors given in the figure legend, are those of a  $8.00 \times 10^{-5}$  M solution. Curve A, 1,8-naphtho-21-crown-6 (2); curve B, 1,8-bis-(methoxymethyl)naphthalene (6); curve C, 1,8-dimethylnaphthalene (7); curve D, naphthalene (10) . . . . . 45
- 3 77 K UV spectra of 1,5-disubstituted naphthalenes in ethanol-methanol (4:1, v/v) glass. See figure legend. Intensities are given in terms of relative absorbancies (see text for explanation). Relative absorbancies for shorter wavelength region are given by the scale on the left; for the longer wavelength region, by the scale on the right. Concentrations (at room temperature) were  $2.00 \times 10^{-4}$  M for the longer wavelength region and  $6.00 \times 10^{-5}$  M for the shorter wavelength region. The scales have been adjusted so that the absorbancies of both sections are those of a  $6.00 \times 10^{-5}$  M solution. Curve A, 1,5-naphtho-22-crown-6 (3); curve B, 1,5-bis-(methoxymethyl)naphthalene (8); curve C, 1,5-dimethylnaphthalene (9); curve D, naphthalene (10) . . . . . 47
- 4 77 K UV spectra of 2,3-naphtho-20-crown-6 (1) alone and with 5:1 added molar excesses of alkali metal chlorides in 95% ethanol-methanol (4:1, v/v) glass. See figure legend. Intensities are given in terms of relative absorbancies (see text for explanation). Relative absorbancies for shorter wavelength

- region are given by the scale on the left;  
for longer wavelength region, by scale on  
right. Crown concentrations (at room tempera-  
ture) were  $4.00 \times 10^{-4}$  M for longer wavelength  
region and  $1.20 \times 10^{-4}$  M for shorter wavelength  
region. The scales have been adjusted so  
that the absorbancies of both sections are  
those of a  $1.20 \times 10^{-4}$  M solution. . . . . 49
- 5 77 K UV spectra of 1,8-naphtho-21-crown-6  
(2) alone and with 5:1 added molar excesses  
of alkali metal chlorides in 95% ethanol-  
methanol (4:1, v/v) glass. See figure legend.  
Intensities are given in terms of relative  
absorbancies (see text for explanation).  
Relative absorbancies for shorter wavelength  
region are given by the scale on the left;  
for longer wavelength region, by scale on right.  
Crown concentrations (at room temperature)  
were  $4.00 \times 10^{-4}$  M for longer wavelength  
region and  $8.00 \times 10^{-5}$  M for shorter wavelength  
region. The scales have been adjusted so that  
the absorbancies of both sections are those of  
a  $8.00 \times 10^{-5}$  M solution. . . . . 51
- 6 77 K UV spectra of 1,5-naphtho-22-crown-6 (3)  
alone and with 5:1 added molar excesses of  
alkali metal chlorides in 95% ethanol-methanol  
(4:1, v/v) glass. See figure legend. Inten-  
sities are given in terms of relative absor-  
bancies (see text for explanation). Relative  
absorbancies for shorter wavelength region  
are given by the scale on the left; for longer  
wavelength region, by scale on right. Crown  
concentrations were  $2.00 \times 10^{-4}$  M for longer

- wavelength region and  $6.00 \times 10^{-5} \text{ M}$  for shorter wavelength region. The scales have been adjusted so that the absorbancies of both sections are those of a  $6.00 \times 10^{-5} \text{ M}$  solution. . . . . 53
- 7 77 K UV spectra of 2,3-naphtho-20-crown-6 (1) alone and with 5:1 added molar excess of ammonium and alkylammonium chlorides in 95% ethanol-methanol (4:1, v/v) glass. See figure legend. Intensities are given in terms of relative absorbancies (see text for explanation). Relative absorbancies for shorter wavelength region are given by the scale on the left; for longer wavelength region, by scale on right. Crown concentrations (at room temperature) were  $4.00 \times 10^{-4} \text{ M}$  for the longer wavelength region and  $1.20 \times 10^{-4} \text{ M}$  for the shorter wavelength region. The scales have been adjusted so that the absorbancies of both sections are those of a  $1.20 \times 10^{-4} \text{ M}$  solution. . . . . 55
- 8 77 K UV spectra of 1,8-naphtho-21-crown-6 (2) alone and with 5:1 added molar excess of ammonium and alkylammonium chlorides in 95% ethanol-methanol (4:1, v/v) glass. See figure legend. Intensities are given in terms of relative absorbancies (see text for explanation). Relative absorbancies for shorter wavelength region are given by scale on left; for longer wavelength region, by scale on right. Crown concentrations (at room temperature) were  $4.00 \times 10^{-4} \text{ M}$  for the longer wavelength region and  $8.00 \times 10^{-5} \text{ M}$  for the shorter wavelength region. The scales have been

	adjusted so that the absorbancies of both sections are those of a $8.00 \times 10^{-5}$ <u>M</u> solution. . . . .	57
9	77 K UV spectra of 1,5-naphtho-22-crown-6 (3) alone and with 100:1 molar excesses of ammonium and <u>n</u> -propylammonium chlorides in ethanol-methanol (4:1, v/v) glass. See figure legend. Intensities are given in terms of relative absorbancies (see text for explanation). Relative absorbancies for shorter wavelength region are given by the scale on the left; for longer wavelength region, by scale on right. Crown concentrations (at room temperature) were $1.00 \times 10^{-4}$ <u>M</u> for the longer wavelength region and $5.00 \times 10^{-5}$ <u>M</u> for the shorter wavelength region. The scales have been adjusted so that the absorbancies of both sections are those of a $5.00 \times 10^{-5}$ <u>M</u> solution. . . . .	59
10	77 K UV spectra of 2,3-naphtho-20-crown-6 (1) alone and with 5:1 added molar excess of bromoalkylammonium chlorides in 95% ethanol-methanol (4:1, v/v) glass and with 12.5:1 added molar excess of iodoalkylammonium chlorides in ethanol-methanol (4:1, v/v) glass. See figure legend. Intensities are given in terms of relative absorbancies (see text for explanation). Relative absorbancies for the shorter wavelength region are given by the scale on the left; for longer wavelength region, by scale on right. The concentration (at room temperature) of crown was $4.00 \times 10^{-4}$ <u>M</u> for the longer wavelength region and $8.00 \times 10^{-5}$ <u>M</u> for the shorter wavelength region. The scales have been	

- adjusted so that the absorbancies of both sections are those of  $8.00 \times 10^{-5}$  M solutions. Baselines: curve F,  $\beta$ -iodoethylammonium chloride; curve G,  $\gamma$ -iodopropylammonium chloride; curve H, 95% ethanol-methanol (4:1, v/v) glass. . . . . 61
- 11 77 K UV spectra of 1,8-naphtho-21-crown-6 (2) alone and with 5:1 added molar excess of bromoalkylammonium chlorides in 95% ethanol-methanol (4:1, v/v) glass and with 12.5:1 added molar excess of iodoalkylammonium chlorides in ethanol-methanol (4:1, v/v) glass. See figure legend. Intensities are given in terms of relative absorbancies (see text for explanation). Relative absorbancies for the shorter wavelength region are given by the scale on the left; for the longer wavelength region, by the scale on the right. The concentration (at room temperature) of crown was  $4.00 \times 10^{-4}$  M for the longer wavelength region and  $8.00 \times 10^{-5}$  M for the shorter wavelength region. The scales have been adjusted so that the absorbancies of both sections are those of a  $8.00 \times 10^{-5}$  M solution. Baselines: curve F,  $\beta$ -iodoethylammonium chloride; curve G,  $\gamma$ -iodopropylammonium chloride; curve H, 95% ethanol-methanol (4:1, v/v) glass . . . . . 63
- 12 77 K UV spectra of 1,5-naphtho-22-crown-6 (3) alone and with 50:1 added molar excess of bromoalkylammonium and iodoalkylammonium chlorides in ethanol-methanol (4:1, v/v) glass. See figure legend. Intensities are

given in terms of relative absorbancies (see text for explanation). Relative absorbancies for the shorter wavelength region are given by the scale on the left; for the longer wavelength region, by the scale on the right. The concentration (at room temperature) of crown was  $1.00 \times 10^{-4}$  M for the longer wavelength region and  $5.00 \times 10^{-4}$  M for the shorter wavelength region. The scales have been adjusted so that the absorbancies of both sections are those of a  $5.00 \times 10^{-5}$  M solution. Baselines: curve F,  $2.50 \times 10^{-3}$  M  $\beta$ -iodoethylammonium chloride; curve G,  $2.50 \times 10^{-3}$  M  $\gamma$ -iodopropylammonium chloride; curve H, ethanol-methanol (4:1, v/v) glass. . . . .

65

13 77 K UV spectra of 2,3-naphtho-20-crown-6 (1) alone and with 5:1 added molar excess of cesium chloride in 95% ethanol-methanol (4:1, v/v) glass and with 12:1 added molar excess of barium bromide in ethanol-methanol (4:1, v/v) glass. See figure legend. Intensities are given in terms of relative absorbancies (see text for explanation). Relative absorbancies for the shorter wavelength region are given by the scale on the left; for the longer wavelength region, by the scale on the right. Crown concentrations (at room temperature) were  $4.00 \times 10^{-4}$  M for the longer wavelength region and  $8.00 \times 10^{-5}$  M for the shorter wavelength region. The scales have been adjusted so that the absorbancies of both sections are those of a  $8.00 \times 10^{-5}$  M solution . . . . .

67



- 14      77 K UV spectra of 1,8-naphtho-21-crown-6  
(2) alone and with 5:1 added molar excess of  
cesium chloride in 95% ethanol-methanol (4:1,  
v/v) glass and with 12:1 added molar excess  
of barium bromide in ethanol-methanol (4:1,  
v/v) glass. See figure legend. Intensities  
are given in terms of relative absorbancies  
(see text for explanation). Relative absor-  
bancies for the shorter wavelength region are  
given by the scale on the left; for the longer  
wavelength region by the scale on the right.  
Crown concentrations (at room temperature)  
were  $4.00 \times 10^{-4}$  M for the longer wavelength  
region and  $8.00 \times 10^{-5}$  M for the shorter wave-  
length region. The scales have been adjusted  
so that the absorbancies of both sections are  
those of a  $8.00 \times 10^{-5}$  M solution. . . . . 69
- 15      77 K UV spectra of 1,5-naphtho-22-crown-6  
(3) alone and with 5:1 added molar excess  
of cesium chloride in 95% ethanol-methanol  
(4:1, v/v) glass and with 50:1 added molar  
excess of barium bromide in ethanol-methanol  
(4:1, v/v) glass. See figure legend. In-  
tensities are given in terms of relative  
absorbancies (see text for explanation).  
Relative absorbancies for the shorter wave-  
length region are given by the scale on the  
left; for the longer wavelength region by the  
scale on the right. Crown concentrations (at  
room temperature) were  $4.00 \times 10^{-4}$  M for the  
longer wavelength region and  $8.00 \times 10^{-5}$  M  
for the shorter wavelength region. The scales  
have been adjusted so that the absorbancies





	of both sections are those of a $8.00 \times 10^{-5}$ <u>M</u> solution . . . . .	71
16	77 K UV spectra of 2,3-naphtho-20-crown-6 (1) alone and with 50:1 added molar excess of silver triflate in ethanol-methanol (4:1, v/v) glass. See figure legend. Intensities are given in terms of relative absorbancies (see text for explanation). Relative ab- sorbancies for the shorter wavelength region are given by the scale on the left; for the longer wavelength region by the scale on the right. Crown concentrations (at room tempera- ture) were $4.00 \times 10^{-4}$ <u>M</u> for the longer wave- length region and $8.00 \times 10^{-5}$ <u>M</u> for the shorter wavelength region. The scales have been adjusted so that the absorbancies of both sections are those of a $8.00 \times 10^{-5}$ <u>M</u> solu- tion . . . . .	73
17	77 K UV spectra of 1,8-naphtho-21-crown-6 (2) alone and with 50:1 added molar excess of silver triflate in ethanol-methanol (4:1, v/v) glass. See figure legend. Intensities are given in terms of relative absorbancies (see text for explanation). Relative ab- sorbancies for the shorter wavelength region are given by the scale on the left; for the longer wavelength region by the scale on the right. Crown concentrations (at room tempera- ture) were $4.00 \times 10^{-4}$ <u>M</u> for the longer wave- length region and $8.00 \times 10^{-5}$ <u>M</u> for the shorter wavelength region. The scales have been adjusted so that the absorbancies of both sections are those of $8.00 \times 10^{-5}$ <u>M</u> solu- tion . . . . .	75

- 18 77 K UV spectra of 1,5-naphtho-22-crown-6 (3) alone and with 200:1 added molar excess of silver triflate in ethanol-methanol (4:1, v/v) glass. See figure legend. Intensities are given in terms of relative absorbancies (see text for explanation). Relative absorbancies for the shorter wavelength region are given by the scale on the left; for the longer wavelength region by the scale on the right. Crown concentrations at room temperature were  $1.00 \times 10^{-4}$  M for the longer wavelength region and  $5.00 \times 10^{-5}$  M for the shorter wavelength region. The scales have been adjusted so that the absorbancies of both sections are those of a  $5.00 \times 10^{-5}$  M solution . . . . . 77
- 19 Corrected fluorescence spectra of  $1.00 \times 10^{-4}$  M 2,3-disubstituted naphthalenes (2,3-naphtho-20-crown-6 (1), curve A; 2,3-bis-(methoxymethyl)naphthalene (4), curve B; 2,3-dimethylnaphthalene (5), curve C; and naphthalene (10), curve D) in uncracked 95% ethanol glass at 77 K. . . . . 86
- 20 Corrected phosphorescence spectra of  $1.00 \times 10^{-4}$  M 2,3-disubstituted naphthalenes (2,3-naphtho-20-crown-6 (1), curve A; 2,3-bis-(methoxymethyl)naphthalene (4), curve B; 2,3-dimethylnaphthalene (5), curve C; and naphthalene (10) curve D) in uncracked 95% ethanol. . . . . 88
- 21 Corrected fluorescence spectra of 1,8-disubstituted naphthalenes (1,8-naphtho-21-crown-6 (2), curve A; 1,8-bis-(methoxymethyl)naphthalene (6), curve B; 1,8-dimethylnaphthalene

	(7), curve C; and naphthalene (10), curve D) in uncracked 95% ethanol at 77 K. Curve D should be multiplied by 3.0. . . . .	89
22	Corrected phosphorescence spectra of 1,8- disubstituted naphthalenes (1,8-naphtho-21- crown-6 (2), curve A; 1,8-bis-(methoxymethyl)- naphthalene (6), curve B; 1,8-dimethylnaphtha- lene (7), curve C; and naphthalene (10), curve D) in uncracked 95% ethanol glass at 77 K. . . . .	90
23	Corrected fluorescence spectra of 1,5-disubsti- tuted naphthalenes (1,5-naphtho-22-crown-6 (3), curve A; 1,5-bis-(methoxymethyl)naphthalene (8) curve B; 1,5-dimethylnaphthalene (9), curve C; and naphthalene (10), curve D) in uncracked 95% ethanol glass at 77 K. . . . .	91
24	Corrected phosphorescence spectra of 1,5- disubstituted naphthalenes (1,5-naphtho-22- crown-6 (3), curve A; 1,5-bis(methoxymethyl)- naphthalene (8), curve B; 1,5-dimethylnaphthalene (9), curve C; and naphthalene (10), curve D) in uncracked 95% ethanol glass at 77 K . . . . .	92
25	Corrected fluorescence spectra of $2.00 \times 10^{-4}$ M 2,3-naphtho-20-crown-6 (1) alone and with 5:1 molar excess of alkali metal chlorides added in uncracked 95% ethanol glass at 77 K . . . . .	93
26	Corrected phosphorescence spectra of $2.00 \times 10^{-4}$ M 2,3-naphtho-20-crown-6 (1) alone and with 5:1 molar excess of added alkali metal chlorides in uncracked 95% ethanol glass at 77 K . . . . .	94
27	Corrected fluorescence spectra of $2.00 \times 10^{-4}$ M 1,8-naphtho-21-crown-6 (2) alone and with 5:1 molar excess of added alkali metal chlorides in uncracked 95% ethanol glass at 77 K. . . . .	95

28	Corrected phosphorescence spectra of $2.00 \times 10^{-4}$ M 1,8-naphtho-21-crown-6 ( $\lambda$ ) alone and with 5:1 molar excess of added alkali metal chlorides in uncracked 95% ethanol glass at 77 K . . . . .	96
29	Corrected fluorescence spectra of $1.00 \times 10^{-4}$ M 1,5-naphtho-22-crown-6 ( $\lambda$ ) alone and with 5:1 molar excess of added alkali metal chlorides in uncracked 95% ethanol glass at 77 K . . . . .	97
30	Corrected phosphorescence spectra of $1.00 \times 10^{-4}$ M 1,5-naphtho-22-crown-6 ( $\lambda$ ) alone and with 5:1 molar excess of added alkali metal chlorides in uncracked 95% ethanol glass at 77 K. . . . .	98
31	Corrected fluorescence spectra of $2.00 \times 10^{-4}$ M 2,3-naphtho-20-crown-6 ( $\lambda$ ) alone and with 5:1 molar excess of added ammonium and alkyl-ammonium chlorides in uncracked 95% ethanol glass at 77 K... . . . .	99
32	Corrected phosphorescence spectra of $2.00 \times 10^{-4}$ M 2,3-naphtho-20-crown-6 ( $\lambda$ ) alone and with 5:1 molar excess of added ammonium and alkylammonium chlorides in uncracked 95% ethanol glass at 77 K. . . . .	100
33	Corrected fluorescence spectra of $2.00 \times 10^{-4}$ M 1,8-naphtho-21-crown-6 ( $\lambda$ ) alone and with 5:1 molar excess of added ammonium and alkyl-ammonium chlorides in uncracked 95% ethanol glass at 77 K. . . . .	101
34	Corrected phosphorescence of $2.00 \times 10^{-4}$ M 1,8-naphtho-21-crown-6 ( $\lambda$ ) alone and with 5:1 molar excess of added ammonium and alkyl-ammonium chlorides in uncracked 95% ethanol glass at 77 K. . . . .	102

35	Corrected fluorescence spectra of $1.00 \times 10^{-4}$ M 1,5-naphtho-22-crown-6 ( $\lambda$ ) alone and with 50:1 and 10:1 added molar excesses of ammonium and n-propylammonium chlorides, respectively, in uncracked 95% ethanol glass at 77 K. . . . .	103
36	Corrected phosphorescence spectra of $1.00 \times 10^{-4}$ M 1,5-naphtho-22-crown-6 ( $\lambda$ ) alone and with 50:1 and 10:1 added molar excesses of ammonium and n-propylammonium chlorides, respectively, in uncracked 95% ethanol glass at 77 K. . . . .	104
37	Corrected fluorescence spectra of 2,3-naphtho-20-crown-6 ( $\lambda$ ) alone and with 5:1 added molar excess of bromoalkylammonium chlorides ( $2.00 \times 10^{-4}$ M crown) and 20:1 added molar excess of iodoalkylammonium chlorides ( $1.00 \times 10^{-4}$ M crown) in uncracked 95% ethanol glass at 77 K. . . . .	105
38	Corrected phosphorescence spectra of 2,3-naphtho-20-crown-6 ( $\lambda$ ) alone and 5:1 molar excess of bromoalkylammonium chlorides ( $2.00 \times 10^{-4}$ M crown) and 20:1 molar excess of iodoalkylammonium chlorides ( $1.00 \times 10^{-4}$ M crown) in uncracked 95% ethanol glass at 77 K. . . . .	106
39	Corrected fluorescence spectra of 1,8-naphtho-21-crown-6 ( $\lambda$ ) alone and with 5:1 added molar excess of bromoalkylammonium chlorides ( $2.00 \times 10^{-4}$ M crown) and with 20:1 added molar excess of iodoalkylammonium chlorides ( $1.00 \times 10^{-4}$ M crown) in uncracked 95% ethanol glass at 77 K. . . . .	107

40	Corrected phosphorescence spectra of 1,8-naphtho-21-crown-6 ( $\lambda$ ) alone and with 5:1 added molar excess of bromoalkylammonium chlorides ( $2.00 \times 10^{-4}$ M crown) and with 20:1 added molar excess of iodoalkylammonium chlorides ( $1.00 \times 10^{-4}$ M crown) in 95% ethanol glass at 77 K. . . . .	108
41	Corrected fluorescence spectra of $1.00 \times 10^{-4}$ M 1,5-naphtho-22-crown-6 ( $\lambda$ ) alone and with 20:1 added molar excess of bromo- and iodoalkylammonium chlorides in uncracked 95% ethanol glass at 77 K. . . . .	109
42	Corrected phosphorescence spectra of $1.00 \times 10^{-4}$ M 1,5-naphtho-22-crown-6 ( $\lambda$ ) alone and with 20:1 added molar excess of bromo- and iodoalkylammonium chlorides in uncracked 95% ethanol glass at 77 K. . . . .	110
43	Corrected fluorescence spectra of 2,3-naphtho-20-crown-6 ( $\lambda$ ) alone and with 5:1 added molar excess of cesium chloride ( $2.00 \times 10^{-4}$ M crown) and 10:1 added molar excess of barium bromide ( $1.00 \times 10^{-4}$ M crown) in uncracked 95% ethanol glass at 77 K. . . . .	111
44	Corrected phosphorescence spectra of 2,3-naphtho-20-crown-6 ( $\lambda$ ) alone and with 5:1 added molar excess of cesium chloride ( $2.00 \times 10^{-4}$ M crown) and 10:1 added molar excess of barium bromide ( $1.00 \times 10^{-4}$ M crown) in uncracked 95% ethanol glass at 77 K. . . . .	112
45	Corrected fluorescence spectra of 1,8-naphtho-21-crown-6 ( $\lambda$ ) alone and with 5:1 added molar excess of cesium chloride ( $2.00 \times 10^{-4}$ M crown) and 10:1 added molar excess of barium	

Figure		Page
	bromide ( $1.00 \times 10^{-4}$ M crown) in uncracked 95% ethanol glass at 77 K. . . . .	113
46	Corrected phosphorescence spectra of 1,8- naphtho-21-crown-6 (2) alone and with 5:1 added molar excess of cesium chloride ( $2.00$ $\times 10^{-4}$ M crown) and 10:1 added molar excess of barium bromide ( $1.00 \times 10^{-4}$ M crown) in uncracked 95% ethanol glass at 77 K. . . . .	114
47	Corrected fluorescence spectra of 1,5-naphtho- 22-crown-6 (3) alone and with 5:1 added molar excess of cesium chloride ( $2.00 \times 10^{-4}$ M crown) and 50:1 added molar excess of barium bromide ( $1.00 \times 10^{-4}$ M crown) in uncracked 95% ethanol glass at 77 K. . . . .	115
48	Corrected phosphorescence spectra of 1,5- naphtho-22-crown-6 (3) alone and with 5:1 added molar excess of cesium chloride ( $2.00$ $\times 10^{-4}$ M crown) and 50:1 added molar excess of barium bromide ( $1.00 \times 10^{-4}$ M crown) in uncracked 95% ethanol glass at 77 K. . . . .	116
49	Corrected fluorescence spectra of $1.00 \times 10^{-4}$ M 2,3-naphtho-20-crown-6 (1) alone and with 50:1 added molar excess of silver triflate in uncracked 95% ethanol glass at 77 K. . . . .	117
50	Corrected phosphorescence spectra of $1.00 \times$ $10^{-4}$ M 2,3-naphtho-20-crown-6 (1) alone and with 50:1 added molar excess of silver triflate in uncracked 95% ethanol glass at 77 K. . . . .	118
51	Corrected fluorescence spectra of $1.00 \times 10^{-4}$ M 1,8-naphtho-21-crown-6 (2) alone and with 50:1 added molar excess of silver triflate in uncracked 95% ethanol at 77 K. . . . .	119



Figure		Page
52	Corrected phosphorescence spectra of $1.00 \times 10^{-4}$ M 1,8-naphtho-21-crown-6 (2) alone and with 50:1 added molar excess of silver triflate in uncracked 95% ethanol glass at 77 K . . . . .	120
53	Corrected fluorescence spectra of $1.00 \times 10^{-4}$ M 1,5-naphtho-22-crown-6 (3) alone and with 200:1 added molar excess of silver triflate in uncracked 95% ethanol glass at 77 K. . . . .	121
54	Corrected phosphorescence spectra of $1.00 \times 10^{-4}$ M 1,5-naphtho-22-crown-6 (3) alone and with 200:1 added molar excess of silver triflate in uncracked 95% ethanol glass at 77 K . . . . .	122
55	Titration of $2.00 \times 10^{-4}$ M 2,3-naphtho-20-crown-6 (1) with alkali metal chlorides in 95% ethanol at 77 K followed by monitoring integrated fluorescence intensity. . . . .	153
56	Titration of $2.00 \times 10^{-4}$ M 2,3-naphtho-20-crown-6 (1) with alkali metal chlorides in 95% ethanol at 77 K followed by monitoring integrated phosphorescence intensity . . . . .	154
57	Titration of $2.00 \times 10^{-4}$ M 1,8-naphtho-21-crown-6 (2) with alkali metal chlorides in 95% ethanol at 77 K followed by monitoring integrated fluorescence intensity. . . . .	155
58	Titration of $2.00 \times 10^{-4}$ M 1,8-naphtho-21-crown-6 (2) with alkali metal chlorides in 95% ethanol at 77 K followed by monitoring integrated phosphorescence intensity . . . . .	156
59	Titration of $1.00 \times 10^{-4}$ M 1,5-naphtho-22-crown-6 (3) with alkali metal chlorides in 95% ethanol at 77 K followed by monitoring integrated fluorescence intensity. . . . .	157

Figure		Page
60	Titration of $1.00 \times 10^{-4}$ M 1,5-naphtho-22-crown-6 (3) with alkali metal chlorides in 95% ethanol at 77 K followed by monitoring integrated phosphorescence intensity . . . . .	158
61	Wavelength positions of peaks and shoulders (half-height lines) for fluorescence spectra of naphthalene and 2,3-, 1,8-, and 1,5-disubstituted naphthalenes in 95% ethanol glass at 77 K. . . . .	207
62	Wavelength positions of peaks and shoulders (half-height lines) for UV absorption spectra of naphthalene and 2,3-, 1,8-, and 1,5-disubstituted naphthalenes in 95% ethanol glass at 77 K. . . . .	210
63	Changes in estimated rate constants caused by 2,3-disubstitution of naphthalene and by alkali metal cation perturbation of the 2,3-crown (1). . . . .	222
64	Changes in estimated rate constants caused by 1,8-disubstitution of naphthalene and by alkali metal cation perturbation of the 1,8-crown (2). . . . .	223
65	Changes in estimates of rate constants caused by 1,5-disubstitution of naphthalene and by alkali metal cation perturbation of the 1,5-crown (3). . . . .	224
66	Plot of $\log k_{dt}$ versus the change in the $T_1-S_0$ energy separation in $\text{cm}^{-1}$ caused by alkali metal, barium, and silver cation perturbation of crowns 1 and 2. . . . .	230
67	Plot of the change in the $S_1 - T_1$ energy separation caused by alkali metal cation perturbation of crowns 1 and 2 versus the polarizing strength of the alkali metal cations . . . . .	233

68	Plot of the change in the $T_1 - S_0$ energy separation caused by alkali metal cation perturbation of crowns $\lambda_1$ and $\lambda_2$ versus the polarizing strength of the alkali metal cations. . . . .	234
69	Changes in rate constants of excited state processes of crowns $\lambda_1$ , $\lambda_2$ , and $\lambda_3$ caused by $K^+$ ( a light cation) and $Cs^+$ (a heavy cation) . . . .	239
70	Plot of $\log k_{dt}$ versus the change in the $T_1 - S_0$ energy separation in $cm^{-1}$ caused by ammonium, alkylammonium, and haloalkylammonium cation perturbation of crowns $\lambda_1$ and $\lambda_2$ . . . . .	253

## PREFACE

This investigation of excited state processes makes use of a new perturbational method, so the introduction will first make some general comments on the nature of perturbational methodology. An analytical consideration of how excited state processes might be studied by perturbational methods will then be presented. Methods which have been used and their relative advantages and disadvantages are noted and compared to those of the method used in this investigation. The problem will then be recast in terms of the methodology presented and the general philosophy of the proposed method of analysis given. A brief background section on heavy atom effects will be presented, since some of the perturbing species used are known to cause what has come to be called "heavy atom effects". After the introduction, results will be presented in a fashion suitable to the proposed method of analysis. The discussion will analyze the results in terms of the questions and problems raised in the introduction.

It should be pointed out at the onset that this investigation is very exploratory in nature. Reasonable sets of experiments in light of what was known and what was learned in the course of the investigation were proposed and carried out. While the results at hand undoubtedly answer some of the questions posed, they may also raise more questions than they answer. But this is the nature of exploratory research.

## INTRODUCTION

### General Methodology

One of the most general ways to study a phenomenon is to characterize it in terms of its behavior. This can be done not only by observing its normal behavior but also by observing how it behaves in response to a variety of stimuli. The Latins had a phrase which summarizes the philosophy of this methodology: Agere sequitur esse (to act follows to be). That is, a thing's behavior is a function of its nature. A problem inherent to all perturbational studies is the possibility that the perturbation applied might change the system to the point that the observed behavior is no longer characteristic of the unperturbed system but characteristic rather of a new system produced by the perturbation.

The phenomenon with which this investigation is concerned is the behavior of electronically excited states produced by electronic excitation in condensed phases. Since the purpose of this investigation is in part to investigate the validity of a new perturbational method and since a general investigation of excited state processes is beyond the scope of any single study, the excited state behavior of a single compound will be investigated using this method. Naphthalene, a member of the aromatic hydrocarbon series, is the model compound selected for the purposes of this investigation. Reasons for its selection will be given later. It might be hoped that what is learned from this investigation based on naphthalene, provided that the perturbational method used can be justified, might be true

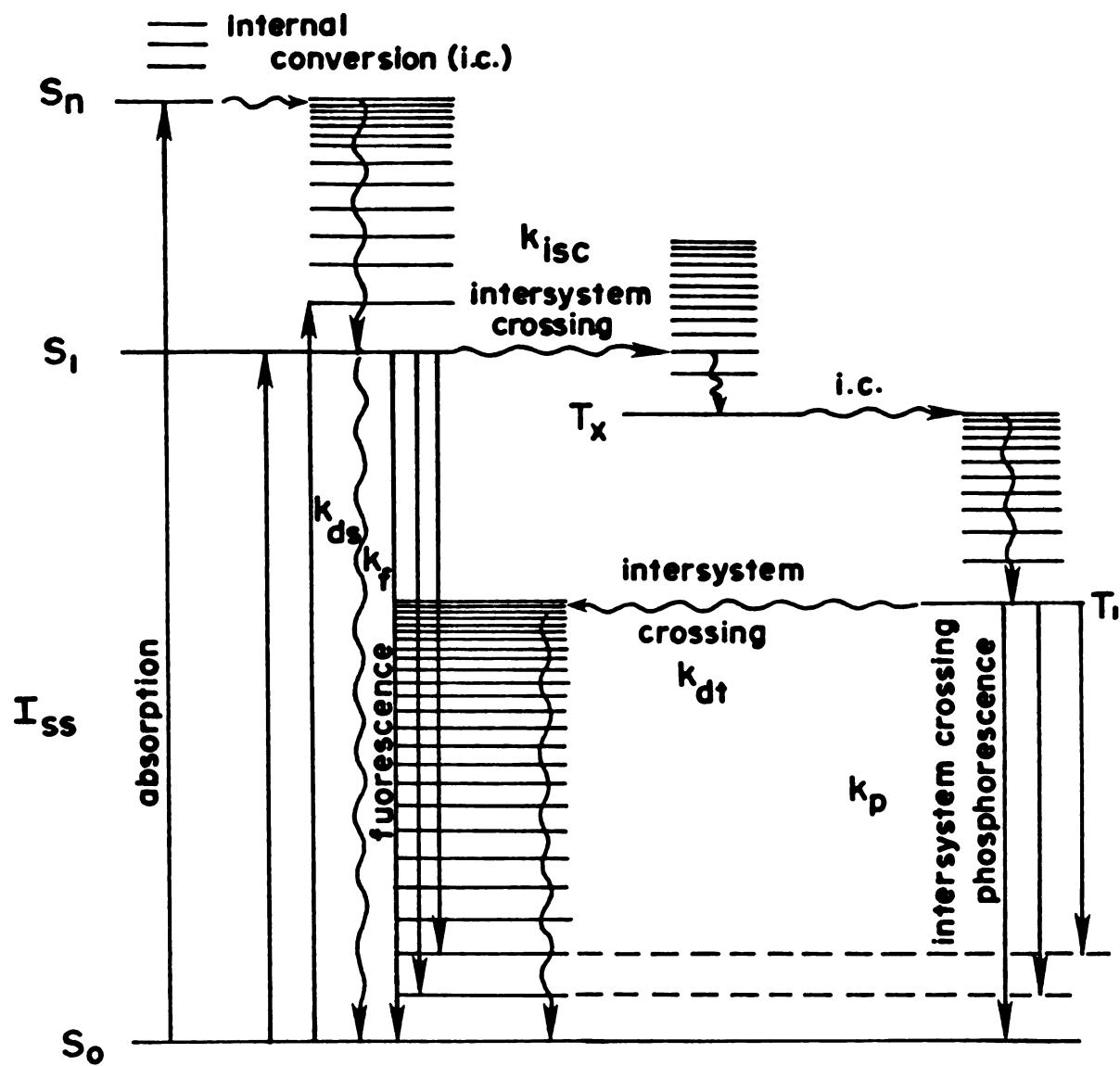
for aromatic hydrocarbons in general. The generality of conclusions reached, however, will not be established by this investigation.

### Excited State Processes<sup>1</sup>

Before considering the variety of ways which might be used to study excited state behavior by perturbational methods, a discussion of what excited states normally do will be given. What excited states do is to dissipate excess energy. What is of interest is how they dissipate energy. The ways in which excited states dissipate energy fall into two classes: radiative (energy dissipated in the form of light) and nonradiative. Nonradiative energy dissipation may occur by energy transfer in the form of heat to the physical surroundings, by energy transfer to another molecule, or via chemical reaction. This investigation is limited to a consideration of photophysical processes of photoexcited molecules in condensed phases, i.e., electronic excited state in the absence of chemical reactions but under the possible physical perturbation of a solvent. The systems studied will be dilute ( $10^{-4}$  M range) solutions in glassy media at 77 K, so nonradiative energy transfer will most likely involve energy transfer to the physical surroundings.

A Jablonski diagram depicting the photophysical processes of a typical aromatic hydrocarbon in condensed medium is given in Scheme 1.<sup>2</sup> Radiative processes are indicated by straight lines, nonradiative by wavy lines. The main processes of interest are: fluorescence (radiative decay of lowest electronically excited singlet state,  $S_1$ ),

Scheme 1.



phosphorescence (radiative decay of the lowest electronically excited triplet state,  $T_1$ ), intersystem crossing (radiationless decay of  $S_1$  involving crossing to the triplet manifold, radiationless decay of  $S_1$  to  $S_0$ , radiationless decay involving intersystem crossing from  $T_1$  to  $S_0$ ). Each of these are unimolecular processes. The rate constants of each of these processes are labeled as follows:  $k_f$  (rate constant for fluorescence),  $k_p$  (rate constant for phosphorescence),  $k_{isc}$  (rate constant for intersystem crossing from  $S_1$  to  $T_1$ ),  $k_{ds}$  (rate constant for radiationless decay from  $S_1$  to  $S_0$ ),  $k_{dt}$  (rate constant for radiationless decay from  $T_1$  to  $S_0$ ). Note that when a process is indicated to occur from one state to another nothing more is intended than an indication of the initial and final states; no implication about how this process occurs is intended. In condensed media, rates of radiationless decay of higher excited singlets to  $S_1$  or higher excited triplets to  $T_1$  (referred to as "internal conversion" in both cases) are much faster than either radiative or radiationless decay of either  $S_1$  or  $T_1$ , so fluorescence and phosphorescence are normally from  $S_1$  and  $T_1$ , respectively.<sup>3</sup>

The rates of radiative and radiationless decays from  $S_1$  and  $T_1$  can be calculated from the following experimentally determined quantities:  $\phi_f$  (quantum yield of fluorescence),  $\phi_p$  (quantum yield of phosphorescence),  $\tau_f$  (lifetime of fluorescence decay),  $\tau_p$  (lifetime of phosphorescence decay), and  $\phi_{isc}$  (quantum yield of intersystem crossing). These quantities are defined by the rates in Scheme 1 as given by the following equations:



$$\phi_f = \frac{k_f}{k_f + k_{ds} + k_{isc}} = k_f \tau_f$$

$$\phi_{isc} = k_{isc} \tau_f$$

$$\phi_p = \phi_{isc} \frac{k_p}{k_p + k_{dt}} = \phi_{isc} k_p \tau_p$$

$\phi_{isc}$  is readily determined in solution, but in glassy media much more complex experiments are required.<sup>5</sup> For many aromatic hydrocarbons, including naphthalene, however, it has been demonstrated (in solution and in glassy media) by the direct determination of the quantum yield of triplet formation, that  $\phi_{isc} = 1 - \phi_f$ .<sup>5</sup> This means that all decay of  $S_1$  is either through fluorescence or through intersystem crossing. Alternatively, it means that  $k_{ds}$  is negligibly small compared to  $(k_f + k_{isc})$ . Thus, the above set of equations reduce to four equations in four unknowns. Solutions for the rate constants in terms of measurable quantities are:

$$k_f = \frac{\tau_f}{\tau_t}$$

$$k_{isc} = \frac{(1 - \phi_f)}{\tau_f}$$

$$k_p = \frac{\phi_p}{(1 - \phi_f)\tau_p}$$

$$k_{dt} = \frac{1}{\tau_p} - k_p$$

Determination of these rate constants for naphthalene and for naphthalene perturbed in a variety of ways will be one way of investigating how excited state processes are affected as a function of the way in which naphthalene is perturbed.

### Perturbational Methods

An analytical consideration of how naphthalene excited states might be studied by perturbational methods will now be given. Ideally a perturbational study would involve taking a single electronically excited naphthalene molecule, bringing a variety of different type perturbers up to it, holding them at a variety of distances and orientations, and characterizing changes in the rates of its excited state processes in terms of these parameters. Several possible orientations are indicated below:



Such a study would reveal the following kinds of information: direction of approach of the perturber which is most effective; the minimum

distance between naphthalene and perturber for perturbation to occur; and which perturbors are most effective at perturbing a given process or group of processes. In the absence of molecular forceps this method is obviously not capable of experimental realization. What are needed, then, are methods which will induce the perturber and perturbed to spend time near each other. Various methods have been used to do this and their relative advantages and disadvantages as perturbational methods will be given below. Finally, the method used in this investigation will be discussed in terms of its relative advantages and disadvantages as a perturbational method.

One of the surest ways of inducing two species to spend time together in a relatively fixed fashion is to hold them together via a covalent bond. Thus, one might investigate changes in naphthalene's excited state processes as a function of position, number and nature of substituents. This has been done for naphthalene using deuterium<sup>6</sup> and halogen<sup>7</sup> substituents in place of protium. The advantage of using deuterium as a perturber is that substitution of deuterium for protium is the smallest possible chemical perturbation that can be made. One advantage of using the halogens as perturbors is that they form a larger series, though different in nature, than the limited isotopes of hydrogen. The disadvantage is that substitution of halogen for hydrogen is a large chemical perturbation. It is well known that the interaction of unshared electron pairs on halogen with adjacent  $\pi$ -systems has been used to explain the greater strength of aryl-halogen and vinyl-halogen bonds as compared to alkyl halogen bonds. Thus, results of such studies have to be treated with the caution

that changes in the rates of excited state processes for different perturbers might not be comparable. The changes, rather than reflecting a change in some fundamental periodic property of the halogens, might instead reflect changes due to chemically altering the substituted nucleus to such an extent that changes observed for different substituents are no longer comparable. The alteration due to different substituents might be due to changes in fundamental periodic properties. The problem is separation of effects, which might be difficult for covalently bonded perturbers.

Both deuterium and halogen substitution have provided useful probes of excited state behavior. The smaller amplitude of a vibrational wavefunction for a deuterium-carbon bond compared to that of a protium-carbon bond of the same energy has proven to be useful in the understanding of radiationless decay processes.<sup>8</sup> The halogens have provided a useful series for investigation of the effects of variation of the atomic number of the perturber on excited state processes. Their effects as perturbers has led to much of what is known about so called "heavy atom effects" (vide infra). McClure, for example, found that the triplet lifetimes of  $\alpha$ - and of  $\beta$ -halonaphthalenes correlated reasonably well with a single atomic parameter of the halogens, the spin-orbital coupling parameter.<sup>9</sup>

Another method of inducing two things to spend time near each other is to simply mix them together. Barring any attractive interactions, statistically they will spend some time in each other's vicinity. The chances of the two species spending time in each other's vicinity can be increased by increasing the concentrations of one or

both species. Results of studies done on compounds in the gas phase and in a condensed phase are often different. In the gas phase, fluorescence from higher electronic states than  $S_1$  and from vibrational levels of electronically excited states has been observed.<sup>10</sup> As was previously noted, however, fluorescence is usually from  $S_1$  when the compound is in the condensed phase. Thus, comparison of excited state behavior in the gas phase and in a condensed phase is one perturbational method of the intermolecular variety.<sup>11</sup> One can also investigate the perturbing effects of one condensed phase relative to another.<sup>12</sup> The advantages of this perturbation method are that 1) it avoids the possible pitfalls of making use of covalent bonding to ensure association, and 2) it allows investigation of perturbations due to species which can't be covalently bonded to a hydrocarbon framework. For this type of study, it is desirable that there be no strong attractive forces between the perturber and the perturbed, i.e., that their association be governed by statistics. Strong attractions between the perturbed and perturber will change both of them and invalidate the perturbational method. This is probably not a problem for cases which require high concentrations of perturber. A disadvantage of this method is that one has no idea of the spatial relationships between perturber and perturbed which give rise to the observed effects. In the absence of attractive interactions there should be a random distribution of perturber around the perturbed species, thus giving rise to an infinite number of interactions. Also, for a given direction of approach, the distance between the perturber and perturbed will vary in a statistical fashion. Since one would not expect all these

interactions to give the same effect, the observed results will be a mixture of effects unless there is only one effective perturbational interaction. Analysis of a mixture of effects is less informative than analysis of isolated effects.

One of the most common types of condensed phases used to study excited state behavior has been alkyl halides, either neat or mixed with some other solvent. Solutions in neat alkyl halides, however, frequently give cracked glasses,<sup>13</sup> which makes accurate quantum yield determinations impossible, and mixed first order triplet decay is invariably observed.<sup>13,14</sup> Thus, actual rate constant calculations can't be done, since the observed quantities are composites. Nevertheless, trends in  $\phi_f$ ,  $\phi_p$ , and  $\tau_p$  have been noted for these studies and interpreted as heavy atom effects (see introduction section on heavy atom effects below). Another problem is that alkyl iodides absorb strongly at wavelengths shorter than 400 nm (see results section for ethyl bromide). Its use for studying a chromophore like naphthalene is impossible except in a very rough way, since naphthalene fluoresces in the 315 to 400 nm region.<sup>15</sup> Condensed phases of rare gases at 4.2 °K have also been used as perturbing media. Condensed phases of this sort are probably less likely to interact chemically with a dissolved species than are any others, which makes them ideal perturbers. Johnson has shown that the triplet lifetimes and phosphorescence spectra of benzene in an argon matrix differ according to the symmetry of the hole benzene is in and he was able to identify the symmetry of one of the holes responsible for a given lifetime and spectrum.<sup>17</sup> A variety of other types of external perturbers have been used: alkali

halide salts (perturbation due to halide),<sup>18</sup> cesium chloride (perturbation due to cesium cation),<sup>19</sup> transition metals,<sup>20,21</sup> and other paramagnetic species such as oxygen.<sup>22</sup> The kinds of perturbers noted above have a wide range of properties and each kind of perturber provides limited information about the nature of excited state processes. The wide variety of perturbers which can be used is one of the advantages of the intermolecular perturbational method. The main disadvantage of this method is the random distribution of perturber, which gives rise to many different interactions. Johnson's work for benzene (vide infra) in rare gas hosts was able to partially overcome this difficulty by being able to control the symmetry of the hole.

Another method which can be used to get two species to spend time together makes use of species which form complexes. Provided that the site of complexation is known, this method has the advantage of being less random than the intermolecular method. These studies depend upon attractive polar interactions involving atoms which are part of the chromophore as the basis for complexation. While such studies may be instructive in their own right, it does not seem to be desirable to base a perturbational method upon this type of interaction. Some examples of this kind of study follow. Yuster and Weissman<sup>23</sup> determined relative fluorescence and phosphorescence intensities and phosphorescence lifetimes for dibenzoylmethane complexes of trivalent ions of aluminum, scandium, yttrium, lanthanum, gadolinium, and lutetium as well as phosphorescence lifetimes for complexes of alkali and alkaline earth metals. It was found that  $\tau_p$  decreased with increasing atomic number for complexes of ions in the same column

of the periodic table. Fluorescence to phosphorescence intensities decreased as  $\tau_p$  decreased. Effects were observed to depend not only on atomic number but also on electronic configuration. The largest effects were observed for paramagnetic gadolinium. Marzzacco<sup>24</sup> determined 77 °K absorption, phosphorescence, and phosphorescence excitation spectra of pyrazine in ethanol with various amounts of lithium, sodium, potassium, and zinc (II) halide salts. Effects were shown to be anion independent, and shown to be a composite of uncomplexed pyrazine, and 1:1 and 2:1 metal:pyrazine complexes (complexation is between metal and nitrogen). Phosphorescence quantum yields were about the same for the 1:1 sodium and potassium complexes ( $0.9 \pm 0.2$ ) and smaller for lithium, zinc, and water 1:1 complexes. Phosphorescence quantum yields were about the same for sodium, potassium, and water 2:1 complexes ( $0.6 \pm 0.3$ ) and smaller for lithium and zinc complexes ( $<0.15$  and  $<0.1$ , respectively). This study did not attempt any interpretation of the results in terms of the properties of the perturbors. Song<sup>25</sup> observed an increase in the fluorescence quantum yield for a complex between retinal and sodium cation relative to the quantum yield for uncomplexed retinal (a similar effect was not observed for retinol). The increase in fluorescence quantum yield was interpreted as an anomalous heavy atom effect. Luminescence properties of complexes of metal ions with porphyrins<sup>26</sup> and of bipyridyl ruthenium complexes have been extensively investigated.<sup>27</sup>

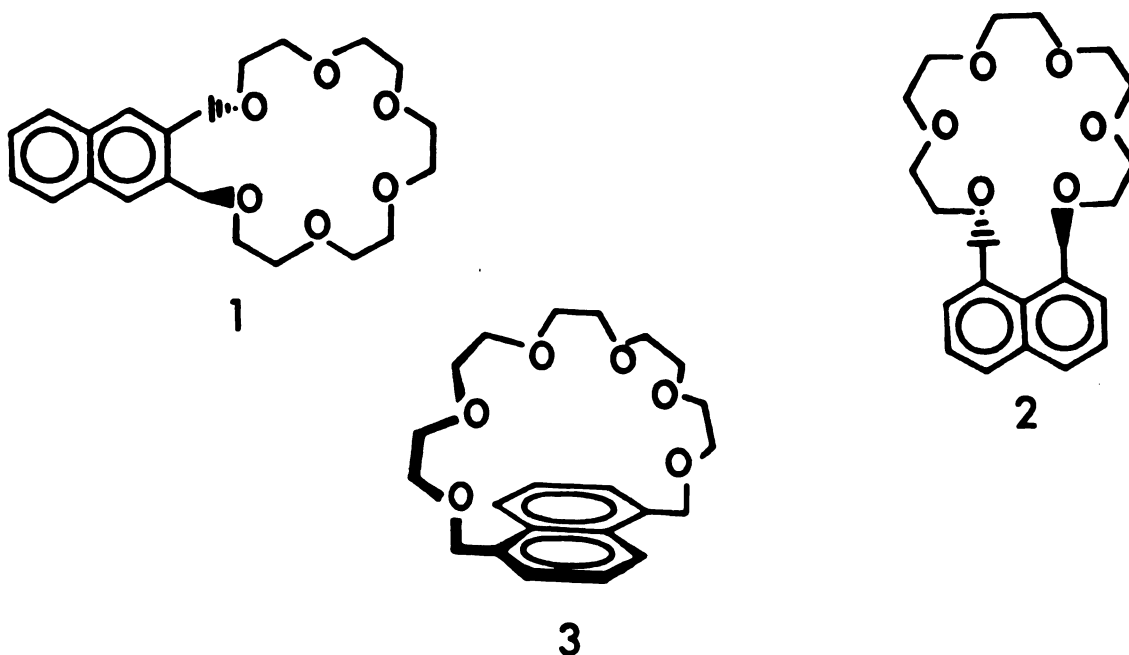
Another method which has been used to induce two species to spend time in the same vicinity is to bond the perturber to a part of the molecule which is not part of the chromophore yet holds the perturber



in the vicinity of the chromophore. Turro<sup>29</sup> made use of the rigidity of the norbornene system fused to the 2,3- positions of naphthalene in an attempt to systematically study the interaction between bromine substituents on the norbornene framework and the naphthalene chromophore. No systematic relationship between the position of bromine and changes in excited state rate constants could be discerned (both mono- and dibromonaphthonorbornenes were investigated in ether-isopentane-ethanol (5:5:2) glass at 77 °K). The puzzling results of this study may be a function of an inadequate understanding of the importance of throughbond interactions, even though the bromine is insulated by several carbon-carbon bonds from the chromophore.

#### Proposed Perturbational Method

This investigation has also relied upon complexation to induce two species to spend time in the same vicinity, but it has done so in a different fashion. The perturber itself is not directly bonded to the chromophore of interest but is held near to it by means of a complexing agent which has been attached. To do this, advantage was taken of the complexing abilities of crown ethers (cyclic polyethers).<sup>29,30</sup> The following crown ether-equipped naphthalene derivatives were synthesized: 2,3-naphtho-20-crown-6 (1), 1,8-naphtho-21-crown-6 (2), and 1,5-naphtho-22-crown-6 (3).



The versatile complexing abilities of crown ethers provide for the study of a wide range of perturbers. Crown ethers are known to complex a variety of cations: alkali metal,<sup>29a,b</sup> alkaline earth,<sup>29a,b</sup> ammonium,<sup>31</sup> primary alkylammonium,<sup>31</sup> diazonium,<sup>32</sup> silver (I),<sup>33</sup> lead (II),<sup>33</sup> mercury (II),<sup>33</sup> thallium (I),<sup>33</sup> and zinc (II)<sup>34</sup> and lanthanides.<sup>35</sup> In nonpolar solvents hydrogen bonding compounds such as alcohols<sup>36</sup> and carboxylic acids<sup>37</sup> are complexed by crown ethers. Crown ethers are reasonably inert chemically. Also, they do not absorb in the near ultraviolet region, so their absorption will not overlap absorption by the chromophore of interest.

This proposed perturbational method has some of the advantages and some of the disadvantages inherent to the intramolecular, intermolecular, and complexation perturbational methods noted above. Like the intramolecular and complexation methods, it has the advantage that complexed perturbers are held in reasonably well-defined positions

relative to the naphthalene nucleus. The position of a complexed perturber is less well-defined, however, than that of a covalently bonded perturber or a perturber which complexes with a given site in a chromophore. This is because the position of a complexed perturber can't be deduced from the structure of the free crown. Also, different perturbors may complex differently. Thus, the distance and position of different perturbors from the naphthalene nucleus may differ. While the positions of complexed perturbors will not be known precisely, at least the direction of approach of a perturber to the naphthalene nucleus is defined by the positions at which the naphthalene nucleus is incorporated into the cycle. Like the intramolecular perturbation method, this method perturbs naphthalene by making use of covalent bonding. On the other hand, crown  $\text{3}$  affords a direction of approach to the naphthalene chromophore not practically possible via covalent bonding, i.e., it allows positioning of a perturber in the vicinity of the  $\pi$ -face of the chromophore. In this case, however, it is the complexing agent, not the perturber, which is covalently bonded. The attachment of the complexing agent itself, of course, is a perturbation. The attachment of the complexing agent, however, was done in such a way as to minimize the perturbation. The purpose of the methylene units inserted between the naphthalene nucleus and the oxygen atoms is to electrically insulate the naphthalene  $\pi$ -system from interaction with unshared electron pairs on oxygen and to minimize differences in inductive effects felt by the naphthalene nucleus from complexed and from uncomplexed oxygen. The problem of perturbing naphthalene by attachment of the complexing agent will be considered

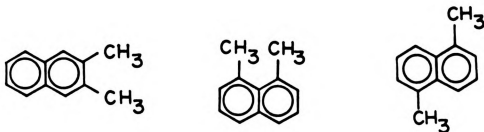
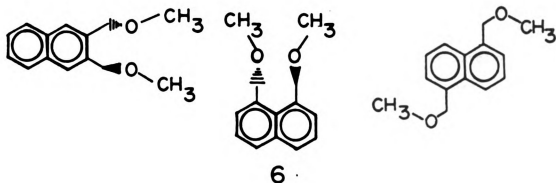
in greater detail below.

Like the intermolecular and complexation perturbational methods noted previously, the proposed method has the advantage of making it possible to investigate the perturbing effects of species which can't be covalently bonded to a hydrocarbon framework. Unlike intermolecular perturbation of naphthalene, however, two of our models, crowns  $\lambda$  and  $\mu$ , have groups which block the approach of the perturber to the side of the chromophore. Thus, for these two crowns, our results will perhaps be more characteristic of bis-(methoxymethyl)-naphthalenes than of naphthalene itself. For crown  $\nu$ , approach to the  $\pi$ -face is not blocked by the methylene units, since they lie in the same plane as the naphthalene nucleus. Depending upon how different ions complex, however, the distance between the  $\pi$ -face and the complexed ion may vary.

There are some practical advantages to the proposed perturbational approach, which are meaningful if the method turns out to be valid. One advantage is that it is easier to make complexes than compounds. Some survey studies have been hampered by the large amount of work involved in preparation and purification of a large group of related derivatives.<sup>6</sup> While synthesis and purification of chromophores equipped with complexing agents may not be trivial, once they have been made and purified, one need only use pure salts and solvents to prepare pure complexes. A wide variety of salts of high purity are commercially available, and impurities in salts are less likely to be troublesome than organic impurities, which may emit or quench excited states. Also, provided that stability constants are reasonably large,

lower concentrations than those required for the intermolecular method can be used. This is especially important for ionic perturbers, since many salts have very low solubilities in organic solvents. Alternatively, crown ethers may increase the solubility of attached hydrocarbons in aqueous media. Also, perturbers which absorb light in the region that absorption or emission occurs may interfere when used at high concentrations but may not interfere at low concentrations. Thus, this investigation was able to determine the intermolecular effect of alkyl iodides via iodoalkylammonium chlorides on excited state behavior using concentrations at which absorption by the iodides did not interfere (vide infra).

The perturbation due to disubstituting naphthalene with crown-methylene groups is potentially serious. A possible consequence of this perturbation would be that rates of excited state processes for crown complexes could not be compared to those of naphthalene. In this case, results for complexes of crowns 1, 2, and 3 could not be compared, although results for different complexes of the same crown might validly be compared. The problem will in part be addressed by comparing rates of excited state processes of 2,3-, 1,8-, and 1,5- dimethyl-, bis-(methoxymethyl)-, and crown-methylene disubstituted naphthalenes to those of naphthalene and to those of crown complexes. The compounds indicated in the above series are 2,3-dimethylnaphthalene (4), 2,3-bis-(methoxymethyl)naphthalene, (5), crown 1, 1,8-dimethylnaphthalene (6), 1,8-bis-(methoxymethyl) naphthalene (7), crown 2, 1,5-dimethylnaphthalene (8), 1,5-bis-(methoxymethyl)naphthalene (9), crown 3, and naphthalene (10).



The problem will also be addressed by comparing 77 K UV absorption and emission spectra. The following sets of spectral comparisons will be made: naphthalene compared to disubstituted naphthalenes, free crown compared to complexes of same crown, and complexes of one crown compared to complexes of another crown. The comparisons will be qualitative in nature. The extent of the comparisons will be to note how similar or dissimilar spectral shapes are. The assumption underlying such comparisons will be that if spectral shapes are the same, so also are the states giving rise to them. When spectral shapes are

different, there is less that can be said here, since this writer is not a theoretical spectroscopist. Full analysis of spectral shapes that are different might reveal how different the states involved are and the nature of the perturbation responsible for their difference. The difficulty of analysis in such cases may also be a function of the chromophore chosen for this model study. While naphthalene is a good candidate for study in many respects (vide infra), interpretation of results may be complicated because of the nature of its absorption ( $S_0 \rightarrow S_1$ ) and fluorescence ( $S_1 \rightarrow S_0$ ), since the orbitally allowed component of these transitions is weak and much of the observed intensity is induced by vibronic coupling with higher electronic states.<sup>38</sup>

Perturbation due to introduction of a substituent may enhance mixing of electronic states resulting in enhanced transition intensities. Naphthalenes phosphorescence, however, is orbitally allowed (though, of course, spin forbidden).<sup>39</sup> Perturbation due to introduction of a substituent may only introduce symmetry restrictions which affect the allowedness of various transitions.<sup>40</sup>

There are several reasons which make naphthalene a good candidate for study. Naphthalene's excited state behavior has been extensively studied, which makes comparison of the proposed perturbational method to previously used perturbational methods much easier than if a little studied system had been chosen. Also, it provides for comparison of results obtained by the proposed method to results previously obtained by other methods. Naphthalene has acceptable photophysical properties, i.e., it both fluoresces and phosphoresces in easily accessible spectral regions. Naphthalene has less symmetry than, say, benzene, and so

provides a better model for probing for directional dependence of external perturbation. Naphthalene derivatives are readily available, thus simplifying the synthetic task, and there was a reasonable chance that the crown derivatives would be crystalline solids. Crystalline solids can be effectively purified by recrystallization, whereas oils are difficult to purify.

Provided that the problems alluded to are not overpowering, crowns like  $\lambda$ ,  $\mu$ , and  $\nu$  offer a new method for the study of excited state processes by nonbonded perturbers. At worst, the excited state behavior of a large variety of complexes of a new variety will have been investigated.

### Proposed Experiments

Previous to this investigation, there were no reports in the literature of perturbation of excited states of aromatic hydrocarbons by alkali, alkaline earth, or by ammonium cations, save one study of the quenching of nine aromatic hydrocarbons by cesium cation.<sup>19</sup> In fact, previous studies using alkali metal halides found that effects were due to the halide, not to the cation.<sup>41</sup> Thus, the alkali metal chlorides should be an interesting series to investigate. Since the cation perturbation studies are exploratory, it is not desirable to prejudice the results by saying that the purpose is to investigate this or that theory or effect. There was very little way to know what to expect. Thus, although the alkali metal cations are isoelectronic with the corresponding halide anions, there is no reason to assume that their effects will be the same or different, since the effect of the positive



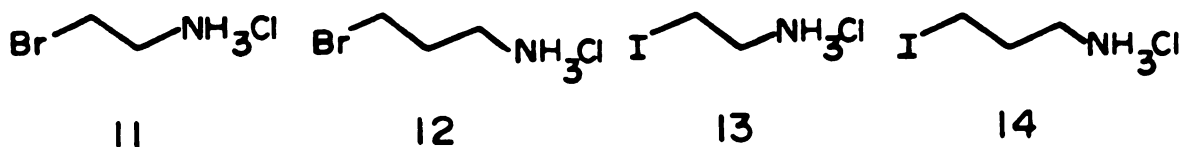
charge is unknown.

It is difficult to say in advance what correlations might be expected between the rates of excited state processes and the atomic parameters of the perturbers. The charge, size, polarizability, atomic number, spin-orbit coupling parameter, electronic configuration, and magnetic properties (diamagnetic, paramagnetic) are atomic parameters of cationic perturbers which can be varied. The alkali metal cations provide a series of cations which all have the same charge but which differ in the remaining atomic parameters. Comparison of cesium and barium cations as perturbers will provide for a comparison of two cations which have similar atomic weights and spin orbit coupling parameters but which differ in size, charge, and polarizability. Investigation of the perturbing effects of silver (I) cation will provide an example of a cation of lower atomic number than cesium or barium, of about the same size as the potassium cation, of greater polarizability than any of the other metal cations investigated, and, unfortunately, the only cation investigated which has an unfilled shell of electrons. These metal cations provide a wide variation of atomic parameters, though they by no means provide a systematic variation of every atomic parameter.

Investigation of the perturbing effects of ammonium and primary alkylammonium salts might be interesting because they are very much different from the alkali metal cations both in nature and in the way they complex with crown ethers.<sup>31</sup> Ammonium salts complex with crown ethers through hydrogen bonding; apparently three hydrogen bonds are necessary, since complexation with 2° and 3° ammonium salts has not

yet been observed. What was to be expected from use of ammonium salts as perturbers was even less certain than for the metal cations. It was thought, however, that introduction of an alkyl group in the vicinity of the excited state in an otherwise very polar medium might provide a useful probe for the susceptibility of excited state behavior to localized changes in solvent polarity.

Complexation of crown ethers with alkylammonium salts provides another method for studying intermolecular perturbations via attachment of the perturber to the alkyl chain of an ammonium salt. This method has been made use of to study the intermolecular heavy atom effect due to the halogens (bromine and iodine). The effects of  $\beta$ -bromoethylammonium chloride (11),  $\gamma$ -bromopropylammonium-chloride (12),  $\beta$ -iodoethyl-ammonium chloride (13), and  $\gamma$ -iodopropylammonium chloride (14) complexed by crowns 1, 2, and 3 were investigated. This method of investigating intermolecular heavy atom effects has the same kind



of disadvantage as do traditional methods, i.e., lack of knowledge of the location of the heavy atom relative to the excited state. Although the alkyl chain does not constrain the halogen to be in any given place, the length of the alkyl chain places constraints on how far away it can be and the site of complexation of the ammonium group places constraints on where it can be. The position of the perturber is more determinate than for the intermolecular perturbation method

but less determinate than for the intramolecular method. While this method has the advantage of avoiding chemical attachment of the heavy atom to the chromophore, it has the potential disadvantage of concurrent perturbation of naphthalene by crown-methylene substitution and by complexation of the ammonium group. The perturbation due to a complexed alkylammonium salt, however, will be available for comparison. An advantage of studying intermolecular perturbation by this method is that a locally high concentration of perturber can be obtained without using a high bulk concentration of perturber. This is an advantage for an investigation of perturbers which absorb light in the same spectral region as absorption and emission of light by the chromophore under investigation. A previous study of alkyl halide perturbation of naphthalene was stymied in the case of ethyl iodide (ethyl iodide-ethanol 1:4, v/v) due to absorption of fluorescence by ethyl iodide.<sup>15</sup> For this investigation, however, the concentrations of haloalkylammonium salts were sufficiently low that absorption of fluorescence by the salt was negligible.

A traditional intermolecular heavy atom study using ethyl bromide-ethanol-methanol (1:4:1, v/v) glass at 77 K as the perturbing medium was done for naphthalene, for crowns  $\lambda_1$ ,  $\lambda_2$ , and  $\lambda_3$ , and for various alkali metal chloride complexes of these crowns. This study was done for a variety of reasons. Changes in rates of excited state processes of the bromoalkylammonium complexes seemed to be somewhat small. It was possible that this might be because the bromine was not in a position where it could perturb effectively or that the susceptibility of the complex to perturbation by the bromine was less than what it

would have been for naphthalene unperturbed by crown-methylene substitution and crown complexation. Thus, it was desirable to investigate the effect of an untethered alkyl bromide. Also, questions about whether or not heavy atom effects are additive have been raised.<sup>42</sup> A combination of cations complexed by crowns  $\lambda$ ,  $\zeta$ , and  $\mathfrak{z}$  and ethyl bromide provides a series where not only the weight but also the position of the cationic perturber can easily be varied. Directional dependence of the intermolecular heavy atom effect has been investigated by using phenyl groups substituted at adjacent positions on naphthalene to sterically block approach of an external heavy atom from that direction.<sup>42</sup> Crowns  $\lambda$ ,  $\zeta$ , and  $\mathfrak{z}$  have very bulky substituents. For  $\mathfrak{z}$ , the crown may sterically block approach to the face of the  $\pi$ -system.

#### Background of Heavy Atom Effects

This background section does not purport to be a complete review of what is known about heavy atom effects (HAE). The emphasis will be on what has been learned from intermolecular HAE due to alkyl halides. HAE and their interpretation will be described. Issues concerning the mechanism of HAE will be briefly indicated, but only those issues which this investigation will have a bearing on will be described in any detail. Differences and similarities between inter- and intramolecular HAE will be briefly noted.

McClure<sup>9</sup> found that  $\tau_p$  decreased regularly within the same series for  $\alpha$ - and  $\beta$ -halonaphthalenes as the atomic number of the halogen (F, Cl, Br, I) increased. The enhanced transition probabilities were

taken as evidence that the transitions were between singlet and triplet states and that the long-lived states of aromatic hydrocarbons are triplet states. The justification for this conclusion was that the results fit the predictions of a first order perturbation treatment (vide infra) which treated the perturbation due to introduction of a halogen in terms of the spin-orbital (SO) coupling operator ( $H_{SO}$ ):

$$\hat{H} = \hat{H}_0 + \hat{H}_{SO}$$

where  $\hat{H}_0$  is the Hamiltonian for the unperturbed system and  $\hat{H}$  is the perturbed Hamiltonian. For a single electron in a central potential field, the SO coupling operator takes the general form

$$\hat{H}_{SO} = k\xi(L \cdot S)$$

where  $k$  is a composite of constants,  $\xi$  is the SO coupling parameter,  $L$  is the orbital angular momentum, and  $S$  is the spin angular momentum ( $\xi$  can be derived from atomic spectra).<sup>43</sup> Its value increases rapidly as the nuclear charge increases. The values of  $\xi$  for F, Cl, Br, and I are, respectively, 272, 587, 2,460, and 5,060  $\text{cm}^{-1}$ .<sup>44</sup> Thus, SO coupling should be most pronounced when an electron is in an orbital which has a high probability of being near a nucleus of high atomic number. Electronic dipole transitions between states of different multiplicity are strictly forbidden. Since it is required only that the total angular momentum be conserved, transitions between states of different multiplicity can occur, provided that the spin and orbital angular

momentum are coupled.<sup>45</sup> The result of SO coupling is that singlet and triplet states which are mixed are no longer pure singlet or triplet states but are contaminated with some triplet and some singlet state character. The wavefunction which results from SO coupling,  $\Psi_{SO}$ , contains a term which is inversely proportional to the difference in energy between the triplet and singlet states mixed.<sup>46</sup> Thus, the effectiveness of SO coupling due to a given heavy atom perturber will depend on this energy difference as well as on the value of  $\xi$ .

$\xi$  for a molecule may be roughly approximated by summing the values for all atoms in the molecule.<sup>9</sup> The results of the first order perturbation treatment by McClure predicted that  $\tau_p \xi^2 = \text{constant}$ . Since  $\xi$  is squared, and, since  $\xi$  for carbon is only  $28 \text{ cm}^{-1}$  and much less for hydrogen,  $\xi$  for the molecule was taken to be the same as for the perturbing halogen. This prediction, despite the approximations involved, was borne out quite well within either the  $\alpha$ - or the  $\beta$ -halonaphthalene series. Thus, McClure's conclusion that the transition observed was between singlet and triplet states based on the correlation between  $\tau_p$  and  $\xi$  is justified. Thus, increased transition probabilities between states of different multiplicities due to the presence of an atom of high atomic number have come to be referred to as "heavy atom effects" (HAE).

Based on McClure's findings, Kasha<sup>47</sup> explored the possibility of increased singlet to triplet absorption transition probabilities due to the presence of an external heavy atom (HA). In what deserves to be called a classic experiment, it was observed that a yellow color was instantly produced upon mixing two colorless liquids,

$\alpha$ -chloronaphthalene and ethyl iodide. Spectroscopic examination showed that the yellow color was due to enhanced  $S_0 \rightarrow T$  absorption. Investigation of the effect of ethyl iodide on the other  $\alpha$ -halonaphthalenes (Br and I) showed that the enhancement of  $S_0 \rightarrow T_1$  absorption was also a function of the internal halogen, the enhancement following the order  $-\text{Cl} < -\text{Br} < -\text{I}$ .

Based on the findings of McClure and Kasha, it is to be expected, in general, that the presence of either inter- or intramolecular HAE should increase the transition probability for any singlet-triplet interconversion process:  $k_{isc}$ ,  $k_{dt}$ ,  $k_p$ , and  $I_{st}$  (rate of  $S_0 \rightarrow T$  absorption). This has generally been found to be the case.

The following kinds of changes are characteristic of inter- or intramolecular heavy atom perturbation: 1)  $\phi_p/\phi_f$  increases, 2)  $\phi_p$  may increase; 3)  $\tau_p$  invariably decreases, and 4) the integrated intensity of  $S_0 \rightarrow T$  absorption increases.<sup>48</sup> Observation of increased  $S_0 \rightarrow T$  absorptivity is the most unambiguous demonstration of the operation of a HAE. These experiments are somewhat difficult to do, however, and a number of conditions must be met for the observation to be accepted as valid.<sup>49</sup> This has come to be regarded as an unambiguous method for establishing true 0-0 phosphorescence bands, since the 0-0 absorption and emission bands should occur at approximately the same frequency. Also, triplet energies can be determined for compounds which don't phosphoresce. Demonstration of HAE on  $k_{isc}$ ,  $k_p$ , and  $k_{dt}$  is more difficult, since their determination requires both quantum yield ( $\phi_f$ ,  $\phi_p$ ,  $\phi_{isc}$ ) and lifetime ( $\tau_f, \tau_p$ ) measurements. Investigations of HAE on these rate-constants based

on both quantum yields and lifetimes are few. Conclusions are often drawn on the basis of increases in  $\phi_p/\phi_f$  or solely on the basis of  $\tau_p$ . Since  $k_f$  is assumed not to be affected by the HAE,<sup>50</sup> and, since  $k_{ds}$  is assumed to be negligible for aromatic hydrocarbons,<sup>51</sup> an increase in  $\phi_p/\phi_f$  is interpreted to be due to an increase in  $k_{isc}$ . Since both radiationless and radiative decay from  $T_1$  are spin forbidden, the operation of a HAE can be concluded solely on the basis of a decrease in  $\tau_p$ . The relative susceptibilities of  $k_p$  and  $k_{dt}$  to the HAE are not known then; however, their relative susceptibilities have been determined in some cases without recourse to quantum yield determinations by determining relative HAE on protiated and deuterated analogs and making use of the supposition that  $k_{dt}$  is small for the deuterated analog.<sup>52</sup> Other studies have determined their relative susceptibilities by making use of electron spin resonance to directly monitor triplet state concentrations.<sup>53</sup> The relative susceptibility of  $k_p$  and  $k_{dt}$  to the HAE is of interest because phosphorescence involves coupling of the electronic field with the photon field while radiationless decay involves coupling of the electronic field with the phonon field. These processes are inherently different and might be expected to be affected differently.<sup>54</sup> There seems to be general agreement that  $k_p$  is generally more susceptible to the HAE than  $k_{dt}$ .<sup>55</sup> This is often assumed rather than demonstrated, however. The susceptibility of  $k_{isc}$  relative to  $k_p$  and  $k_{dt}$  is not as well known, since its unambiguous determination requires determination of  $\phi_f$ ,  $\phi_{isc}$ , and  $\tau_f$ . As noted above, two simplifying assumptions are frequently made, and an increase in



$k_{isc}$  is presumed based solely upon a decrease in  $\phi_f$  or increase in  $\phi_p/\phi_f$ . These observed changes in quantum yields could be accounted for by a decrease in  $k_f$ . Relatively little is known about how  $k_f$  is affected, since techniques for determining lifetimes in the nano-second range are relatively recent. Some authors have proposed "inverse HAE" to account for apparent decreases in  $k_{isc}$ .<sup>28b</sup> But these evaluations of  $k_{isc}$  were based on less than complete data and a decrease in  $k_{isc}$  could also be accounted for in terms of an increase in the energy separation between the singlet and triplet states involved. It has been shown, for instance, that for some aromatic hydrocarbons (e.g., perylene)  $\phi_f$  is decreased by neither internal nor external HAE.<sup>56</sup> It was shown that if  $k_{isc} < 10^2 k_f$ , there is no increase in  $k_{isc}$  due to presence of a heavy atom. It was concluded that if the energy gap between the singlet and triplet states is larger than 10 kK, that there will be no quenching of fluorescence by either internal or external heavy atoms. For naphthalene,  $T_2$  is close in energy to  $S_1$  and it is thought that intersystem crossing is via  $T_2$ , not directly to  $T_1$ .<sup>57</sup> Therefore,  $k_{isc}$  for naphthalene may be sensitive to changes in energy levels due to substitution and consequent changes in solvation.

This investigation may add to what is known about the relative susceptibilities of  $k_f$ ,  $k_{isc}$ ,  $k_p$ , and  $k_{dt}$  to external perturbors since both quantum yields and lifetimes have been determined with the exception of  $\phi_{isc}$  (see introduction section on excited state processes). It is possible, however, that there is no general order of relative susceptibilities to external perturbors. The

relative susceptibilities may depend upon both the chromophore and the perturber.

The interpretation of enhanced transition probabilities between states of different multiplicity in the presence of a heavy atom is universally accepted as being due to enhanced SO coupling. Thus "HAE" has come to be used as a synonym for "SO coupling". There has, however, been considerable controversy over the mechanism of SO coupling for inter- and intramolecular HA perturbation. One issue is the identity of the perturbing singlet state, i.e., whether it is one or more singlet states of the chromophore, whether it is an excited singlet state of the heavy atom,<sup>13</sup> or whether it is a singlet charge transfer state of a molecule-perturber complex.<sup>68</sup> On the basis of complete depolarization of phosphorescence in heavy atom containing glass (vide infra), Kearns<sup>14</sup> concluded that the perturbing singlet state could not be one of the chromophore and, therefore, must be a singlet state of the heavy atom.<sup>57</sup>

Another issue is whether the interaction is best described theoretically in charge transfer (CT) terms or in exchange terms. McGlynn<sup>58</sup> points out that it is difficult to make a choice between these descriptions on theoretical grounds, but prefers a CT description, based on what are thought to be various, experimental indications of CT complexes. There is disagreement, however, based on the insensitivity of  $T_1 \leftrightarrow S_0$  frequencies to solvent effects.<sup>59</sup> This finding is countered by McGlynn on the basis of his own results. McGlynn had found that the 0-0 phosphorescence band of naphthalene in propyl halide glasses was red shifted relative to the frequency of the

0-0 band in EPA (ether-isopentane-alcohol (5:5:2, v/v) by the following amounts:  $55\text{ cm}^{-1}$  (propyl chloride),  $155\text{ cm}^{-1}$  (propyl bromide), and  $325\text{ cm}^{-1}$  (propyl iodide). McGlynn<sup>13</sup> noted that the difference in  $\text{cm}^{-1}$  in going from propyl bromide to propyl iodide was larger than difference in going from propyl chloride to propyl bromide. He also noted that the decrease in  $\tau_p$  (or increase in  $S_0 \rightarrow T$  absorptivity) was larger in going from propyl chloride to propyl bromide than in going from propyl bromide to propyl iodide. McGlynn concludes that the spin-orbital coupling interaction between naphthalene and the propyl halide medium cannot be primarily responsible for the observed red shifts, since, if it was, one would expect to see a correspondence between the cases where the largest increase in red shift is produced and where there is the largest increase in SO coupling (as evidenced by largest decrease in  $\tau_p$  or increase in  $S_0 \rightarrow T$  absorptivity). Since SO coupling can't be primarily responsible for the red shifts, something else must be. This something else could be any perturbing singlet state higher in energy than the triplet state. McGlynn notes that, while it could be a CT singlet state, the results warrant only that it is some singlet state higher in energy than the triplet. The observed red shifts are used to favor CT interactions as the dominant effect because of the presumed insensitivity of the  $T_1 \leftrightarrow S_0$  frequency to solvent effects by an exchange mechanism.

While McGlynn is of the opinion that CT complexes are required for an external HAE, Kearns<sup>14</sup> counters with evidence (vide infra) that CT complexes aren't essential at all. The results of the present investigation may have some bearing on the importance of CT

complexes to the external HAE.

The issue concerning the external HAE on which this investigation will have the largest bearing is the directional dependence of the effect. That there is such a dependence and that an aromatic hydrocarbon is most susceptible to external perturbation in the vicinity of the  $\pi$ -face is suggested but not experimentally proven by previous investigations. By monitoring the optical density for  $S_0 \rightarrow T$  absorption and the refractive index of mixtures of  $\alpha$ -chloronaphthalene and ethyl iodide, McGlynn<sup>60</sup> was able to show evidence for at least weak complexes (stabilization energy of about 0.6 kcal, equilibrium constant approximately 0). The stoichiometry of the complex was 1:1, though the existence of other stoichiometries were evident but much less preponderant. McGlynn<sup>13</sup> found, however, that phosphorescence decay curves for solutes in alkyl halide glasses could only be reproduced analytically by a sum of several first order single exponential decays. This fact was interpreted as an indication that the conformation of the complex could vary widely about some most probable configuration. Evidence for a 1:1 complex was used to favor a CT mechanism rather than exchange, since, it was contended, an exchange mechanism would not require such specific interaction.<sup>58</sup> It does not seem, however, that McGlynn's interpretations of either the room temperature data or of the multiexponential decay character in a glass are interpretations required by the data. The seeming preponderance of a 1:1 complex at room temperature could also be accounted for by many different interaction geometries which all give rise to about the same effect. A heavy

atom anywhere in the vicinity of the  $\pi$ -face might have a large effect. Furthermore, interpretation of the multiexponential decay character in terms of conformational variation around some most probable configuration is not consistent with Kearns'<sup>14</sup> finding that there is complete depolarization of the phosphorescence of aromatic hydrocarbons (including naphthalene) in ethyl iodide-EPA glasses at 77 K, since, according to Kearns, complete depolarization requires a completely random distribution of perturbers. Also, while Kearns<sup>14</sup> observed multiexponential phosphorescence decay character from solutes in heavy atom glasses, he observed single exponential decay for naphthalene in crystals of polyhalobenzenes. Furthermore, Kearns<sup>14</sup> observed that naphthalene was more perturbed in crystals of *p*-dibromo- and sym-tetrabromobenzene ( $\tau_p \approx 33$  msec), compounds which don't form strong CT complexes with naphthalene, than it was in a strong CT complex with tetrabromophthalic anhydride ( $\tau_p \approx 390$  msec). While the shorter naphthalene lifetime in the crystals is probably in part due to the higher number of bromines around the naphthalene, the comparison is sufficiently accurate to show that the presence of low-lying CT states in the naphthalene-tetrabromophthalic anhydride complex has not enhanced the magnitude of the external HAE relative to external heavy atom perturbers which contain the same heavy atoms but which do not form CT complexes.

Other arguments by McGlynn in favor of the mediation of CT states in the external HAE are based on the similarities in  $\phi_f/\phi_p$  and  $\tau_p$  behavior for CT complexes to those produced by external heavy atoms.<sup>61</sup> For the sym-trinitrobenzene complex of anthracene, for

example,  $\tau_p$  decreases and  $\phi_p$  increases relative to uncomplexed anthracene. Examples of a wide variety of CT complexes for which  $\tau_p$  decreases by an order of magnitude are cited. It is also noted that  $\phi_p/\phi_f$  increases for some of these CT complexes which don't contain any heavy atoms. Enhancement of  $S_0 \rightarrow T$  absorptivity due to oxygen is also noted and mediation of CT complexes invoked.

While it may very well be true that CT states can enhance SO coupling in a molecule, it cannot be concluded from this that the external HAE also involves CT states. HAEs and effects produced by CT complexation may be similar because they both promote SO coupling, and, therefore, lead to enhanced transition probabilities for spin-forbidden processes. However, the basis for SO coupling induced by a heavy atom is the high nuclear charge of the heavy atom. While the effect of this high nuclear charge must in some way be mediated to the perturbed species, it is not at all clear that an interaction as strong as a CT interaction need be invoked to accomplish the mediation. While the external HAE certainly involves some distance dependence,<sup>62</sup> it is not known experimentally what this dependence is. But  $\pi$  orbitals extend further than the van der Waals radius of a molecule (theoretically, indefinitely), so an exchange mechanism is reasonable. It cannot be assumed that because heavy atoms produce effects similar to those produced by other kinds of perturbations that, therefore, the mechanism of the interaction is the same in all cases. Oxygen is paramagnetic, and formation of a CT complex has to be admitted to be a rather gross perturbation of a chromophore. A whole new set of states is produced in a CT complex.

These are evidenced by the appearance of broad characterless absorption and emission bands.<sup>63</sup> Thus, this investigator finds it difficult to accept McGlynn's arguments for mediation of the external HAE by CT states based on the similarity of effects observed for heavy atoms, paramagnetic species, and CT complexes.

Kearns<sup>14</sup> attempted an investigation of the distance dependence of the external HAE by making use of known crystal structure data. He was not able to find any correlation between the distance of the heavy atom to an arbitrary reference point and the effectiveness of the crystal as a perturber. It was concluded that relative orientations must be important for the external HAE.

Berlman's<sup>42</sup> work also suggests that relative orientations are important for the external HAE. From measurements of  $\phi_f$  in benzene and in bromobenzene, it was found that phenyl substituents on naphthalene and anthracene reduced the efficiency of quenching by bromobenzene relative to the unsubstituted system. The reduced efficiency was explained in terms of reduced perturbation of energy transfer to bromobenzene (due to red shift induced by phenyl groups) and in terms of steric hindrance of approach to the external heavy atom due to steric hindrance by the noncoplanar phenyl groups. Also, it was noted that planar aromatic hydrocarbons which are susceptible to heavy atom quenching are also susceptible to concentration quenching (anthracene) or excimer formation (naphthalene). The quenching was interpreted as collisional in nature and the steric hindrance as evidence that the collisional quenching was short range in nature and involved a close encounter between the  $\pi$ -system and the quencher. The close encounter was viewed as involving overlap of a p orbital

of the halogen with a  $\pi$  orbital of the chromophore. While the interpretation of reduced quenching efficiency as partially due to steric hindrance seems to be warranted, the more detailed analysis of the data seems not to be warranted. As McGlynn<sup>13</sup> has pointed out, the external HAE does not require collisions, since his work has demonstrated that the external HAE at room temperature (evidence from increased  $S_0 \rightarrow T$  absorptivity) is the same as the external HAE in heavy atom glasses at 77 K (evidence from  $\tau_p$ ) (vide infra). Furthermore, no evidence beyond the steric inhibition of quenching was advanced to warrant the analysis of the close encounter thought to be necessary. The indications of steric inhibition do seem to indicate that aromatic hydrocarbons are most susceptible to external HAE in the vicinity of the  $\pi$ -face. The strength of the evidence alone, however, would not preclude the possibility that aromatic hydrocarbons are most susceptible to the external HAE in the nodal plane. Investigation of the external HAE of ethyl bromide on naphthalene and crowns 1, 2, and 3 will provide a means of systematically blocking approach of an external heavy atom to the naphthalene chromophore from a variety of directions.

Internal and external HAE have been compared in a variety of ways. Based on the following experiments, it was concluded by McGlynn<sup>13</sup> that they are similar, though judgment on the generality of the conclusion was reserved.  $\tau_p$  and phosphorescence spectra were determined for each of the  $\alpha$ -halonaphthalenes (-F, -Cl, -Br, -I) in each of the following solvents: EPA, propyl chloride, propyl bromide, and propyl iodide. The triplet decays were all non-single exponential, so



"first half-lives" were reported. It was found that  $(\xi_I + \xi_E)^2 \tau_p$  was roughly constant within a range of  $10^2$ .  $\xi_I$  is the SO coupling parameter for the internal halogen and  $\xi_E$  is the SO coupling parameter for the external halogen. It was noted, however, that there were regular variations in  $(\xi_I^2 + \xi_E^2) \tau_p$ .  $(\xi_I + \xi_E)^2 \tau_p$  increases as  $\xi_E$  increases ( $\xi_I$  constant) and  $(\xi_I + \xi_E)^2 \tau_p$  decreases as  $\xi_I$  increases ( $\xi_E$  constant). It was suggested that these variations might be accounted for in terms of 1) a larger effect of  $\xi_E$  on  $k_p$  than  $k_{dt}$  (would explain increase in  $(\xi_I + \xi_E)^2 \tau_p$  as  $\xi_E$  increases) and/or 2) lack of constancy of overlap factors in the integral  $(\phi_0^T \hat{H}_{SO} \phi_0^{sp})$ , where  $\phi_0^T$  is the zeroth order triplet wavefunction,  $\hat{H}_{SO}$  is the SO coupling Hamiltonian, and  $\phi_0^{sp}$  is the zeroth order perturbing singlet wavefunction. An alternative explanation is that  $k_{dt}$  and/or  $k_p$  are less susceptible to  $\xi_E$  than  $\xi_I$ .

Increases in  $S_0 \rightarrow T$  absorptivity for the  $\alpha$ -halonaphthalenes at room temperature due to propyl iodide perturbation were also determined.<sup>13</sup> A remarkable parallel was found between the increases in  $S_0 \rightarrow T_1$  absorptivity and the decreases in  $\tau_p$  due to propyl iodide perturbation. In both cases, as  $\xi_I$  increases, the ratio of the external to the internal effect decreases.

Based on the results of alkyl halide perturbation of the  $S_0 \rightarrow T$  absorptivity of naphthalene, McGlynn<sup>13</sup> also suggested that external SO coupling will be greatest when the internal SO coupling is greatest. Patterson<sup>19</sup> tested this suggestion by determining the rate constant for quenching ( $k_q$ ) of nine aromatic hydrocarbons by cesium chloride in methanol. A log-log plot of  $k_q$  vs  $k_{isc}$  showed

a reasonably good linear correlation between increases in  $\log k_q$  and  $\log k_{isc}$  ( $k_{isc}$  provides a measure of the inherent SO coupling between  $S_1$  and the triplet to which intersystem crossing occurs). (Linear log-log plots of rate constants for spin-forbidden processes vs  $\xi^2$  for internal and external HAE have been reported.)<sup>64</sup>

The investigation reported herein will provide a somewhat different test for the ratio of external to internal perturbation as a function of increasing  $\xi_1$ . Perturbation of crowns  $\bar{1}$ ,  $\bar{2}$ , and  $\bar{3}$  containing light and heavy cations by ethyl bromide was investigated. Since complexed cations are really external perturbers, the investigation is more appropriately described as a test of the effect of an external perturber as a function of the SO perturbation already present due to a complexed external perturber.

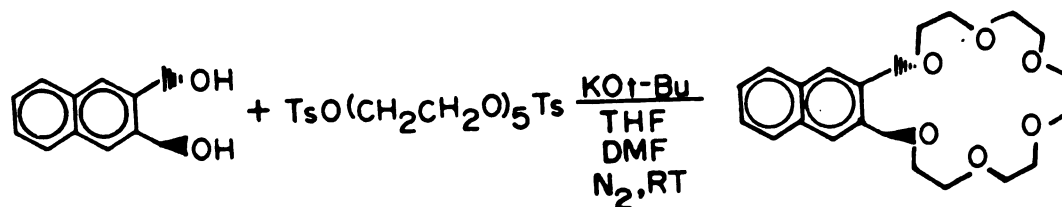
Internal and external HAE have been investigated spectroscopically by Coulson and Gash.<sup>40</sup> The phosphorescence and  $T_1$  absorption spectra of naphthalene in p-dihalogenated benzene host crystals at 4.2 K were determined and found to be composed of only totally symmetric vibrational modes. The phosphorescence spectrum of naphthalene in perdeutereonaphthalene is composed of non-totally symmetric as well as totally symmetric modes. From the fact that only totally symmetric modes are enhanced by externally induced SO coupling, it is concluded that the external HAE is purely electronic in nature. The internal HAE, however, is shown to enhance the totally symmetric modes of the parent naphthalene and to vibronically enhance out-of-plane halogen modes. This is viewed as being reasonable, since out-of-plane modes probably enhance the totally symmetric modes

of the parent naphthalene and to vibronically enhance out-of-plane halogen modes. The out-of-plane modes for naphthalene are of only moderate intensity. The same conclusion was reached by El-Sayed and Pavlopoulos<sup>65</sup> based on phosphorescence polarization measurements on naphthalene and naphthalene derivatives at 77 K.

## RESULTS<sup>66</sup>

### Synthesis

2,3-Naphtho-20-crown-6 (1) and 1,8-naphtho-21-crown-6 (2) were synthesized by room temperature reaction of the appropriate bis-(hydroxymethyl)-naphthalene and pentaethyleneglycol ditosylate in tetrahydrofuran dimethylformamide (9:1) with potassium t-butoxide used as



base. Isolated yields of 1 and 2 following careful alumina chromatography and crystallization from ether-pentane averaged 16% and 8%, respectively. 1,5-Naphtho-22-crown-6 (3) was synthesized by reaction of 1,5-bis-(bromomethyl)naphthalene with pentaethylene glycol in tetrahydrofuran with potassium t-butoxide present as base.<sup>1</sup> 3 was isolated in 14% yield after careful alumina chromatography and repeated recrystallization from ether-pentane and then cyclohexane. The 2,3-, 1,8-, and 1,5-bis-(methoxymethyl)naphthalenes (4, 6, and 8, respectively) were also prepared by a Williamson ether synthesis using the bis-(hydroxymethyl)naphthalenes and methyl iodide in the case of

4 and 6 and the bis-(bromomethylnaphthalene and sodium methoxide in the case of 8).

The alkyl ammonium chloride salts were obtained by passing gaseous hydrochloric acid through an ethereal solution of the parent amine. The iodo- and bromoalkylammonium chloride salts were prepared from the corresponding iodide and bromide salts via anion exchange. 3-Iodopropylamine hydrochloride was obtained from treatment of 3-bromopropylamine hydrobromide with excess sodium iodide in acetone at room temperature.

#### Ultraviolet Absorption Spectra

The following general comments apply to Figures 1 through 18. The 77 K ultraviolet (UV) absorption spectra were recorded on samples in either 95% ethanol-methanol (4:1, v/v) or ethanol-methanol (4:1, v/v) uncracked glasses (methanol added to prevent cracking). For spectra of crown complexes, sufficient salt (as determined from quantum yield titrations, vide infra) is present to assure that absorption is essentially from only complexed crown. The spectral shapes and intensities of Figures 1 through 18 are reproducible with a given tube and dewar (see Experimental), and the relative intensities at a given wavelength are meaningful, but the relative intensities at two different wavelengths are somewhat distorted from what the true relative intensities would be, due to the use of non-identical reference sample (a nitrogen purged atmosphere was used as the reference). Salt and substituent induced changes in the energies and intensities of absorption peaks are evident and will

Figure 1. 77 K UV spectra of 2,3-disubstituted naphthalenes in 95% ethanol-methanol (4:1, v/v) glass. See figure legend. Intensities are given in terms of relative absorbancies (see text for explanation). Relative absorbancies for shorter wavelength region are given by the scale on the left; for longer wavelength region, by scale on the right. Concentrations (at room temperature) were  $4.00 \times 10^{-4}$  M for longer wavelength region and  $1.20 \times 10^{-4}$  M for shorter wavelength region (except for naphthalene,  $1.00 \times 10^{-4}$  M). The scales have been adjusted so that the absorbancies, of both sections, after multiplication if necessary by the factors given in the figure legend, are those of a  $8.00 \times 10^{-5}$  M solution. Curve A, 2,3-naphtho-20-crown-6 ( $\frac{1}{\lambda}$ ); curve B, 2,3-bis-(methoxymethyl) naphthalene ( $\frac{4}{\lambda}$ ); curve C, 2,3-dimethylnaphthalene ( $\frac{5}{\lambda}$ ); curve D, naphthalene ( $\frac{10}{\lambda}$ ).

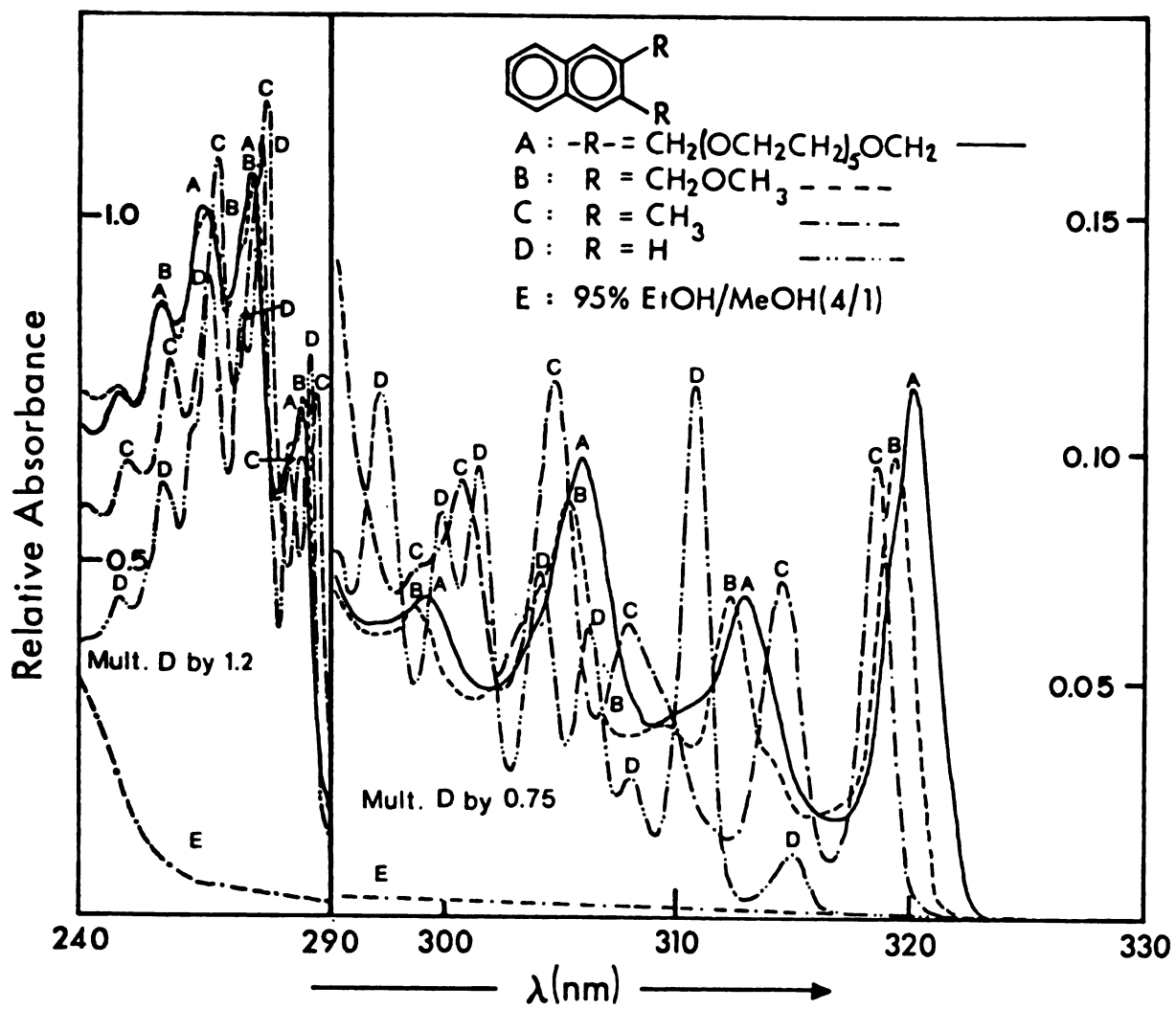


Figure 1

Figure 2. 77 K UV spectra of 1,8-disubstituted naphthalenes in 95% ethanol-methanol (4:1, v/v) glass. Intensities are given in terms of relative absorbancies (see text for explanation). Relative absorbancies for shorter wavelength region are given by the scale on the left; for longer wavelength region, by the scale on the right. Concentrations (at room temperature) were  $4.00 \times 10^{-4}$  M for longer wavelength region and  $8.00 \times 10^{-5}$  M for shorter wavelength region (except for naphthalene,  $1.00 \times 10^{-4}$  M). The scales have been adjusted so that the absorbancies of both sections, after multiplication if necessary by the factors given in the figure legend, are those of a  $8.00 \times 10^{-5}$  M solution. Curve A, 1,8-naphtho-21-crown-6 (2); curve B, 1,8-bis-(methoxymethyl)naphthalene (6); curve C, 1,8-dimethylnaphthalene (7); curve D, naphthalene (10).



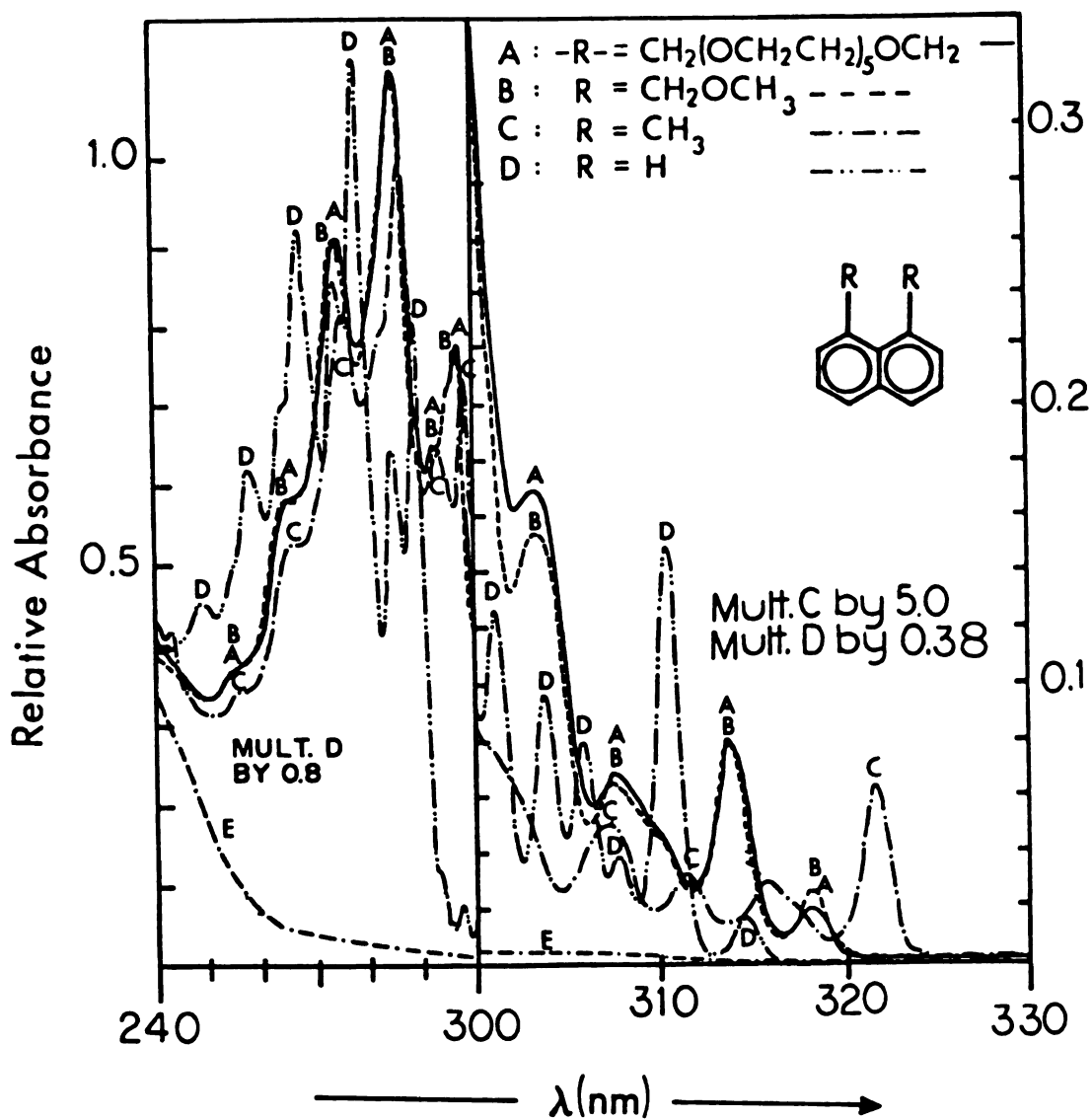


Figure 2

Figure 3. 77 K UV spectra of 1,5-disubstituted naphthalenes in ethanol-methanol (4:1, v/v) glass. See figure legend. Intensities are given in terms of relative absorbancies (see text for explanation). Relative absorbancies for shorter wavelength region are given by the scale on the left; for the longer wavelength region, by the scale on the right. Concentrations (at room temperature) were  $2.00 \times 10^{-4}$  M for the longer wavelength region and  $6.00 \times 10^{-5}$  M for the shorter wavelength region. The scales have been adjusted so that the absorbancies of both sections are those of a  $6.00 \times 10^{-5}$  M solution. Curve A, 1,5-naphtho-22-crown-6 (3); curve B, 1,5-bis-(methoxymethyl)naphthalene (8); curve C, 1,5-dimethylnaphthalene (9); curve D, naphthalene (10).

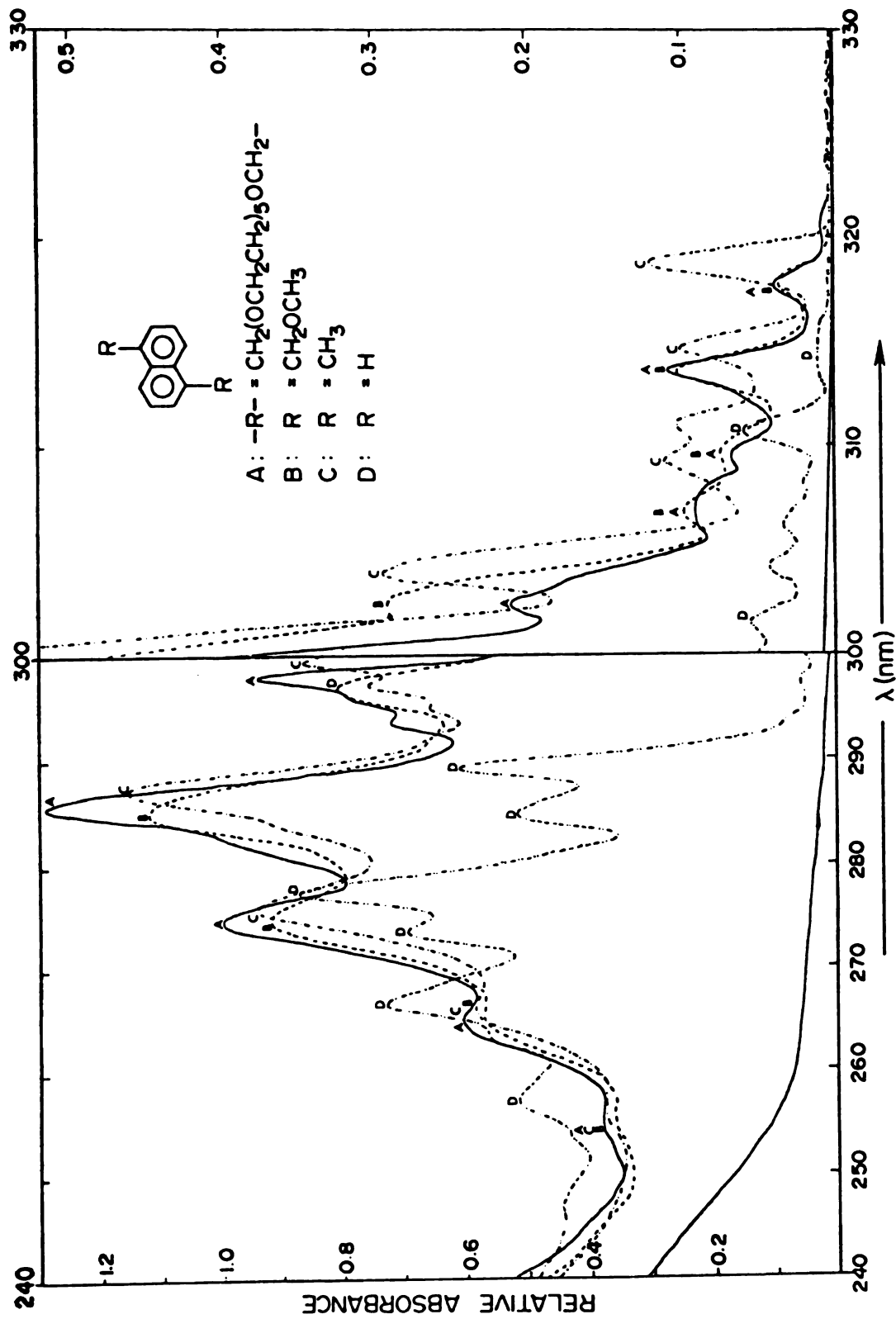


Figure 3

Figure 4. 77 K UV spectra of 2,3-naphtho-20-crown-6 (1) alone and with 5:1 added molar excesses of alkali metal chlorides in 95% ethanol-methanol (4:1, v/v) glass. See figure legend. Intensities are given in terms of relative absorbancies (see text for explanation). Relative absorbancies for shorter wavelength region are given by the scale on the left; for longer wavelength region, by scale on right. Crown concentrations (at room temperature) were  $4.00 \times 10^{-4}$  M for longer wavelength region and  $1.20 \times 10^{-4}$  M for shorter wavelength region. The scales have been adjusted so that the absorbancies of both sections are those of a  $1.20 \times 10^{-4}$  M solution.

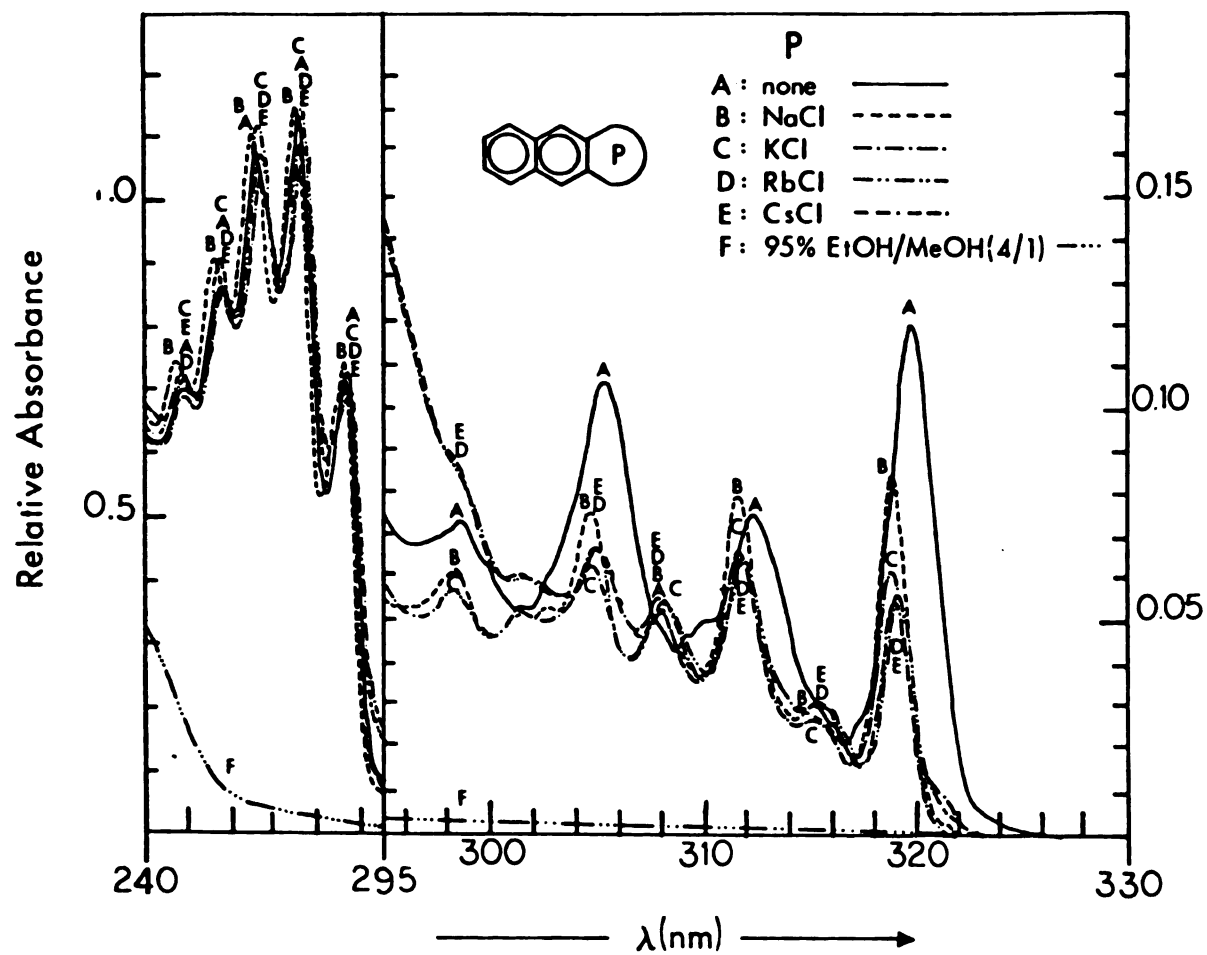


Figure 4

Figure 5. 77 K UV spectra of 1,8-naphtho-21-crown-6 (2) alone and with 5:1 added molar excesses of alkali metal chlorides in 95% ethanol-methanol (4:1, v/v) glass. See figure legend. Intensities are given in terms of relative absorbancies (see text for explanation). Relative absorbancies for shorter wavelength region are given by the scale on the left; for longer wavelength region, by scale on right. Crown concentrations (at room temperature) were  $4.00 \times 10^{-4}$  M for longer wavelength region and  $8.00 \times 10^{-5}$  M for shorter wavelength region. The scales have been adjusted so that the absorbancies of both sections are those of a  $8.00 \times 10^{-5}$  M solution.

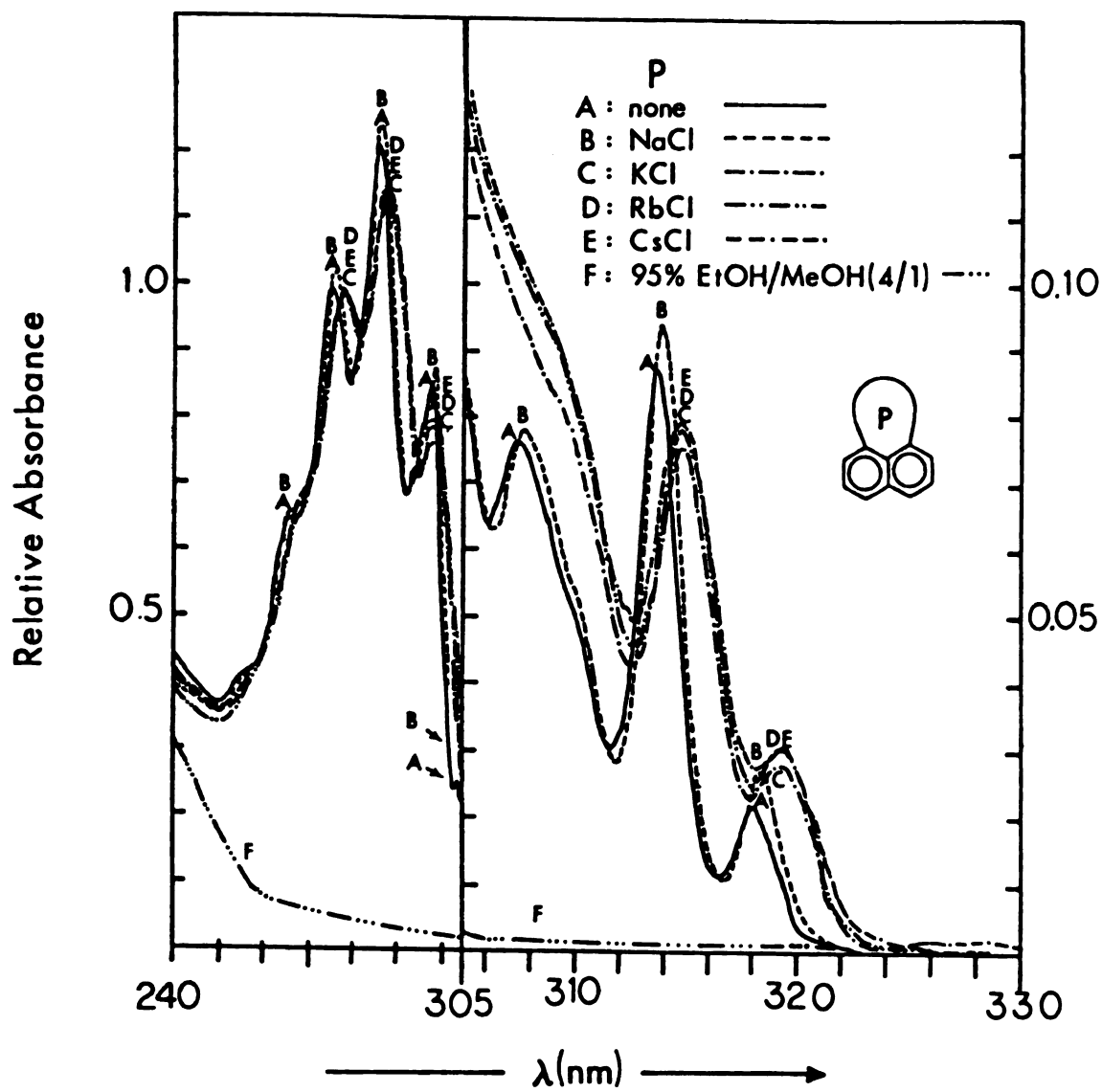


Figure 5

Figure 6. 77 K UV spectra of 1,5-naphtho-22-crown-6 (3) alone and with 5:1 added molar excesses of alkali metal chlorides in 95% ethanol-methanol (4:1, v/v) glass. See figure legend. Intensities are given in terms of relative absorbancies (see text for explanation). Relative absorbancies for shorter wavelength region are given by the scale on the left; for longer wavelength region, by scale on right. Crown concentrations were  $2.00 \times 10^{-4}$  M for longer wavelength region and  $6.00 \times 10^{-5}$  M for shorter wavelength region. The scales have been adjusted so that the absorbancies of both sections are those of a  $6.00 \times 10^{-5}$  M solution.



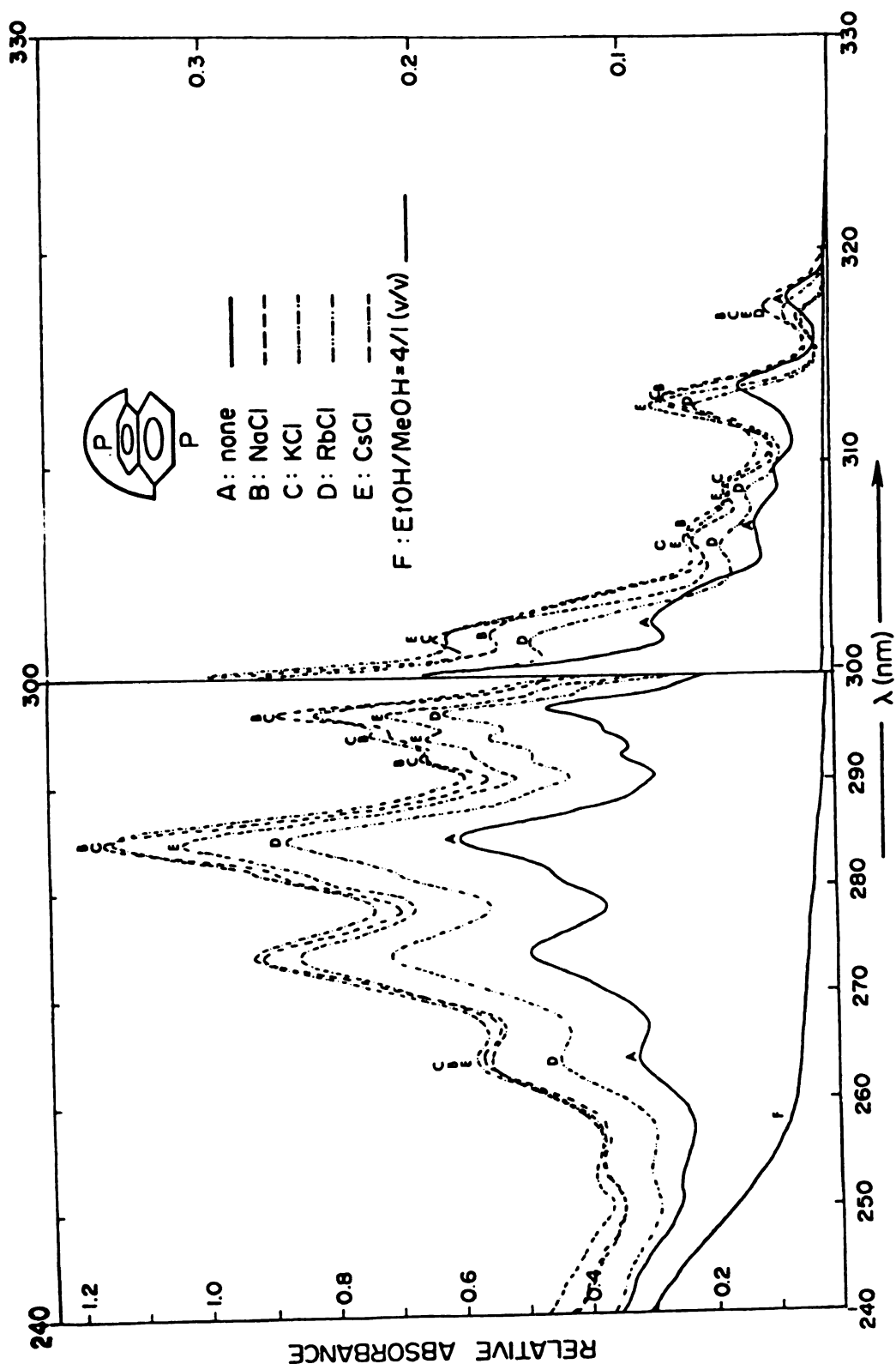


Figure 6

Figure 7. 77 K UV spectra of 2,3-naphtho-20-crown-6 (1) alone and with 5:1 added molar excess of ammonium and alkylammonium chlorides in 95% ethanol-methanol (4:1, v/v) glass. See figure legend. Intensities are given in terms of relative absorbancies (see text for explanation). Relative absorbancies for shorter wavelength region are given by the scale on the left; for longer wavelength region, by scale on right. Crown concentrations (at room temperature) were  $4.00 \times 10^{-4}$  M for the longer wavelength region and  $1.20 \times 10^{-4}$  M for the shorter wavelength region. The scales have been adjusted so that the absorbancies of both sections are those of a  $1.20 \times 10^{-4}$  M solution.

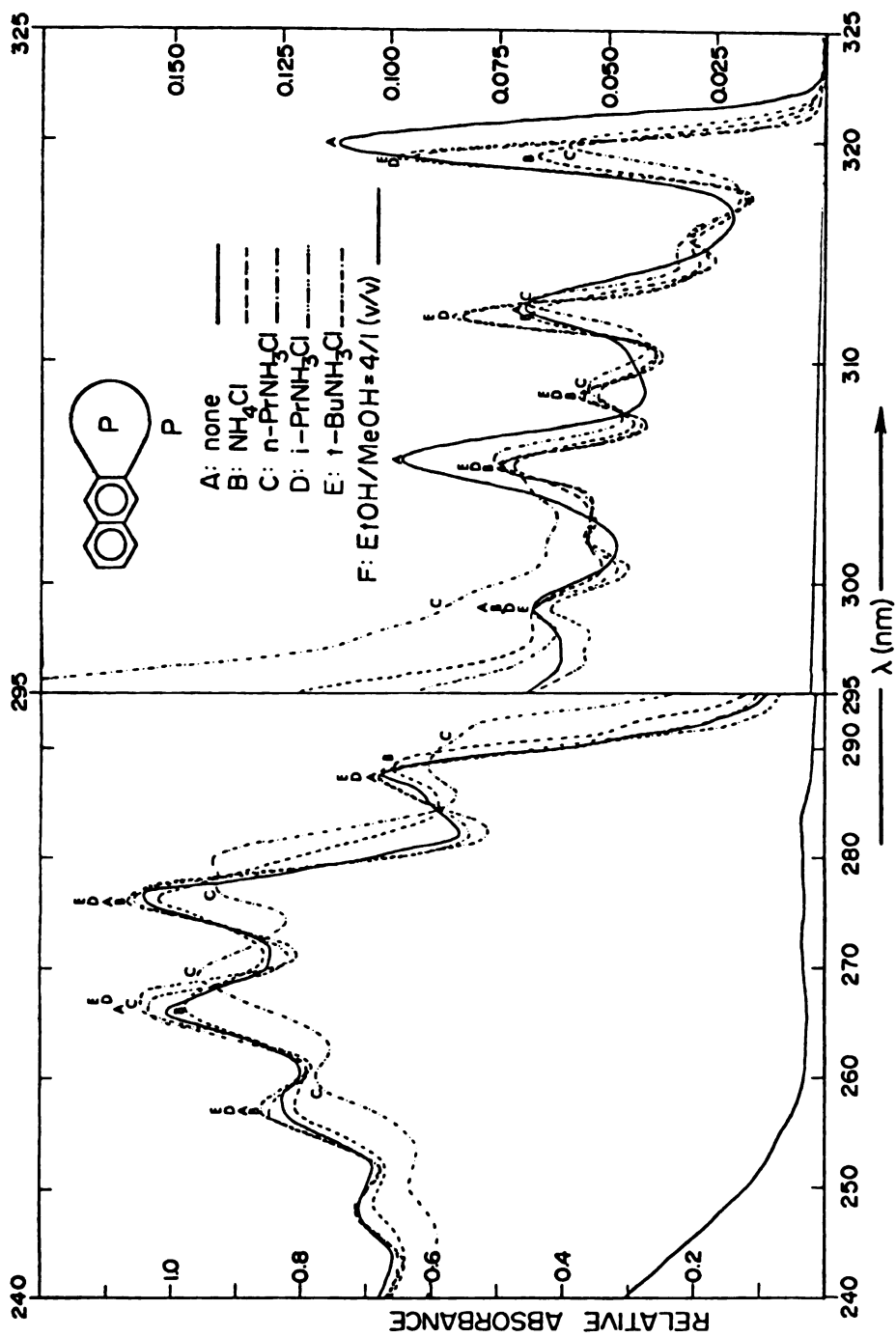


Figure 7

Figure 8. 77 K UV spectra of 1,8-naphtho-21-crown-6 ( $\lambda$ ) alone and with 5:1 added molar excess of ammonium and alkylammonium chlorides in 95% ethanolmethanol (4:1, v/v) glass. See figure legend. Intensities are given in terms of relative absorbancies (see text for explanation). Relative absorbancies for shorter wavelength region are given by scale on left; for longer wavelength region, by scale on right. Crown concentrations (at room temperature) were  $4.00 \times 10^{-4}$  M for the longer wavelength region and  $8.00 \times 10^{-5}$  M for the shorter wavelength region. The scales have been adjusted so that the absorbancies of both sections are those of a  $8.00 \times 10^{-5}$  M solution.

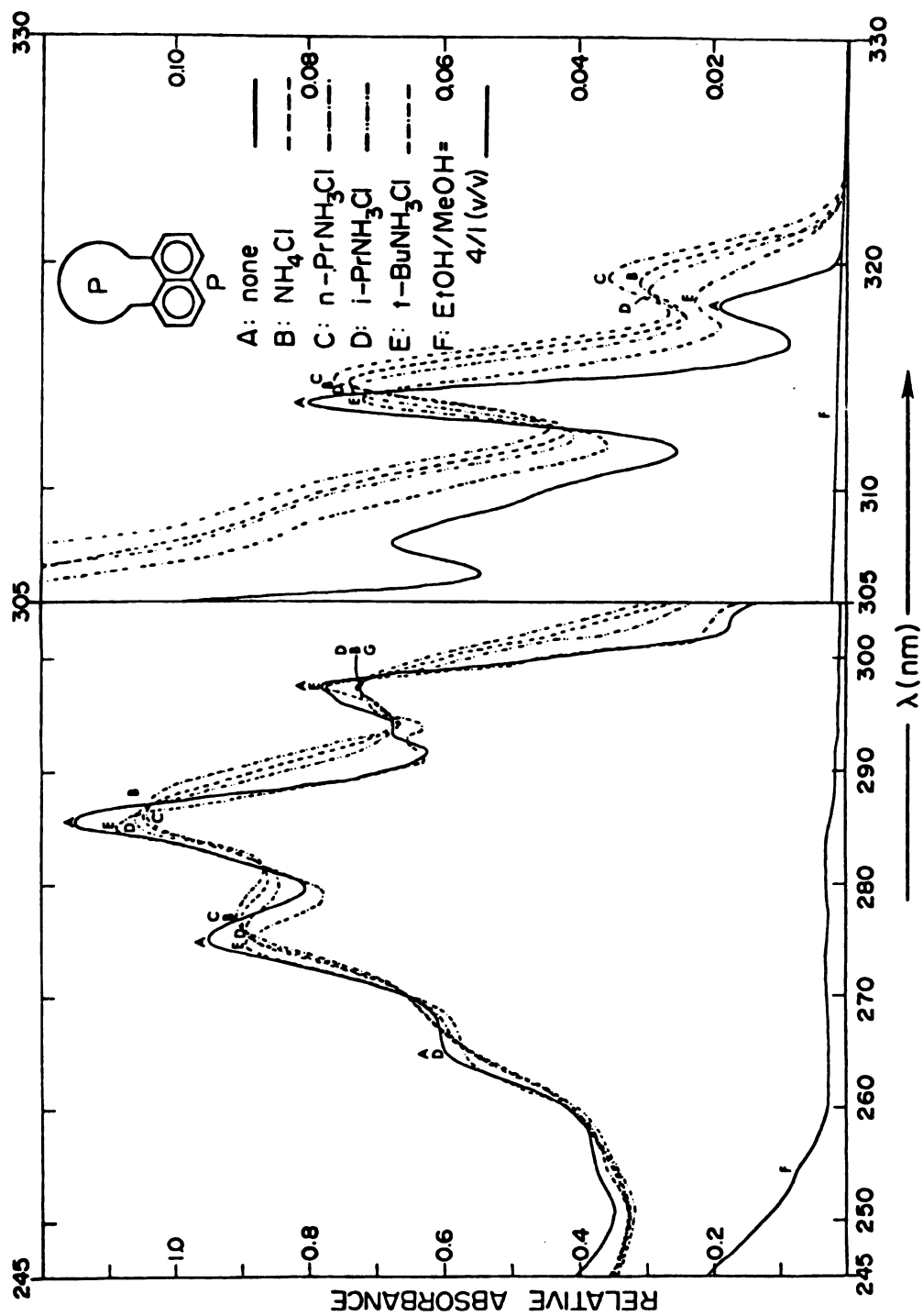


Figure 8

Figure 9. 77 K UV spectra of 1,5-naphtho-22-crown-6 (3) alone and with 100:1 molar excesses of ammonium and n-propylammonium chlorides in ethanol-methanol (4:1, v/v) glass. See figure legend. Intensities are given in terms of relative absorbancies (see text for explanation). Relative absorbancies for shorter wavelength region are given by the scale on the left; for longer wavelength region, by scale on right. Crown concentrations (at room temperature) were  $1.00 \times 10^{-4}$  M for the longer wavelength region and  $5.00 \times 10^{-5}$  M for the shorter wavelength region. The scales have been adjusted so that the absorbancies of both sections are those of a  $5.00 \times 10^{-5}$  M solution.

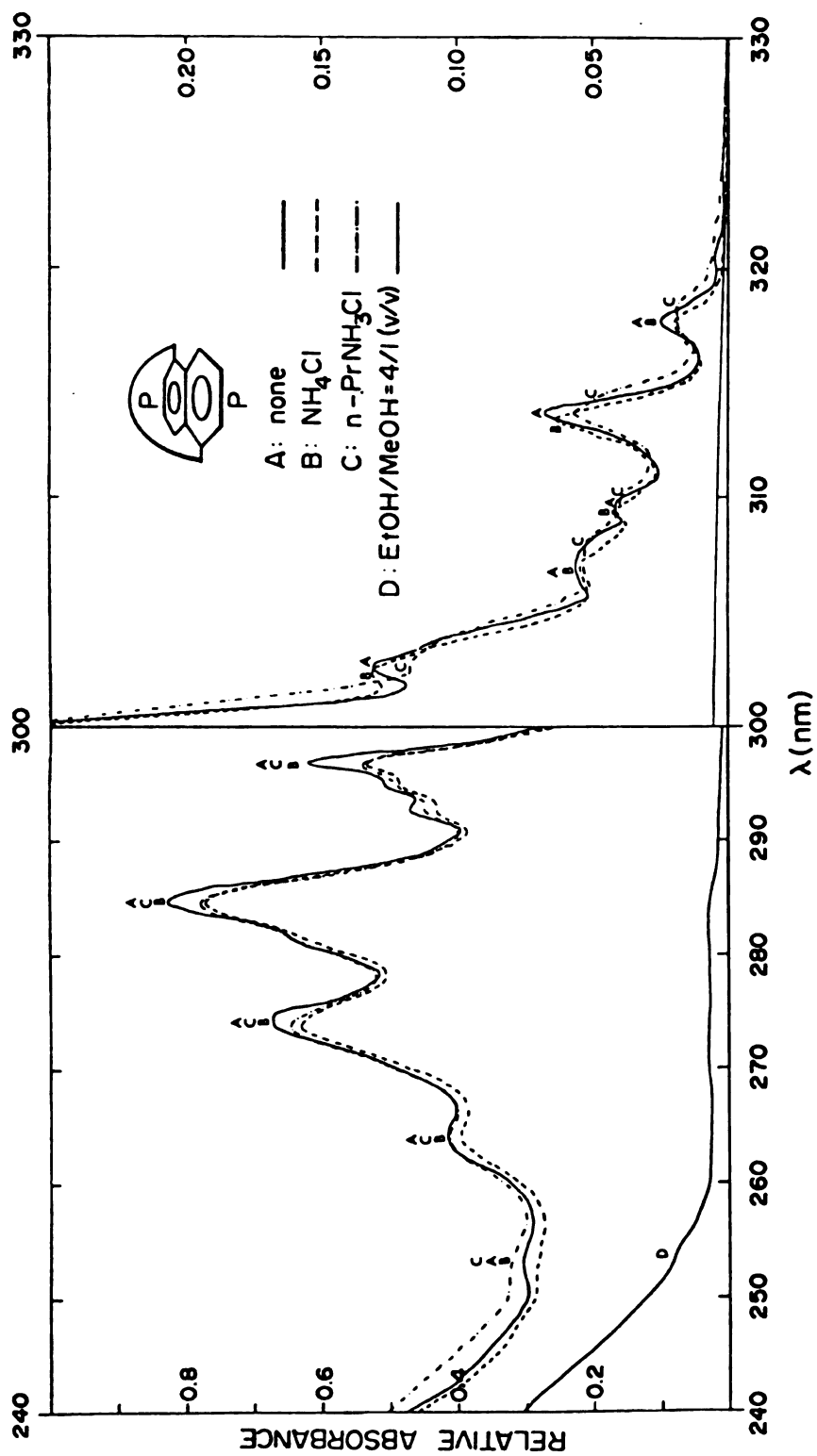


Figure 9

Figure 10. 77 K UV spectra of 2,3-naphtho-20-crown-6 (1) alone and with 5:1 added molar excess of bromoalkylammonium chlorides in 95% ethanol-methanol (4:1, v/v) glass and with 12.5:1 added molar excess of iodalkylammonium chlorides in ethanol-methanol (4:1, v/v) glass. See figure legend. Intensities are given in terms of relative absorbancies (see text for explanation). Relative absorbancies for the shorter wavelength region are given by the scale on the left; for longer wavelength region, by scale on right. The concentration (at room temperature) of crown was  $4.00 \times 10^{-4}$  M for the longer wavelength region and  $8.00 \times 10^{-5}$  M for the shorter wavelength region. The scales have been adjusted so that the absorbancies of both sections are those of  $8.00 \times 10^{-5}$  M solutions. Baselines: curve F,  $\beta$ -iodoethylammonium chloride; curve G,  $\gamma$ -iodopropylammonium chloride; curve H, 95% ethanol-methanol (4:1, v/v) glass.



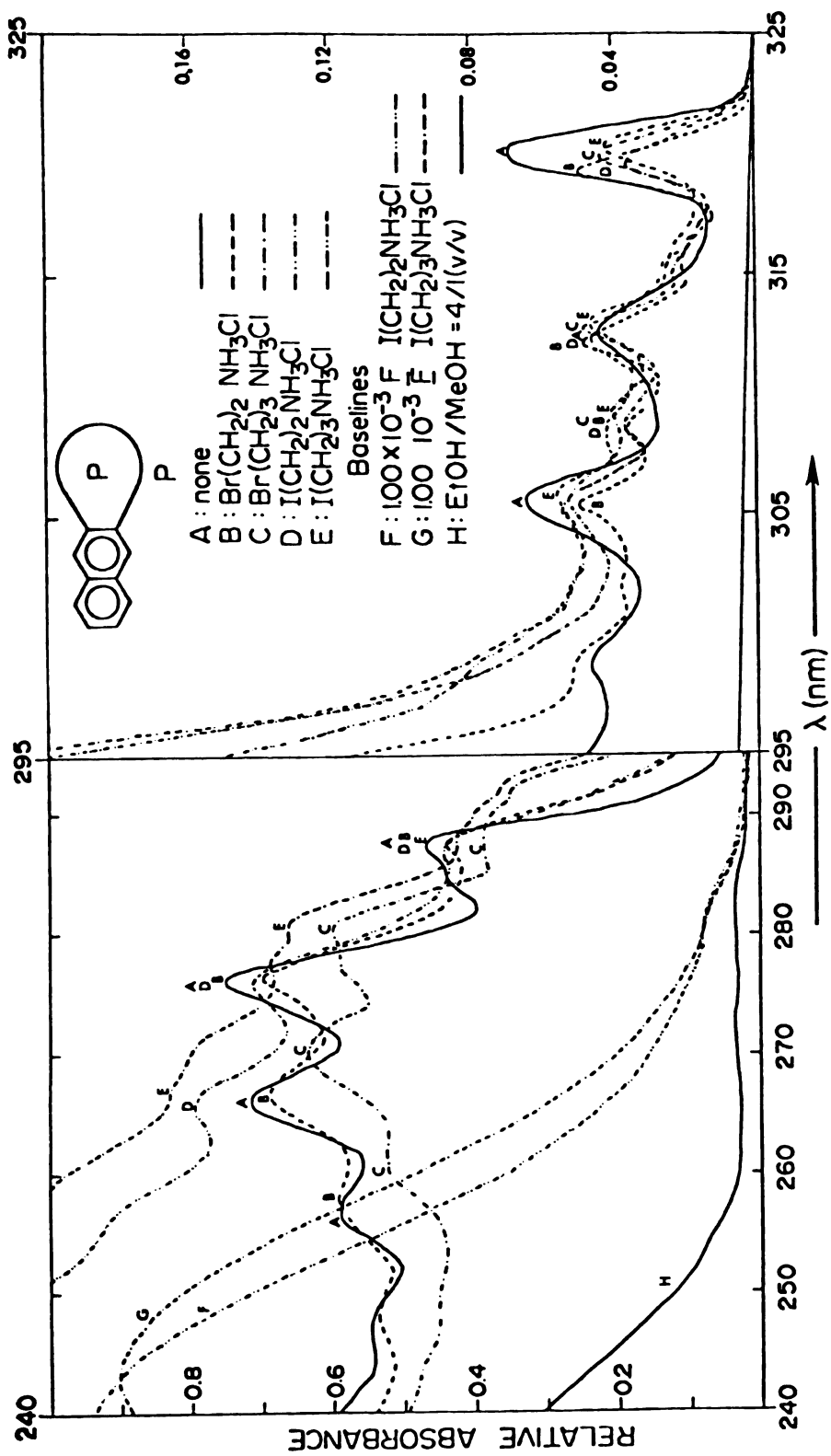


Figure 10

Figure 11. 77 K UV spectra of 1,8-naphtho-21-crown-6 ( $\lambda$ ) alone and with 5:1 added molar excess of bromoalkylammonium chlorides in 95% ethanol-methanol (4:1, v/v) glass and with 12.5:1 added molar excess of iodoalkylammonium chlorides in ethanol-methanol (4:1, v/v) glass. See figure legend. Intensities are given in terms of relative absorbancies (see text for explanation). Relative absorbancies for the shorter wavelength region are given by the scale on the left; for the longer wavelength region, by the scale on the right. The concentration (at room temperature) of crown was  $4.00 \times 10^{-4}$  M for the longer wavelength region and  $8.00 \times 10^{-5}$  M for the shorter wavelength region. The scales have been adjusted so that the absorbancies of both sections are those of a  $8.00 \times 10^{-5}$  M solution. Baselines: curve F,  $\beta$ -iodoethylammonium chloride; curve G,  $\gamma$ -iodopropylammonium chloride; curve H, 95% ethanol-methanol (4:1, v/v) glass.

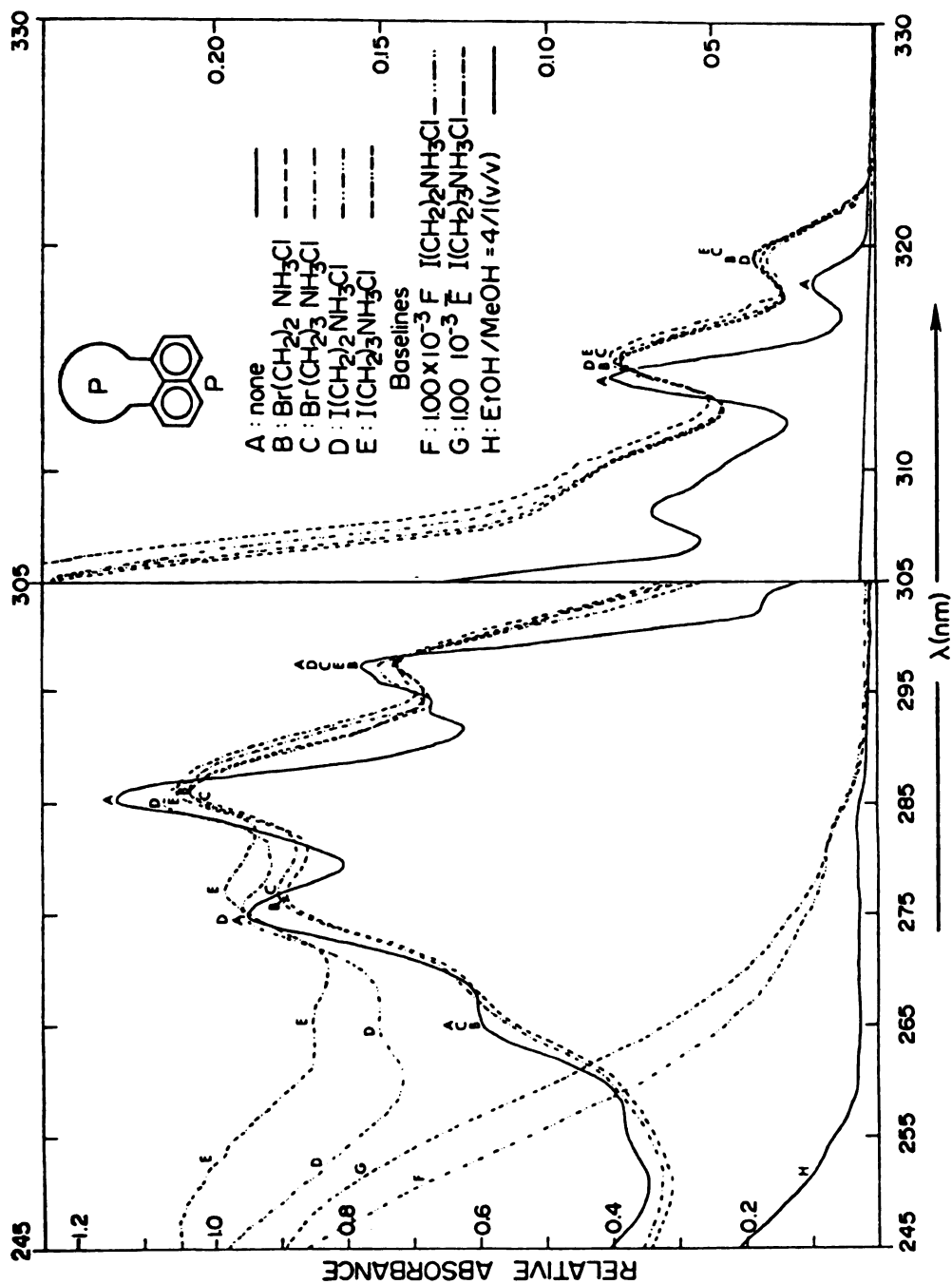


Figure 11

Figure 12. 77 K UV spectra of 1,5-naphtho-22-crown-6 (3) alone and with 50:1 added molar excess of bromoalkylammonium and iodoalkylammonium chlorides in ethanol-methanol (4:1, v/v) glass. See figure legend. Intensities are given in terms of relative absorbancies (see text for explanation). Relative absorbancies for the shorter wavelength region are given by the scale on the left; for the longer wavelength region, by the scale on the right. The concentration (at room temperature) of crown was  $1.00 \times 10^{-4}$  M for the longer wavelength region and  $5.00 \times 10^{-4}$  M for the shorter wavelength region. The scales have been adjusted so that the absorbancies of both sections are those of a  $5.00 \times 10^{-5}$  M solution. Baselines: curve F,  $2.50 \times 10^{-3}$  M  $\beta$ -iodoethylammonium chloride; curve G,  $2.50 \times 10^{-3}$  M  $\gamma$ -iodopropylammonium chloride; curve H, ethanol-methanol (4:1, v/v) glass.

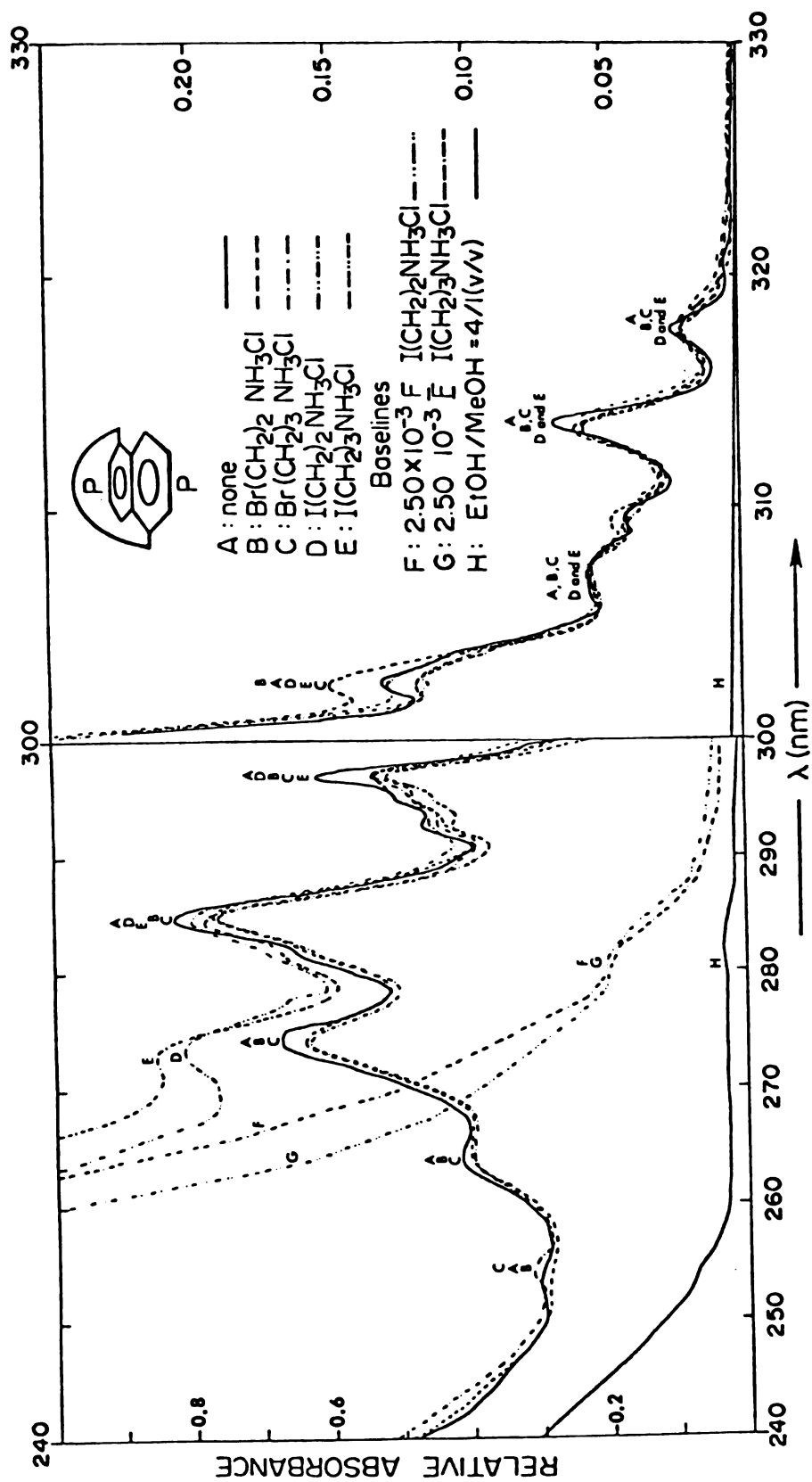


Figure 12

Figure 13. 77 K UV spectra of 2,3-naphtho-20-crown-6 (1) alone and with 5:1 added molar excess of cesium chloride in 95% ethanol-methanol (4:1, v/v) glass and with 12:1 added molar excess of barium bromide in ethanol-methanol (4:1, v/v) glass. See figure legend. Intensities are given in terms of relative absorbancies (see text for explanation). Relative absorbancies for the shorter wavelength region are given by the scale on the left; for the longer wavelength region, by the scale on the right. Crown concentrations (at room temperature) were  $4.00 \times 10^{-4}$  M for the longer wavelength region and  $8.00 \times 10^{-5}$  M for the shorter wavelength region. The scales have been adjusted so that the absorbancies of both sections are those of a  $8.00 \times 10^{-5}$  M solution.

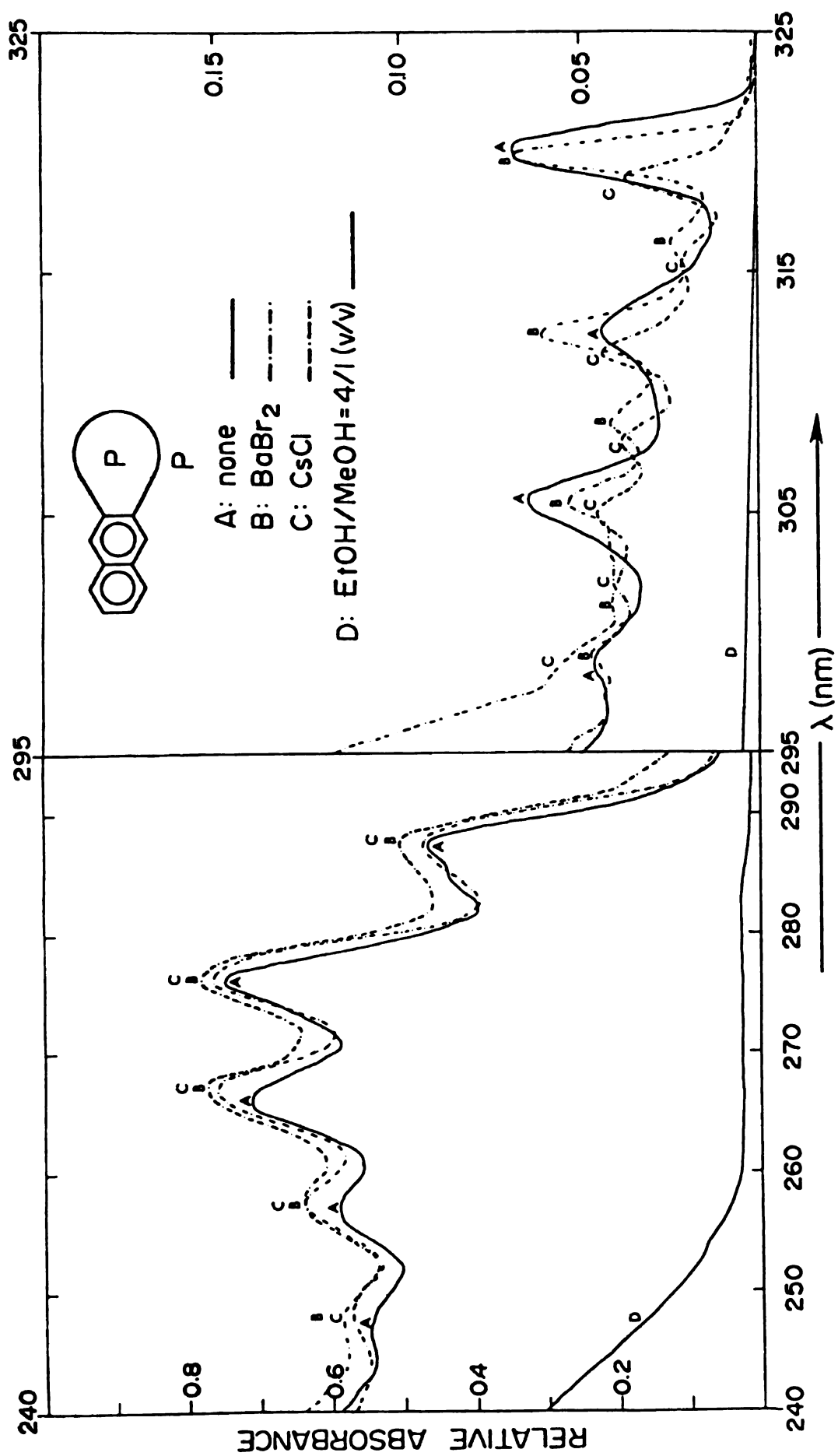


Figure 13

Figure 14. 77 K UV spectra of 1,8-naphtho-21-crown-6 (2) alone and with 5:1 added molar excess of cesium chloride in 95% ethanol-methanol (4:1, v/v) glass and with 12:1 added molar excess of barium bromide in ethanol-methanol (4:1, v/v) glass. See figure legend. Intensities are given in terms of relative absorbancies (see text for explanation). Relative absorbancies for the shorter wavelength region are given by the scale on the left; for the longer wavelength region by the scale on the right. Crown concentrations (at room temperature) were  $4.00 \times 10^{-4}$  M for the longer wavelength region and  $8.00 \times 10^{-5}$  M for the shorter wavelength region. The scales have been adjusted so that the absorbancies of both sections are those of a  $8.00 \times 10^{-5}$  M solution.



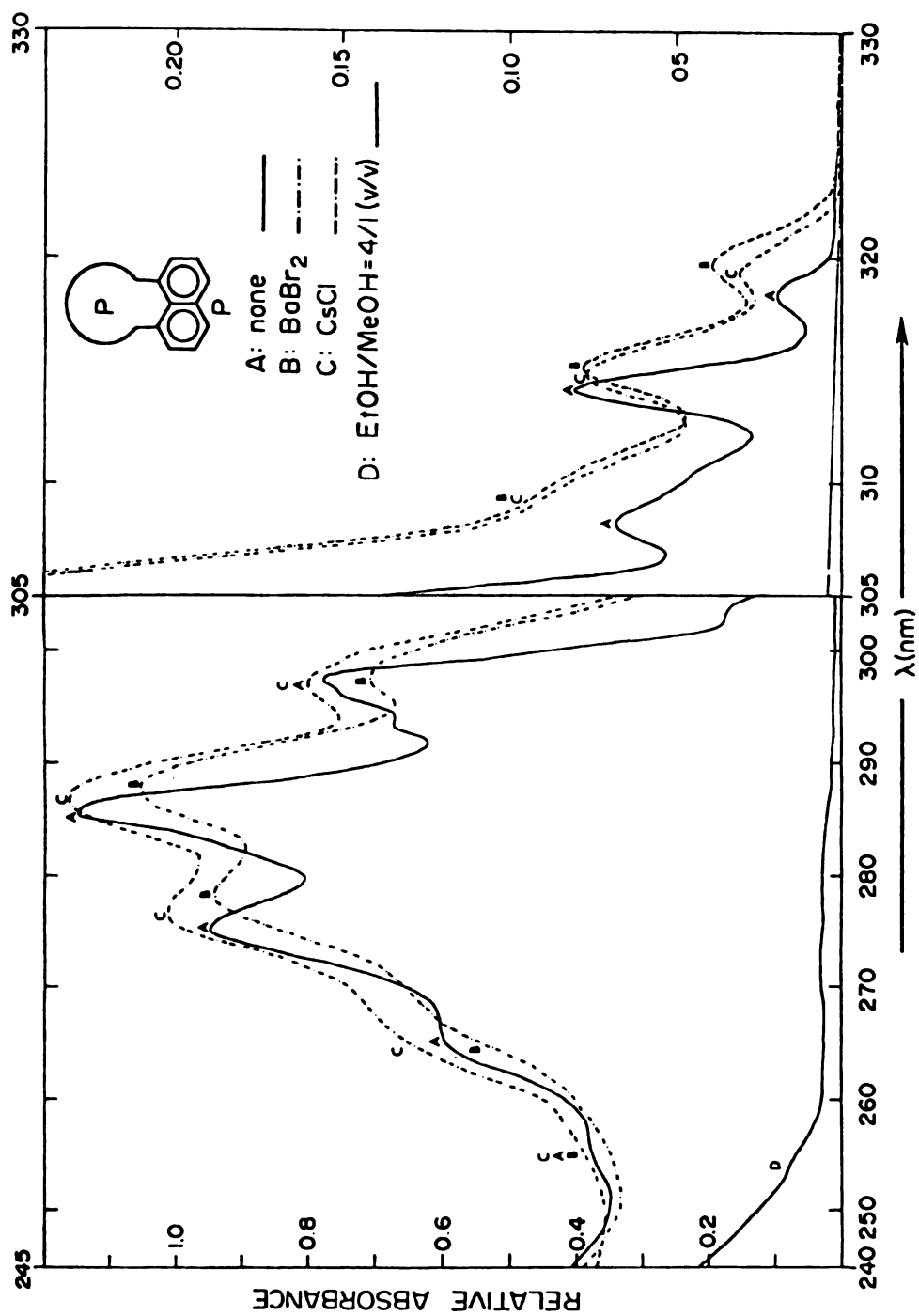


Figure 14

Figure 15. 77 K UV spectra of 1,5-naphtho-22-crown-6 (3) alone and with 5:1 added molar excess of cesium chloride in 95% ethanol-methanol (4:1, v/v) glass and with 50:1 added molar excess of barium bromide in ethanol-methanol (4:1, v/v) glass. See figure legend. Intensities are given in terms of relative absorbancies (see text for explanation). Relative absorbancies for the shorter wavelength region are given by the scale on the left; for the longer wavelength region by the scale on the right. Crown concentrations (at room temperature) were  $4.00 \times 10^{-4}$  M for the longer wavelength region and  $8.00 \times 10^{-5}$  M for the shorter wavelength region. The scales have been adjusted so that the absorbancies of both sections are those of a  $8.00 \times 10^{-5}$  M solution.

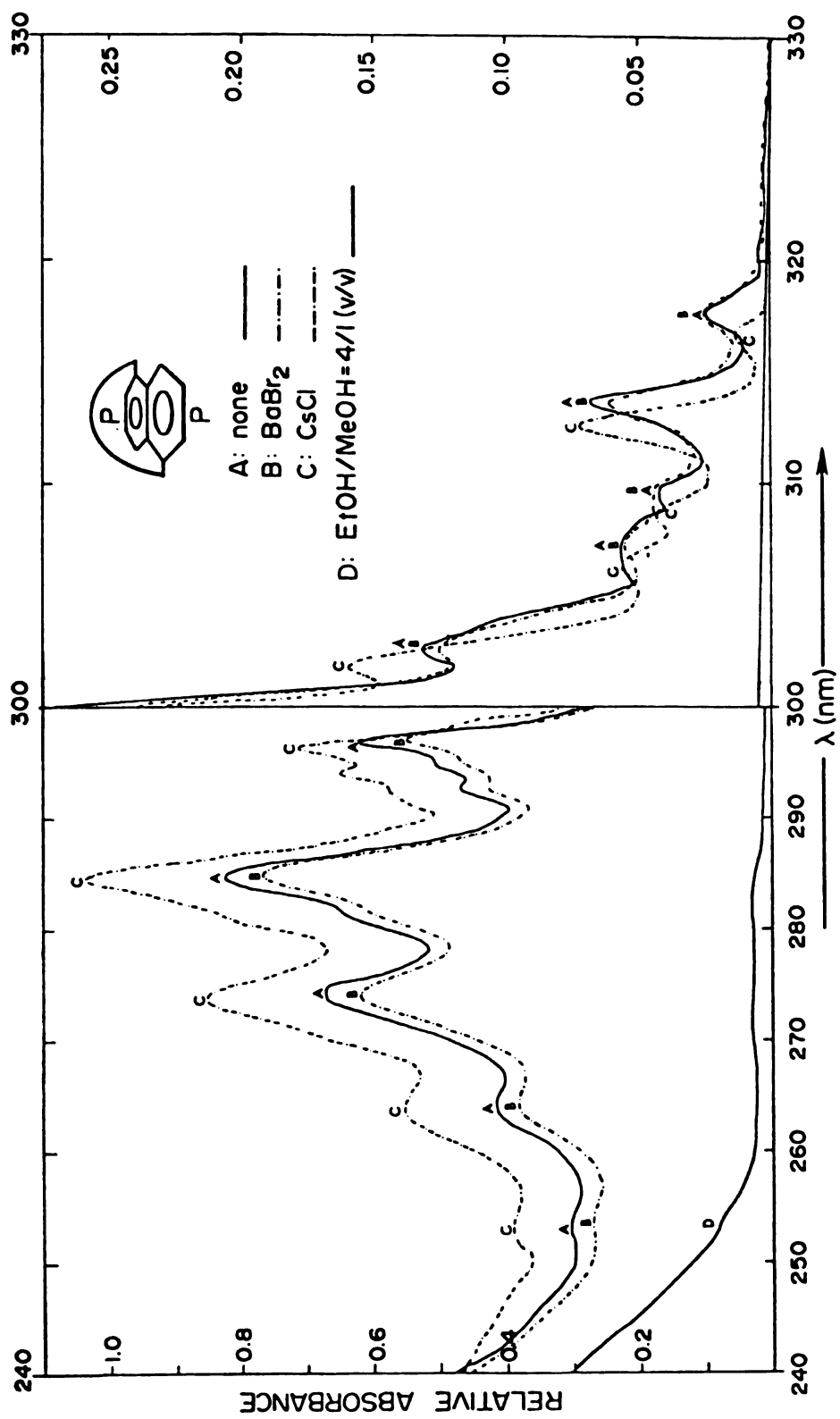


Figure 15

Figure 16. 77 K UV spectra of 2,3-naphtho-20-crown-6 (1) alone and with 50:1 added molar excess of silver triflate in ethanol-methanol (4:1, v/v) glass. See figure legend. Intensities are given in terms of relative absorbancies (see text for explanation). Relative absorbancies for the shorter wavelength region are given by the scale on the left; for the longer wavelength region by the scale on the right. Crown concentrations (at room temperature) were  $4.00 \times 10^{-4}$  M for the longer wavelength region and  $8.00 \times 10^{-5}$  M for the shorter wavelength region. The scales have been adjusted so that the absorbancies of both sections are those of a  $8.00 \times 10^{-5}$  M solution.

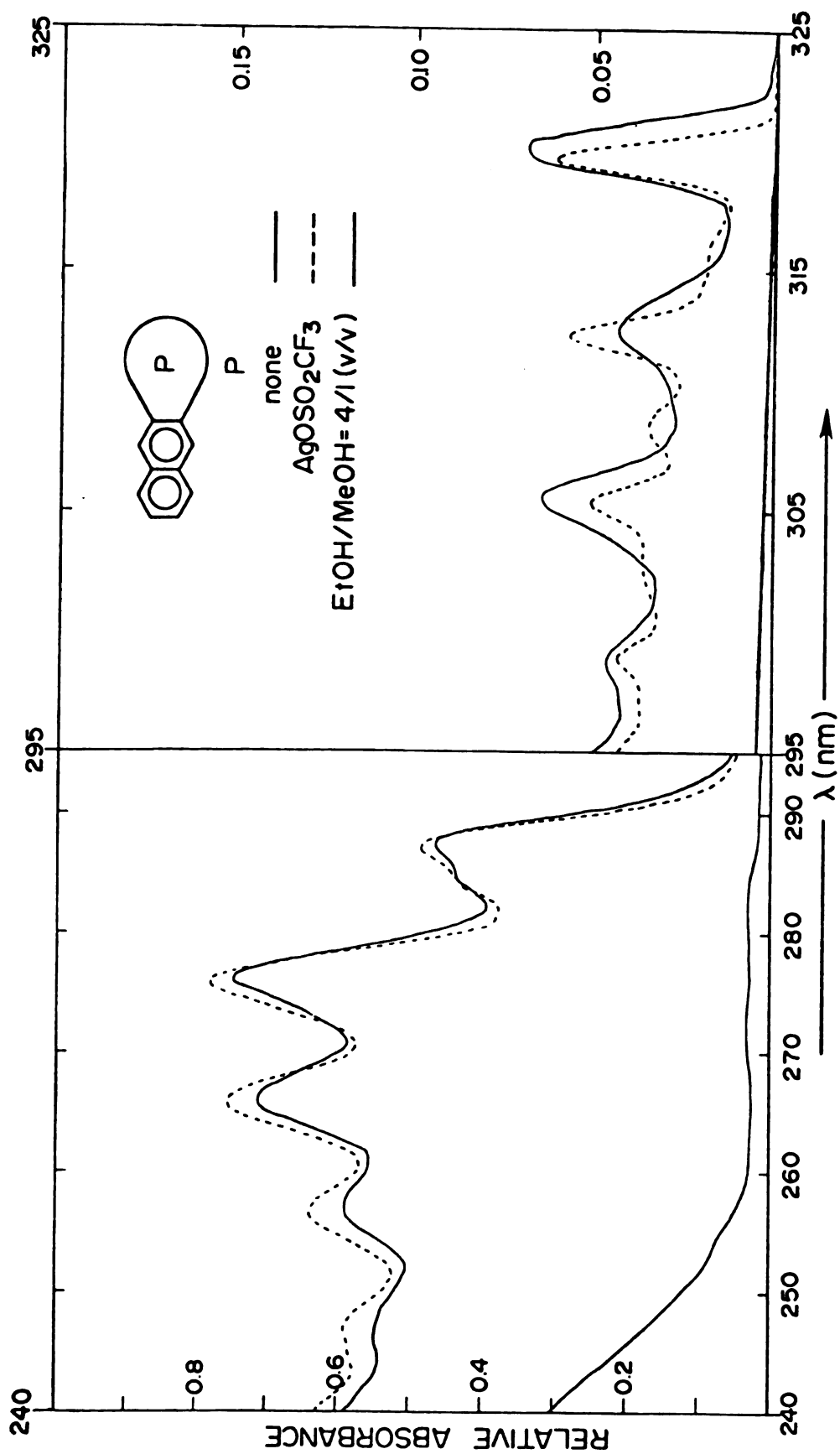


Figure 16



Figure 17. 77 K UV spectra of 1,8-naphtho-21-crown-6 (2) alone and with 50:1 added molar excess of silver triflate in ethanol-methanol (4:1, v/v) glass. See figure legend. Intensities are given in terms of relative absorbancies (see text for explanation). Relative absorbancies for the shorter wavelength region are given by the scale on the left; for the longer wavelength region by the scale on the right. Crown concentrations (at room temperature) were  $4.00 \times 10^{-4}$  M for the longer wavelength region and  $8.00 \times 10^{-5}$  M for the shorter wavelength region. The scales have been adjusted so that the absorbancies of both sections are those of  $8.00 \times 10^{-5}$  M solution.

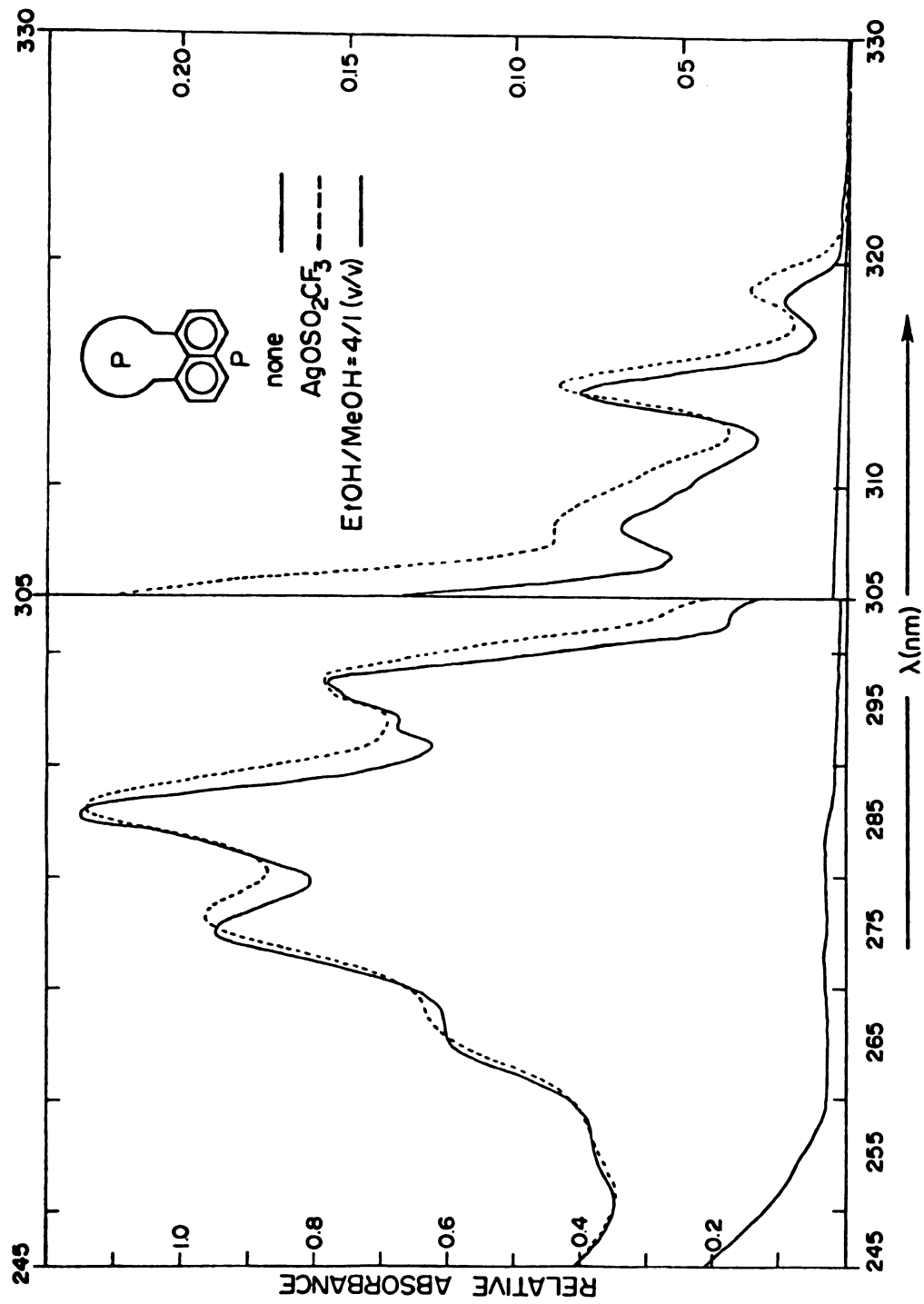


Figure 17



Figure 18. 77 K UV spectra of 1,5-naphtho-22-crown-6 (3) alone and with 200:1 added molar excess of silver triflate in ethanol-methanol (4:1, v/v) glass. See figure legend. Intensities are given in terms of relative absorbancies (see text for explanation). Relative absorbancies for the shorter wavelength region are given by the scale on the left; for the longer wavelength region by the scale on the right. Crown concentrations at room temperature were  $1.00 \times 10^{-4}$  M for the longer wavelength region and  $5.00 \times 10^{-5}$  M for the shorter wavelength region. The scales have been adjusted so that the absorbancies of both sections are those of a  $5.00 \times 10^{-5}$  M solution.

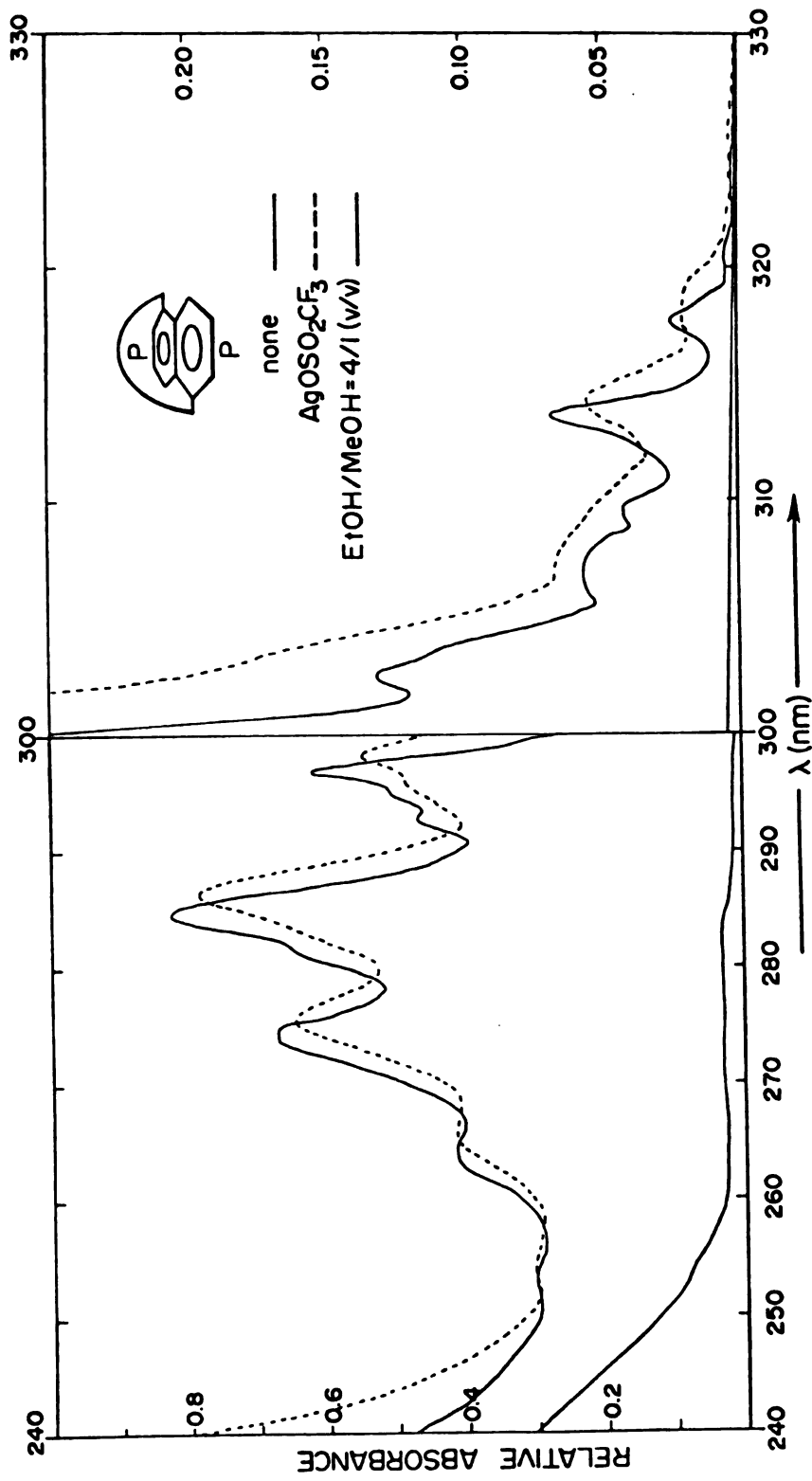


Figure 18

be qualitatively noted. Precise energies will be given below in the results section on energy shifts. The lowest energy peak (longest wavelength) which is apparent will be referred to as the "0-0 band". Discussion of whether or not these are true 0-0 bands will be given later. The lower energy absorption band (from approximately 330 to 300 nm) will be referred to as the " $S_1$  band".<sup>67</sup> Here "band" is used to refer to a whole series of peaks belonging to the same electronic level. The  $S_1$  band, for instance, is comprised of transitions from the ground state to various levels of the first electronically excited singlet. The higher energy absorption band (from approximately 240 to 300 nm) will be referred to as the " $S_2$  band". Absorption bands higher in energy than the  $S_2$  band were not easily experimentally accessible due to significant absorption by the alcoholic solvent below 240 nm.

Figures 1, 2, and 3 show, respectively, the 77 K UV spectra for 2,3-, 1,8-, and 1,5-disubstituted naphthalenes and naphthalene itself. The substituents in each case are methyl, methoxymethyl, and crown-methyl. The solvent is 95% ethanol-methanol glass (4:1, v/v) for the 2,3- and 1,8- derivatives and ethanol-methanol glass (4:1, v/v) for the 1,5- derivatives. The absorbancies shown (after correction by the multiplicative factors given in the figures in some cases) are those of  $8.00 \times 10^{-5}$  M (at room temperature) solutions. For ethanol-methanol (4:1, v/v) glass the contraction factor is 0.802 (Volume at 77°K/volume at 293°K).<sup>69</sup>

For the 2,3- disubstituted naphthalenes, the  $S_2$  bands of the derivatives are quite similar to naphthalene in fine structure,

energies, and intensities, but the  $S_1$  bands of the derivatives appear to be quite dissimilar relative to naphthalene. For both bands, however, note that the crown and methoxymethyl derivatives have very similar fine structure and energies. The 0-0 bands are all red shifted relative to naphthalene. The shifts are of similar magnitude, but largest for the crown and smallest for the dimethyl derivative. For the  $S_2$  bands of these derivatives, the entire band is red shifted for the 2,3-dimethyl derivative, whereas the entire band is blue shifted for the crown and methoxymethyl derivatives. The situation is not quite so simple for the  $S_1$  bands, however, since all of the derivatives have less fine structure than naphthalene.

As is seen for the 2,3-derivatives, the 1,8-crown and methoxymethyl derivatives have absorption spectra which are similar in intensity, fine structure, and energy (Figure 2). The  $S_2$  bands of the 1,8-derivatives have fine structure which is similar to that of naphthalene but all these bands are considerably red shifted relative to naphthalene (by about  $1000\text{ cm}^{-1}$ ). As is seen for the 2,3-derivatives, the  $S_1$  bands of the 1,8-derivatives show much less fine structure than does naphthalene. The 0-0 bands are all red shifted, but the 0-0 band of the 1,8-dimethyl derivative is red shifted most, whereas the crown was red shifted most for the 2,3-derivatives. The red shift of the  $S_2$  band is also largest for the 1,8-dimethyl derivative.

Comparison of the 77 K UV spectra of the 1,5- and 1,8-disubstituted naphthalenes shows that they are quite similar in most respects: fine structure, energy shifts, and, for the  $S_2$  band,

relative intensities.

The following differences for the  $S_1$  region are noted by comparison of Figures 2 and 3. The  $S_1$  band of the 1,8-dimethyl derivative is about three times more intense than for the 1,5-dimethyl derivative. The 1,5-dimethyl derivative has a peak at 303.8, whereas there is only a shoulder in this region for the 1,8-derivative. The 1,5-crown and methoxymethyl derivatives absorb approximately two times more intensely in the  $S_1$  region than do the corresponding 1,8-derivatives. These differences aside, the two sets of absorption spectra are quite similar.

Figures 4, 5, and 6 show, respectively, the effects of 5:1 molar excesses of alkali metal chloride salts on the 77 K UV absorption spectra of crowns  $\lambda$ ,  $\zeta$ , and  $\xi$ . The absorption spectra of the complexes are very much like those of the parent crown in many respects.

For crown  $\lambda$ , the complexes and free crown have similar fine structure, energies, and intensities. The  $S_1$  bands of the complexes, however, have three small peaks not observed for the free crown. The 0-0 band and whole spectrum of each complex are slightly blue shifted relative to free crown.

For crown  $\zeta$ , the  $S_2$  bands of the complexes and of free crown  $\zeta$ , as for crown  $\lambda$ , are very similar in fine structure, intensity, and energy (complexes are slightly red shifted relative to free crown). For the potassium, rubidium, and cesium chloride complexes, there is some broadening of the  $S_2$  band in the 305 nm region. Thus, the peaks at approximately 308 nm for crown  $\zeta$  and for its sodium complex

in the  $S_1$  region, appear only as shoulders for the other complexes (see note in results section on quantum yield titrations for sodium complex of crown  $\lambda$ ). This difference aside, the  $S_1$  bands of free crown  $\lambda$  and of its complexes are quite similar. The 0-0 bands and whole  $S_1$  band of each complex are slightly red shifted relative to free crown.

For crown  $\lambda$ , the  $S_2$  and  $S_1$  bands of complexes and free crown shown in Figure 6 have very similar fine structure and the 0-0 band and whole spectrum of each complex are slightly blue shifted relative to free crown. Both the  $S_2$  and  $S_1$  bands of the complexes are relatively more intense than those of the free crown. For the  $S_2$  band, all peaks of a given complex are increased in intensity by about the same amount relative to free crown. The increase is largest for the sodium and potassium complexes and smallest for the cesium complex. For the  $S_1$  band, the intensities of various peaks are affected differently for different complexes.

Many of the comments made above concerning changes in fine structure and the direction of energy shifts for complexes of crowns  $\lambda$ ,  $\lambda$ , and  $\lambda$  relative to the respective free crowns are also true for other complexes of these crowns which were investigated: alkyl and haloalkylammonium chlorides, barium bromide, and silver triflate complexes. In relating the results for the 77 K UV spectra of these other complexes, only differences between the results for the alkali metal chloride complexes will be noted.

Figures 7 and 8 show the effects of 5:1 molar excesses of ammonium and alkylammonium chloride salts on the 77 K UV absorption spectra

of crowns  $1$  and  $2$  in 95% ethanol-methanol (4:1, v/v) glass. The effects of 100:1 molar excesses of ammonium and n-propylammonium chlorides on the 77 K UV absorption spectrum of crown  $3$ , in ethanol-methanol glass (4:1, v/v), are shown in Figure 9.

For the alkylammonium complexes of crown  $1$ , the energy shifts are all small blue shifts, as is typical for complexes of this crown, except for the n-propylammonium complex, for which the whole  $S_2$  band is significantly red shifted (by approximately  $500\text{ cm}^{-1}$ ). Also, an extra peak appears for this complex in the 280 nm region, although the dip is small enough that it may be due to curvature in the baseline. The alkylammonium complexes of crown  $2$  require no special comments. The ammonium and n-propyl complexes of crown  $3$  have absorption spectra which are practically identical to that of free crown. Note, however, that the 0-0 band is slightly red shifted for the n-propyl complex but slightly blue shifted for the ammonium chloride complex. The alkali metal chloride complexes were slightly blue shifted. In contrast to the alkali metal complexes of crown  $3$ , these complexes show very little change in absorption intensity relative to the free crown.

The effects of excess bromoalkyl and iodoalkylammonium chloride salts on the 77 K UV absorption spectra of crowns  $1$  (5 to 12.5-fold molar excess of salt),  $2$  (5 to 12.5-fold molar excess of salt), and  $3$  (50-fold molar excesses of salt) are shown in Figures 10, 11, and 12, respectively. The spectra for the bromoalkylammonium complexes of crowns  $1$  and  $2$  are from 95% ethanol-methanol glass (4:1, v/v). The remainder of spectra in these figures are from ethanol-methanol

glass (4:1, v/v). Absorption due to excess iodoalkylammonium chloride salts becomes appreciable at wavelengths shorter than 280 nm. Baselines corresponding to the amount of excess salt present are shown in the figures. While absorption by excesses of these salts obscure the higher energy portion of the  $S_2$  bands, the spectra as presented are sufficiently undistorted by this extra absorption for most of the  $S_2$  band so that accurate comparison to absorption by free crown and other complexes can be made.

For crown 1, the entire  $S_2$  band of both  $\gamma$ -halopropylammonium complexes is significantly red shifted relative to free crown (approximately  $500\text{ cm}^{-1}$ ), as is also the case for the  $n$ -propylammonium complex. The haloalkylammonium complexes of crown  $2_{\lambda}$  give spectra and energy shifts similar to those of the alkali metal cation complexes. For crown  $3_{\lambda}$ , note that the complexes and free crown have very similar absorbancies, which is in contrast to the differences seen for the alkali metal chloride complexes.

Figures 13, 14 and 15 show, respectively, the effects of excess cesium chloride and barium bromide on the 77 K UV absorption spectra of crowns  $1_{\lambda}$  (5-fold molar excess cesium chloride, 12-fold molar excess barium bromide),  $2_{\lambda}$  (5-fold molar excess cesium chloride, 12-fold excess barium bromide), and  $3_{\lambda}$  (5-fold molar excess cesium chloride, 50-fold molar excess barium bromide). These spectra require no further comments beyond those made for the alkali metal chloride complexes, except to note that both the  $S_1$  and  $S_2$  bands of the barium complex of crown  $3_{\lambda}$  are more similar in energy and intensity to free crown than are those of the cesium complex.



The effects of excess silver triflate on the 77 K UV absorption spectra of crowns  $\lambda_1$  (50:1 molar excess),  $\lambda_2$  (50:1 molar excess), and  $\lambda_3$  (200:1 molar excess) in ethanol-methanol glass (4:1, v/v) are shown in Figures 16, 17, and 18, respectively. These spectra require no further comment except for the spectrum of the silver complex of crown 3. This is the only complex of this crown for which the  $S_2$  and  $S_1$  bands are significantly red shifted ( $-150\text{ cm}^{-1}$  and  $-50\text{ cm}^{-1}$ , respectively). All other complexes are slightly blue shifted relative to free crown  $\lambda_3$ , except for the n-propylammonium chloride complex, which is slightly red shifted.

At room temperature, with concentrations similar to those of Figures 1 and 2 added alkali metal chlorides do not appreciably change the UV spectra of crowns  $\lambda_1$  and  $\lambda_2$ . The intensities change by less than 5% and energy shifts are not discernible. It should be noted, however, that the extent of complexation of crowns  $\lambda_1$  and  $\lambda_2$  under the given conditions ( $2.00 \times 10^{-4}\text{ M}$  crown, 5:1 molar excess of salt) is not known precisely but is estimated to be approximately 60 to 80%. For crown  $\lambda_3$ , however, added alkali metal salts do change the room temperature absorption spectra relative to free crown. The shapes remain the same, but the intensities of both the  $S_1$  and  $S_2$  absorption bands are increased by approximately the same factor in each case as for the 77 K spectrum. Also, the order of the intensity increases at room temperature are the same as for the  $S_2$  band of the low temperature spectra ( $\text{KCl} \approx \text{NaCl} > \text{RbCl} > \text{CsCl}$ ). The intensity of the  $S_3$  absorption band for room temperature spectra is also increased by added alkali metal chloride salts by approximately

50% in each case ( $1.20 \times 10^{-6}$  M crown with 5-fold molar excess of salt present). The room temperature complexation constants for crown 3 with alkali metal chlorides must be large ( $10^6$ ), since the absorbance after dilution from  $6.00 \times 10^{-5}$  to  $1.20 \times 10^{-6}$  is only a few percent less than it would be assuming no increase in dissociation upon dilution.

#### Low Temperature (77 K) Fluorescence and Phosphorescence Spectra

The following general comments apply to Figures 19 through 54. All spectra are from solutions in uncracked 95% ethanol and are corrected. The spectra were recorded with instrument settings appropriate for obtaining maximum resolution, but the excitation band passes were too broad to allow the resolved spectra to also accurately indicate relative quantum yields. Furthermore, differences in absorption are not taken into account. Thus, the relative intensities of two different curves are only approximately correct. They do, however, in most cases, qualitatively indicate the trend of the corresponding relative quantum yields. More importantly, they indicate the presence or absence of changes in spectral shapes and energies. The term "0-0 band" will be used to refer to the highest energy (lowest wavelength) band observed in a spectrum (see Discussion section). In the case of spectra of crown complexes, sufficient salt is present in each case to ensure that the emission is essentially due only to complexed crown. The amount of excess salt required was determined from quantum yield titrations (vide infra). The molar (room temperature) concentrations of naphthalene and naphthalene

# Fluorescence of 2,3-Disubstituted Naphthalenes

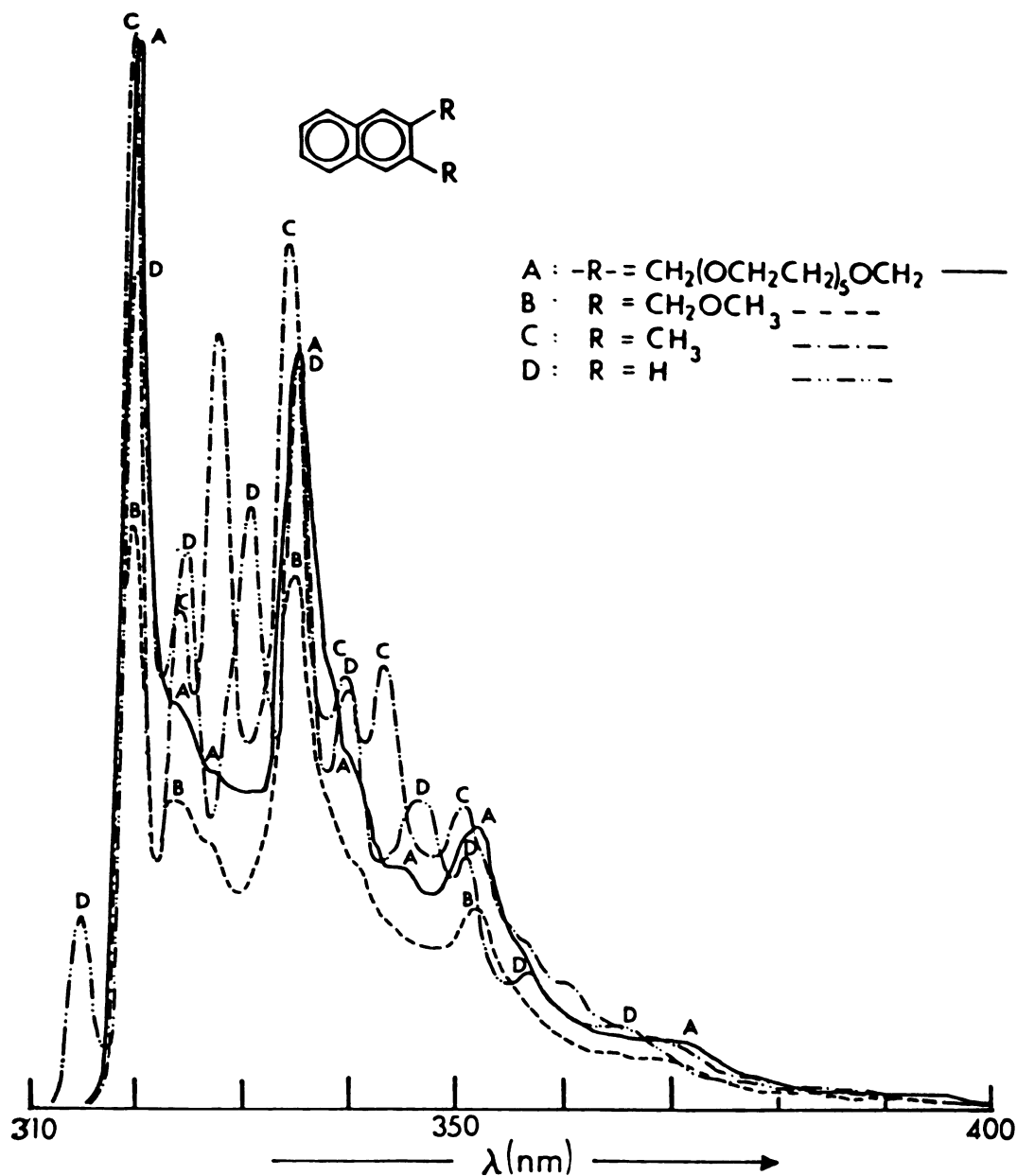


Figure 19. Corrected fluorescence spectra of  $1.00 \times 10^{-4} \text{ M}$  2,3-disubstituted naphthalenes (2,3-Naphtho-20-Crown-6 (1), Curve A; 2,3-Bis-(methoxymethyl)naphthalene (4), Curve B; 2,3-dimethylnaphthalene (5), Curve C; and naphthalene (10), Curve D) in ncracked 95% ethanol glass at 77 K.

Figure 20. Corrected phosphorescence spectra of  $1.00 \times 10^{-4}$  M 2,3-disubstituted naphthalenes (2,3-naphtho-20-crown-6 (1), curve A; 2,3-Bis-(methoxymethyl)naphthalene (4), curve B; 2,3-dimethylnaphthalene (5), curve C; and naphthalene (10) curve D) in uncracked 95% ethanol.

## Phosphorescence of 2,3-Disubstituted Naphthalenes

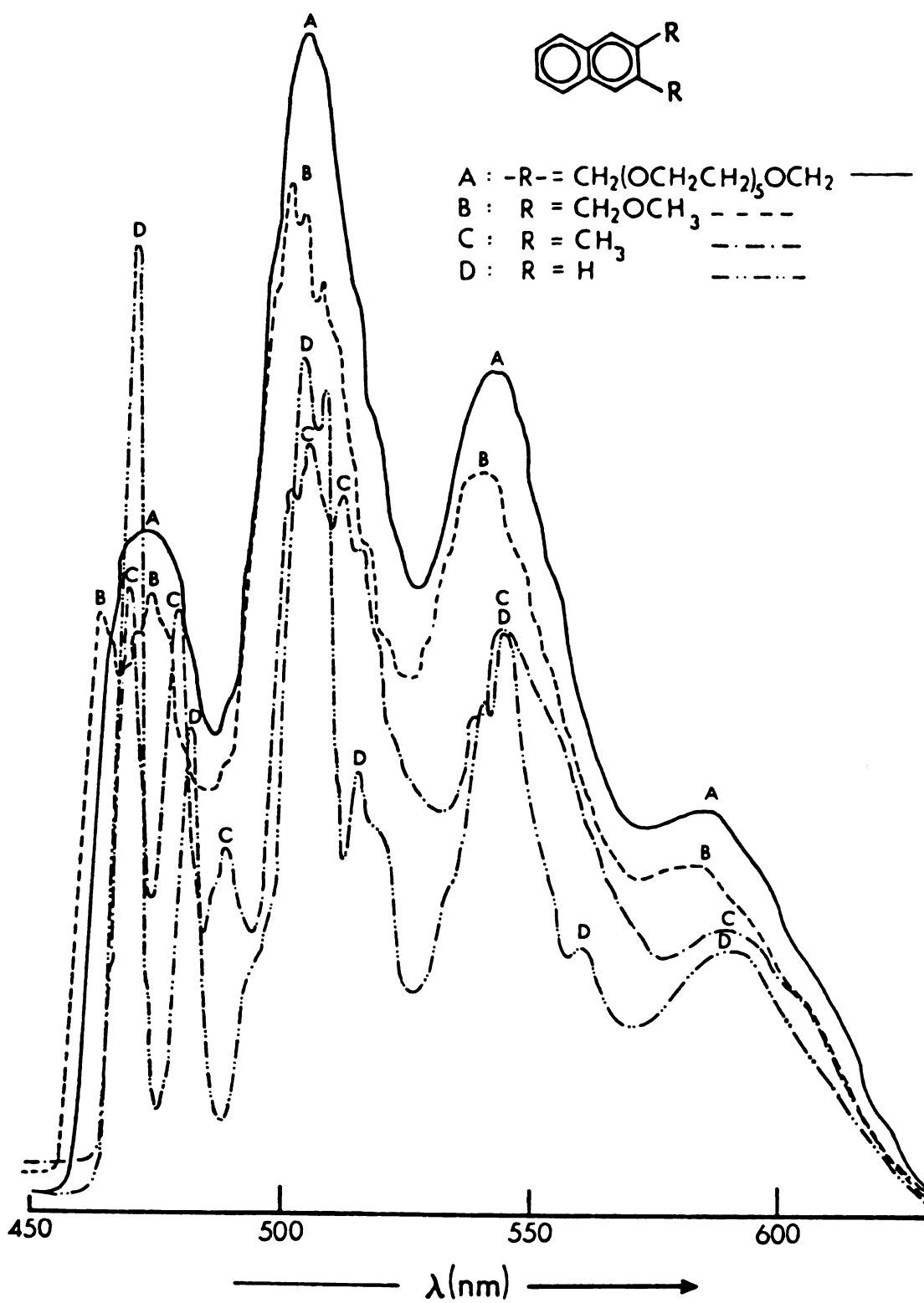


Figure 20

## Fluorescence of 1,8-Disubstituted Naphthalenes

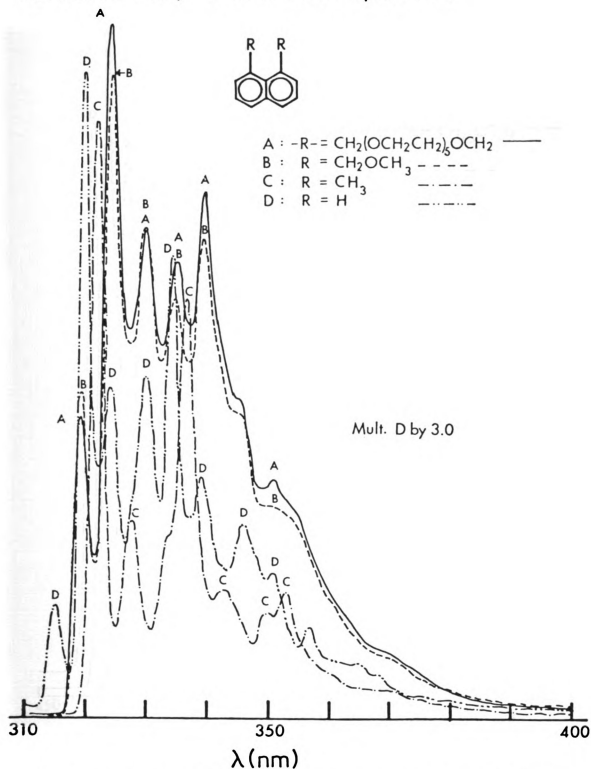


Figure 21. Corrected fluorescence spectra of 1,8-disubstituted naphthalenes (1,8-naphtho-21-crown-6 (2), curve A; 1,8-Bis-(methoxymethyl)naphthalene (6), curve B; 1,8-dimethylnaphthalene (7), curve C; and naphthalene (10), curve D) in uncracked 95% ethanol at 77 K. Curve D should be multiplied by 3.0.

## Phosphorescence of 1,8-Disubstituted Naphthalenes

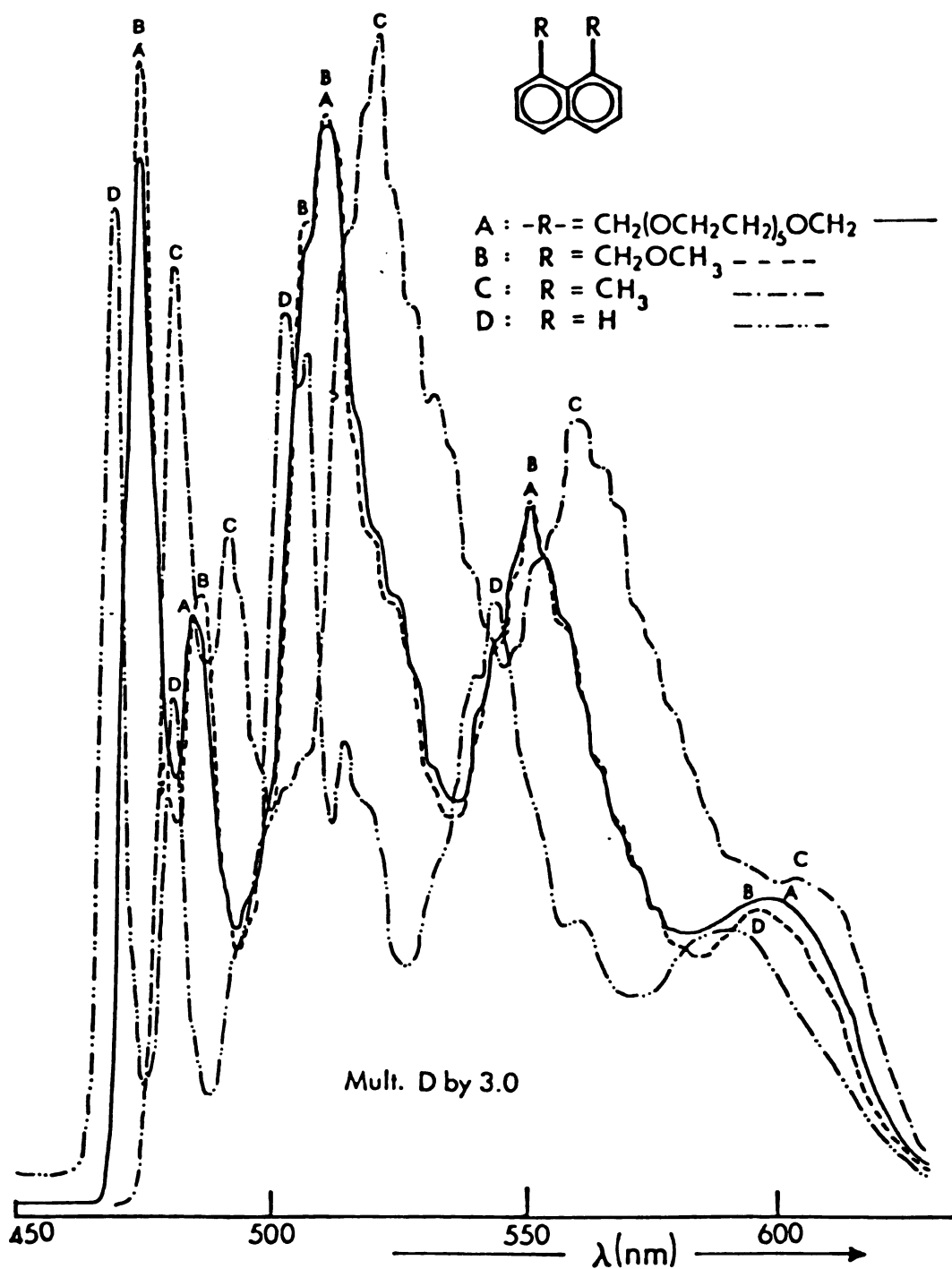


Figure 22. Corrected phosphorescence spectra of 1,8-disubstituted-naphthalenes (1,8-naphtho-21-crown-6 ( $\lambda$ ), curve A; 1,8-Bis-(methoxymethyl)naphthalene ( $\lambda$ ), curve B; 1,8-dimethylnaphthalene ( $\lambda$ ), curve C; and naphthalene ( $\lambda$ ), curve D) in uncracked 95% ethanol glass at 77 K.

## Fluorescence of 1,5-Disubstituted Naphthalenes

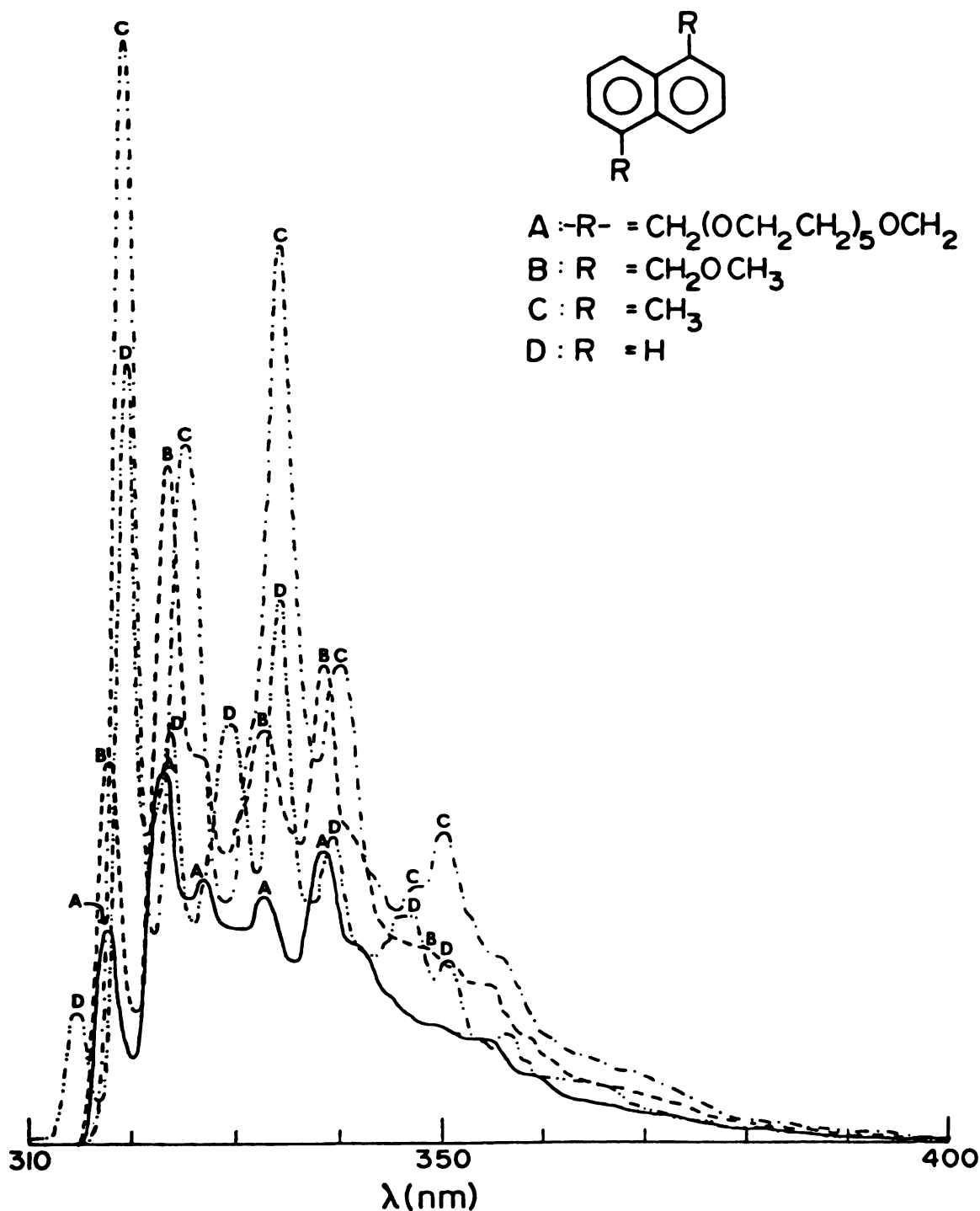


Figure 23. Corrected fluorescence spectra of 1,5-disubstituted-naphthalenes (1,5-naphtho-22-crown-6 (3), curve A; 1,5-Bis-(methoxymethyl)naphthalene (8), curve B; 1,5-dimethylnaphthalene 9, curve C; and naphthalene (10), curve D) in uncracked 95% ethanol glass at 77 K.



## Phosphorescence of 1,5-Disubstituted Naphthalenes

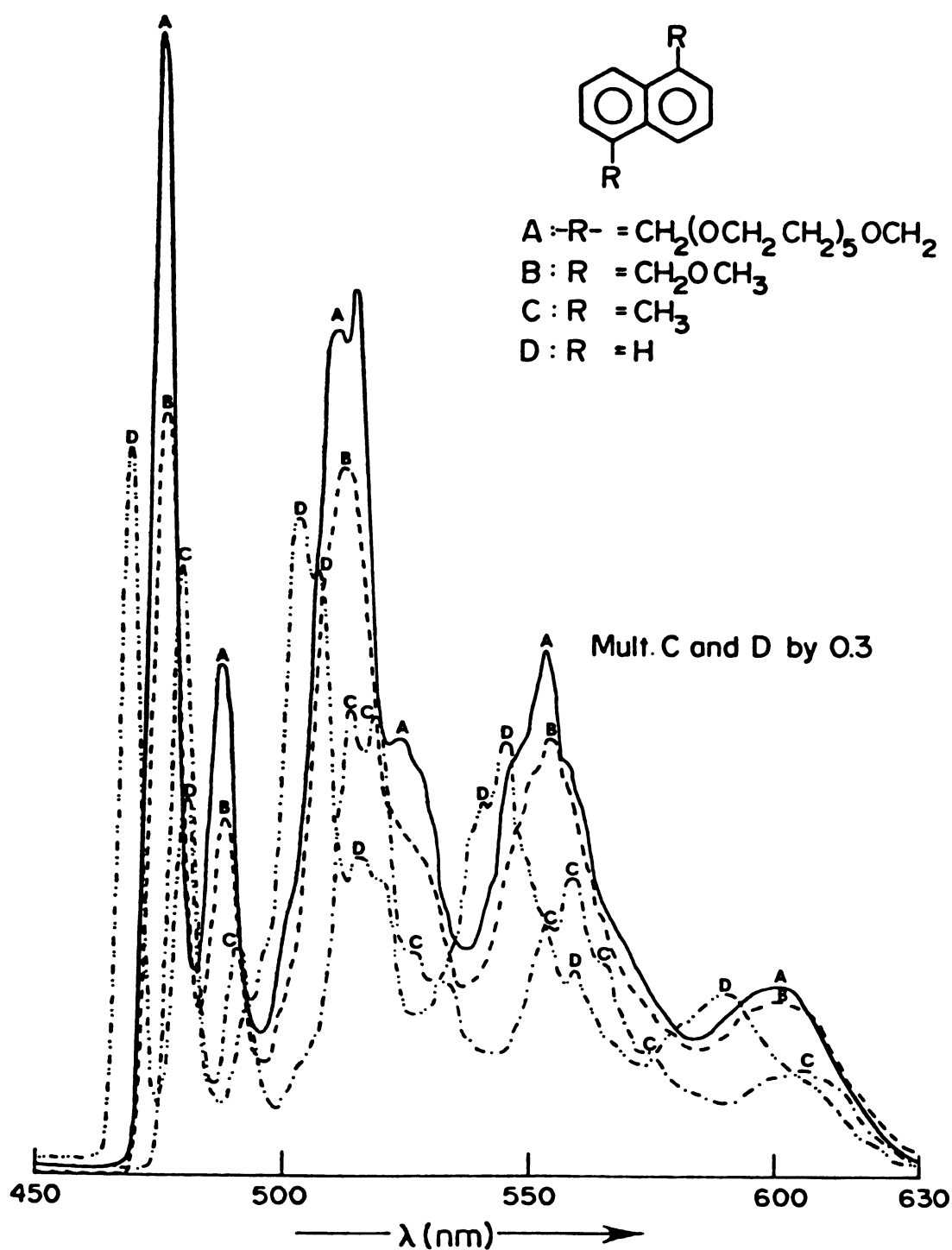


Figure 24. Corrected phosphorescence spectra of 1,5-disubstituted-naphthalenes (1,5-naphtho-22-crown-6 (3), curve A; 1,5-Bis(methoxymethyl)naphthalene (8), curve B; 1,5-dimethylnaphthalene (9), curve C; and naphthalene (10), curve D) in uncracked 95% ethanol glass at 77 K.

# Perturbed Fluorescence of 2,3-Naph-20-Cr-6

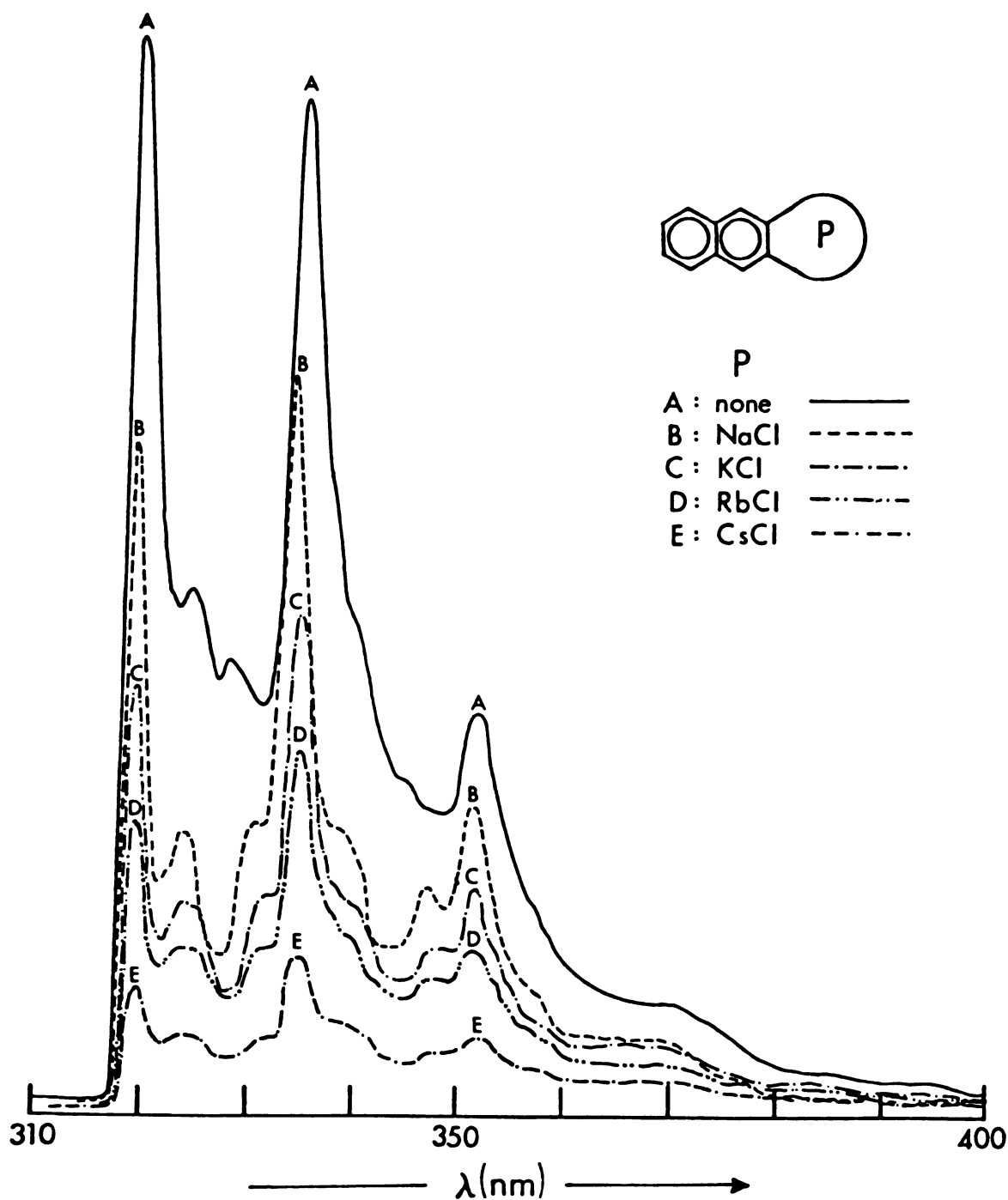


Figure 25. Corrected fluorescence spectra of  $2.00 \times 10^{-4}$  M 2,3-naphtho-20-crown-6 (1) alone and with 5:1 molar excess of alkali metal chlorides added in uncracked 95% ethanol glass at 77 K.

# Perturbed Phosphorescence of 2,3-Naph-20-Cr-6

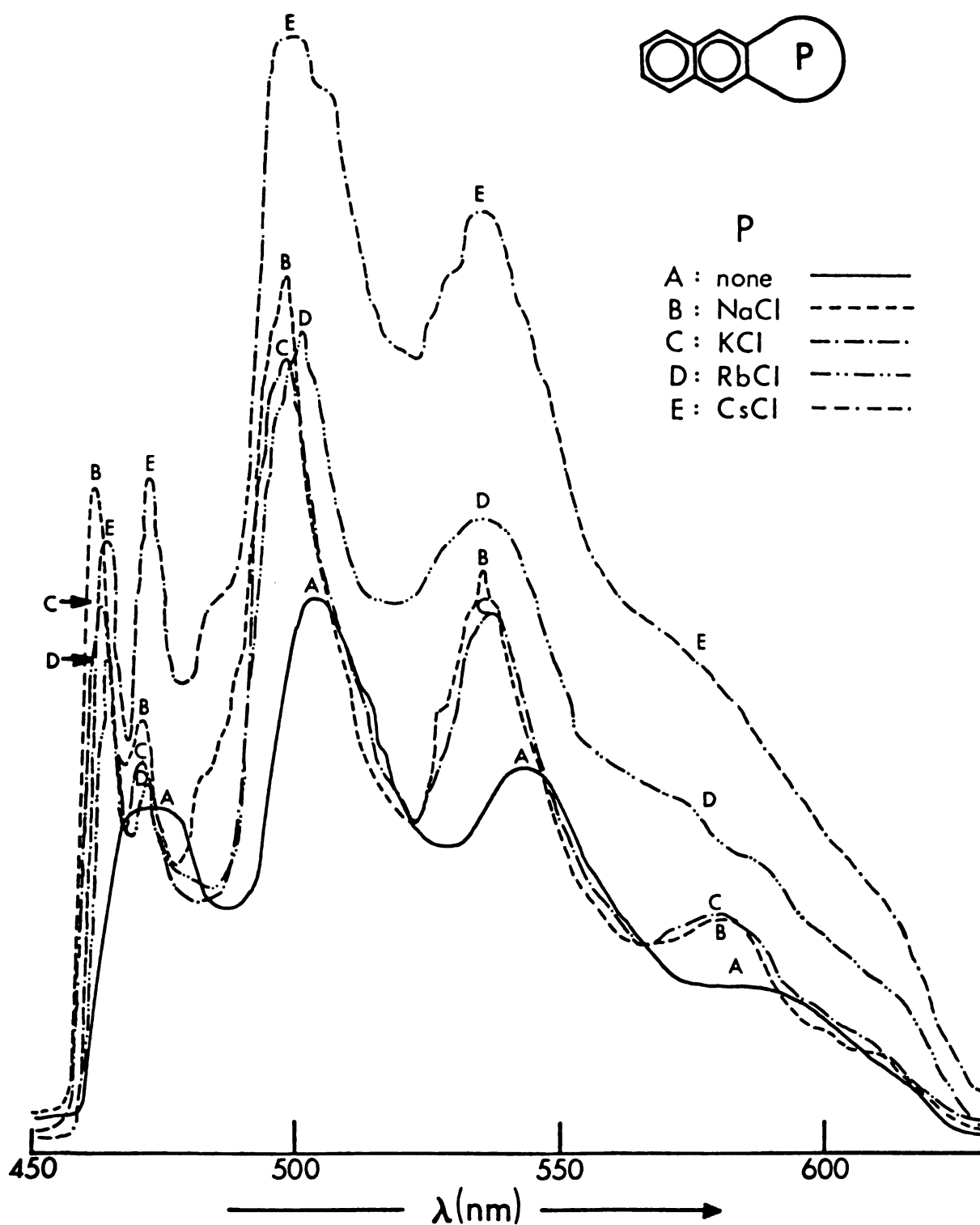


Figure 26. Corrected phosphorescence spectra of  $2.00 \times 10^{-4} \text{ M}$  2,3-naphtho-20-crown-6 ( $\text{P}$ ) alone and with 5:1 molar excess of added alkali metal chlorides in uncracked 95% ethanol glass at 77 K.

# Perturbed Fluorescence of 1,8-Naph-21-Cr-6

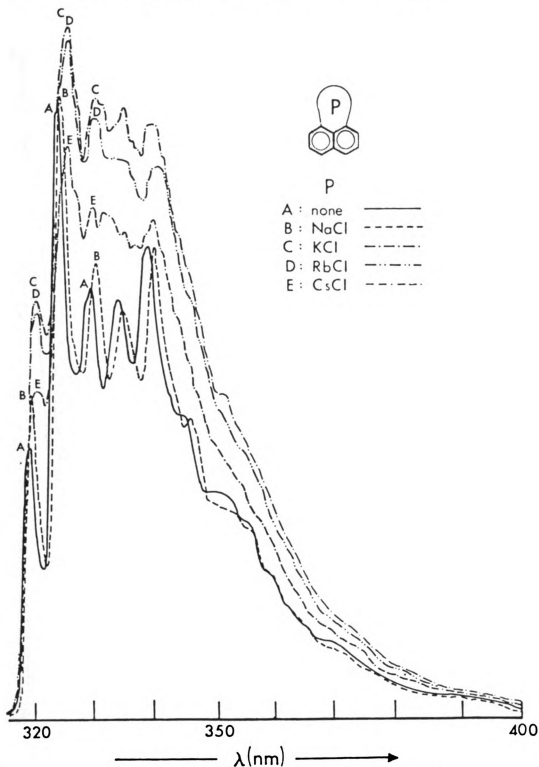


Figure 27. Corrected fluorescence spectra of  $2.00 \times 10^{-4}$  M 1,8-naphtho-21-crown-6 (2) alone and with 5:1 molar excess of added alkali metal chlorides in uncracked 95% ethanol glass at 77 K.

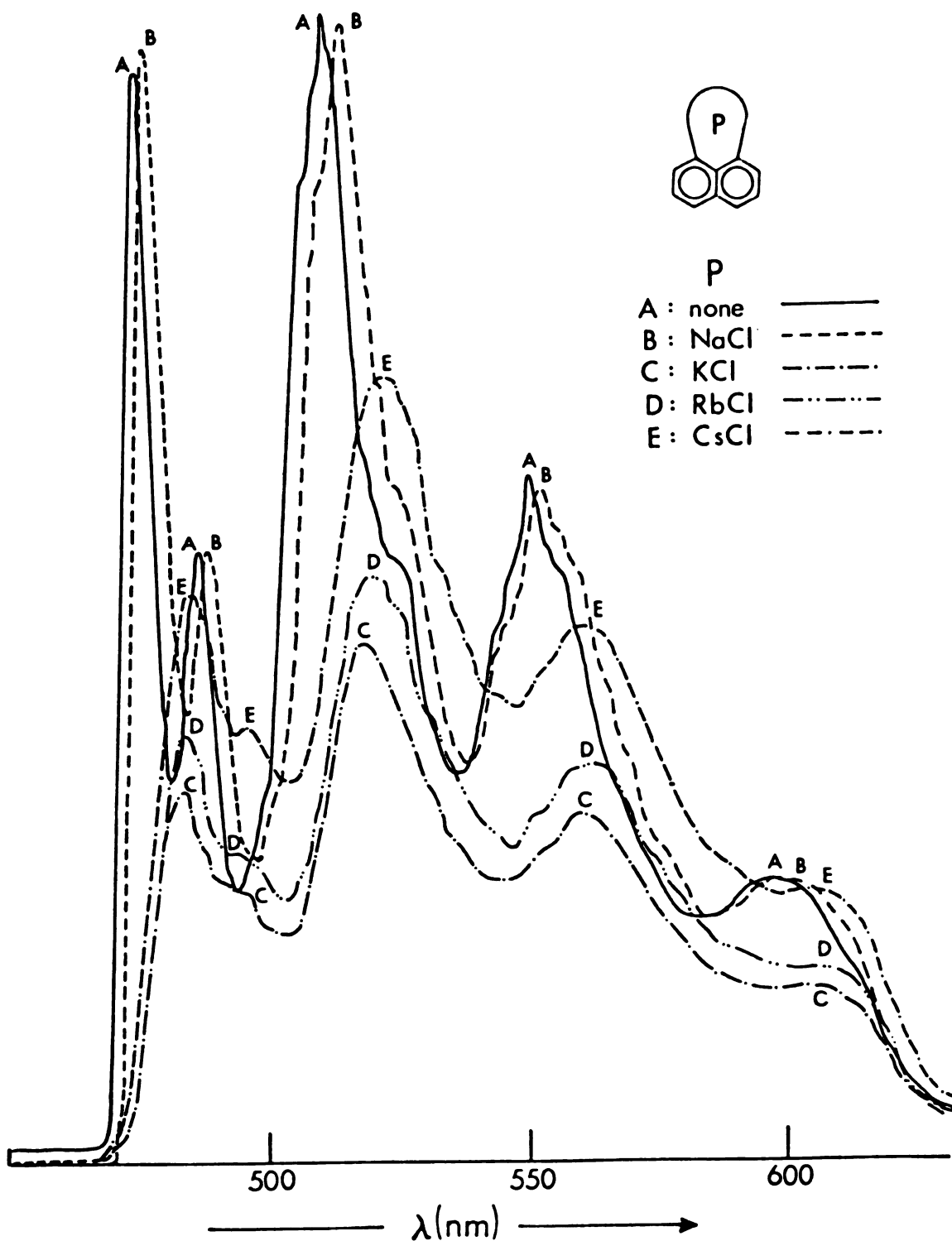


Figure 28. Corrected phosphorescence spectra of  $2.00 \times 10^{-4}$  M 1,8-naphtho-21-crown-6 (2) alone and with 5:1 molar excess of added alkali metal chlorides in uncracked 95% ethanol glass at 77 K.

# Perturbed Fluorescence of 1,5-Naphtho-22-Crown-6

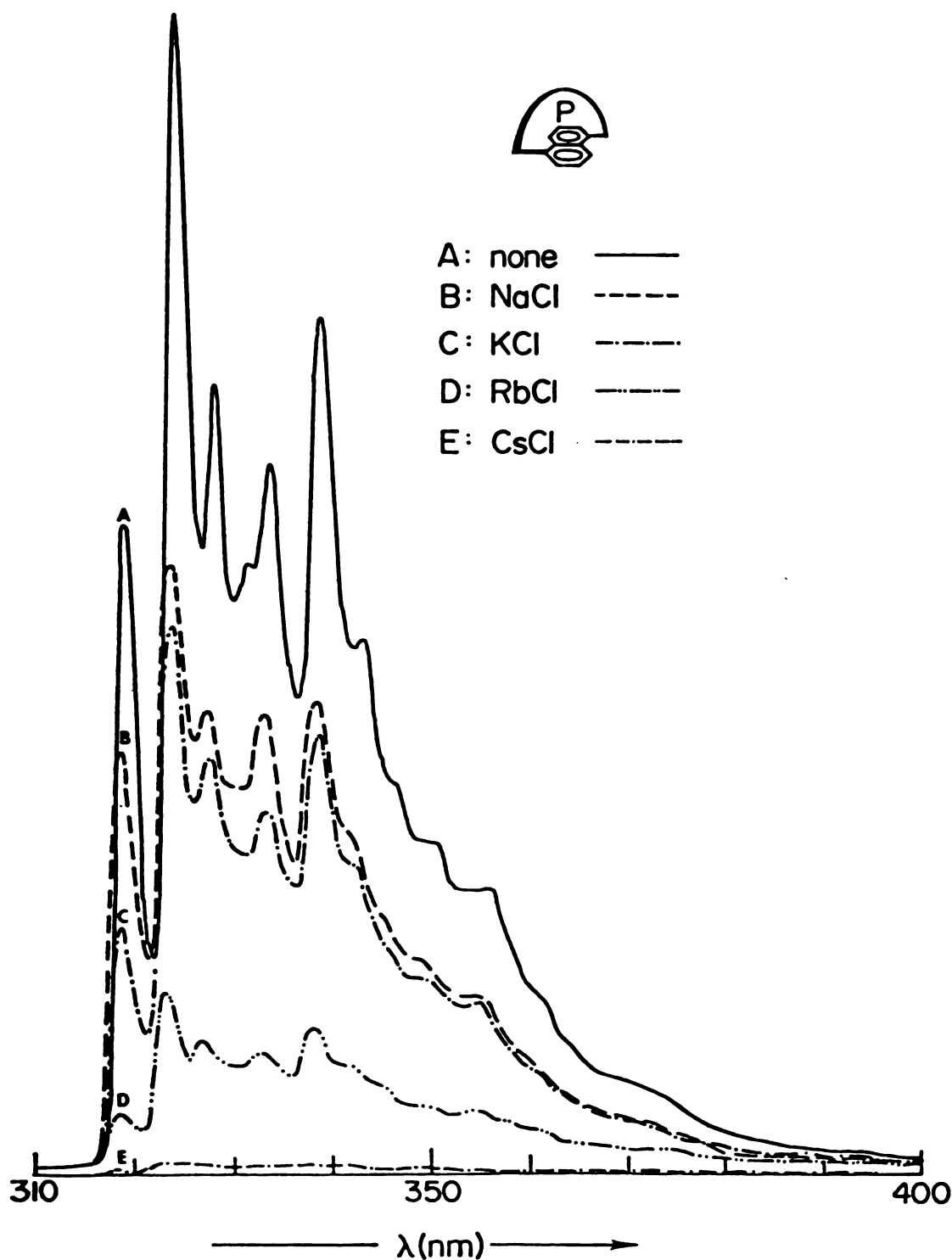


Figure 29. Corrected fluorescence spectra of  $1.00 \times 10^{-4} \text{ M}$  1,5-naphtho-22-crown-6 (3) alone and with 5:1 molar excess of added alkali metal chlorides in uncracked 95% ethanol glass at 77 K.

# Perturbed Phosphorescence of 1,5-Naphtho-22-Crown-6

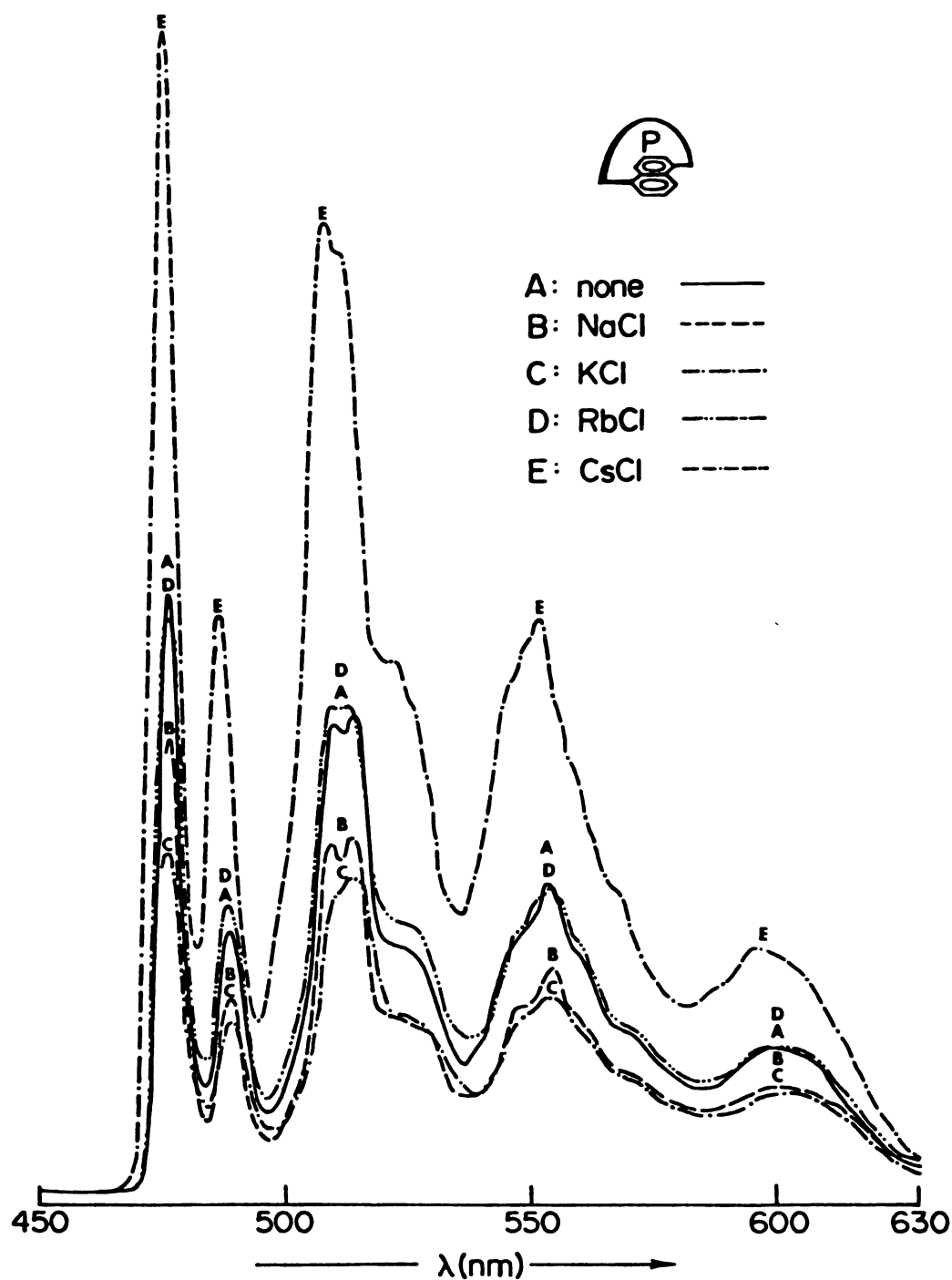


Figure 30. Corrected phosphorescence spectra of  $1.00 \times 10^{-4} \text{ M}$  1,5-naphtho-22-crown-6 (3) alone and with 5:1 molar excess of added alkali metal chlorides in uncracked 95% ethanol glass at 77 K.

# Perturbed Fluorescence of 2,3-Naphtho-20-Crown-6

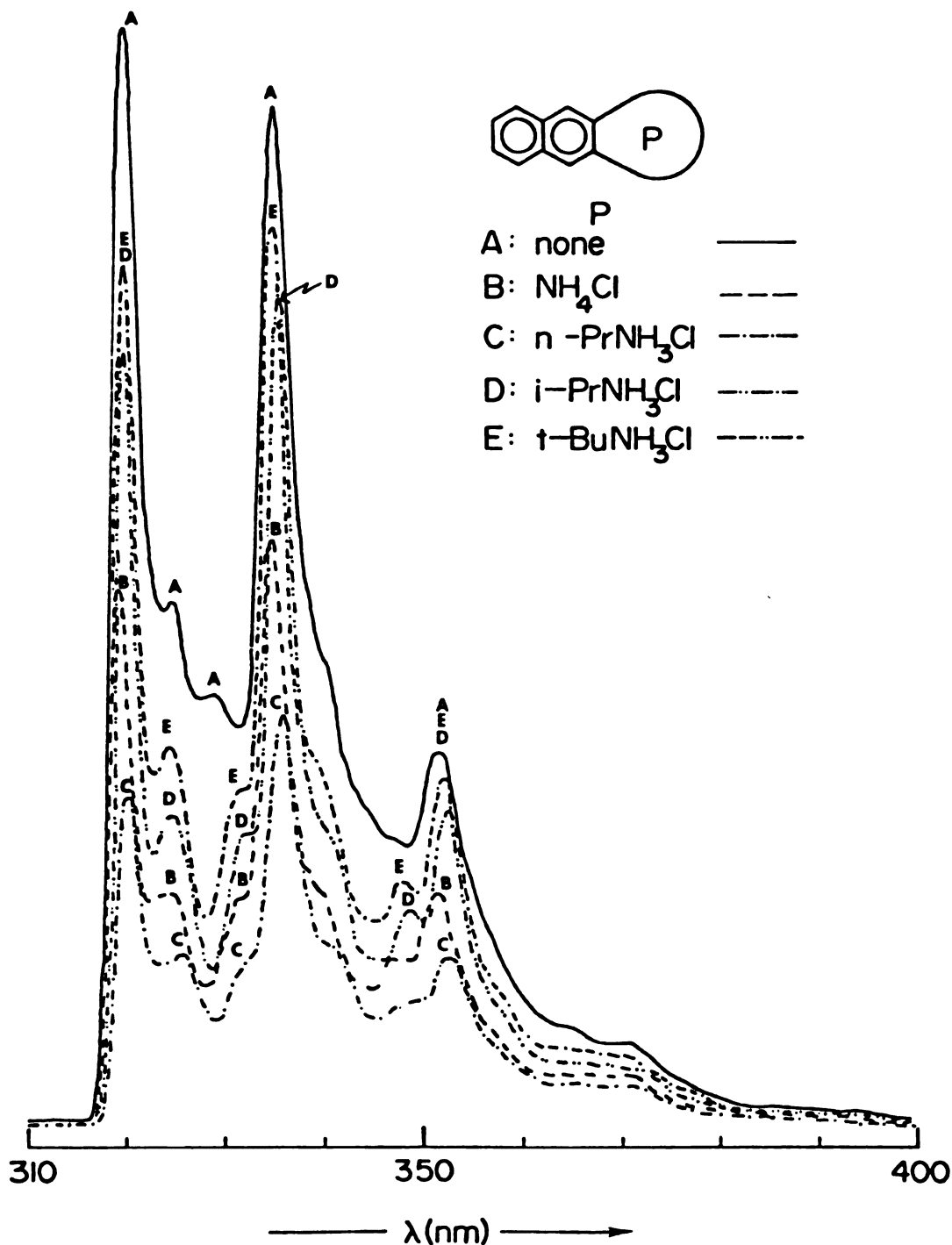


Figure 31. Corrected fluorescence spectra of  $2.00 \times 10^{-4} \text{ M}$  2,3-naphtho-20-crown-6 (1) alone and with 5:1 molar excess of added ammonium and alkylammonium chlorides in un-cracked 95% ethanol glass at 77 K.



# Perturbed Phosphorescence of 2,3-Naphtho-20-Crown-6

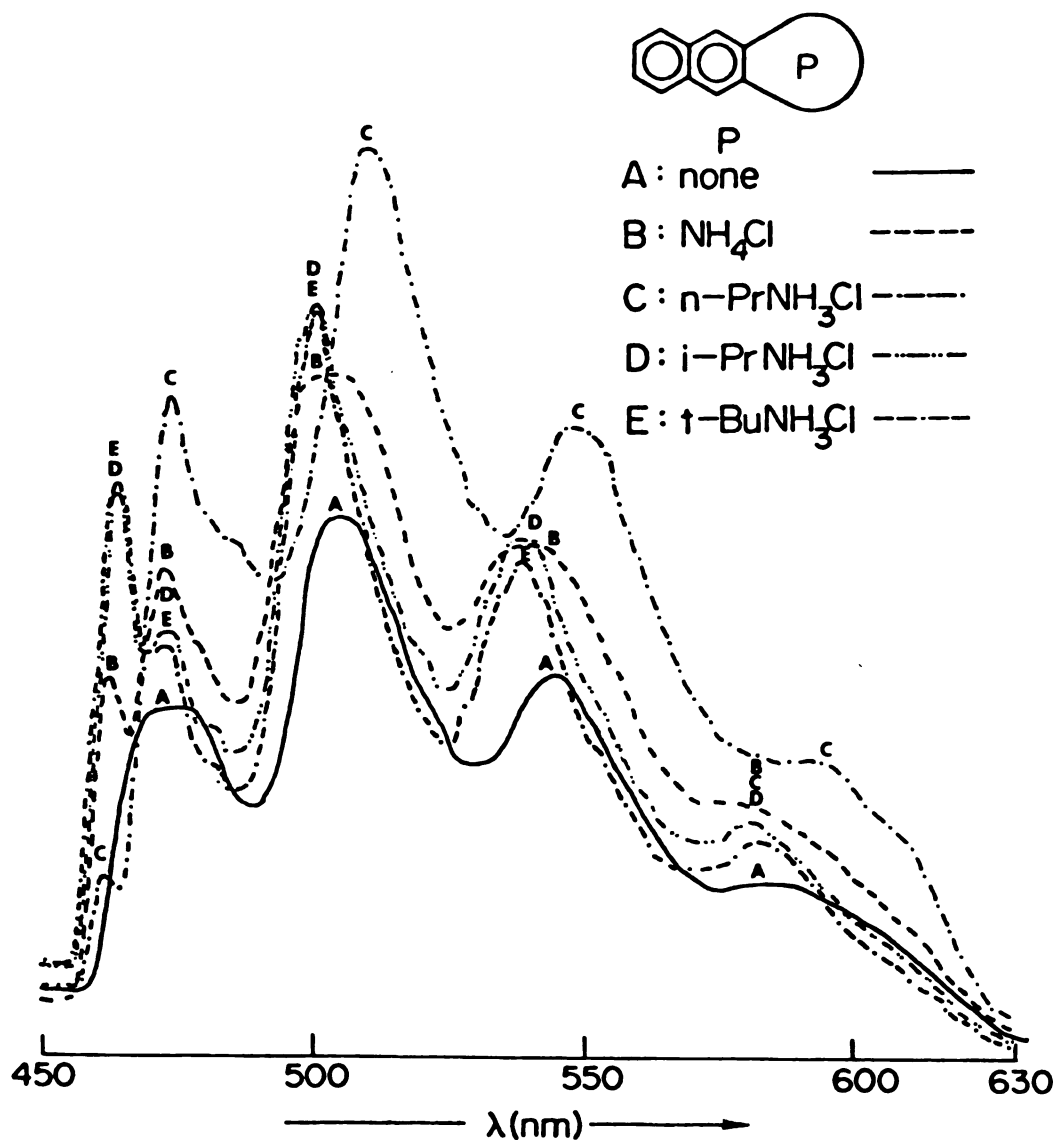


Figure 32. Corrected phosphorescence spectra of  $2.00 \times 10^{-4} \text{ M}$  2,3-naphtho-20-crown-6 ( $\text{P}$ ) alone and with 5:1 molar excess of added ammonium and alkylammonium chlorides in uncracked 95% ethanol glass at 77 K.

# Perturbed Fluorescence of 1,8-Naphtho-21-Crown-6

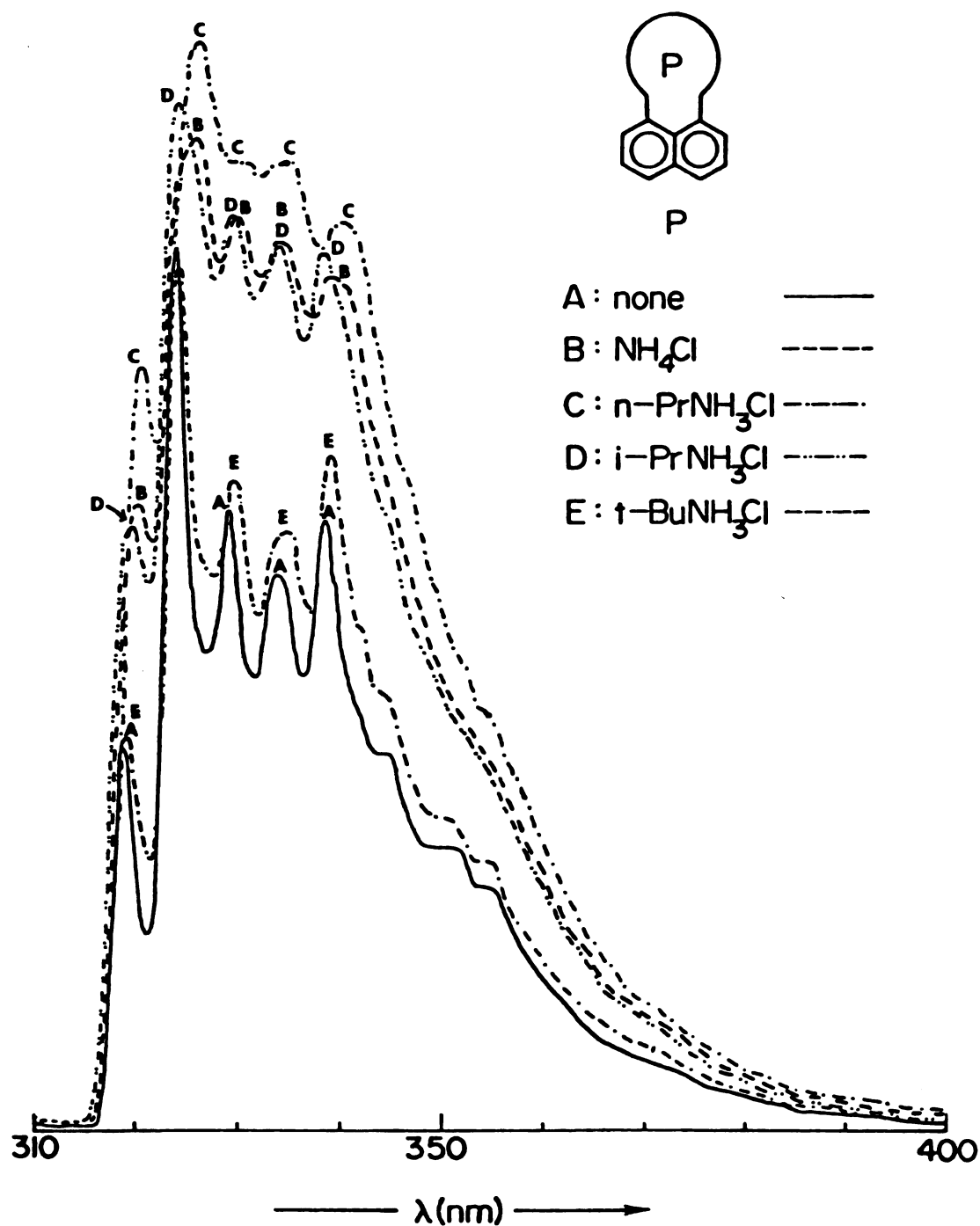
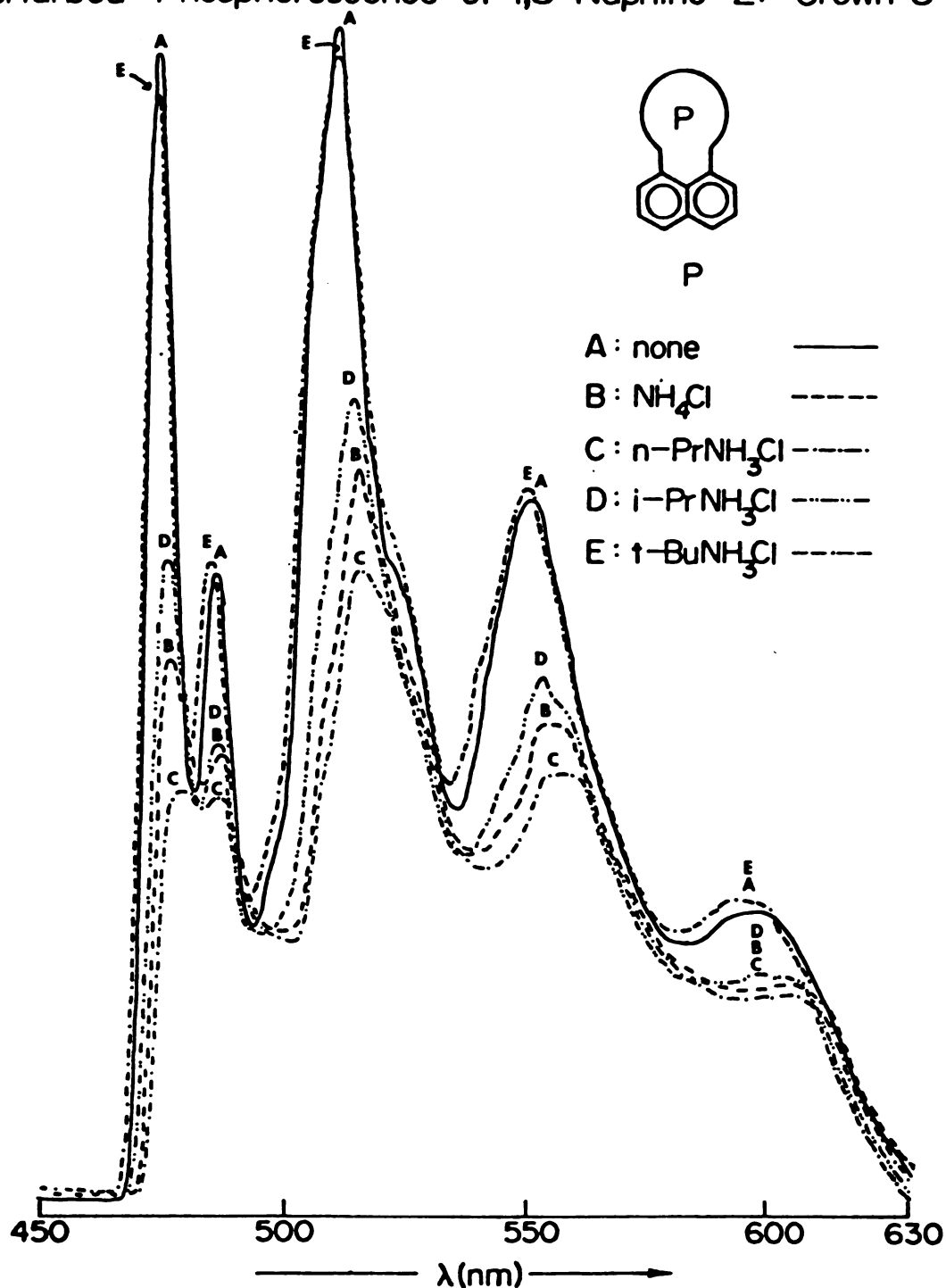


Figure 33. Corrected fluorescence spectra of  $2.00 \times 10^{-4}$  M 1,8-naphtho-21-crown-6 (P) alone and with 5:1 molar excess of added ammonium and alkylammonium chlorides in uncracked 95% ethanol glass at 77 K.

# Perturbed Phosphorescence of 1,8-Naphtho-21-Crown-6



# Perturbed Fluorescence of 1,5-Naphtho-22-Crown-6

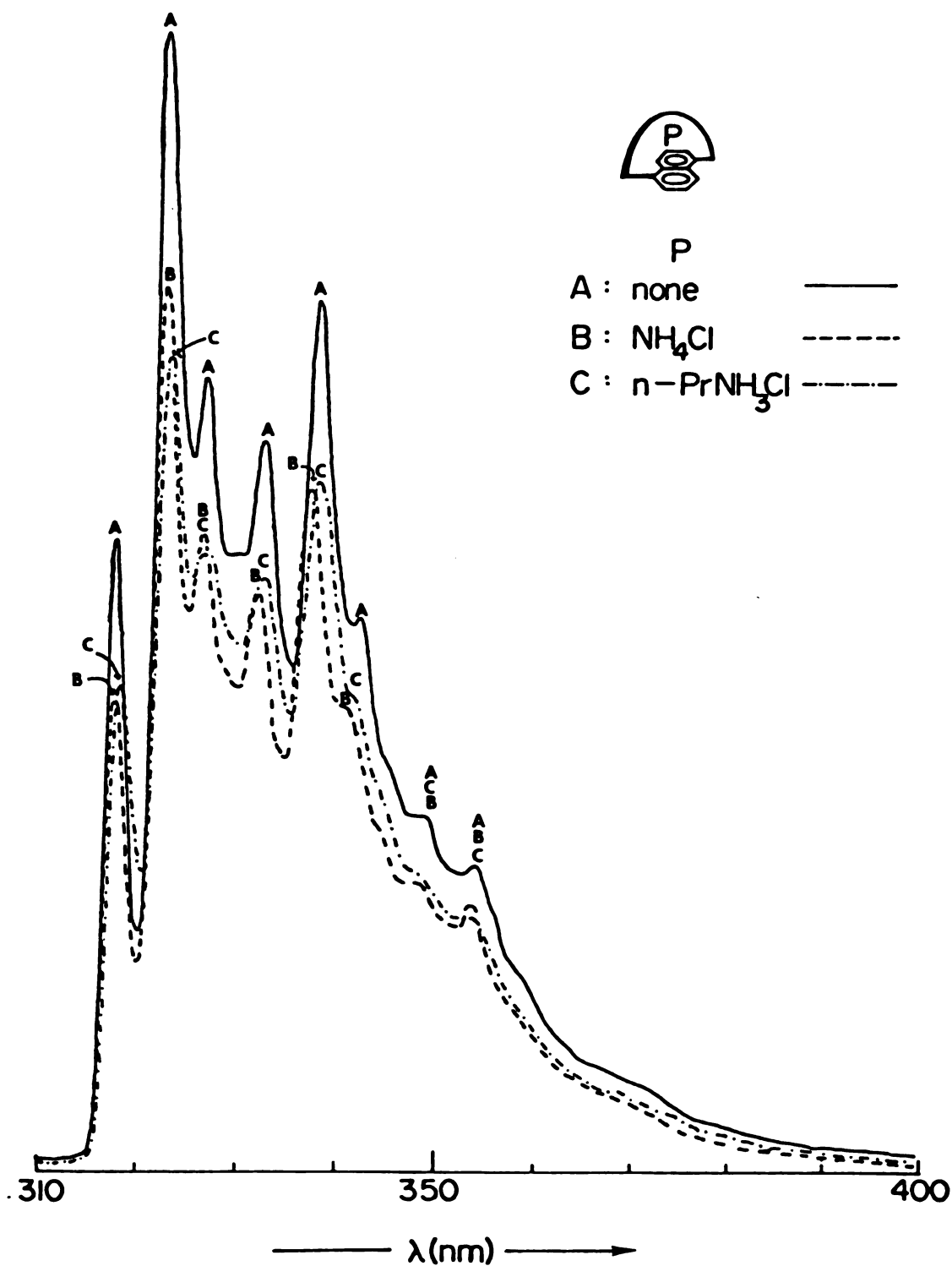


Figure 35. Corrected fluorescence spectra of  $1.00 \times 10^{-4} \text{ M}$  1,5-naphtho-22-crown-6 ( $\text{P}$ ) alone and with 50:1 and 10:1 added molar excesses of ammonium and *n*-propylammonium chlorides, respectively, in uncracked 95% ethanol glass at 77 K.

# Perturbed Phosphorescence of 1,5-Naphtho-22-Crown-6

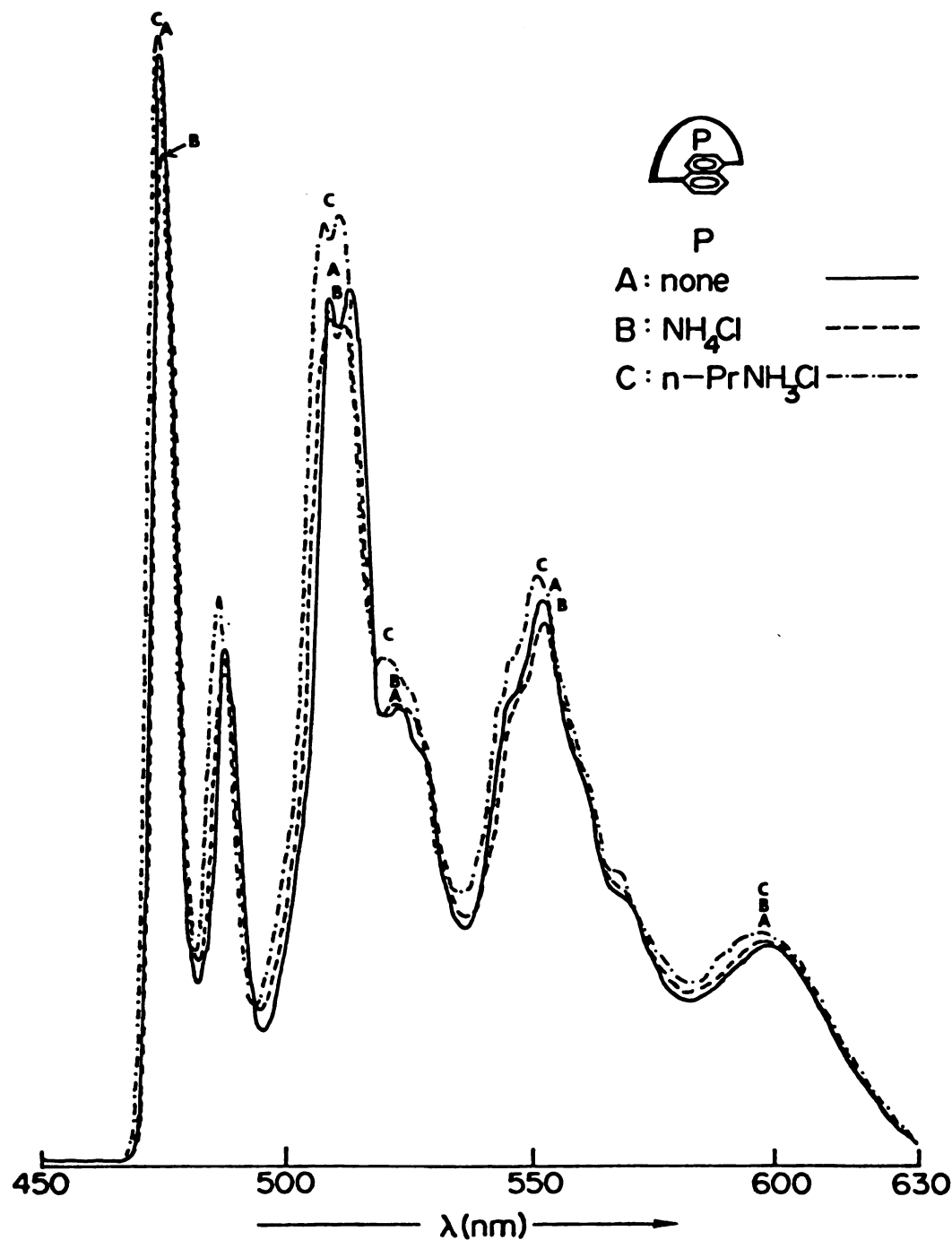


Figure 36. Corrected phosphorescence spectra of  $1.00 \times 10^{-4} \text{ M}$  1,5-naphtho-22-crown-6 ( $\text{P}$ ) alone and with 50:1 and 10:1 added molar excesses of ammonium and *n*-propylammonium chlorides, respectively, in uncracked 95% ethanol glass at 77 K.

# Perturbed Fluorescence of 2,3-Naphtho-20-Crown-6

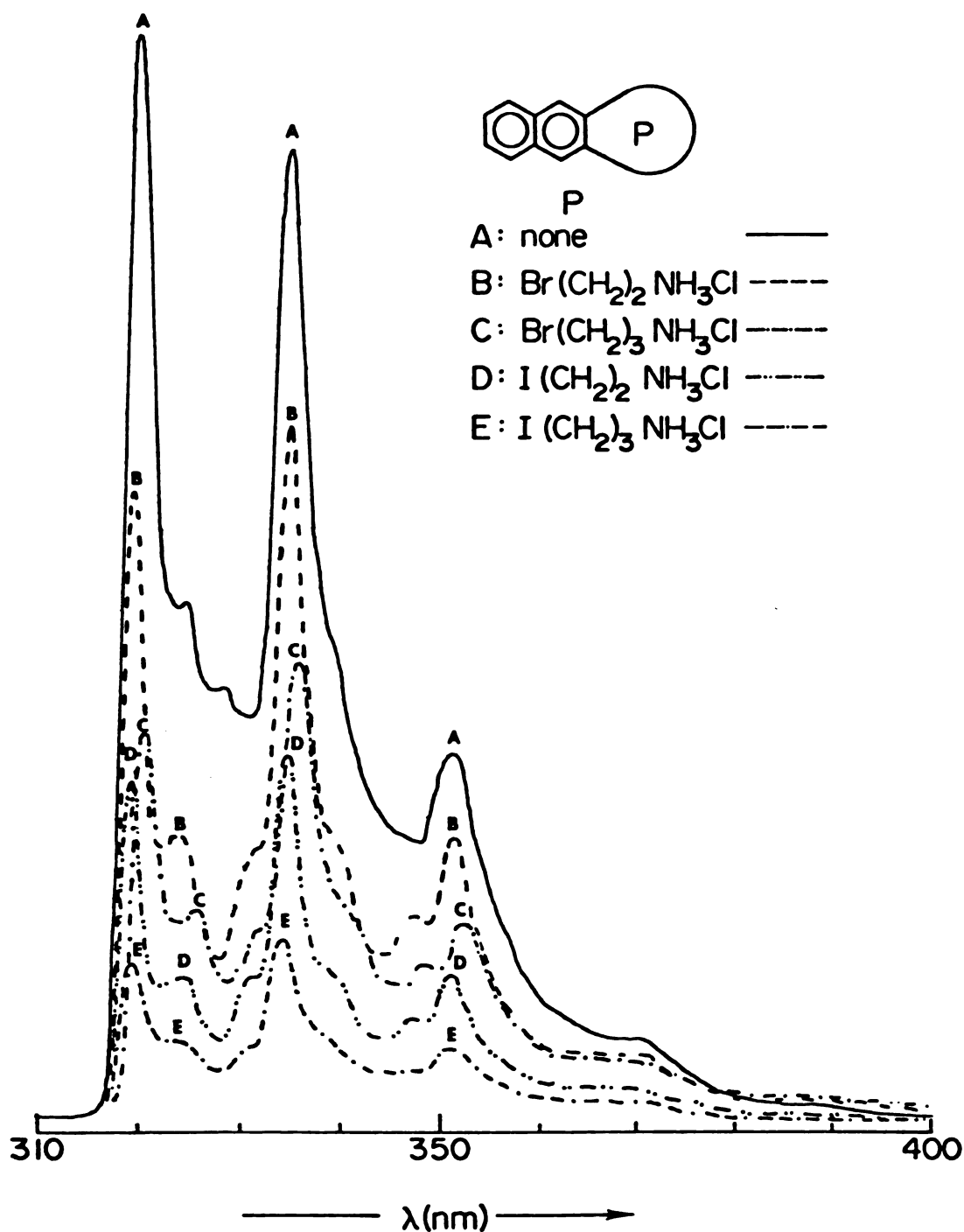


Figure 37. Corrected fluorescence spectra of 2,3-naphtho-20-crown-6 (1) alone and with 5:1 added molar excess of bromoalkylammonium chlorides ( $2.00 \times 10^{-4} \text{ M}$  crown) and 20:1 added molar excess of iodoalkylammonium chlorides ( $1.00 \times 10^{-4} \text{ M}$  crown) in uncracked 95% ethanol glass at 77 K.

# Perturbed Phosphorescence of 2,3-Naphtho-20-Crown-6

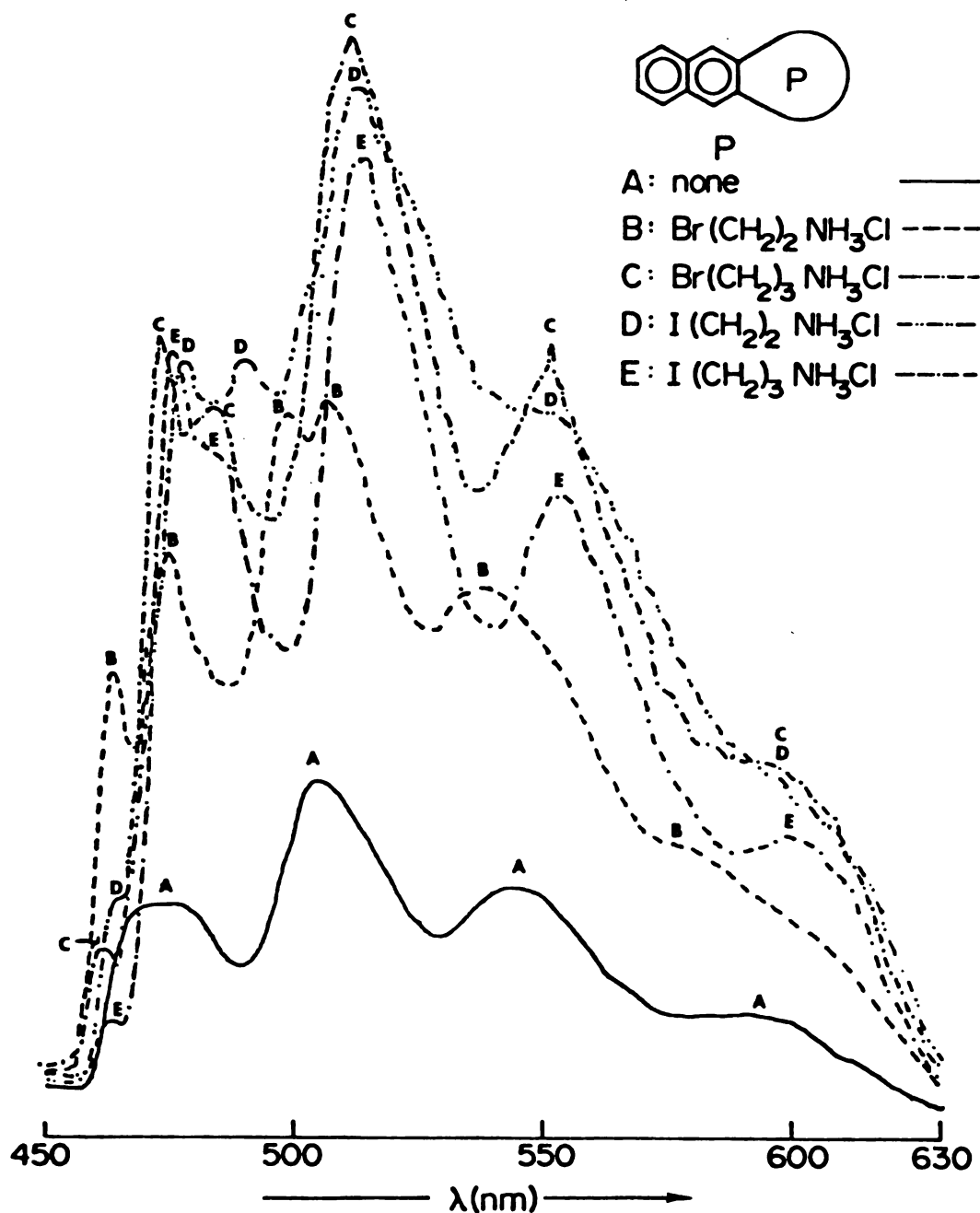


Figure 38. Corrected phosphorescence spectra of 2,3-naphtho-20-crown-6 (1) alone and 5:1 molar excess of bromoalkylammonium chlorides ( $2.00 \times 10^{-4}$  M crown) and 20:1 molar excess of iodoalkylammonium chlorides ( $1.00 \times 10^{-4}$  M crown) in uncracked 95% ethanol glass at 77 K.

# Perturbed Fluorescence of 1,8-Naphtho-21-Crown-6

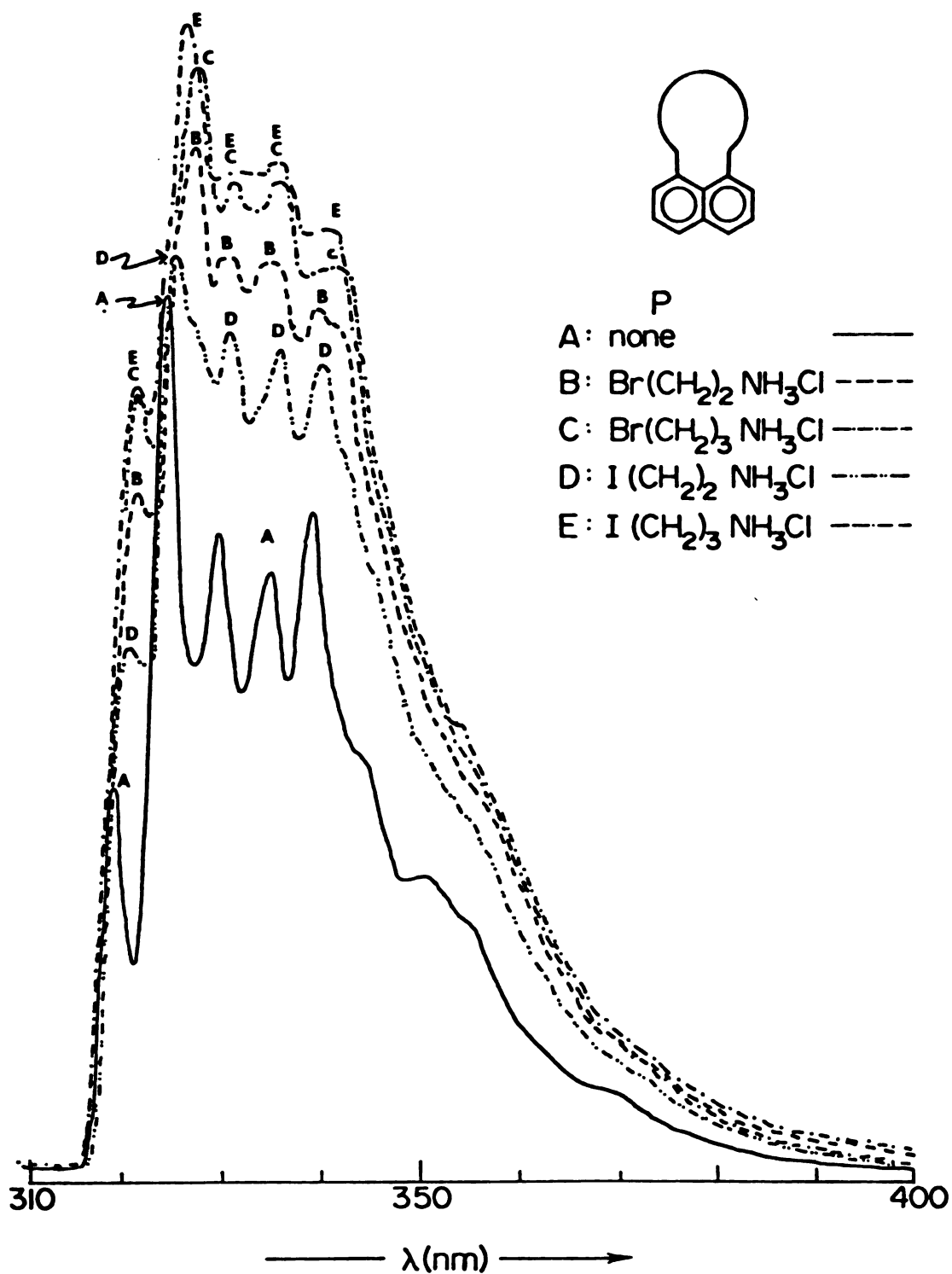


Figure 39. Corrected fluorescence spectra of 1,8-naphtho-21-crown-6 ( $\lambda$ ) alone and with 5:1 added molar excess of bromoalkylammonium chlorides ( $2.00 \times 10^{-4}$  M crown) and with 20:1 added molar excess of iodoalkylammonium chlorides ( $1.00 \times 10^{-4}$  M crown) in uncracked 95% ethanol glass at 77 K.



# Perturbed Phosphorescence of 1,8-Naphtho-21-Crown-6

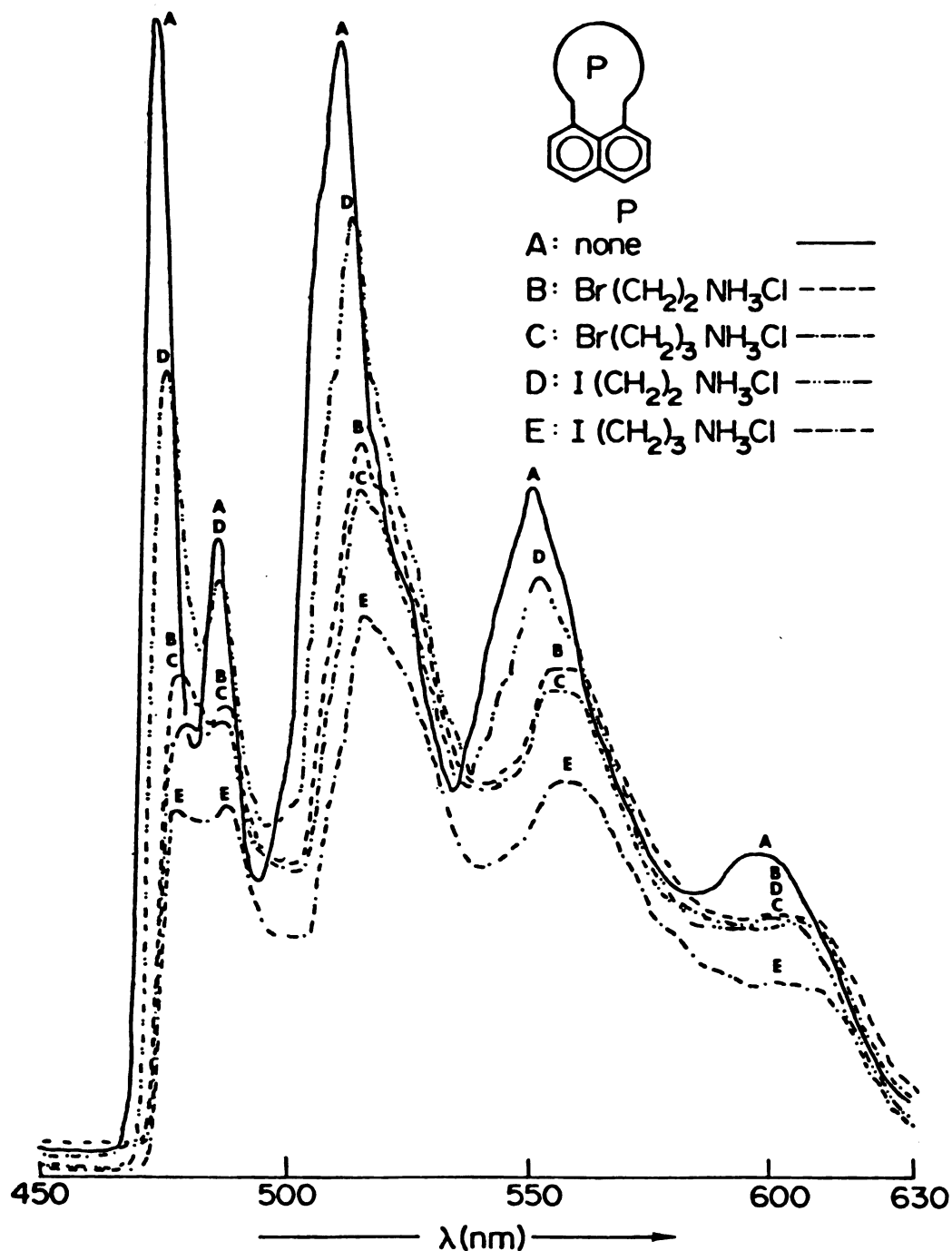


Figure 40. Corrected phosphorescence spectra of 1,8-naphtho-21-crown-6 (2) alone and with 5:1 added molar excess of bromoalkylammonium chlorides ( $2.00 \times 10^{-4}$  M crown) and with 20:1 added molar excess of iodoalkylammonium chlorides ( $1.00 \times 10^{-4}$  M crown) in 95% ethanol glass at 77 K.

# Perturbed Fluorescence of 1,5-Naphtho-22-Crown-6

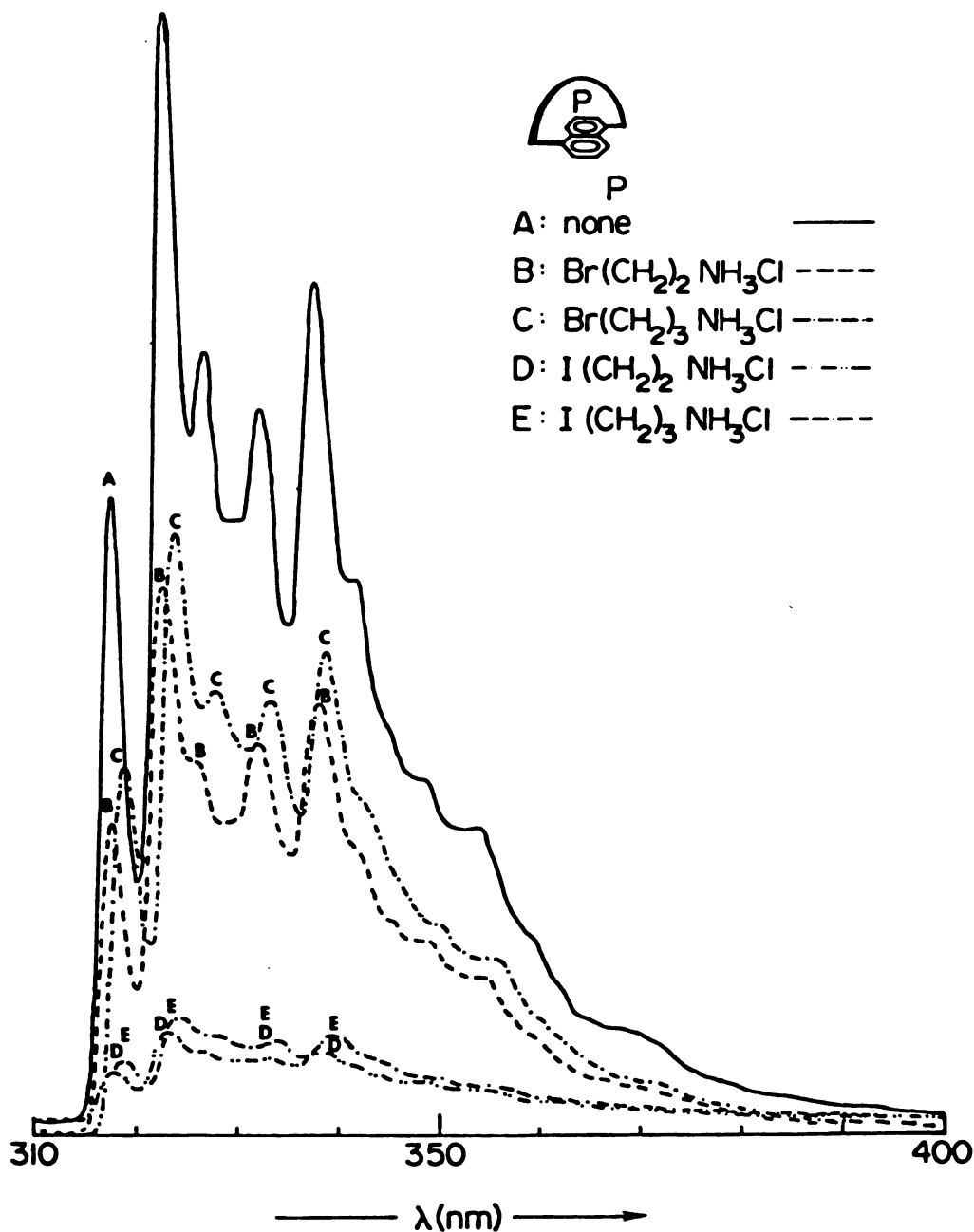


Figure 41. Corrected fluorescence spectra of  $1.00 \times 10^{-4}$  M 1,5-naphtho-22-crown-6 (P) alone and with 20:1 added molar excess of bromo- and iodoalkylammonium chlorides in uncracked 95% ethanol glass at 77 K.

# Perturbed Phosphorescence of 1,5-Naphtho-22-Crown-6

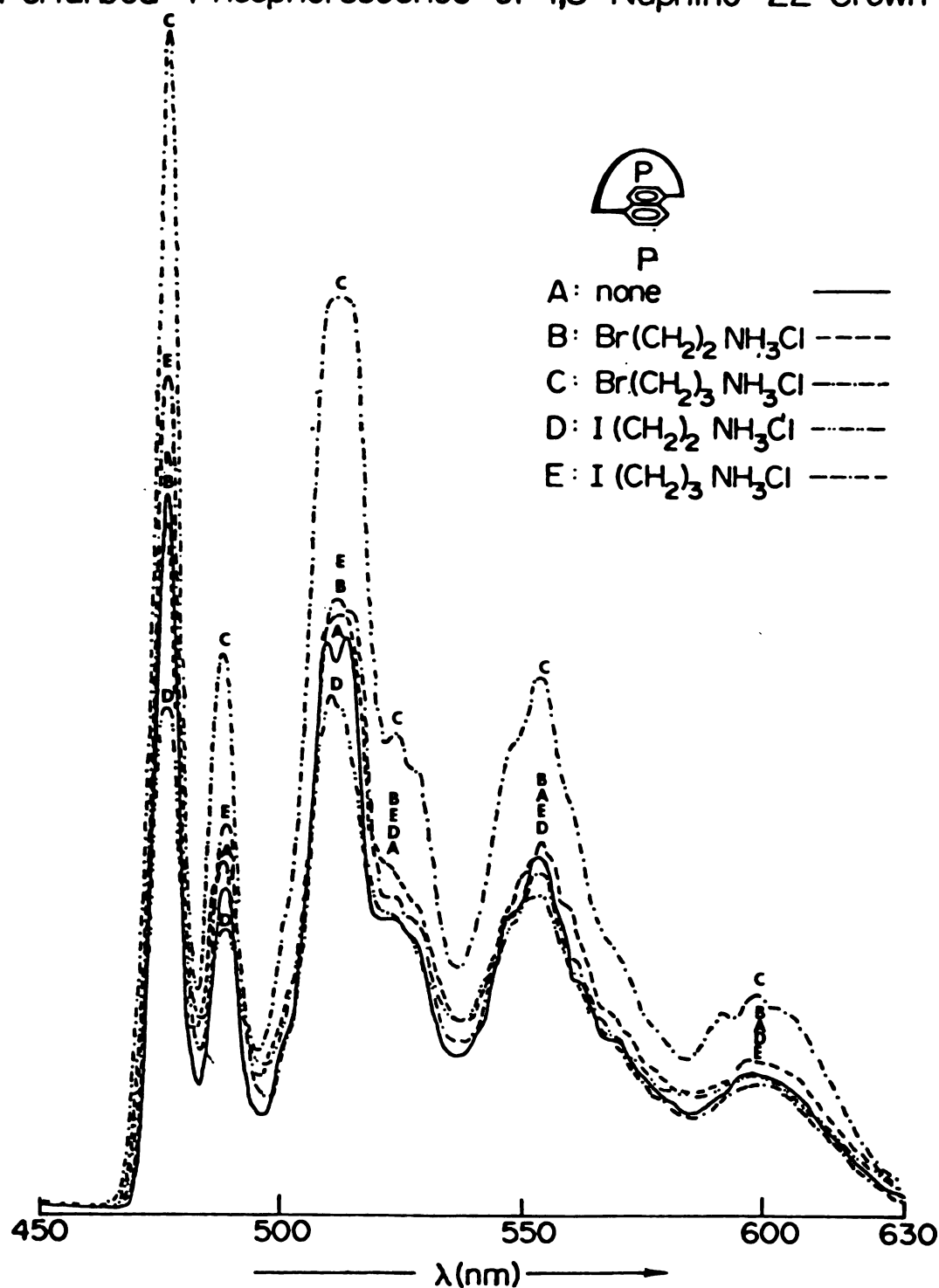


Figure 42. Corrected phosphorescence spectra of  $1.00 \times 10^{-4} \text{ M}$  1,5-naphtho-22-crown-6 (3) alone and with 20:1 added molar excess of bromo- and iodoalkylammonium chlorides in uncracked 95% ethanol glass at 77 K.

# Perturbed Fluorescence of 2,3-Naphtho-20-Crown-6

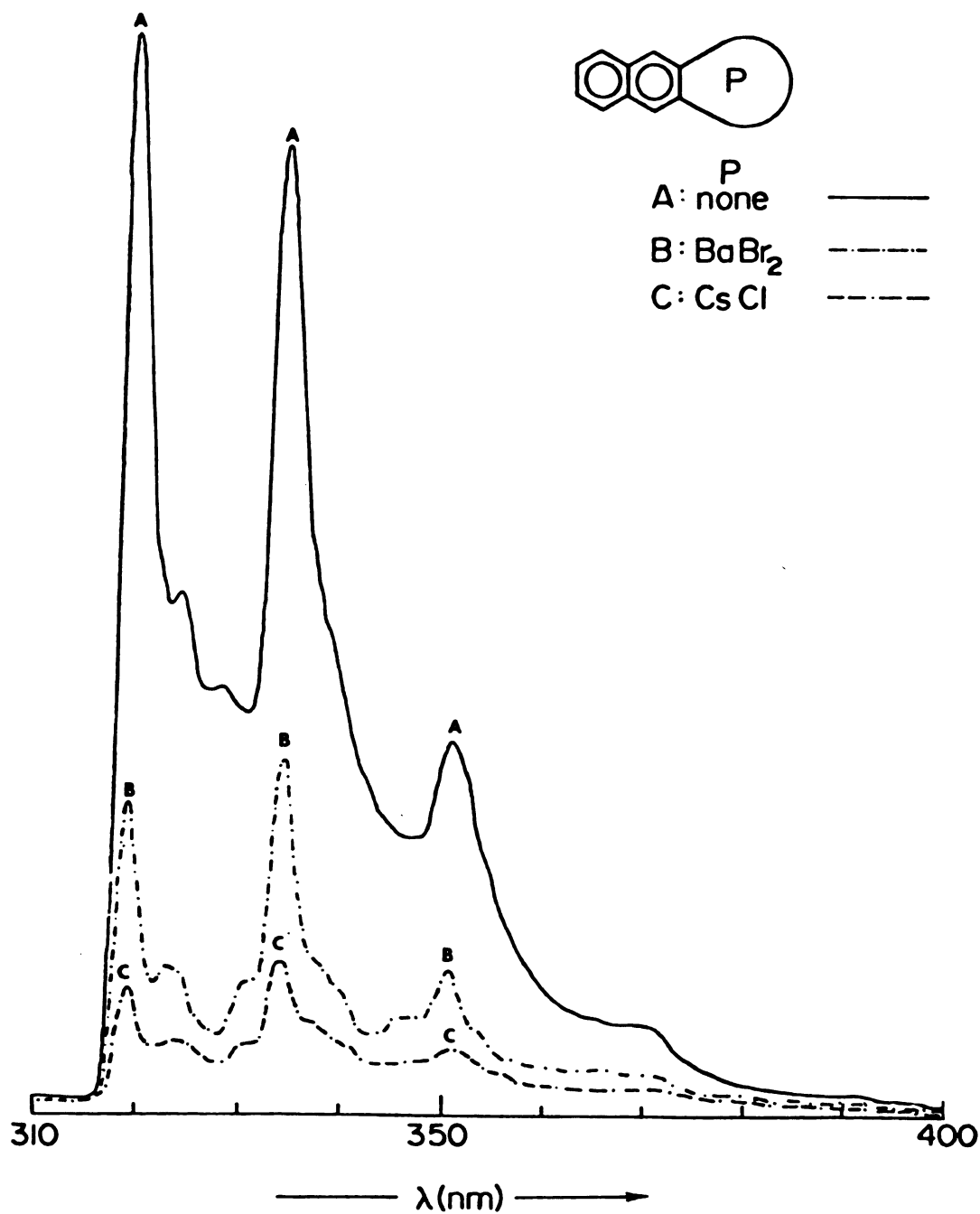


Figure 43. Corrected fluorescence spectra of 2,3-naphtho-20-crown-6 (1) alone and with 5:1 added molar excess of cesium chloride ( $2.00 \times 10^{-4}$  M crown) and 10:1 added molar excess of barium bromide ( $1.00 \times 10^{-4}$  M crown) in uncracked 95% ethanol glass at 77 K.

# Perturbed Phosphorescence of 2,3-Naphtho-20-Crown-6

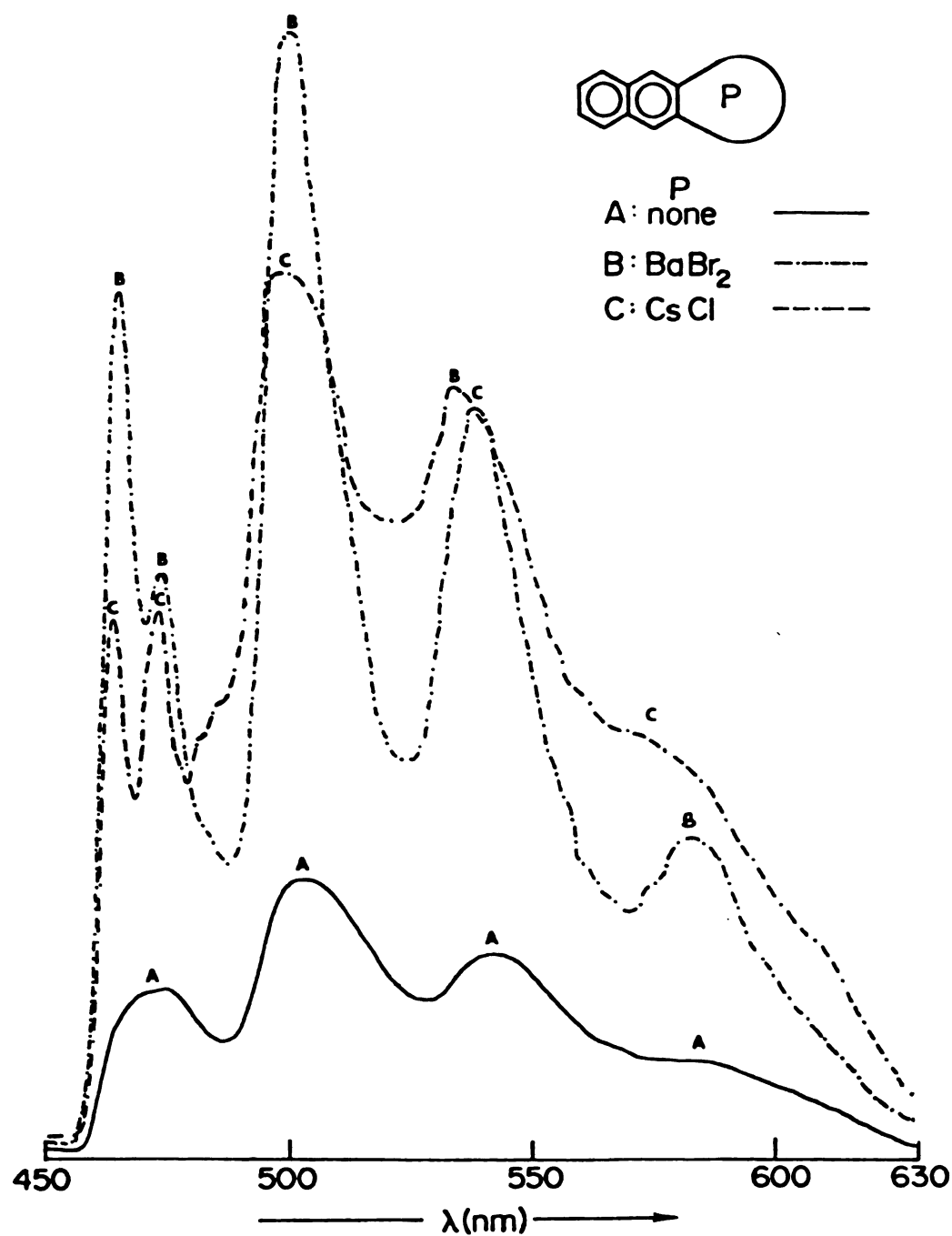


Figure 44. Corrected phosphorescence spectra of 2,3-naphtho-20-crown-6 (1) alone and with 5:1 added molar excess of cesium chloride ( $2.00 \times 10^{-4}$  M crown) and 10:1 added molar excess of barium bromide ( $1.00 \times 10^{-4}$  M crown) in uncracked 95% ethanol glass at 77 K.

# Perturbed Fluorescence of 1,8-Naphtho-21-Crown-6

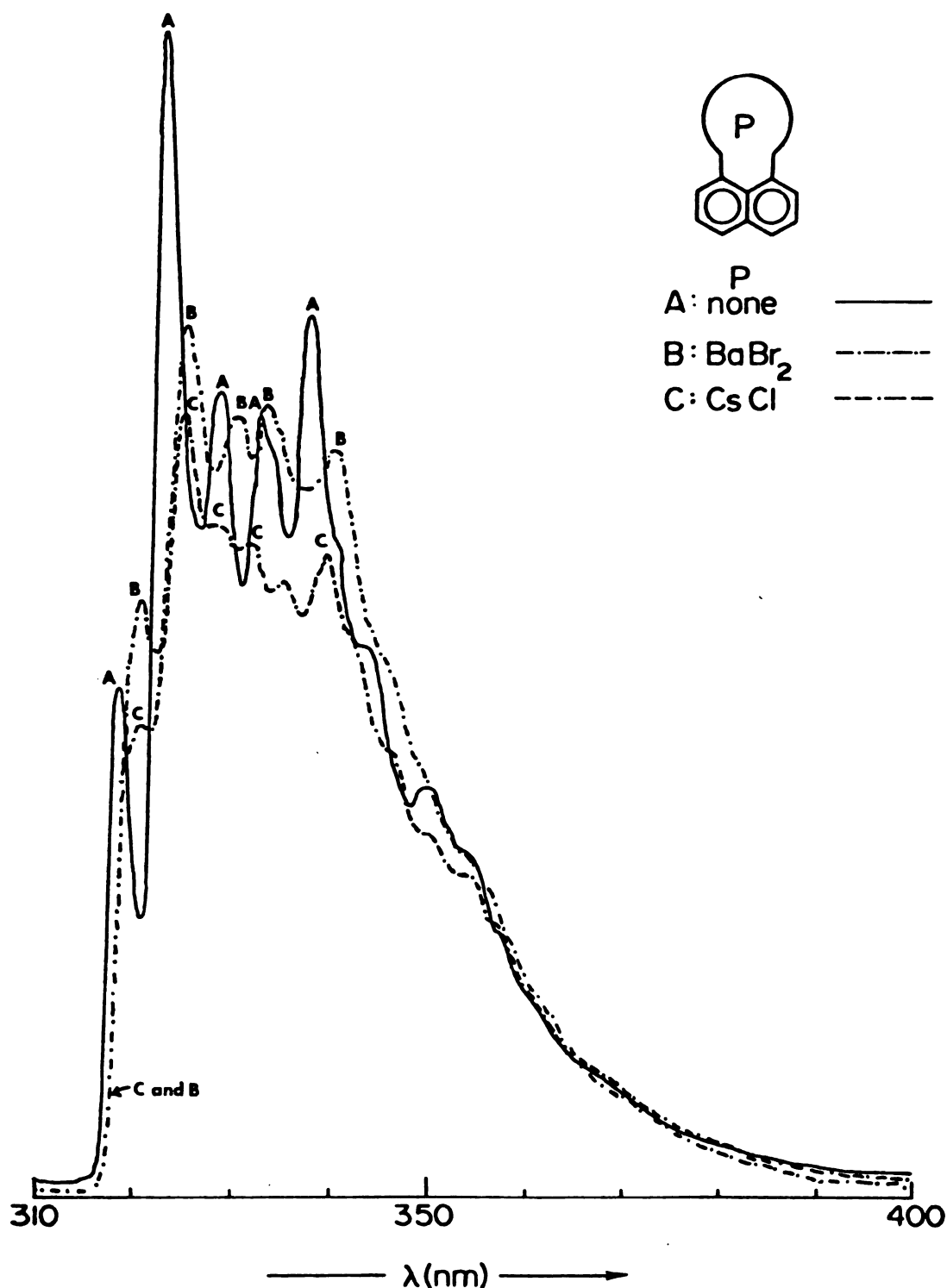


Figure 45. Corrected fluorescence spectra of 1,8-naphtho-21-crown-6 (2) alone and with 5:1 added molar excess of cesium chloride ( $2.00 \times 10^{-4}$  M crown) and 10:1 added molar excess of barium bromide ( $1.00 \times 10^{-4}$  M crown) in uncracked 95% ethanol glass at 77 K.

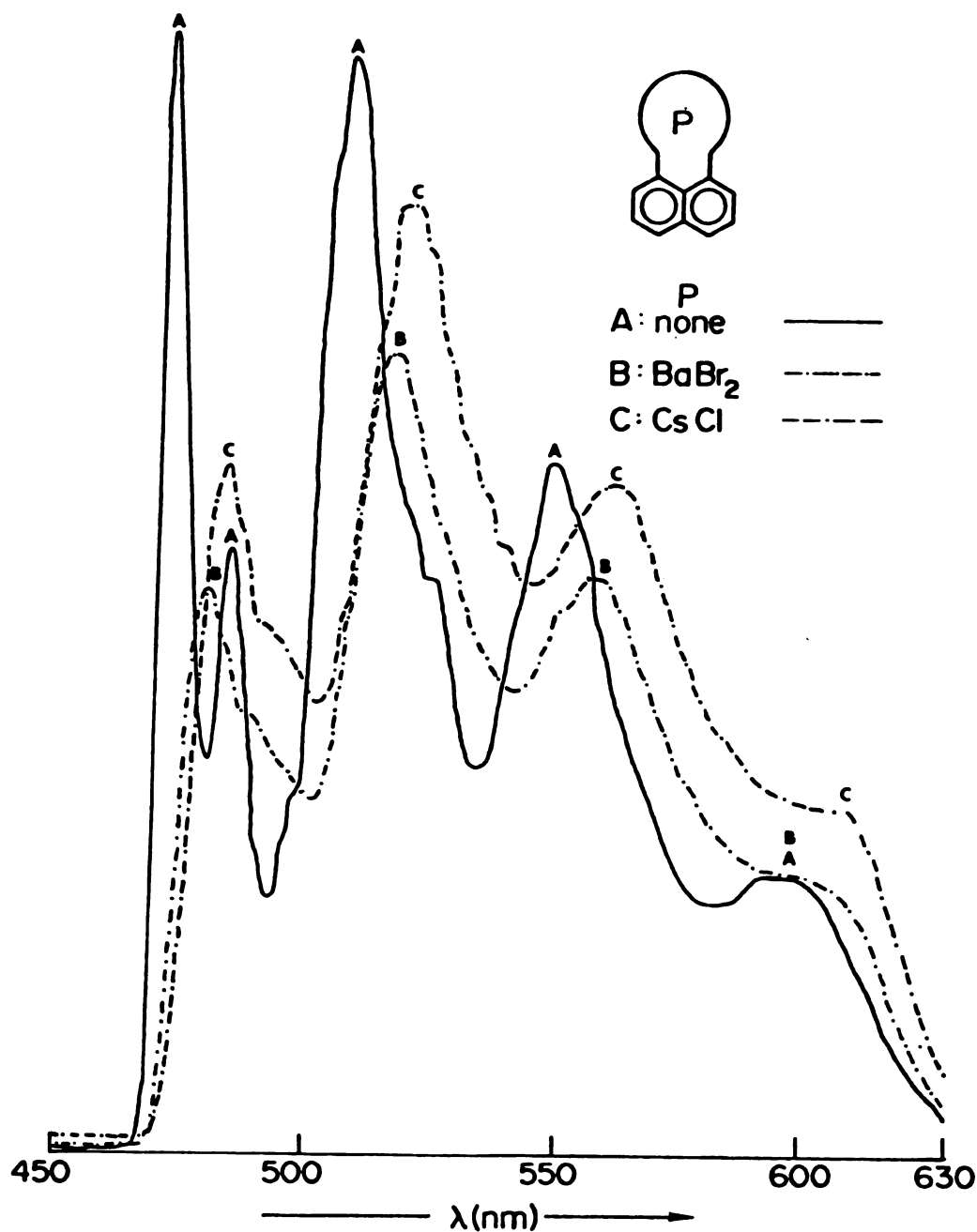


Figure 46. Corrected phosphorescence spectra of 1,8-naphtho-21-crown-6 (2) alone and with 5:1 added molar excess of cesium chloride ( $2.00 \times 10^{-4}$  M crown) and 10:1 added molar excess of barium bromide ( $1.00 \times 10^{-4}$  M crown) in uncracked 95% ethanol glass at 77 K.

# Perturbed Fluorescence of 1,5-Naphtho-22-Crown-6

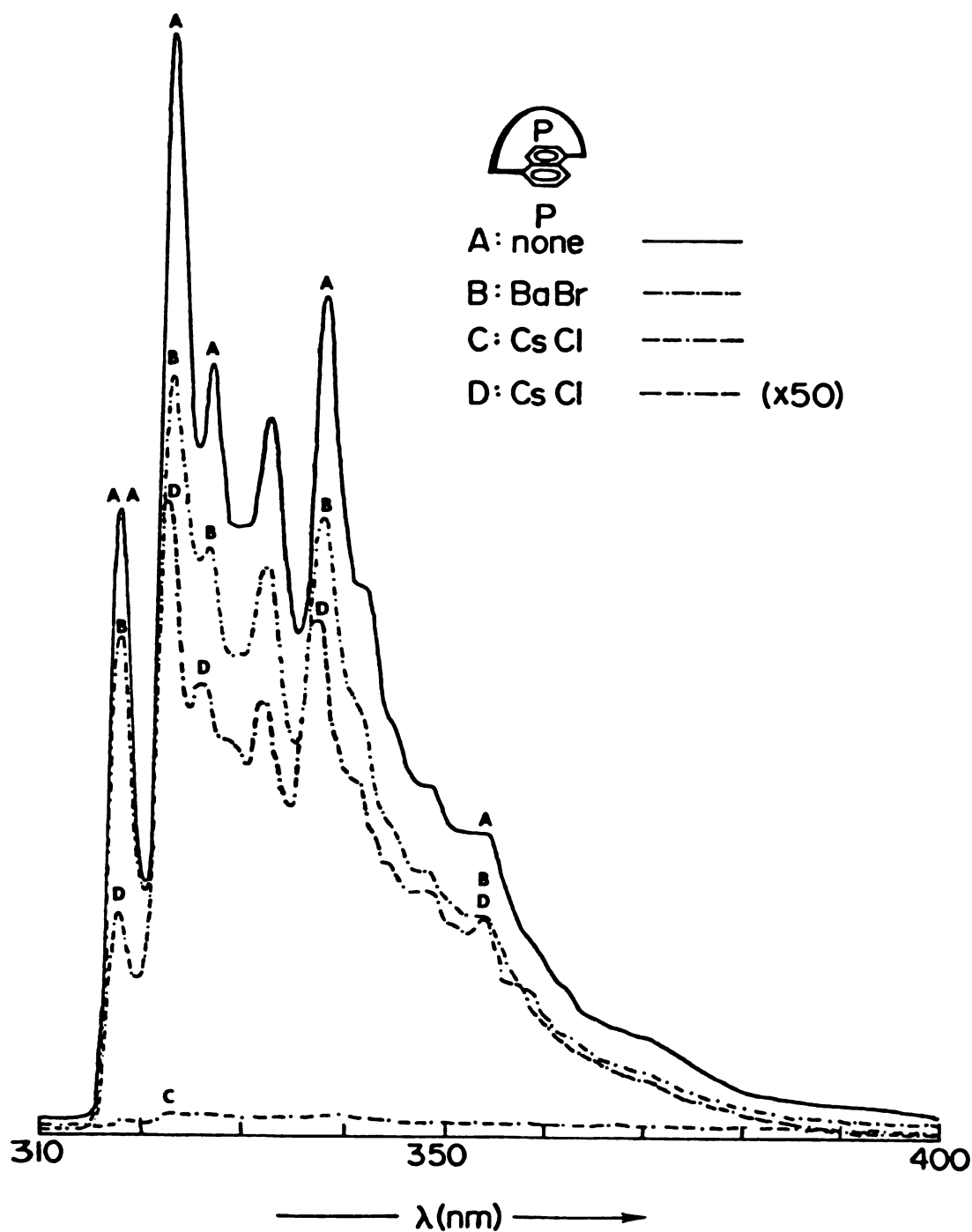


Figure 47. Corrected fluorescence spectra of 1,5-naphtho-22-crown-6 (3) alone and with 5:1 added molar excess of cesium chloride ( $2.00 \times 10^{-4}$  M crown) and 50:1 added molar excess of barium bromide ( $1.00 \times 10^{-4}$  M crown) in uncracked 95% ethanol glass at 77 K.



# Perturbed Phosphorescence of 1,5-Naphtho-22-Crown-6

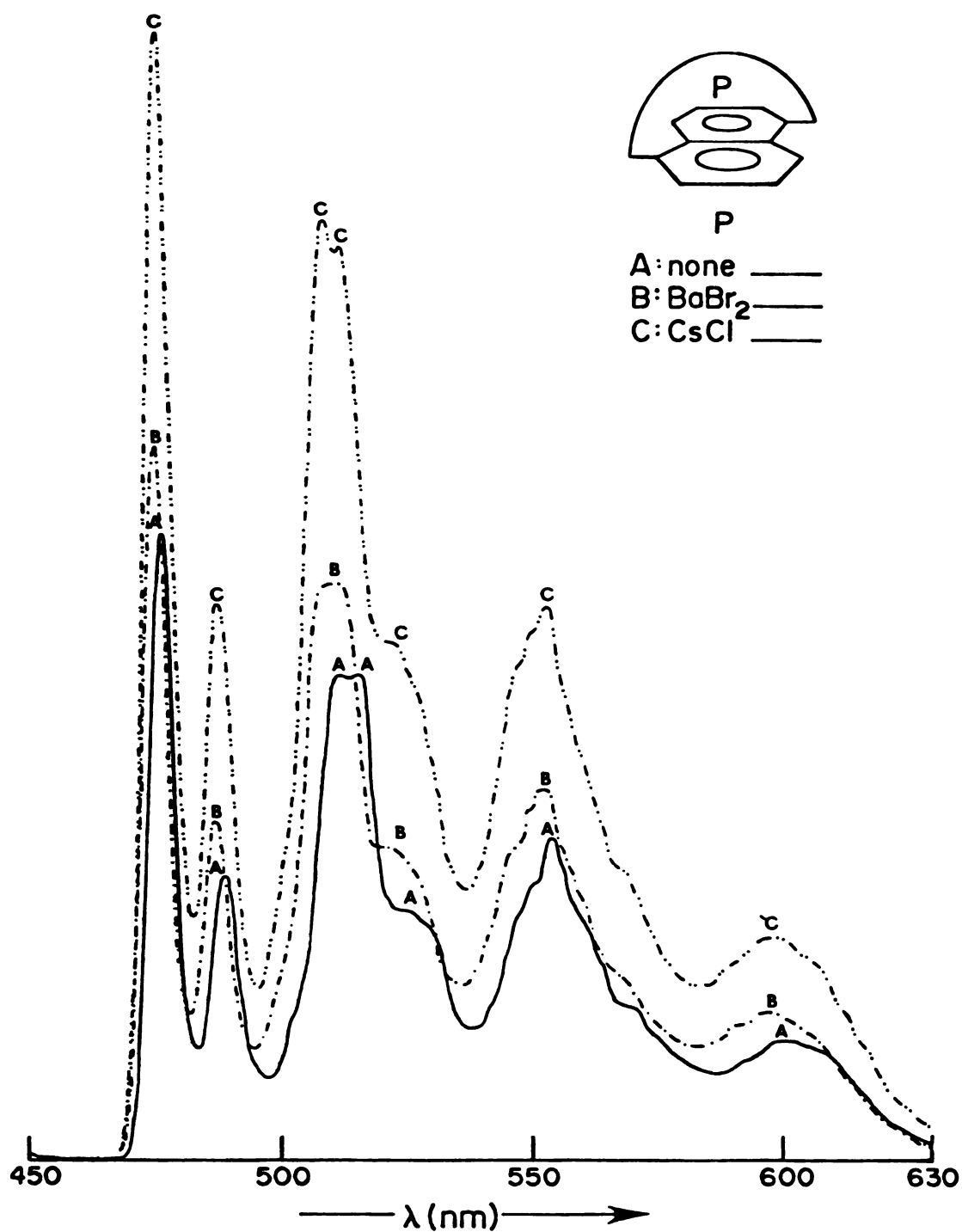


Figure 48. Corrected phosphorescence spectra of 1,5-naphtho-22-crown-6 (P) alone and with 5:1 added molar excess of cesium chloride ( $2.00 \times 10^{-4}$  M crown) and 50:1 added molar excess of barium bromide ( $1.00 \times 10^{-4}$  M crown) in uncracked 95% ethanol glass at 77 K.

# Perturbed Fluorescence of 2,3-Naphtho-20-Crown-6

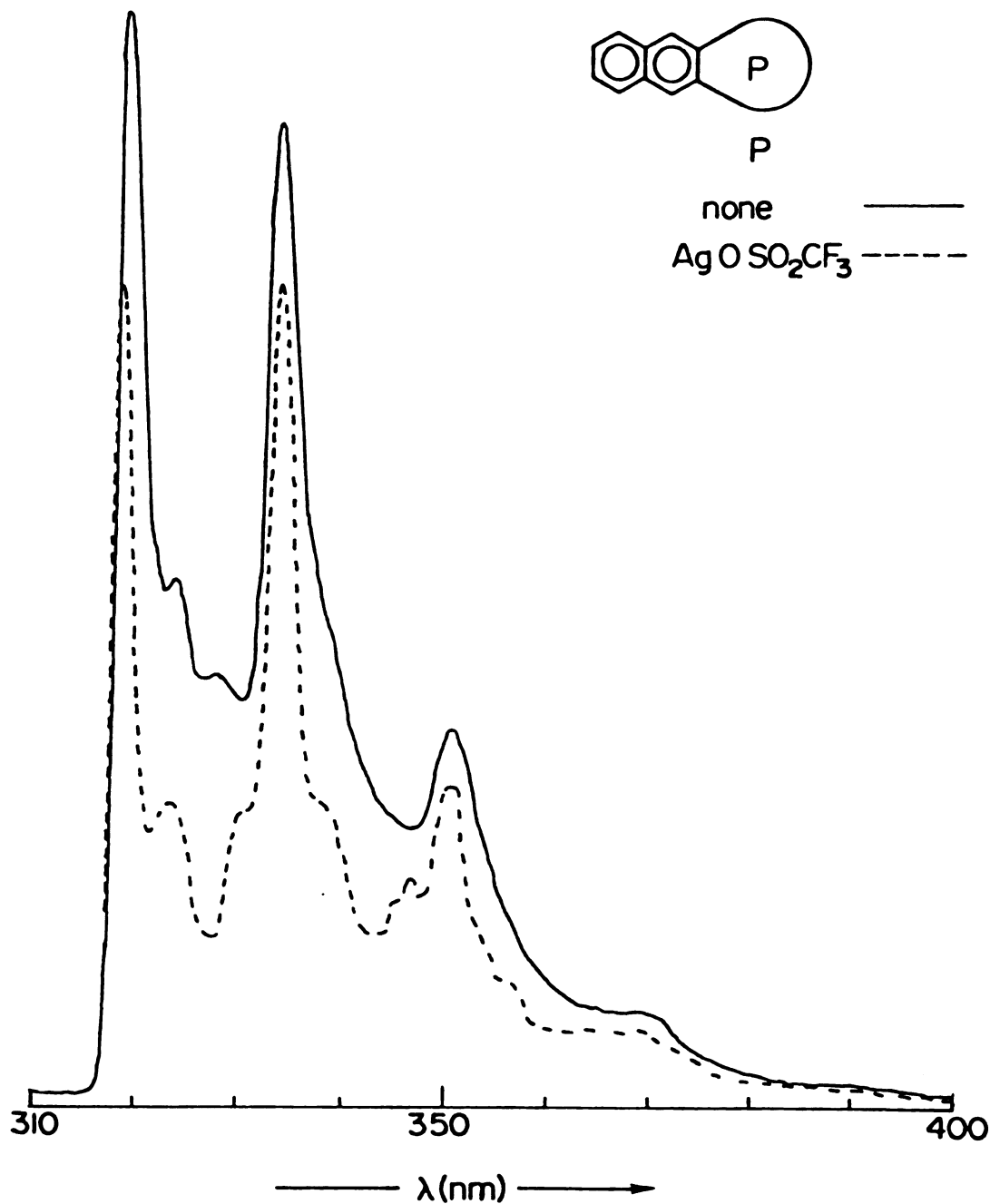
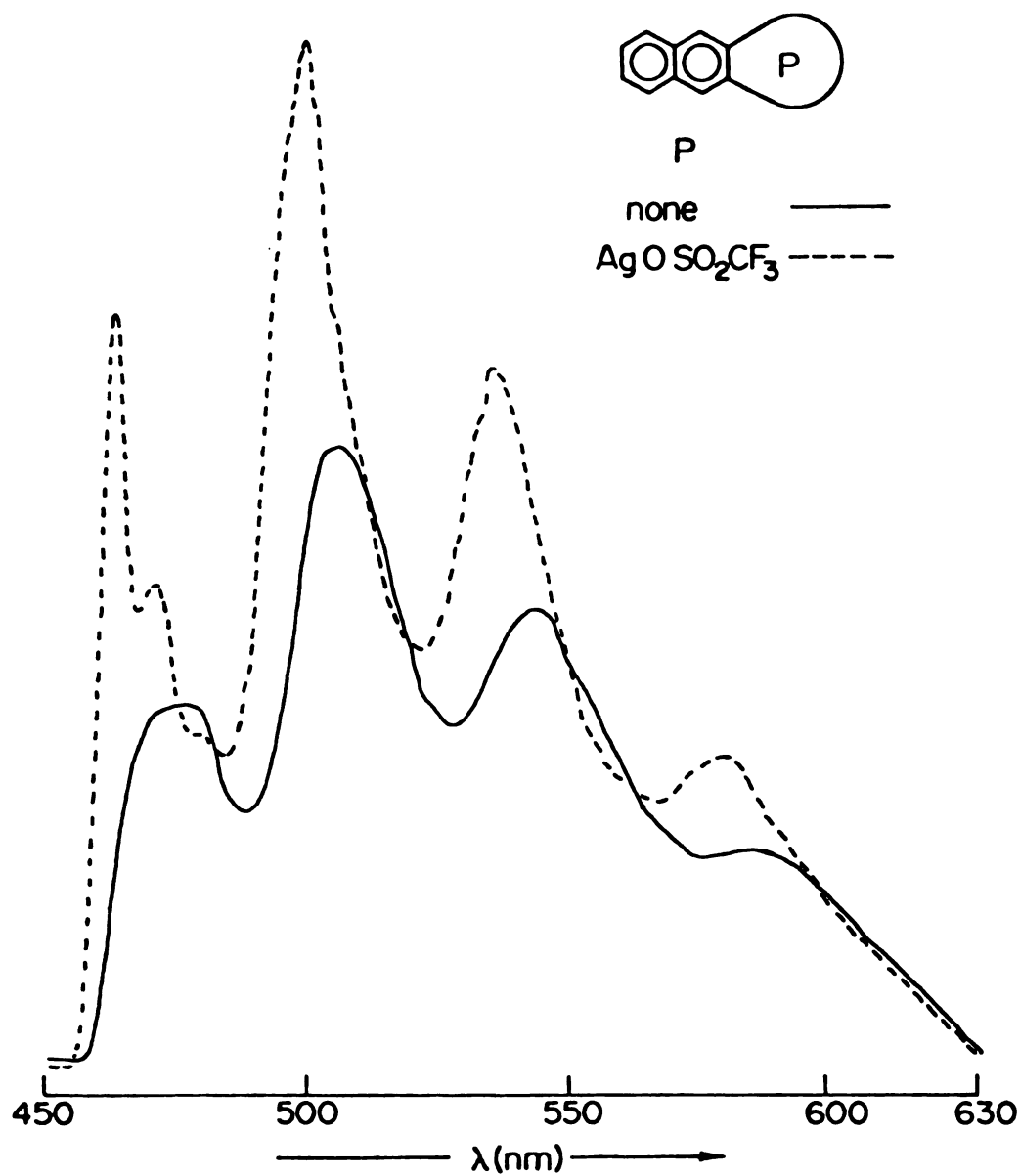


Figure 49. Corrected fluorescence spectra of  $1.00 \times 10^{-4}$  M 2,3-naphtho-20-crown-6 (1) alone and with 50:1 added molar excess of silver triflate in uncracked 95% ethanol glass at 77 K.

# Perturbed Phosphorescence of 2,3-Naphtho-20-Crown-6



# Perturbed Fluorescence of 1,8-Naphtho-21-Crown-6

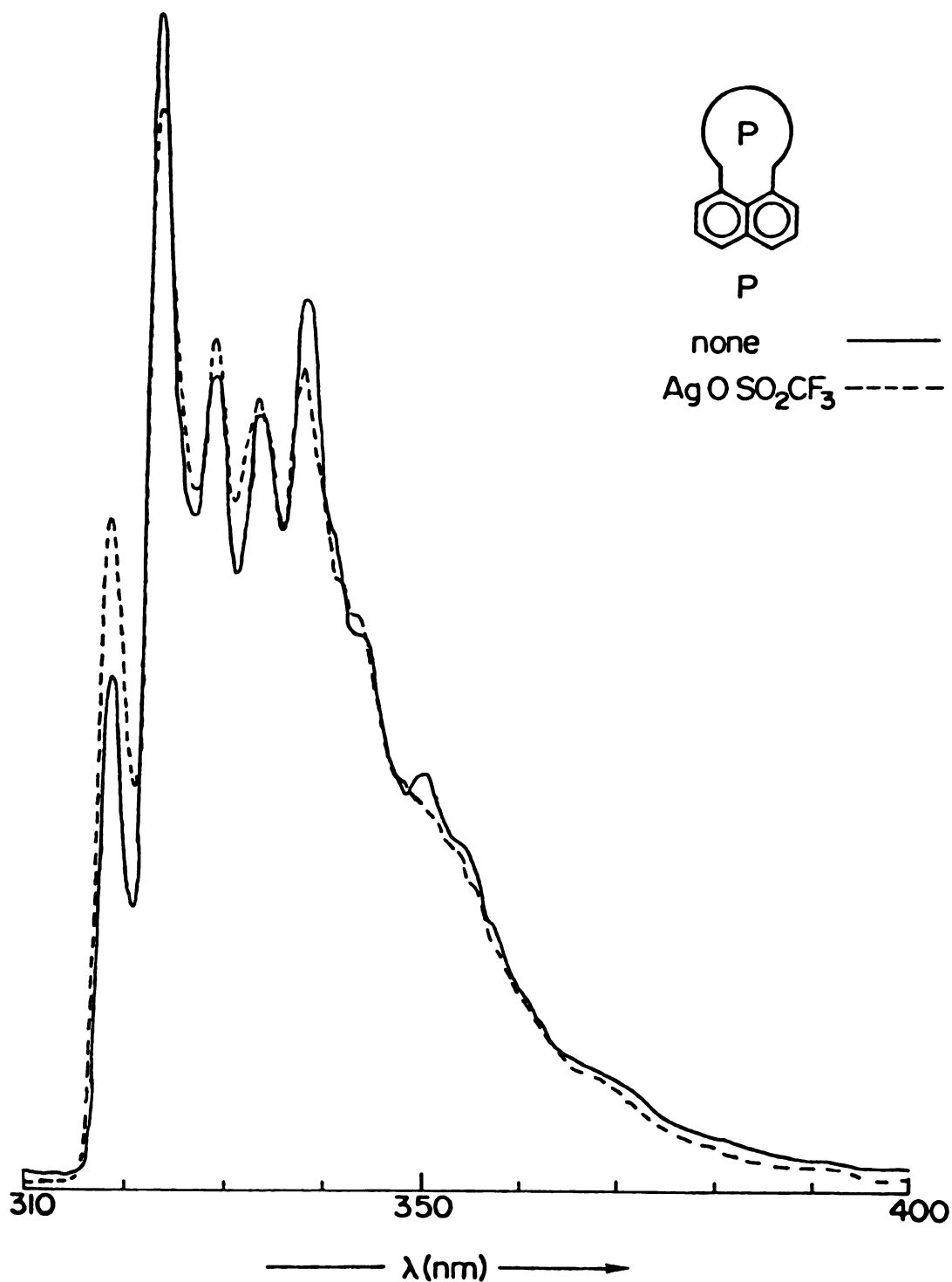


Figure 51. Corrected fluorescence spectra of  $1.00 \times 10^{-4}$  M 1,8-naphtho-21-crown-6 (2) alone and with 50:1 added molar excess of silver triflate in uncracked 95% ethanol at 77 K.

# Perturbed Phosphorescence of 1,8-Naphtho-21-Crown-6

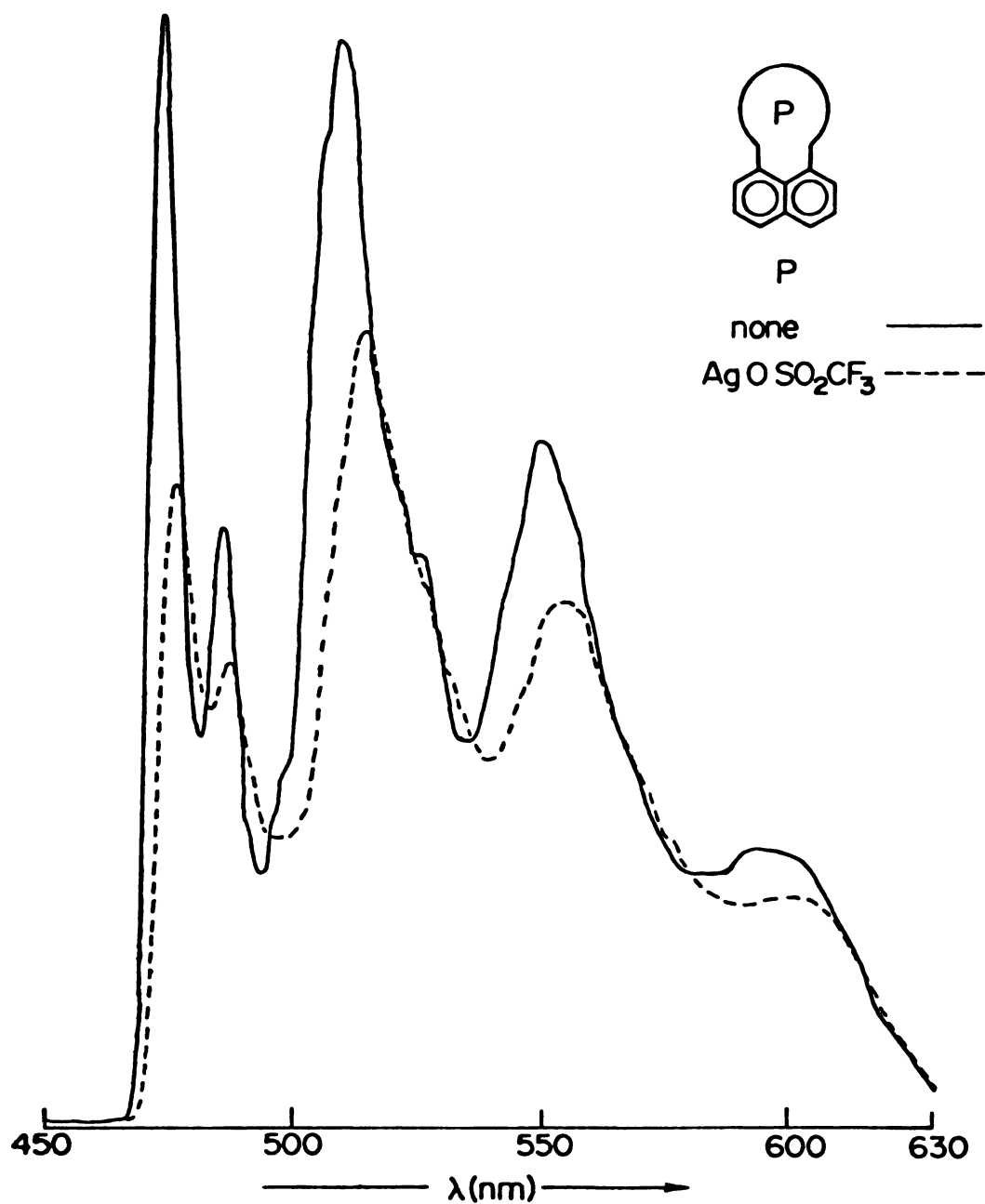


Figure 52. Corrected phosphorescence spectra of  $1.00 \times 10^{-4}$  M 1,8-naphtho-21-crown-6 ( $\text{P}$ ) alone and with 50:1 added molar excess of silver triflate in uncracked 95% ethanol glass at 77 K.

# Perturbed Fluorescence of 1,5-Naphtho-22-Crown-6

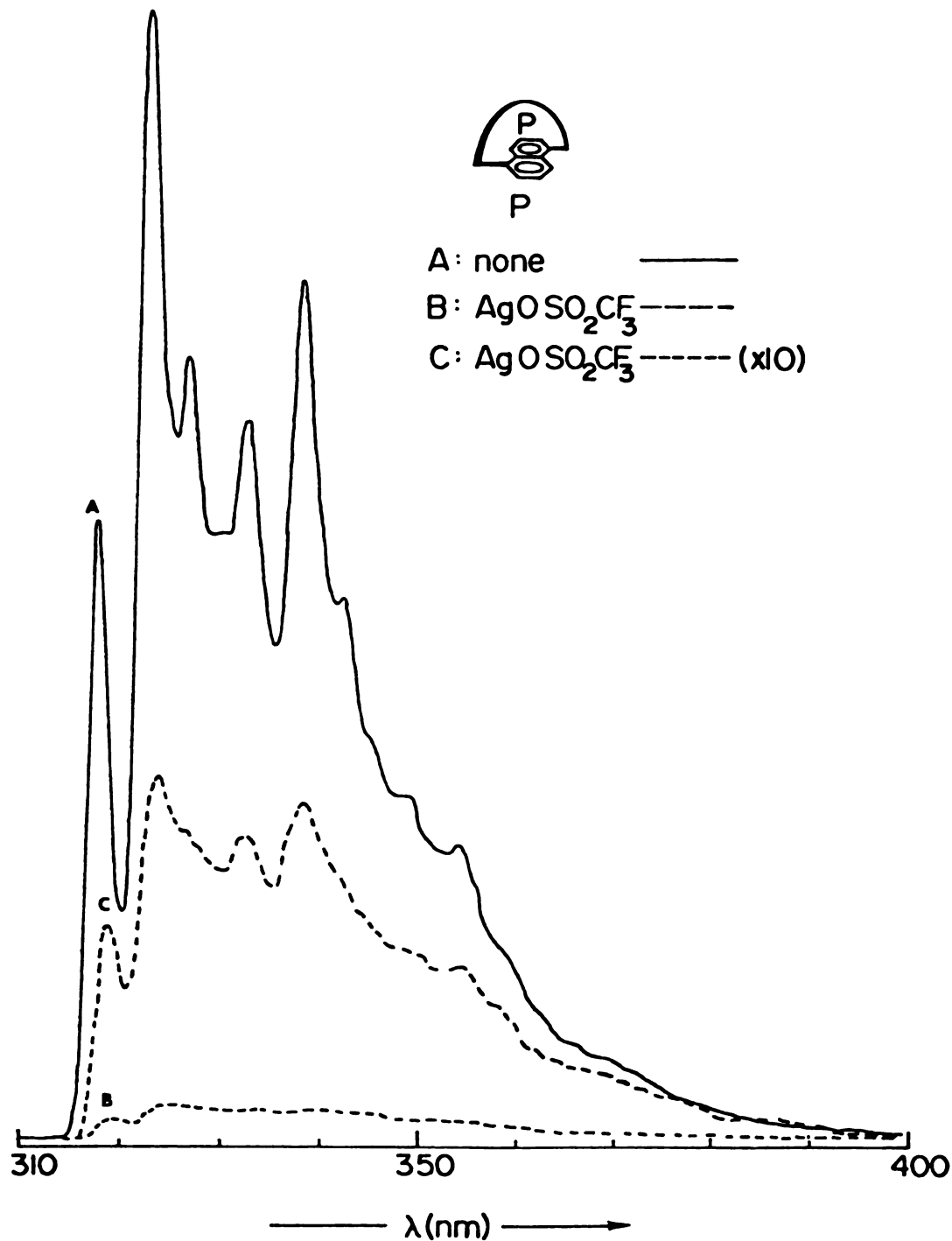


Figure 53. Corrected fluorescence spectra of  $1.00 \times 10^{-4} \text{ M}$  1,5-naphtho-22-crown-6 (3) alone and with 200:1 added molar excess of silver triflate in uncracked 95% ethanol glass at 77 K.

# Perturbed Phosphorescence of 1,5-Naphtho-22-Crown-6

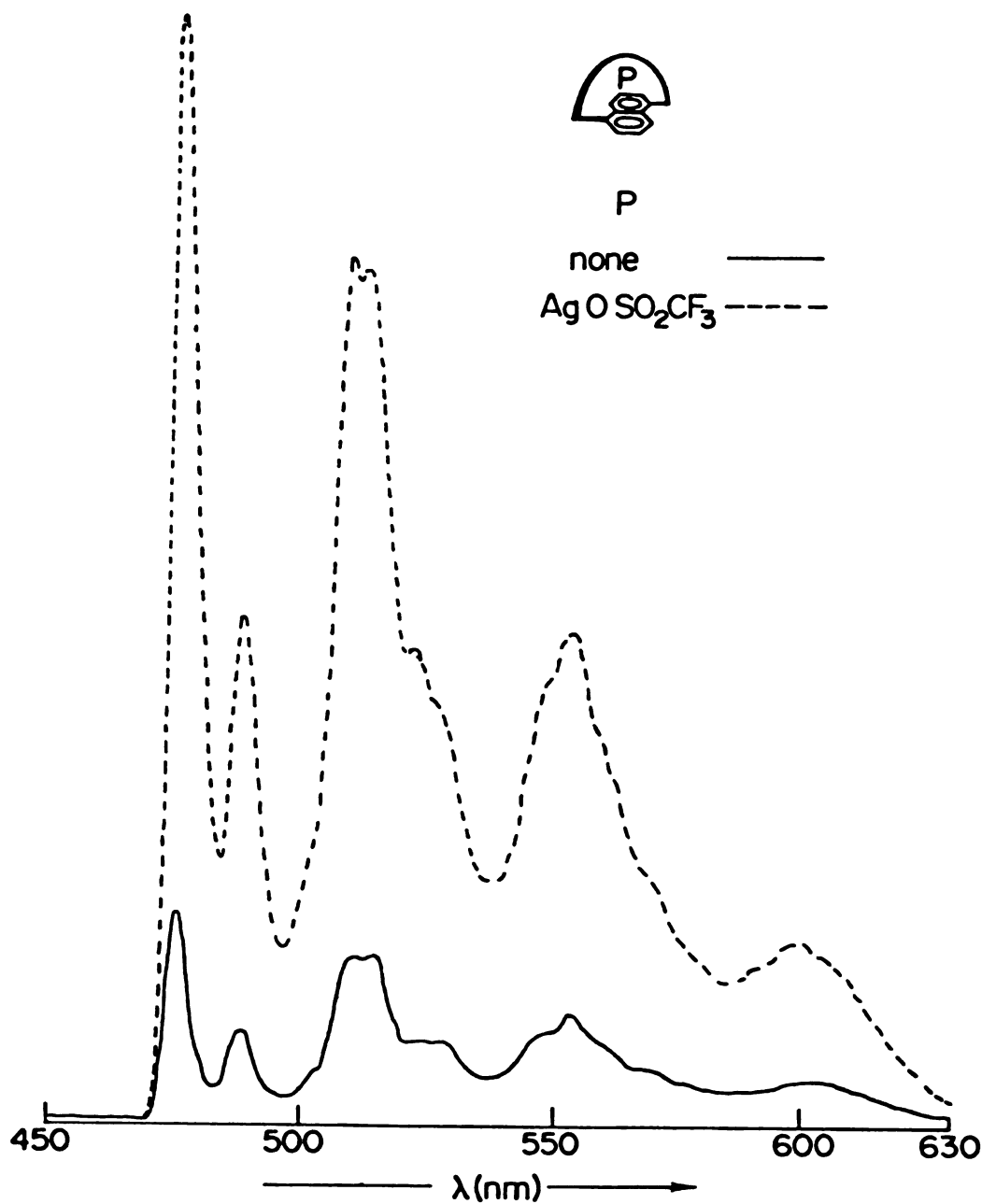


Figure 54. Corrected phosphorescence spectra of  $1.00 \times 10^{-4}$  M 1,5-naphtho-22-crown-6 (P) alone and with 200:1 added molar excess of silver triflate in uncracked 95% ethanol glass at 77 K.

derivatives were  $1.00 \times 10^{-4}$  M. The molar concentrations of crowns in the cases with added salts were either  $2.00 \times 10^{-4}$  M or  $1.00 \times 10^{-4}$  M. Solvent blanks gave essentially flat baselines under similar conditions.

Figures 19, 21, and 23 show the low temperature (77 K) fluorescence spectra for naphthalene disubstituted at the 2,3-, 1,8-, and 1,5-positions, respectively. In each case, substituents are methyl, methoxymethyl, and crown-methyl (naphthalene spectra are also included for comparison). The analogous set of phosphorescence spectra are shown in Figures 20, 22, and 24.

For the fluorescence spectra of the 2,3-disubstituted naphthalenes note that the spectra for the crown and for the methoxymethyl substituted naphthalenes are quite similar, with the latter being somewhat less intense. The fluorescence of 2,3-dimethylnaphthalene exhibits fine structure that is significantly more pronounced than that of the crown or of the methoxymethyl derivatives but includes all the peaks seen for methoxymethyl and crown substitution. The spectra are all red shifted compared to naphthalene by similar but slightly different amounts. Precise substituent and complexation induced energy shifts will be presented below and discussed later.

The phosphorescence spectrum of 2,3-dimethylnaphthalene is quite similar to that of naphthalene. As is also the case for the fluorescence spectra, the crown and methoxymethyl derivatives exhibit less pronounced fine structure. This is especially true for the crown, the highest energy band of which appears as a broad rounded hump. By comparison, naphthalene and its methyl and methoxymethyl



derivatives have two peaks in this region. The spectra are all blue shifted relative to naphthalene. The "0-0 band" for the 2,3-crown will receive special discussion later.

For the fluorescence spectra of the 1,8-disubstituted naphthalenes, note that, as for the 2,3-series, the spectra for the crown and for the methoxymethyl substituted naphthalenes are quite similar both in intensity and in energy. As is also the case for 2,3-dimethylnaphthalene, 1,8-dimethylnaphthalene exhibits fine structure which is significantly more pronounced than for the crown or methoxymethyl derivatives. The spectra are all red shifted relative to naphthalene, as for the 2,3-series, but the red shift is much larger for dimethyl substitution in the 1,8- series.

The phosphorescence spectra of the 1,8-disubstituted naphthalenes are all very naphthalene-like. They are all red shifted compared to naphthalene. The dimethyl derivative, as for the fluorescence spectrum, is red shifted much more than the crown or dimethyl derivatives. Also, as with the 2,3- series, the crown and methoxymethyl derivatives have similar intensities and energies.

Considering the fluorescence spectra of the 1,5-disubstituted naphthalenes, the crown and methoxymethyl derivatives have fine structure and energies which are quite similar, as is also the case for the analogous 2,3- and 1,8- derivatives. The fluorescence quantum yields for the 1,5-crown and methoxymethyl derivatives are more similar than the relative spectral intensities shown would indicate (vide infra). As is also the case for 2,3- and 1,8-dimethylnaphthalene, the fluorescence of 1,5-dimethylnaphthalene exhibits

fine structure which is more pronounced but otherwise similar to that of the crown or methoxymethyl derivatives. The fluorescence spectra of the 1,5-derivatives are all red shifted relative to naphthalene, as is also the case for the 2,3- and 1,8-derivatives. The red shift is much larger for 1,5-dimethyl substitution as is also the case for the 1,8-series.

The phosphorescence spectra of all the 1,5-derivatives are remarkably naphthalene like, which is also the case for the 1,8- and, to a lesser extent, for the 2,3- derivatives (vide supra). The 1,5-crown and methoxymethyl derivatives have fine structure and energies which are quite similar, though the fine structure of the methoxymethyl derivative is slightly less pronounced than that of the crown. The 1,5-dimethyl derivative has somewhat more pronounced fine structure and is red shifted (relative to naphthalene) much more than the 1,5-crown and methoxymethyl derivatives. A much larger red shift is also seen for 1,8-dimethylnaphthalene. The relative phosphorescence intensities shown for the 1,5-derivatives are in the right relative order, but the curves for naphthalene and 1,5-dimethylnaphthalene should be about three times less intense than shown.

Figures 25, 27, and 29 show, respectively, the effects of 5-fold molar excesses of alkali metal chloride salts on the fluorescence spectra of crowns  $\lambda_1$ ,  $\lambda_2$ , and  $\lambda_3$ . The analogous set of phosphorescence spectra are presented in Figures 26, 28, and 30. The molar concentration of crown is  $2.00 \times 10^{-4}$  M for crowns  $\lambda_1$ , and  $\lambda_2$  and  $1.00 \times 10^{-4}$  M for crown  $\lambda_3$ .

The fluorescence spectra for the alkali metal cation complexes

of crown  $\text{1}$  are all decreased in intensity relative to free crown, the decrease being smallest for the sodium complex and largest for the cesium complex. The spectra of these complexes are similar to each other but somewhat different from that of the free crown.

A comparison of Figure 25 to Figures 31, 37, 43, and 49 will show that all other complexing species investigated have fine structure which is similar to that of the alkali metal cation complexes. The 0-0 fluorescence bands of the alkali metal complexes are slightly blue shifted relative to free crown. Inspection of Figures 31, 37, 43, and 49 or reference to the results section on energy shifts will show that all of the other complexes of this crown which were investigated also have 0-0 fluorescence bands which are slightly blue shifted relative to free crown  $\text{1}$ . Some bands in the spectra of these complexes are red shifted relative to what appear to be the corresponding bands of the free crown, however, and one cannot say that the entire spectrum of a given complex is blue shifted.

The phosphorescence spectra of the alkali metal cation complexes of crown  $\text{1}$  (Figure 26) are all increased in intensity relative to free crown, the increase being largest for cesium and smallest for sodium. The gross structures of the phosphorescence spectra of these complexes are similar to that of the free crown, but the complexes have somewhat different fine structure. The high energy band for the crown is a broad, rounded hump (as noted above), whereas there are two peaks in this region for each of the alkali metal complexes (two peaks are also seen for naphthalene, naphthalene derivatives  $\text{4}$  and  $\text{5}$ , and, as will be pointed out in further detail

below, for other naphthalene derivatives and salt-crown complexes). The relative intensities of these two peaks change in going from the sodium complex to the cesium complex. For the sodium complex, the higher energy peak is more intense than the lower energy peak, whereas, for the cesium complex, the higher energy peak is less intense. The 0-0 phosphorescence band and the entire spectrum of each of these complexes are blue shifted relative to free crown 1. Comparison of Figure 26 to Figures 38, 42, and 48 or reference to the results section on energy shifts will show that all other complexes of this crown which were investigated also have 0-0 phosphorescence bands which are blue shifted relative to free crown 1. Also, it is generally true that entire phosphorescence spectrum of each complex is blue shifted relative to free crown 1. (Curves C, D, and E of Figure 42 are exceptions.)

For crown 2, the potassium, rubidium, and cesium complexes have fluorescence spectra which all have similar fine structure but which appear to be somewhat different from free crown. There is a general muddling of fine structure and an increase in fluorescence intensity for these complexes. A comparison of Figure 27 to Figures 33, 39, 45, and 51 will show that most of the complexes investigated show a similar muddling of fine structure and increased fluorescence intensity relative to free crown. Note that crown 2 and the related methoxymethyl derivative 6 also exhibit less well defined fine structure than either naphthalene or 1,8-dimethylnaphthalene (See Figure 21). The spectrum of the sodium complex of crown 2, however, is similar to that of free crown. But see the note on complexation of crown 2

with sodium in the results section on quantum yield titrations. The 0-0 fluorescence bands of these complexes are slightly red shifted relative to those of free crown  $\lambda$ . Comparison of Figure 27 to Figures 33, 39, 45, and 51 or reference to the results section on energy shifts will show that all other complexes of crown  $\lambda$  which were investigated also have 0-0 fluorescence bands which are red shifted relative to free crown. Though the fine structure of the fluorescence spectra of these complexes is muddled, there appears to be a general red shift of the entire spectrum of each complex relative to free crown  $\lambda$ . Note that this general red shift contrasts with the general blue shift of at least the 0-0 band for complexes of crown  $\lambda$ .

The phosphorescence spectra of the alkali metal complexes of crown  $\lambda$  show decreased intensities relative to free crown. As is the case for the fluorescence spectra, the fine structure of the complexes is less pronounced than that of the free crown, though the difference is qualitatively less than the difference between the fluorescence spectra of the complexes and free crown. The high energy region is most affected by complexation with alkali metal cations. The crown itself has two reasonably well defined peaks in this region (at approximately 475 and 487 nm) which become less well defined for the potassium, rubidium, and cesium complexes. This is the converse of what is observed in the phosphorescence spectra of the alkali metal cation complexes of crown  $\lambda$ : the high energy region for crown  $\lambda$  (a broad, rounded hump) is less well defined than the high energy region of its complexes (two peaks are evident; see

Figure 26). Thus, the fine structure of the phosphorescence spectra of alkali metal cation complexes of crowns  $1_{\sim}$  and  $2_{\sim}$  end up having a fine structure pattern which is more similar than that for the crowns themselves.

The 0-0 phosphorescence band and the whole spectrum of each alkali metal chloride complex of crown  $2_{\sim}$  are all red shifted relative to the free crown. Inspection of Figures 28, 34, 40, 46, and 52 or reference to the results section on energy shifts will show that the same is true of all investigated complexes of crown  $2_{\sim}$ .

Note that the phosphorescence spectrum of the sodium complex of crown  $2_{\sim}$  is very similar in intensity and energy to that of free crown. This is also the case for the fluorescence spectra (vide infra).

The fluorescence spectra for the alkali metal cation complexes of crown  $3_{\sim}$  are all decreased in intensity relative to the free crown, the decrease being about the same for the sodium and potassium complexes, greater for the rubidium complex, and very much greater for the cesium complex. See Figure 47 for an expanded fluorescence spectrum of the cesium complex. The phosphorescence spectra are decreased in intensity for the sodium and potassium complexes, about the same for the rubidium complex, and increased for the cesium complex, relative to free crown  $3_{\sim}$ . In contrast to crowns  $1_{\sim}$  and  $2_{\sim}$ , the alkali metal cation complexes of crown  $3_{\sim}$  have fine structure which is very similar to that of the free crown. Also, energy shifts of the spectra of the complexes relative to free crown are sufficiently small so as not to be evident from the figures.

(See results section on energy shifts.) Comparison of Figures 29 and 30 to Figures 35, 36, 41, 42, 47, 48, 53 and 54 will show that all of the complexes of crown  $\mathfrak{z}$  investigated have fluorescence and phosphorescence spectra which have fine structure which is very similar to those of the free crown. Also, in general, energy shifts relative to free crown  $\mathfrak{z}$  are small.

The effects of excess alkylammonium chloride salts (ammonium, n-propyl, i-propyl, and t-butyl) on the fluorescence spectra of crowns  $\mathfrak{1}$  (5-fold molar excesses of salts),  $\mathfrak{2}$  (5-fold molar excesses of salts) and  $\mathfrak{3}$  (100:1 molar excess of ammonium chloride, 20-fold molar excess of n-propylammonium chloride) are given, respectively, in Figures 31, 33, and 35. The corresponding set of phosphorescence spectra are given in Figures 32, 34, and 36.

The fluorescence spectra of the alkylammonium chloride complexes of crown  $\mathfrak{1}$  all are decreased in intensity relative to free crown. The decrease is largest for n-propyl and smallest for t-butyl. Note that the fluorescence spectra of these complexes fit the generalizations about fine structure and energy shifts made for complexes of crown  $\mathfrak{1}$  in relating the results for the alkali metal chloride complexes.

The phosphorescence spectra of the alkylammonium complexes of crown  $\mathfrak{1}$  are all of higher intensity than the free crown, with the n-propylammonium complex showing the largest increase. The fine structure of the phosphorescence spectra of these complexes is similar to that observed for the alkali metal cation complexes (See Figure 26). The difference in relative intensities for the

two highest energy peaks (at approximately 463 and 472 nm) is much larger than for the alkali metal cation complexes, but otherwise the fine structure is quite similar. The 0-0 phosphorescence bands of these complexes are all blue shifted relative to free crown  $1_{\lambda}$ . Also, the whole spectrum of a complex is blue shifted except for the n-propyl complex, which has many bands which are red shifted.

The fluorescence spectra of the ammonium, n-propylammonium, i-propylammonium, and t-butylammonium complexes of crown  $2_{\lambda}$  are all increased in intensity relative to free crown. This contrasts with the decrease seen for complexes of crown  $1_{\lambda}$ . The increase is largest for the n-propyl complex and smallest for the t-butyl complex. Note that the fluorescence spectra of these complexes fit the generalizations made above for the alkali metal cation complexes of crown  $2_{\lambda}$ .

The phosphorescence spectra of the alkylammonium complexes of crown  $2_{\lambda}$  are all decreased in intensity relative to free crown. This contrasts with the increases seen for complexes of crown  $1_{\lambda}$ . The decrease is greatest for the n-propyl complex and smallest for the t-butyl complex. All these complexes show fine structure in their phosphorescence spectra which is similar to that of free crown  $2_{\lambda}$  and which is similar to that of the alkali metal complexes of crown  $2_{\lambda}$  (See Figure 28).

The fluorescence spectra of the ammonium and n-propylammonium chloride complexes of crown  $3_{\lambda}$  are only slightly diminished in intensity relative to free crown. The fine structure of the fluorescence spectra of these complexes is essentially the same as that of the



free crown. Small but discernible spectral energy shifts are observed for these complexes relative to free crown. The 0-0 band and whole spectrum of the ammonium complex are blue shifted slightly relative to free crown, as is the case for the alkali metal cation complexes of crown  $\beta$ . The 0-0 band and whole spectrum of the n-propylammonium chloride complex, however, are slightly red shifted. The converse is true for the phosphorescence spectra of these complexes: the 0-0 band and whole spectrum of the ammonium complex are slightly red shifted (as is the case for the alkali metal cation complexes), whereas the 0-0 band and whole spectrum is slightly blue shifted for the n-propylammonium chloride complex. The differences in spectral shapes and intensities of the phosphorescence spectra of these complexes are very small.

The effects of excess bromoalkyl and iodoalkylammonium chloride salts on the fluorescence spectra of crowns  $\beta$  (5-fold molar excesses of bromoalkyl and 20:1 molar excesses of iodoalkylammonium chloride salts),  $\gamma$  (5-fold molar excesses of bromoalkyl and 20-fold molar excesses of iodoalkylammonium chloride salts), and  $\delta$  (20-fold molar excesses of bromoalkyl and iodoalkylammonium chloride salts) are shown, respectively, in Figures 37, 39, and 41. For crowns  $\beta$  and  $\gamma$ , the bromoalkyl work used  $2.00 \times 10^{-4}$  M crown and the ammonium chloride work which was done later, used  $1.00 \times 10^{-4}$  M crown. The crown reference spectra were of approximately the same arbitrary intensity in both cases, however, so the comparison of the relative emission intensities of the bromoalkylammonium chloride complexes to those of the iodoalkylammonium chloride complexes is qualitatively

correct. The corresponding set of phosphorescence spectra are shown in Figures 38, 40, and 42.

The fluorescence spectra of the  $\beta$ -bromo- and  $\beta$ -iodoethylammonium and  $\gamma$ -bromo- and  $\gamma$ -iodopropylammonium chloride complexes of crown  $\text{18-crown-6}$  are all decreased in intensity relative to free crown. In each case, the decrease is larger for the  $\gamma$ -halopropylammonium complex than for the  $\beta$ -bromoethylammonium complex, with the largest decrease being for the  $\beta$ -iodopropylammonium complex. The fluorescence spectra of these complexes of crown  $\text{18-crown-6}$  look remarkably like the fluorescence spectra for other complexes of this crown which are reported here (Figures 25, 31, 43, and 49). The 0-0 band of each of these complexes is somewhat blue shifted relative to free crown. The shift is smallest for the  $\gamma$ -bromoammonium complex and larger by approximately the same amount for the other complexes. The whole fluorescence spectrum of each of these other complexes is blue shifted relative to the fluorescence spectrum of the  $\gamma$ -bromoammonium complex. For other complexes of crown  $\text{18-crown-6}$  it is not possible to tell whether or not the whole fluorescence spectrum follows the blue shift of the 0-0 band, since the spectral shapes are all similar and the magnitudes of the 0-0 band shifts are all similar.

The phosphorescence spectra of the haloalkylammonium chloride complexes of crown  $\text{18-crown-6}$  are all increased in intensity relative to free crown. In each case, the increase is larger for the  $\gamma$ -halopropyl than for the  $\gamma$ -haloethylammonium complex. At first sight, the fine structure of the phosphorescence spectra of these complexes appears to be much different than that of the other complexes of crown  $\text{18-crown-6}$ .

referred to previously. However, comparison to Figures 20, 26, and 32, for example, suggests that the prominent peak at approximately 495 nm for the  $\beta$ -bromoethyl 480 nm for the  $\gamma$ -bromopropyl, 487 nm for the  $\beta$ -iodoethyl, and the shoulder at 480 nm for the  $\gamma$ -iodopropylammonium chloride complexes may correspond to the less prominent peaks or shoulders in this region of the other phosphorescence spectra. With this in mind, the high energy sections of the phosphorescence spectra of these complexes may be considered to be similar to those of other complexes of both crowns  $\text{1}$  and  $\text{2}$ . As in the phosphorescence spectra of other complexes of crowns  $\text{1}$  and  $\text{2}$ , there is a marked change in the relative intensity of the two highest energy peaks. In these cases, the peaks in the 470 to 475 region are of about equal intensity for the  $\gamma$ -bromo,  $\beta$ -iodo, and  $\gamma$ -iodoalkylammonium complexes, but the intensity of the 0-0 bands change. The 0-0 bands are least intense for the  $\gamma$ -halopropylammonium complexes, the 0-0 band for the  $\gamma$ -iodo being less intense than that for the  $\gamma$ -bromopropylammonium complex. The 0-0 bands for the  $\beta$ -haloethylammonium complexes are more intense than for the  $\gamma$ -analogs, the 0-0 band for the  $\beta$ -iodo complex again being less intense than for the  $\beta$ -bromo complex. All the phosphorescence 0-0 bands of these complexes of crown  $\text{1}$  are blue shifted relative to the free crown, as is also the case for other complexes of this crown (vide supra). The bands in the 510, 550, and 600 nm region for the  $\gamma$ -halopropyl and  $\beta$ -iodoethylammonium complexes, however, are all red shifted relative to free crown. The bands at approximately 540 and 585 nm for the  $\beta$ -bromoethylammonium complex, however, are blue shifted. The

relative intensities and energies of bands in the phosphorescence spectrum of the  $\beta$ -bromo complex are qualitatively different from those of the other haloalkylammonium complexes of crown  $\lambda$ .

The fluorescence spectra of the haloalkylammonium chloride complexes of crown  $\lambda_2$  are all increased in intensity relative to free crown. The increase is largest for the  $\gamma$ -halopropylammonium complexes. The fluorescence spectra of these complexes have the same muddled fine structure as other complexes of crown  $\lambda_2$ , as was previously noted to be the case in general. Also, note that the red shifts of the 0-0 bands and the general red shift of the whole spectrum of each complex relative to free crown  $\lambda_2$  fits the generalization made previously.

The phosphorescence spectra of the haloalkylammonium chloride complexes of crown  $\lambda_2$  are all decreased in intensity relative to free crown, the decrease being greatest for the  $\gamma$ -iodopropyl complex and smallest for the  $\beta$ -iodopropylammonium complex. In contrast to the differences seen for the phosphorescence spectra of the haloalkylammonium complexes of crown  $\lambda_1$  compared to other complexes of crown  $\lambda_1$ , the phosphorescence spectra of the haloalkylammonium complexes of crown  $\lambda_2$  are quite similar to other complexes of crown  $\lambda_2$ . Again, the changes in relative intensities of various bands are largest for the two highest energy bands. The 0-0 band and whole spectrum of each of these complexes of crown  $\lambda_2$  are red shifted, in accord with the generalization made previously.

For crown  $\lambda_3$ , the fluorescence spectra of the haloalkylammonium chloride complexes are all decreased in intensity, the decrease

being much larger for the iodo than for the bromoalkylammonium complexes. The fluorescence spectra of these complexes all have essentially the same fine structure as for the free crown and spectral energy shifts are small. This is in keeping with the previously made generalizations for complexes of crown  $\mathfrak{3}$  (vide supra). However, as is also the case for the n-propylammonium complex, there is a discernible red shift of the 0-0 band and of the whole spectrum for the  $\gamma$ -bromo and  $\gamma$ -iodoammonium complexes relative to crown  $\mathfrak{3}$ . And, as is also the case for the ammonium chloride complex, there is a blue shift for the  $\beta$ -bromo and  $\beta$ -iodoammonium chloride complexes relative to free crown.

The phosphorescence spectra of the haloalkylammonium chloride complexes of crown  $\mathfrak{3}$  are all approximately of the same intensity as the free crown, except for the spectrum of the  $\beta$ -bromopropyl complex, which is approximately twice as intense. In contrast to the fluorescence spectral energies, the phosphorescence spectral energies are essentially unchanged. Also, there are only small changes in fine structure for the complexes relative to free crown  $\mathfrak{3}$ .

Figures 43, 45, and 47 compare, respectively, the effects of cesium chloride and barium bromide on the fluorescence of crowns  $\mathfrak{1}$  (5:1 molar excess cesium chloride, 10:1 molar excess barium bromide),  $\mathfrak{2}$  (5:1 molar excess cesium chloride, 10:1 molar excess barium bromide), and  $\mathfrak{3}$  (5:1 molar excess cesium chloride, 50:1 molar excess barium bromide). The corresponding set of phosphorescence spectra are found in Figures 44, 46, and 48. For crowns  $\mathfrak{1}$  and  $\mathfrak{2}$ , the crown concentration was  $2.00 \times 10^{-4}$  M for the cesium chloride work

and  $1.00 \times 10^{-4}$  M for the barium bromide work. For crown 3, the crown concentration was  $1.00 \times 10^{-4}$  M. The spectra for the cesium complexes are also given elsewhere (Figures 25 through 30).

The barium bromide and cesium chloride complexes of crown 1 both have much lower fluorescence intensities than the free crown. The relative fluorescence intensities of the barium and cesium complexes as shown in Figure 43 are significantly more different than their relative quantum yields, which are essentially the same (vide infra). This is primarily due to the different absorbancies of the complexes in the region in which they were excited. Note that the fine structure of the fluorescence spectra of these complexes is essentially the same. Spectral energy shifts are not easily discerned from Figure 43, but see the results section on energy shifts for precise values. The phosphorescence quantum yields for these two complexes are also essentially the same, a conclusion one would not arrive at from the relative phosphorescence intensities shown in Figure 44. The 0-0 bands and the whole spectrum of both complexes are blue shifted relative to free crown and the spectra of the complexes have fine structure which is very similar.

As in the case of the barium bromide and cesium chloride complexes of crown 1, the fluorescence and phosphorescence quantum yields of the barium and cesium complex of crown 2 are more similar (approximately the same, vide infra) than the relative spectral intensities would indicate. The fluorescence spectra of these two complexes have the same muddled appearance as do other complexes of this crown. Also, as for other complexes of this crown, the 0-0 band

and whole spectrum of each complex are red shifted relative to free crown. The phosphorescence spectra of these complexes are also very similar, although the whole spectrum of the cesium complex is red shifted further than is the barium complex relative to free crown  $\lambda$ .

Whereas the intensities of the fluorescence and phosphorescence spectra of the barium bromide and cesium chloride complexes of crowns  $\lambda$  and  $\lambda$  are similar, the barium and cesium complexes of crown  $\lambda$  are greatly different (the fluorescence spectrum of the cesium complex is approximately 50 times less intense than that of the barium complex; and the phosphorescence spectrum of the cesium complex is approximately twice as intense as that of the barium complex). As is usual for this crown, both fluorescence and phosphorescence fine structures and spectral energies are similar for both the complexes and the free crown.

Figures 49, 51, and 53 show, respectively, the effects of silver triflate on the fluorescence of crowns  $\lambda$  (50-fold molar excess of salt),  $\lambda$  (50-fold molar excess of salt), and  $\lambda$  (100-fold molar excess of salt). The corresponding set of phosphorescence spectra are found in Figures 50, 52, and 54.

The fluorescence intensities of the silver triflate complexes of crowns  $\lambda$ ,  $\lambda$ , and  $\lambda$  relative to free crown are as follows: somewhat less intense for the complex of crown  $\lambda$ ; of approximately equal intensity for the complex of crown  $\lambda$ ; but of greatly decreased intensity for the complex of crown  $\lambda$  (decrease is similar to that for the cesium complex of crown  $\lambda$ ). And the phosphorescence intensities

relative to free crown: moderate increase for complex of crown 1; small decrease for complex of crown 2; and very large increase for complex of crown 3 (a much larger increase than for cesium complex of crown 3). The fluorescence 0-0 bands of the silver triflate complexes of crowns 1, 2, and 3 are shifted as follows relative to free crown: blue shift for complex of crown 1; red shift for complex of crown 2; and negligible blue shift for complex of crown 3, and the phosphorescence 0-0 bands relative to free crown: blue shift for complex of crown 1; red shift for complex of crown 2; and negligible blue shift for complex of crown 3. The complexes of crowns 1 and 2 show changes in the fine structure of their fluorescence and phosphorescence spectra relative to free crown which are similar to changes seen for other complexes of crowns 1 and 2. As with other complexes of crown 3, the fine structure of the spectra of the silver complex is essentially the same as that of free crown 3.

### Spectroscopic Energies

In the two preceding sections on absorption and emission spectra, qualitative comments concerning the direction and size of spectral energy shifts for naphthalene derivatives relative to naphthalene and crown complexes relative to parent free crown were made. Tables 1 through 7 gather together precise values (in  $\text{cm}^{-1}$ ) for frequencies of the 0-0 bands of absorption ( $S_1$  and  $S_2$ ) and emission (fluorescence and phosphorescence) for naphthalene (10), naphthalene derivatives (compounds 4 through 9), crowns 1, 2, and 3, and complexes of these crowns. Also, values for energy differences ( $\Delta E$ , in  $\text{cm}^{-1}$ )



Table 1. Absorption and Emission Frequencies and Changes in Energy Level Separations (all in  $\text{cm}^{-1}$ ) for 2,3-, 1,8-, and 1,5-Disubstituted Naphthalenes in Alcohol Glasses at 77 K.

Naphthalene Substitution	Absorption <sup>a,c</sup>		Emission <sup>a,d</sup>		Changes in Energy Level Separations Relative to Naphthalene <sup>b</sup>			
	$L_a(S_2)$	$L_bS_1;0-0)$	Fluor. (0-0)	Phos. (0-0)	$\Delta(E_{S_2-S_0})^e$	$\Delta(E_{S_1-S_0})^f$	$\Delta(E_{T_1-S_0})^g$	$\Delta(E_{S_1-T_1})^h$
None (10)	34696	31779	31742	21285	0	-380	160	-470
2,3-Dimethyl (4)	34389	31407	31369	21382	-310	-380	670	-680
2,3-Bis(methoxy- methyl) (5)	34783	31332	31328	32549	90	-414	670	-680
2,3-Crown-6 (1)	34758	31279	31206	21399 <sup>1</sup>	60	-540	630	-650
1,8-Dimethyl (6)	33535	31082	31058	20748	-1160	-680	-540	-150
1,8-Bis(methoxy- methyl) (7)	33695	31437	31396	21055	-1000	-350	-230	-120
1,8-Crown-6 (2)	33683	31441	31390	21060	-1010	-350	-220	-130
1,5-Dimethyl (8)	33242	31273	31256	20842	-1450	-490	-440	-40
1,5-Bis(methoxy- methyl) (9)	33777	31465	31447	20990	-920	-300	-300	0
1,5-Crown-6 (3)	33691	31479	31430	21009	-1000	-310	-280	-40

<sup>a</sup> Errors are  $\pm 10 \text{ cm}^{-1}$  for absorption,  $\pm 20 \text{ cm}^{-1}$  for fluorescence, and  $\pm 10 \text{ cm}^{-1}$  for positions of phosphorescence maxima. <sup>b</sup> A positive number indicates that the energy separation increases. <sup>c</sup> All absorption data is from 95% ethanol-methanol (4:1, v/v) glass except that for 3, 8, and 9, which is from ethanol-methanol (4:1, v/v) glass. <sup>d</sup> All emission data are from uncracked 95% ethanol glass. <sup>e</sup>  $\pm 1.5 \text{ cm}^{-1}$ . <sup>f</sup> Difference is for emission data;  $30 \text{ cm}^{-1}$ . <sup>g</sup>  $\pm 20 \text{ cm}^{-1}$ . <sup>h</sup>  $\pm 30 \text{ cm}^{-1}$ . <sup>i</sup> This is an estimate of the true 0-0 energy (see discussion).

Table 2. Absorption and Emission Frequencies and Changes in Energy Level Separations (Relative to Free Crown  $\lambda$ ) for Alkali Metal Chloride, Barium Bromide, and Silver Triflate Complexes of 2,3-Naphtho-20-Crown-6 ( $\lambda$ ) at 77 K in Alcohol Glass. All Numbers in  $\text{cm}^{-1}$ .<sup>a</sup>

Absorption		Emission		Changes in Energy Level Separations Relative to Crown $\lambda$			
$L_a(S_2)$	$L_b(S_1; 0-0)$	Fluor. (0-0)	Phos. (0-0)	$\Delta(E_{S_2-S_0})$	$\Delta(E_{S_1-S_0})$	$\Delta(E_{T_1-S_0})$	$\Delta(E_{S_1-T_1})$
<hr/>							
2,3-Crown-6( $\lambda$ )	34758	31279	31206	21400	0	0	0
$\lambda + \text{NaCl}$	34864	31375	31309	21624	110	100	130
$\lambda + \text{KCl}$	34861	31376	31306	21570	100	100	-70
$\lambda + \text{RbCl}$	34820	31344	31305	21518	60	90	-20
$\lambda + \text{CsCl}$	34840	31362	31311	21548	80	110	-40
<hr/>							
$\lambda + \text{BaBr}_2$	34800	31269	31274	21515	42	70	-50
$\lambda + \text{AgOSO}_2\text{CF}_3$	34828	31286	31279	21622	70	70	-150

<sup>a</sup>See notes a, b, and d through i for Table 1. Absorption data for barium bromide and silver triflate complexes are from ethanol-methanol (4:1, v/v) glass; all other absorption data are from 95% ethanol-methanol glass. Crown concentration is in the  $10^{-4}$  M range (see text).

Table 3. Absorption and Emission Frequencies and Changes in Energy Level Separations (Relative to Free Crown 2) for Alkali Metal Chloride, Barium Bromide, and Silver Triflate Complexes of 1,8-Naphtho-21-Crown-6 ( $\zeta$ ) in Alcohol Glass at 77 K. All Numbers in  $\text{cm}^{-1}$ .<sup>a</sup>

Absorption		Emission		Changes in Energy Level Separations Relative to Crown 2			
$L_a(S_2)$	$L_b(S_1;0-0)$	Fluor. (0-0)	Phos. (0-0)	$\Delta(E_{S_2-S_0})$	$\Delta(E_{S_1-S_0})$	$\Delta(E_{T_1-S_0})$	$\Delta(E_{S_1-T_1})$
1,8-Crown-6( $\zeta$ )	33683	31441	31390	21040	0	0	0
$\zeta$ + NaCl	33602	31412	31358	20977	-80	-30	-80
$\zeta$ + KCl	33656	31327	31160	20715	-30	-230	-340
$\zeta$ + RbCl	33669	31315	31146	20649	-10	-240	-310
$\zeta$ + CsCl	33641	31314	31146	20628	-40	-240	-430
$\zeta$ + BaBr <sub>2</sub>	33611	31278	31152	20816	-70	-160	-240
$\zeta$ + AgOSO <sub>2</sub> CF <sub>3</sub>	33618	31370	31323	20941	-70	--70	-120

<sup>a</sup>See notes a, c, and d through h in Table 1. Absorption data for the barium bromide and silver triflate complexes are from ethanol-methanol (4:1, v/v) glass; all other absorption data are from 95% ethanol-methanol (4:1, v/v) glass. Crown concentration is in  $10^{-4}$  M range (see text).

Table 4. Absorption and Emission Frequencies and Changes in Energy Level Separations (Relative to Free Crown  $\lambda$ ) for Alkali Metal Chloride, Barium Bromide, and Silver Triflate Complexes of 1,5-Naphtho-22-Crown-6 ( $\lambda$ ) at 77 K in Alcohol Glass. All numbers in  $\text{cm}^{-1}$ .<sup>a</sup>

	Absorption		Emission		Changes in Energy Level Separations Relative to Crown $\lambda$				
	$L_a(S_2)$	$L_b(S_1; 0-0)$	Fluor. (0-0)	Phos (0-0)	$\Delta(E_{S_2}-S_0)$	$\Delta(E_{S_1}-S_0)$	$\Delta(E_{T_1}-S_0)$	$\Delta(E_{S_1}-T_1)$	
1,5-Crown-6( $\lambda$ )	33691	31479	31421	21012	0	0	0	0	
$\lambda$ + NaCl	33707	31517	31460	21047	20	40	40	0	
$\lambda$ + KCl	33722	31536	31470	20990	30	50	-20	70	
$\lambda$ + RbCl	33741	31578	31502	21030	50	80	20	60	
$\lambda$ + CsCl	33743	31580	31438	21040	50	20	30	-10	
$\lambda$ + BaBr <sub>2</sub>	33681	31495	31422	21022	-10	0	10	-10	
$\lambda$ + AgOSO <sub>2</sub> CF <sub>3</sub>	33542	31426	31372	20992	-150	-50	-20	-30	

<sup>a</sup>See notes a, b, and d through h for Table 1. Absorption data for barium bromide and silver triflate complexes are from ethanol-methanol (4:1, v/v) glass; all other absorption data are from 95% ethanol-methanol (4:1, v/v) glass. Crown concentration is in  $10^{-3}$  M range (see text).

Table 5. Absorption and Emission Frequencies and Changes in Energy Level Separations (Relative to Free Crown  $\text{I}$ ) for Alkyl and Haloalkylammonium Chloride Complexes of 2,3-Naphtho-20-Crown-6 ( $\text{I}$ ) at 77 K in Alcohol Glass. All Numbers in  $\text{cm}^{-1}$ .<sup>a</sup>

Absorption		Emission		Changes in Energy Level Separations Relative to Crown $\text{I}$				
$\text{L}_a(\text{S}_2)$	$\text{L}_b(\text{S}_1; 0-0)$	Fluor. (0-0)	Phos. (0-0)	$\Delta(\text{E}_{\text{S}_2-\text{S}_0})$	$\Delta(\text{E}_{\text{S}_1-\text{S}_0})$	$\Delta(\text{E}_{\text{T}_1-\text{S}_0})$	$\Delta(\text{E}_{\text{S}_1-\text{T}_1})$	
2,3-Crown-6( $\text{I}$ )	34758	31279	31206	21400	0	0	0	0
$\text{I} + \text{NH}_4\text{Cl}$	34824	31317	31284	21617	70	80	220	-140
$\text{I} + \text{n-PrNH}_3\text{Cl}$	34675	31267	31241	21639	-480	40	240	-200
$\text{I} + \text{i-PrNH}_3\text{Cl}$	34809	31319	31300	21577	50	90	180	-80
$\text{I} + \text{t-BuNH}_3\text{Cl}$	34806	31325	31296	21565	50	90	170	-80
$\text{I} + \text{Br}(\text{CH}_2)_2\text{NH}_3\text{Cl}$	34806	31316	31297	21575	50	90	180	-90
$\text{I} + \text{Br}(\text{CH}_2)_3\text{NH}_3\text{Cl}$	34744	31260	31241	21616	-510	40	240	-200
$\text{I} + \text{I}(\text{CH}_2)_2\text{NH}_3\text{Cl}$	34871	31283	31302	21513	110	100	110	-10
$\text{I} + \text{I}(\text{CH}_2)_3\text{NH}_3\text{Cl}$	34231	31231	31286	21560	-530	80	160	-80

<sup>a</sup>See notes a, b, and d through i for Table 1. Absorption data for the iodoalkyl ammonium chloride complexes of crown 1 are from ethanol-methanol (4:1, v/v) glass; all other absorption data are from 95% ethanol-methanol (4:1, v/v) glass. Crown concentration is in the  $10^{-4}$  M range (see text).

Table 6. Absorption and Emission Frequencies and Changes in Energy Level Separations (Relative to Free Crown  $\mathcal{L}$ ) for Alkyl and Haloalkylammonium Chloride Complexes of 1,8-Naphtho-21-Crown-6 ( $\mathcal{L}$ ) at 77 K in Alcohol Glass. All Numbers in  $\text{cm}^{-1}$ .<sup>a</sup>

Absorption		Emission		Changes in Energy Level Separations Relative to Crown $\mathcal{L}$				
$L_a(S_2)$	$L_b(S_1; 0-0)$	Fluor. (0-0)	Phos. (0-0)	$\Delta(E_{S_2-S_0})$	$\Delta(E_{S_1-S_0})$	$\Delta(E_{T_1-S_0})$	$\Delta(E_{S_1-T_1})$	
1,8-Crown-6 ( $\mathcal{L}$ )	33683	31441	31390	21040	0	0	0	
$\mathcal{L} + \text{NH}_4\text{Cl}$	33645	31337	31202	20966	-40	-190	-80	
$\mathcal{L} + n\text{-PrNH}_3\text{Cl}$	33637	31315	31171	20938	-50	-220	-100	
$\mathcal{L} + i\text{-PrNH}_3\text{Cl}$	33641	31369	31248	20988	-40	-140	-70	
$\mathcal{L} + t\text{-BuNH}_3\text{Cl}$	33633	31407	31364	21040	-50	-30	-10	
$\mathcal{L} + \text{Br}(\text{CH}_2)_2\text{NH}_3\text{Cl}$	33635	31302	31154	20930	-50	-240	-110	
$\mathcal{L} + \text{Br}(\text{CH}_2)_3\text{NH}_3\text{Cl}$	33627	31306	31153	20791	-60	-240	+30	
$\mathcal{L} + \text{I}(\text{CH}_2)_2\text{NH}_3\text{Cl}$	33675	31312	31221	20969	-80	-170	-80	
$\mathcal{L} + \text{I}(\text{CH}_2)_3\text{NH}_3\text{Cl}$	33627	31301	31172	20868	-60	-220	-20	

<sup>a</sup>See notes a, b, and d through h for Table 1. Absorption data for the iodoalkyl ammonium chloride complexes of crown  $\mathcal{L}$  are from ethanol-methanol (4:1, v/v) glass; all other absorption data are from 95% ethanol-methanol (4:1, v/v) glass. Crown concentration is in the  $10^{-4}$  \_ range (see text).

Table 7. Absorption and Emission Frequencies and Changes in Energy Level Separations (Relative to Free Crown  $\lambda$ ) for Alkyl and Haloalkylammonium Chloride Complexes of 1,5-Naphtho-22-Crown-6 ( $\lambda$ ) at 77 K in Alcohol Glass. All numbers in  $\text{cm}^{-1}$ .<sup>a</sup>

Absorption		Emission		Changes in Energy Level Separations Relative to Crown $\lambda$				
$L_a(S_2)$	$L_b(S_1; 0-0)$	Fluor. (0-0)	Phos. (0-0)	$\Delta(E_{S_2}-S_0)$	$\Delta(E_{S_1}-S_0)$	$\Delta(E_{T_1}-S_0)$	$\Delta(E_{S_1}-T_1)$	
1,5-Crown-6 ( $\lambda$ )	33685	31478	31424	21012	0	00	00	
$\lambda + \text{NH}_4\text{Cl}$	33710	31498	31454	20999	30	-10	40	
$\lambda + \text{n-PrNH}_3\text{Cl}$	33721	31465	31374	21022	40	-50	-60	
$\lambda + \text{Br}(\text{CH}_2)_2\text{NH}_3\text{Cl}$	33673	31496	31429	20984	-10	50	80	
$\lambda + \text{Br}(\text{CH}_2)_3\text{NH}_3\text{Cl}$	33691	31478	31384	21025	10	-40	-50	
$\lambda + \text{I}(\text{CH}_2)_2\text{NH}_3\text{Cl}$	33710	31486	31426	21022	30	20	10	
$\lambda + \text{I}(\text{CH}_2)_3\text{NH}_3\text{Cl}$	33691	31477	31370	21033	10	-50	-70	

<sup>a</sup> See notes a, b, and d through h for Table 1. All absorption data are from ethanol-methanol (4:1, v/v) glass. Crown concentration is in the  $10^{-4}$  M range (see text).

between the 0-0 bands of naphthalene and those of naphthalene derivatives and between the 0-0 bands of crowns and those of their complexes are given. These differences are given for  $S_2$  0-0 absorption bands ( $\Delta(E_{S_2} - S_0)$ ), 0-0 fluorescence bands ( $\Delta(E_{S_1} - S_0)$ ), and 0-0 phosphorescence bands ( $\Delta(E_{T_1} - S_0)$ ). Differences in the singlet-triplet energy gap ( $E_{S_1} - T_1$ ) between naphthalene and naphthalene derivatives and between crowns and their complexes are also given. These differences ( $\Delta(E_{S_1} - T_1)$ ) indicate whether the singlet-triplet gap gets larger or smaller for derivatives of naphthalene relative to naphthalene or for complexes of crowns relative to free crowns. A positive number indicates that the energy separation increases.

See the general introductory comments made in the results section on UV spectra for definitions of the terms "band", "0-0 band", " $S_1$ ", and " $S_2$ ". Here we use the term "0-0 band" to refer to the lowest energy (longest wavelength) peak in the  $S_2$  band. The table headings also give the Platt<sup>68</sup> notations for the  $S_1$  and  $S_2$  bands: "La", for the  $S_2$  band; and " $L_b$ ", for the  $S_1$  band. Discussion of whether or not the values given are for true 0-0 bands and special discussion of the 0-0 phosphorescence band for crown 1 will be given later.

Table 1 gives the errors appropriate to each kind of frequency measurement and, also, errors appropriate to the changes in energy separations derived from them. While most of the absorption data are from 95% ethanol-methanol (4:1, v/v) glass, some of the later data are from ethanol-methanol (4:1, v/v) glass. There is no



significant difference for absorption frequencies for naphthalene or for the crowns in these slightly different glasses. Thus, all of the absorption data should be comparable. As noted in the tables, all emission data is from 95% ethanol glass. Sample concentrations are the same as those for the corresponding absorption and emission spectra and can be found in the results sections describing these spectra.

#### Fluorescence and Phosphorescence Quantum Yields at 77 K

The following general comments apply to all reported quantum yields. All quantum yields are from determinations made in uncracked 95% ethanol glass at 77 K and were determined by the relative method.<sup>69</sup> The 77 K UV absorption spectra reported in Figures 1 through 18 were the basis for selecting appropriate excitation wavelengths at which to make quantum yield comparisons, and the relative extinction coefficients from these spectra were used to either adjust concentrations before making the quantum yield comparison or to correct the apparent relative quantum yields. The experimental section should be consulted for a fuller accounting of procedures used for quantum yield determinations.

Four types of quantum yield experiments were carried out. The first involved determination of quantum yields of naphthalene derivatives, compounds 1 through 9, relative to naphthalene (10), which is the standard to which all reported quantum yields are ultimately referred. The fluorescence ( $\phi_f$ ) and phosphorescence ( $\phi_p$ ) quantum yields of naphthalene were set (somewhat arbitrarily) at 0.3 and

0.03, respectively, after Ermolaev.<sup>70</sup> The quantum yields reported for naphthalene derivatives in Table 8 are the result in most cases of determinations made at three different excitation wavelengths. See the experimental section for excitation wavelengths and the number of determinations made at each wavelength. The values given in Table 8 are not overall averages of all determinations but averages of the average values obtained at different excitation wavelengths. The standard deviation, in relative terms, for these averages range from about 2% to 10%. Even for the less precise cases, the precision is good considering the numerous factors affecting the values obtained (monochromaticity of exciting light and errors in the relative extinction coefficients obtained from 77 K UV spectra, for example). Thus, the precision of these quantum yield values which are the result of determinations made using several different excitation wavelengths is probably also a good indication of the accuracy of these values relative to the quantum yield values set for naphthalene.

The second type of measurement involved determination of the integrated fluorescence or phosphorescence intensity for a given crown as a function of the concentration of added salt. These experiments establish the molar excess of salt required for essentially complete complexation, indicate the stoichiometry of the complexes, and allow estimates of complexation constants. These are not true quantum yield experiments in that they do not meet the requirement that the two systems compared absorb the same amount of light at the wavelength at which they are excited or that the difference in relative

Table 8. Emission Quantum Yields ( $\phi_f$  and  $\phi_p$ ) and Lifetimes ( $\tau_f$  and  $\tau_p$ ) for Naphthalene and 2,3-, 1,8-, and 1,5-Disubstituted Naphthalenes in Alcohol Glass at 77 K.

Naphthalene Substitution	$\phi_f^b$	$\tau_f(\text{ns})^{c,e}$	$\phi_p^b$	$\tau_p(\text{s})^{b,e}$
None ( $\text{10}$ )	0.30 <sup>a</sup>	215	0.030	2.5
2,3-Dimethyl ( $\text{4}$ )	0.34 $\pm$ 0.01 <sup>d</sup>	144	0.022 $\pm$ 0.001 <sup>a</sup>	2.7
2,3-Bis(methoxymethyl) ( $\text{5}$ )	0.224 $\pm$ 0.006	91	0.031 $\pm$ 0.001	2.8
2,3-Crown-6 ( $\text{1}$ )	0.26 $\pm$ 0.01	94	0.049 $\pm$ 0.002	2.8
1,8-Dimethyl ( $\text{6}$ )	0.39 $\pm$ 0.01	81	0.012 $\pm$ 0.001	1.8
1,8-Bis(methoxymethyl) ( $\text{7}$ )	0.100 $\pm$ 0.002	49	0.070 $\pm$ 0.006	2.3
1,8-Crown-6 ( $\text{2}$ )	0.106 $\pm$ 0.006	44	0.075 $\pm$ 0.006	2.4
1,5-Dimethyl ( $\text{8}$ )	0.45 $\pm$ 0.02	109	0.022 $\pm$ 0.003	2.6
1,5-Bis(methoxymethyl) ( $\text{9}$ )	0.13 $\pm$ 0.01	76	0.08 $\pm$ 0.01	2.5
1,5-Crown-6 ( $\text{3}$ )	0.114 $\pm$ 0.006	35	0.16 $\pm$ 0.02	2.2

<sup>a</sup>Assumed values (see text). All other quantum yields are relative to these values chosen for naphthalene.

<sup>b</sup>In uncracked 95% ethanol glass.

- <sup>c</sup>All  $\tau_f$  values are from 95% ethanol glass except those for  $\lambda$  and  $\lambda$ , which are from ethanol-methanol (4:1, v/v) glass.
- <sup>d</sup>The errors indicated for quantum yields are standard deviations for averages of quantum yield comparisons made at three different wavelengths.
- <sup>e</sup>Estimated relative errors are  $\pm 5\%$ .

absorption be correctable. This is because the comparisons are between a mixture (free crown and complexed crown) and a single compound (free crown) and because the free crown and complexed crown, in general, do not have identical absorption spectra. Furthermore, care was not taken as to the precise excitation wavelength used, and somewhat larger excitation bandpasses were used to reduce the emission noise level. In fact, in some cases, an excitation wavelength which took advantage of differences in absorption spectra was used. Provided, however, that the optical densities of the solutions compared are sufficiently low, the observed integrated intensities can be reexpressed as a linear combination of the quantum yields of free and of complexed crown (see experimental).

Integrated emission intensity titrations (reexpressed in terms of quantum yields of free and complexed crowns) were performed for the alkali metal chloride complexes of crowns  $\lambda_1$ ,  $\lambda_2$ , and  $\lambda_3$ . The results are presented graphically in Figures 55 through 61. Results from titrations monitored by following both fluorescence and phosphorescence integrated intensities are given to illustrate, for example, the difference in quantum yield behavior for crowns  $\lambda_1$  and  $\lambda_2$ . For crown  $\lambda_1$ ,  $\phi_f$  is decreased by alkali metal ion complexation, whereas, for crown  $\lambda_2$ ,  $\phi_f$  is increased. In contrast,  $\phi_p$  is increased by alkali metal ion complexation, for crown  $\lambda_1$ , whereas, for crown  $\lambda_2$ ,  $\phi_p$  is decreased. Figure 59 graphically points out the very large decrease in  $\phi_f$  due to complexation of crown  $\lambda_3$  by cesium cation as compared to the relatively small decreases due to sodium or potassium

# Perturbed 2,3-Naph-20-cr-6 $\phi_{\text{fluor.}}$

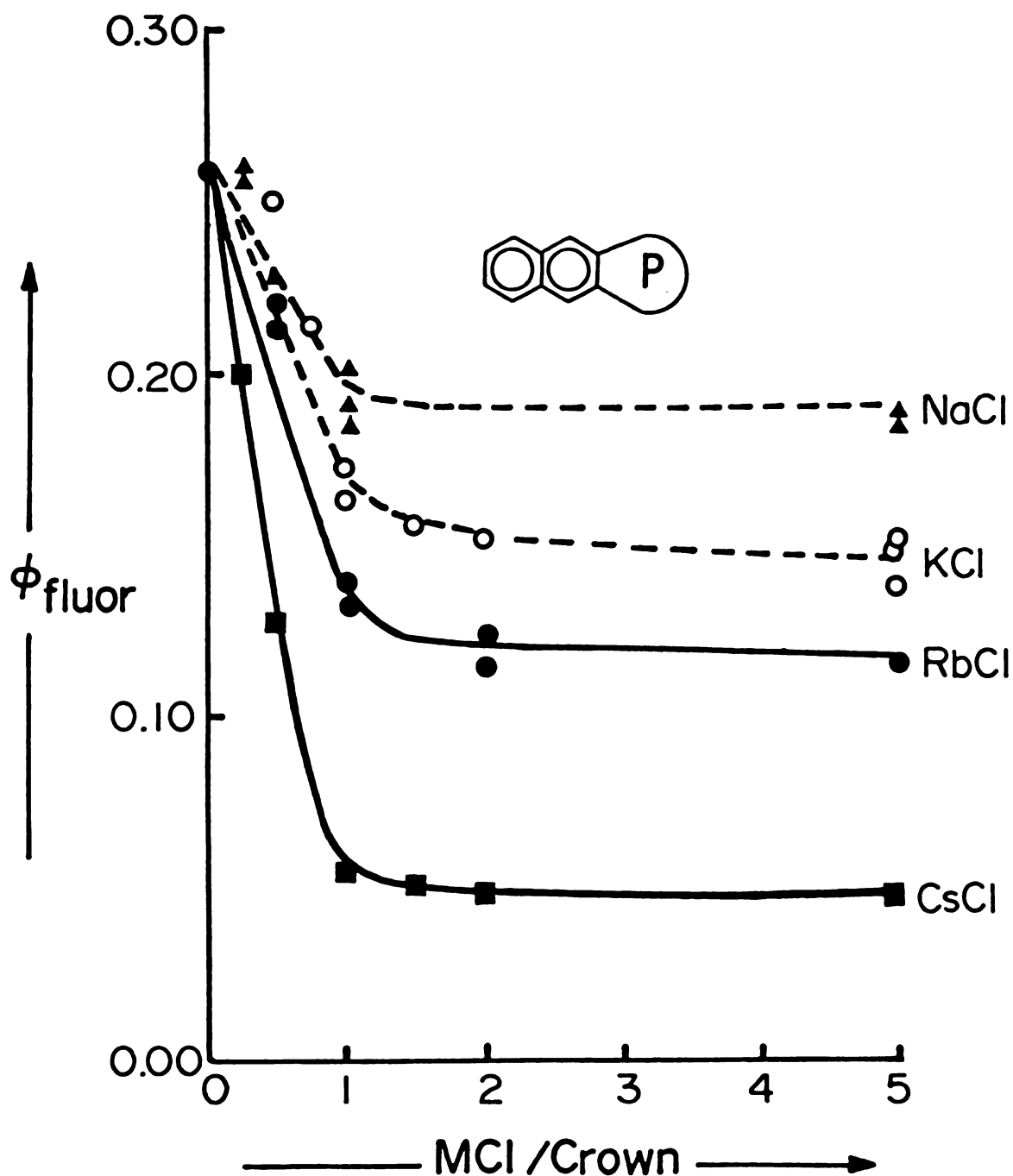


Figure 55. Titration of  $2.00 \times 10^{-4} \text{ M}$  2,3-naphtho-20-crown-6 (1) with alkali metal chlorides in 95% ethanol at 77 K followed by monitoring integrated fluorescence intensity.

# Perturbed 2,3-Naph-20-cr-6 $\phi_{\text{phos}}$ .

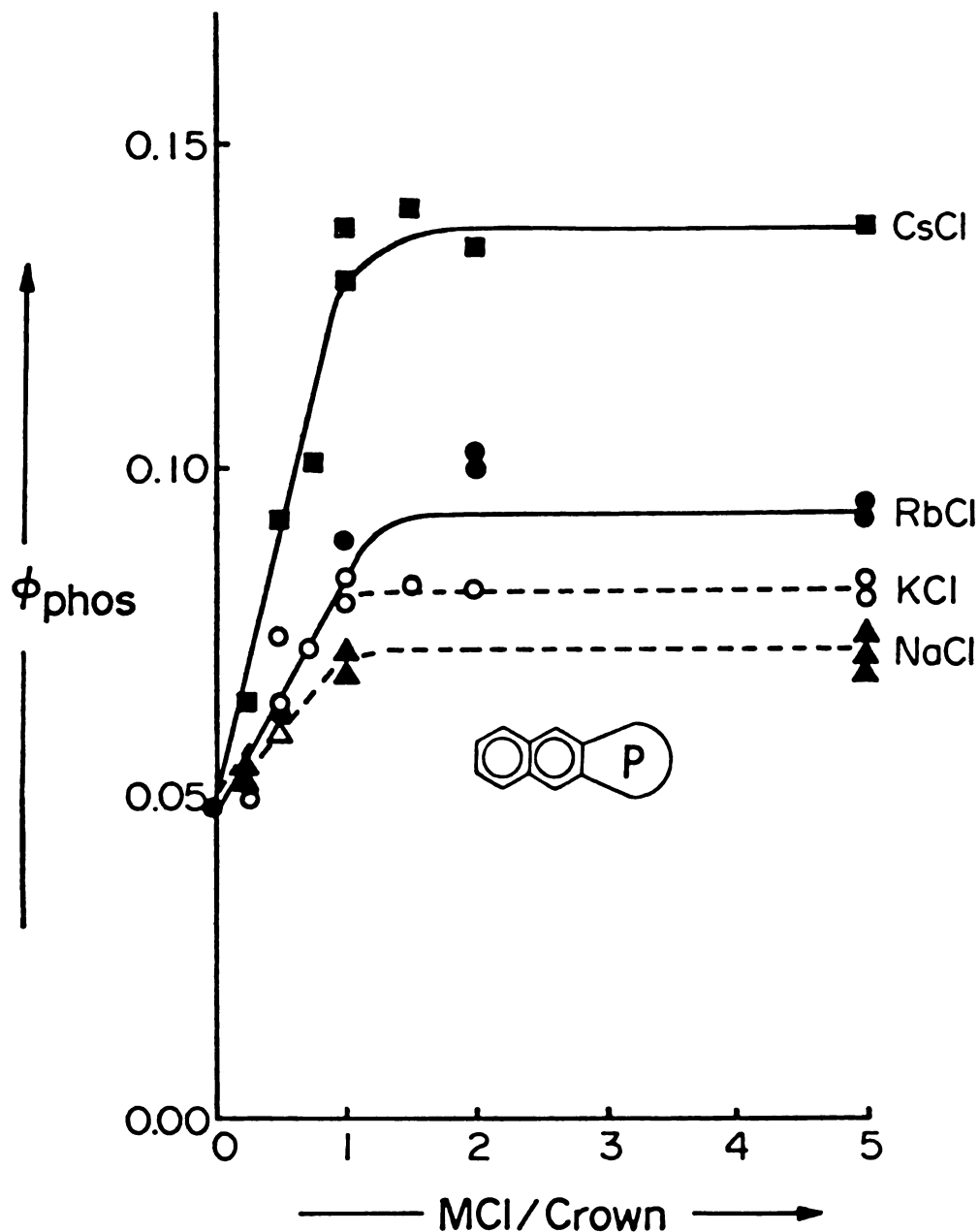


Figure 56. Titration of  $2.00 \times 10^{-4}$  M 2,3-naphtho-20-crown-6 (1) with alkali metal chlorides in 95% ethanol at 77 K followed by monitoring integrated phosphorescence intensity.

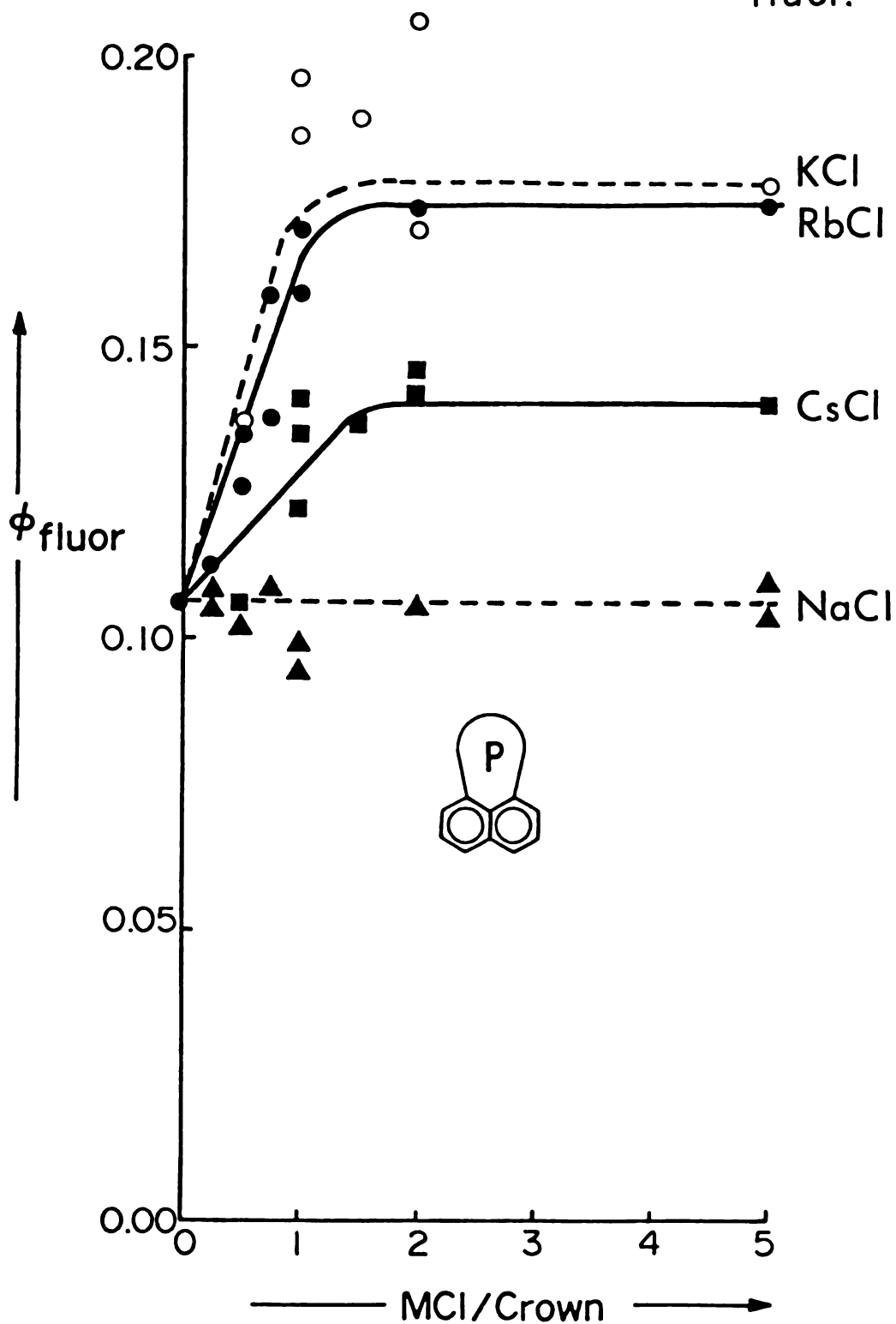


Figure 57. Titration of  $2.00 \times 10^{-4}$  M 1,8-naphtho-21-crown-6 (2) with alkali metal chlorides in 95% ethanol at 77 K followed by monitoring integrated fluorescence intensity.



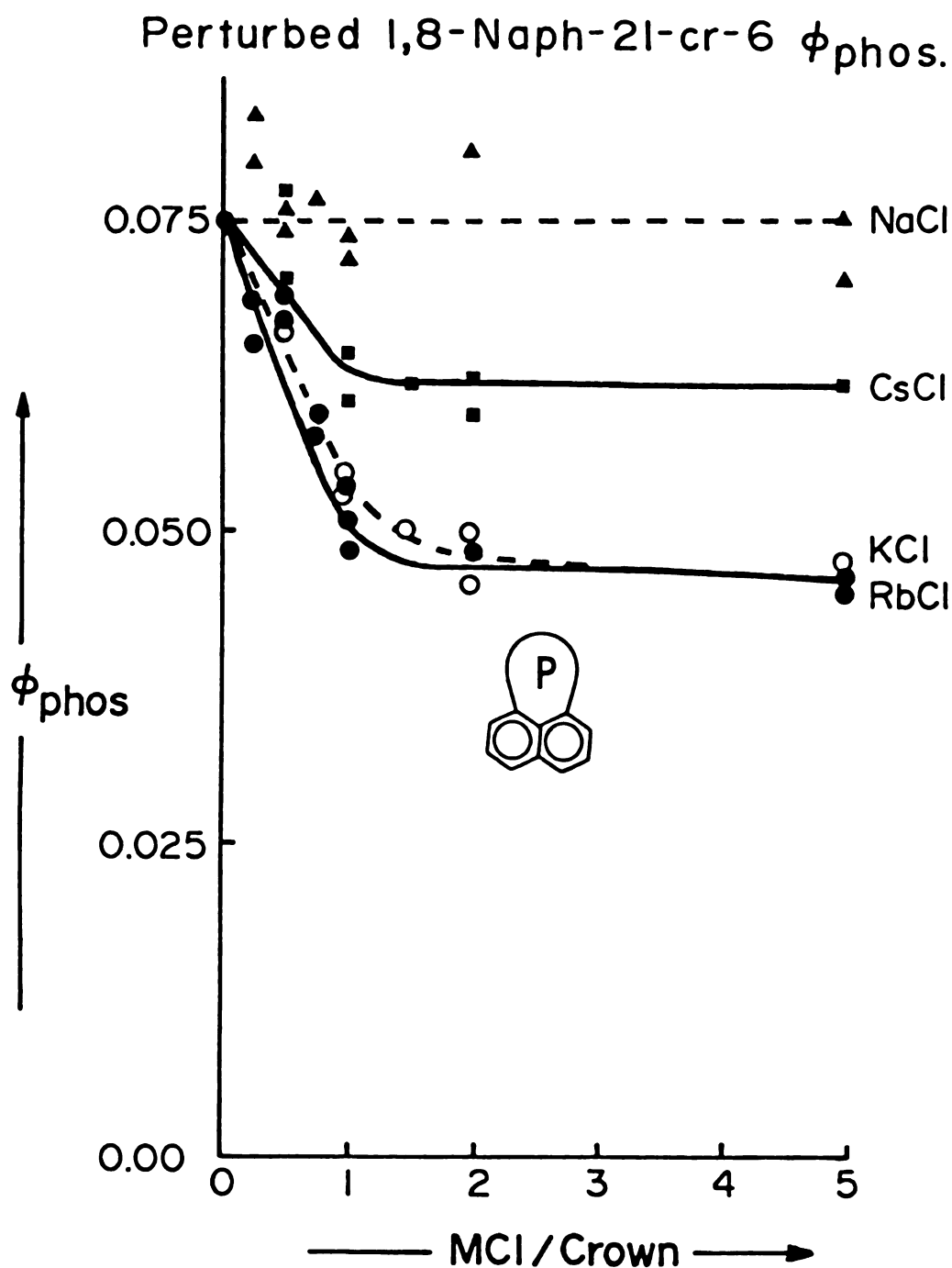


Figure 58. Titration of  $2.00 \times 10^{-4}$  M 1,8-naphtho-21-crown-6 (2) with alkali metal chlorides in 95% ethanol at 77 K followed by monitoring integrated phosphorescence intensity.

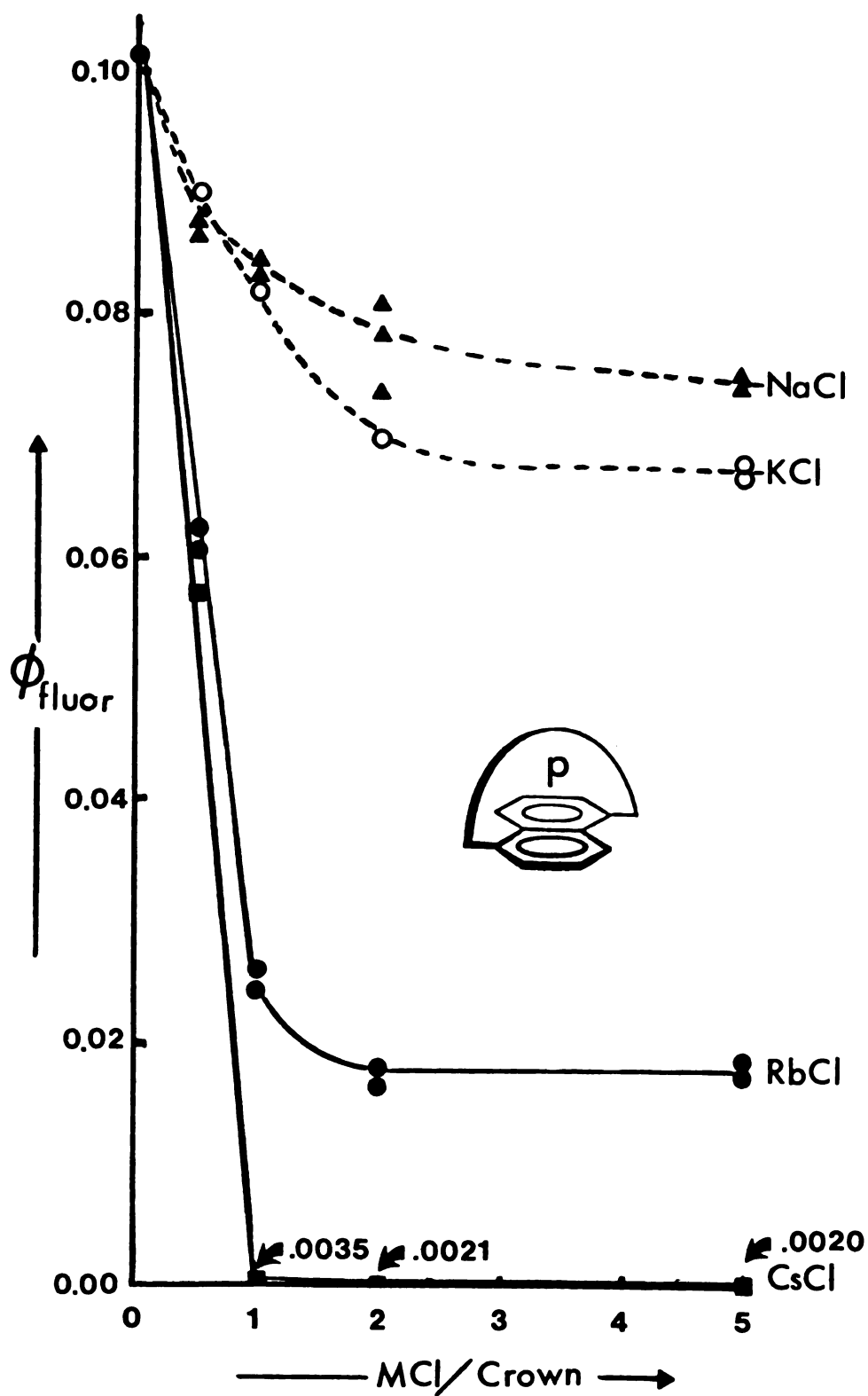


Figure 59. Titration of  $1.00 \times 10^{-4}$  M 1,5-naphtho-22-crown-6 (3) with alkali metal chlorides in 95% ethanol at 77 K followed by monitoring integrated fluorescence intensity.

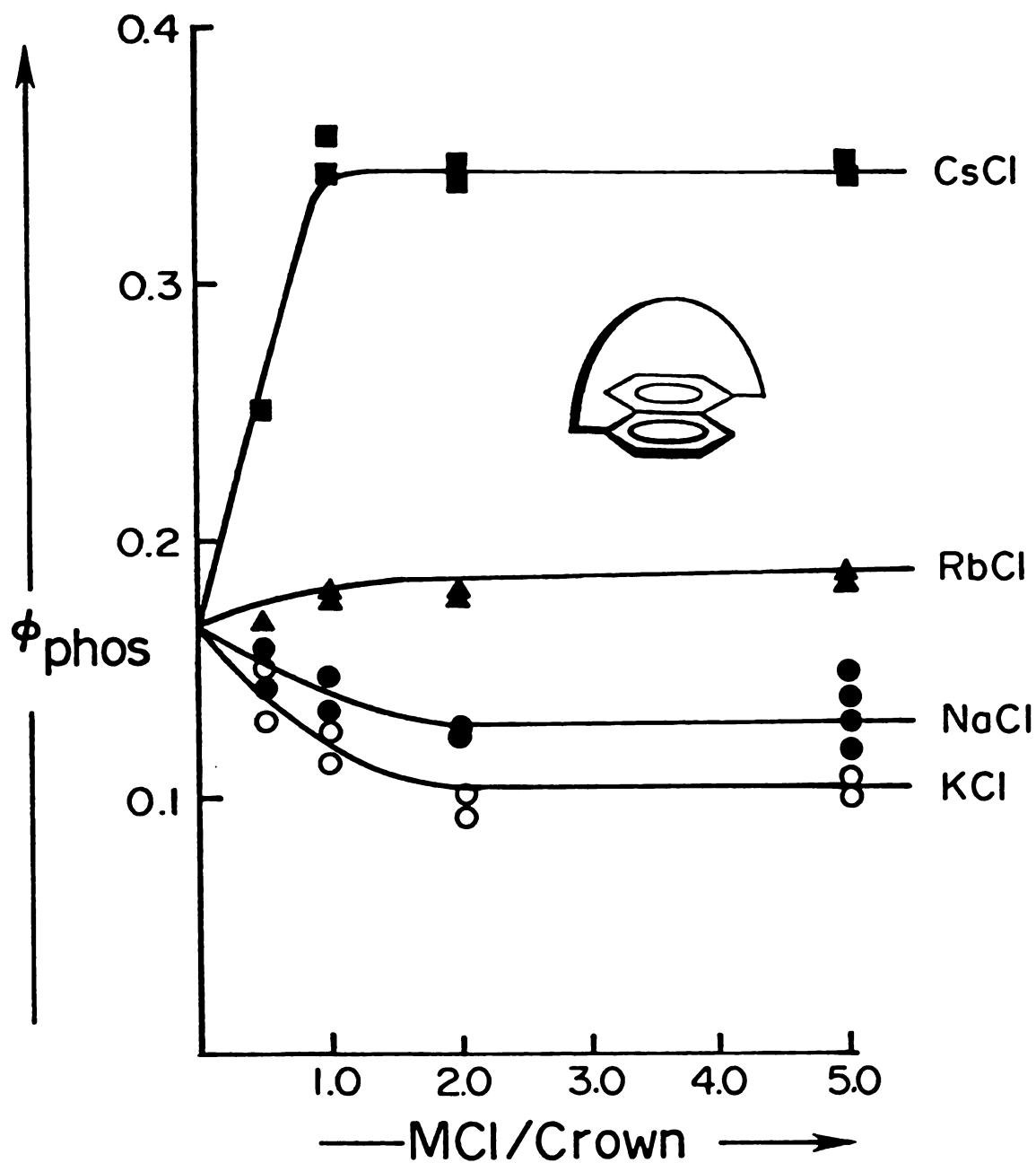


Figure 60. Titration of  $1.00 \times 10^{-4} \text{ M}$  1,5-naphtho-22-crown-6 (3) with alkali metal chlorides in 95% ethanol at 77 K followed by monitoring integrated phosphorescence intensity.

or even due to complexation of rubidium. The relatively sharp breaks at the 1:1 salt to crown ratio are important features of these figures (which are not due to reexpression of the integrated intensities in terms of quantum yields). These sharp breaks indicate the formation of 1:1 complexes with high ( $>10^5$ ) complexation constants. The apparent degree of decrease (or increase) of the quantum yields of complexed crown relative to free crown is meaningful in Figures 55 through 59 only because the data have been reexpressed in terms of carefully determined quantum yields of completely free and completely complexed crown. For example, the decreases in  $\phi_f$  for the alkali metal complexes of crown  $\lambda$  relative to free crown  $\lambda$  shown in Figure 55 are less dramatic than the decreases in the corresponding integrated fluorescence intensities. This is because the complexes all absorb less strongly than free crown in the region in which they were excited (approximately 306 nm).

The remainder of the titration data is presented in tabular form. Since, as remarked previously, the main purpose of these titrations is to establish the molar excess of salt required to achieve essentially complete complexation of the crown, it is only necessary that either the fluorescence or phosphorescence intensity be monitored as a function of added salt, whichever happens to be experimentally easier to do.

For the ammonium, alkylammonium, and bromoalkylammonium complexes of crowns  $\lambda$  and  $\lambda$ , sufficiently accurate integrated intensities are not available (see the experimental section for the variety of ways integrated intensities were obtained). For these complexes,

relative peak intensities (complex intensity/free crown intensity) are tabulated. See Tables 9, 10, 12, and 13. The data are somewhat more scant than for other cases (relative intensities are only available for 1:2, 1:1, and 5:1 salt to crown ratios), but in most cases the relative peak intensities are approximately the same for the 1:1 and for the 5:1 salt to crown ratio. In a few cases (e.g., ammonium chloride complex of crown  $\text{1}$ ), there is a somewhat larger difference. But, at the crown concentration used ( $2.00 \times 10^{-4} \text{ M}$ ), even if there were 20% dissociation for the 1:1 point, there would be only 2% dissociation at the 5:1 point. The tabulated relative peak intensities are referred to as "arbitrary relative peak intensities" in the tables because they depend not only upon the excitation wavelength and band passes used but also on which peaks are compared.

Table 11 gives relative integrated emission intensities for crown  $\text{3}$  as a function of the mole ratio of ammonium and n-propylammonium chlorides to free crown. Tables 12, 13, and 14 give relative integrated emission intensities for crowns  $\text{1}$ ,  $\text{2}$ , and  $\text{3}$  as a function of the mole ratio of iodoalkylammonium chlorides to free crown. Table 14 also gives relative integrated emission intensities for crown  $\text{3}$  as a function of the mole ratio of bromoalkylammonium chlorides to free crown. Tables 15, 16, and 17 give relative integrated emission intensities for crowns  $\text{1}$ ,  $\text{2}$ , and  $\text{3}$  as a function of mole ratio of barium bromide (not for crown  $\text{2}$ ) and silver triflate to free crown. The integrated intensities reported in these tables have been made proportional to the quantum yield of free

Table 9. Titration of 2,3-Naphtho-20-Crown-6 ( $\text{I}$ ) with Ammonium and Alkylammonium Chloride Salts in Un-cracked 95% Ethanol Glass at 77 K Followed by Monitoring Relative Fluorescence Peak Intensities.

Salt/2,3-Cr-6(1) <sup>a</sup>	Arbitrary Relative Intensity <sup>b</sup>			
	$\text{NH}_4\text{Cl}$	$\text{n-PrNH}_3\text{Cl}$	$\text{i-PrNH}_3\text{Cl}$	$\text{t-BuNH}_3\text{Cl}$
None	1.00	1.00	1.00	1.00
1/2	$0.73 \pm 0.01$ (2) <sup>c</sup>	$0.56 \pm 0.01$ (2)	$0.74 \pm 0.01$ (2)	$0.90 \pm 0.02$ (2)
1/1	$0.53 \pm 0.01$ (2)	$0.30 \pm 0.01$ (2)	$0.66 \pm 0.01$ (2)	$0.80 \pm 0.02$ (2)
5/1	$0.41 \pm .01$ (4)	$0.28 \pm 0.01$ (4)	$0.65 \pm .02$ (2)	$0.74 \pm 0.01$ (3)

<sup>a</sup>Molar crown concentration (room temperature) is  $2.00 \times 10^{-4}$  M.

<sup>b</sup>The shortest wavelength fluorescence peak was used. The relative intensity is given in terms of the intensity of the crown peak divided by the intensity of the complex peak.

<sup>c</sup>The errors given are standard deviations; the number in parentheses is the number of comparisons made.

Table 10. Titration of  $2.00 \times 10^{-4}$  M 1,8-Naphtho-21-Crown-6 ( $\lambda$ ) with Ammonium and Alkyl Ammonium Chlorides in Uncracked 95% Ethanol Glass at 77 K Followed by Monitoring Relative Phosphorescence Peak Intensities.

Salt/1,8-Cr-6( $\lambda$ ) <sup>a</sup>	Arbitrary Relative Intensity <sup>b</sup>			
	NH <sub>4</sub> Cl	n-PrNH <sub>3</sub> Cl	i-PrNH <sub>3</sub> Cl	t-BuNH <sub>3</sub> Cl <sup>d</sup>
None	1.00	1.00	1.00	1.00
1/2	$0.71 \pm 0.031$ (2) <sup>c</sup>	$0.63 \pm 0.05$ (3)	$0.80 \pm 0.01$ (2)	$1.02 \pm 0.01$ (2)
1/1	$0.39 \pm 0.01$ (2)	$0.30 \pm 0.05$ (2)	$0.45 \pm 0.01$ (2)	$1.00 \pm 0.01$ (2)
5/1	$0.34 \pm 0.02$ (4)	$0.31 \pm 0.05$ (4)	$0.43 \pm 0.01$ (5)	$0.98 \pm 0.02$ (2)

<sup>a</sup>Molar concentration (room temperature) is  $2.00 \times 10^{-4}$  M.

<sup>b</sup>The shortest wavelength phosphorescence peak was used. The relative intensity is given in terms of the intensity of the crown peak divided by the intensity of the complex.

<sup>c</sup>The error is given in terms of the standard deviation; the number in parentheses is the number of comparisons made.

<sup>d</sup>proof of complexation established by changes in 77 K UV spectra. See text.

Table 11. Titration of 1,5-Naphtho-22-Crown-6 (3) with Ammonium and n-Propylammonium Chlorides in Uncracked 95% Ethanol Glass at 77 K Followed by Monitoring Relative Integrated Fluorescence Intensities.

Salt/1,5-Cr-6 (3) <sup>a</sup>	NH <sub>4</sub> Cl	<u>n</u> -PrNH <sub>3</sub> Cl
None	0.114	0.114
5/1	0.102 ± .002 (3) <sup>b</sup>	0.090 ± .002 (2)
10/1	0.097 ± .001 (3)	0.089 ± .005 (2)
20/1	0.089 ± .002 (6)	0.091 ± .003 (2)
50/1	0.089 ± .002 (6)	-----
100/1	0.091 ± .003 (7)	-----

<sup>a</sup> Molar crown concentration (room temperature) is  $1.00 \times 10^{-4}$  M.

<sup>b</sup> The error given is in terms of the standard deviation. The number in parentheses is the number of comparisons made.



Table 12. Titration of 2,3-Naphtho-20-Crown-6 ( $\lambda$ ) with Haloalkylammonium Chlorides in Uncracked 95% Ethanol Glass at 77 K Followed by Monitoring Relative Fluorescence Intensities.

Salt/2,3-Cr-6 ( $\lambda$ )	Arbitrary Relative Intensity			
	$\text{Br}(\text{CH}_2)_2\text{NH}_3\text{Cl}^{\text{a}}$	$\text{Br}(\text{CH}_2)_3\text{NH}_3\text{Cl}^{\text{a}}$	$\text{I}(\text{CH}_2)_2\text{NH}_3\text{Cl}^{\text{d}}$	$\text{I}(\text{CH}_2)_3\text{NH}_3\text{Cl}^{\text{d}}$
None	1.00	1.00	0.26	0.26
1/2	0.67 <sup>b</sup>	$0.58 \pm 0.01$ (2) <sup>c</sup>	$0.160 \pm .001$ (2)	$0.150 \pm .007$ (2)
1/2	----	$0.29 \pm 0.01$ (2)	$0.068 \pm .001$ (2)	$0.043 \pm .003$ (2)
2/1	0.43	$0.29 \pm 0.01$ (2)	$0.049 \pm .002$ (2)	$0.032 \pm .001$ (2)
5/1	0.43	$0.29 \pm 0.02$ (2)	$0.049 \pm .001$ (2)	$0.030 \pm .001$ (2)
10/1	----	----	$0.049 \pm .002$ (4)	$0.030 \pm .002$ (4)
20/1	----	----	$0.057 \pm .004$ (9)	$0.030 \pm .004$ (8)

<sup>a</sup>Molar crown concentration (room temperature) is  $2.00 \times 10^{-4}$  M. Results are given in terms of the intensity of the shortest wavelength fluorescence peak of the complex divided by the intensity of the shortest wavelength peak of the free crown.

<sup>b</sup>Single determinations.

<sup>c</sup>The error is given in terms of the standard deviation. The number in parentheses is the number of comparisons made.

<sup>d</sup>Molar crown concentration (room temperature) is  $1.00 \times 10^{-4}$  M. Results are from integrated relative intensities.

Table 13. Titration of 1,8-Naphtho-21-Crown-6 (2) with Haloalkyl Ammonium Chlorides in Uncracked 95% Ethanol Glass at 77 K Followed by Monitoring Relative Integrated Emission Intensities.

Salt/1,8-Cr-6 (2)	Arbitrary Relative Intensity			
	$\text{Br}(\text{CH}_2)_2\text{NH}_3\text{Cl}^a$	$\text{Br}(\text{CH}_2)_3\text{NH}_3\text{Cl}^a$	$\text{I}(\text{CH}_2)_2\text{NH}_3\text{Cl}^b$	$\text{I}(\text{CH}_2)_3\text{NH}_3\text{Cl}^b$
None	0.076 (Phos.)	0.076 (Phos.)	0.076 (Phos.)	0.106 (Fluor.)
1/2	$0.045 \pm 0.001$ (2) <sup>c</sup>	$0.040 \pm 0.002$ (2)	$0.067 \pm .001$ (2)	$0.137 \pm .007$ (4)
1/1	$0.027 \pm 0.001$ (2)	$0.022 \pm$ (1)	$0.059 \pm .001$ (2)	$0.170 \pm .006$ (4)
2/1	$0.032 \pm 0.001$ (2)	$0.022 \pm 0.00$ (2)	-----	$0.167 \pm .005$ (4)
2.5/1	-----	-----	$0.056 \pm .006$ (5)	-----
5/1	$0.031 \pm 0.001$ (2)	$0.030 \pm 0.002$ (2)	$0.057 \pm .002$ (6)	$0.172 \pm .006$ (4)
10/1	-----	-----	$0.059 .004$ (6)	$0.165 \pm .004$ (4)

<sup>a</sup>Molar crown concentration (room temperature) is  $2.00 \times 10^{-4}$  M.

<sup>b</sup>Molar crown concentration (room temperature) is  $1.00 \times 10^{-4}$  M.

<sup>c</sup>The error is given in terms of the standard deviation. The number in parentheses is the number of comparisons made.

Table 14. Titration of 1,5-Naphtho-22-Crown-6 (3) with Haloalkylammonium Chlorides in Uncracked 95% Ethanol Glass at 77 K Followed by Monitoring Relative Integrated Fluorescence Intensity.

Salt/1,5-Cr-6 (3) <sup>a</sup>	Arbitrary Relative Intensity		
	Br(CH <sub>2</sub> ) <sub>2</sub> NH <sub>3</sub> Cl	Br(CH <sub>2</sub> ) <sub>3</sub> Cl	I(CH <sub>2</sub> ) <sub>2</sub> NH <sub>3</sub> Cl
None	0.114	0.114	0.114
1/2	0.091 ± .001 (3) <sup>b</sup>	0.093 ± .002 (3)	0.076 ± .003 (2)
1/1	0.077 ± .001 (2)	0.080 ± .001 (2)	0.043 ± .001 (2)
2/1	0.066 ± .002 (2)	0.068 ± .002 (2)	0.032 ± .001 ( )
5/1	-----	0.064 ± .001 (2)	0.012 ± .003 ( )
10/1	0.058 ± .001 (4)	0.065 ± .001 (2)	0.012 ± .003 ( )
20/1	0.057 ± .005 (4)	0.066 ± .001 (2)	0.013 ± .002 (7)
			0.0158 ± .0003 (4)
			0.0166 ± .0007 (3)
			0.0171 ± .0006 (4)

<sup>a</sup>Molar crown concentration (room temperature) at 1.00 x 10<sup>-4</sup> M.

<sup>b</sup>The error is given in terms of the standard deviation. The number in parentheses is the number of comparisons made.

Table 15. Titration of 2,3-Naphtho-20-Crown-6 (1) with Barium Bromide and Silver Triflate in Uncracked 95% Ethanol Glass at 77 K Followed by Monitoring Relative Integrated Fluorescence Intensities.

Salt/2,3-Cr-6(1) <sup>a</sup>	Arbitrary Relative Intensity	
	BaBr <sub>2</sub>	AgOSO <sub>2</sub> CF <sub>3</sub>
None	0.26	0.26
1/2	0.119 ± .004 (2) <sup>b</sup>	----
1/1	0.063 ± .001 (2)	0.253 ± .001 (2)
2.5/1	0.064 ± .006 (2)	----
5/1	0.065 ± .002 (2)	0.217 ± .001 (2)
10/1	0.065 ± .003 (2)	0.180 ± .002 (2)
20/1	----	0.165 ± .003 (2)
50/1	----	0.165 ± .003 (2)
100/1	----	0.164 ± .001 (2)

<sup>a</sup>Molar crown concentration (at room temperature) at  $1.00 \times 10^{-4}$  M.

<sup>b</sup>Error is given in terms of the standard deviation. The number in parentheses is the number of determinations made.

Table 16. Titration of 1,8-Naphtho-21-Crown-6 (2) With Silver Tri-  
 flate in Uncracked 95% Ethanol Glass at 77 K Followed by  
 Monitoring Relative Integrated Phosphorescence Intensity.

AgOSO <sub>2</sub> CF <sub>3</sub> /1,8-Cr-6 (2) <sup>a</sup>	Arbitrary Relative Intensity
None	0.076
1/2	0.0748 ± .0005 (2) <sup>b</sup>
1/1	0.0748 ± .0002 (2)
2.5/1	0.0742 ± .0006 (2)
5/1	0.0710 ± .001 (6)
10/1	0.0675 ± .002 (12)
20/1	0.0681 ± .003 (12)
50/1	0.0660 ± .008 (8)

<sup>a</sup>Molar crown concentration (room temperature) is  $1.00 \times 10^{-4}$  M.

<sup>b</sup>The error is given in terms of the standard deviation. The number in parentheses is the number of comparisons made.

Table 17. Titration of 1,5-Naphtho-22-Crown-6 (3) with Barium Bromide and Silver Triflate in Uncracked 95% Ethanol Glass at 77 K Followed by Monitoring Relative Integrated Emission Intensities.

Salt/1,5-Cr-6 (3) <sup>a</sup>	Arbitrary Relative Intensity	
	BaBr <sub>2</sub>	AgOSO <sub>2</sub> CF <sub>3</sub>
None	0.114 (Fluor.)	0.16 (Phos.)
1/2	0.115 ± .003 (3) <sup>b</sup>	0.152 ± .004 (2)
1/1	0.110 ± .003 (3)	0.177 ± .008 (2)
2/1	0.108 ± .003 (2)	----
5/1	0.104 ± .001 (2)	0.38 ± .01 (2)
10/1	0.0944 ± .005 (2)	0.64 ± .03 (2)
25/1	0.0837 ± .0002 (2)	0.86 ± .03 (2)
50/1	0.0837 ± .0002 (2)	1.02 ± .04 (3)
100/1	0.0846 ± .0003 (2)	1.02 ± .06 (3)
200/1	----	1.02 ± .03 (3)

<sup>a</sup>Molar crown concentration (room temperature) is  $1.00 \times 10^{-4}$  M.

<sup>b</sup>The error is given in terms of the standard deviation. The number in parentheses is the number of comparisons made.

crown but have not been modified in any other way. As tabulated, they provide information on the extent of complexation as a function of added salt. They are referred to as "arbitrary relative integrated intensities" in the tables because they depend upon the choice of experimental conditions (excitation wavelength and width of band-pass).

The errors given in Tables 9 through 17 are standard deviations. The number of values averaged in each case is given in parentheses after the error.

There are several special cases in which changes in both fluorescence and phosphorescence intensities are too small to be reliable indicators of the extent of complexation. In two cases, the extent of complexation was established through competition experiments: a crown/salt mixture which has a quantum yield greatly different from that of the crown alone is titrated with the species which does not cause a very large change in intensity. Relative equilibrium constants can be calculated (see experimental section), thus allowing one to calculate how much salt would be necessary for complete complexation in the absence of competition, provided that there is an independent estimate for one of the equilibrium constants available.

The results of a competition study between sodium chloride and crown  $\lambda$ /rubidium chloride are given in Table 18. The integrated intensities are expressed relative to that of rubidium chloride/crown  $\lambda$  = 2/1, formal crown concentration at  $1.00 \times 10^{-4}$  M. The results from systems containing 100:2:1 and 50:2:1 mole ratios of

Table 18. Competition for  $1.00 \times 10^{-4}$  M 1,8-Naphtho-21-Crown-6 (2) in Uncracked 95% Ethanol Glass at 77 K by Sodium and Rubidium Chlorides Followed by Monitoring Arbitrary Relative Integrated Intensity.

System	Arbitrary Rel. Integrated Intensity	Rel. Equil. Constant $K_{\text{Rb}^+}/K_{\text{Na}^+}$
RbCl/ $\lambda$ = 2/1	1.00	
1,8-Cr-6 (2)	0.47	
NaCl/ $\lambda$ = 100/1	$0.49 \pm .04$ (3)	
NaCl/RbCl/ $\lambda$ = 100/2/1	$0.71 \pm .05$ (3)	50
NaCl/RbCl/ $\lambda$ = 50/2/1	$0.8 \pm .1$ (2)	60
NaCl/RbCl/ $\lambda$ = 10/2/1	$0.96 \pm .04$ (2)	100

<sup>a</sup>Errors are given in terms of the standard deviation. The number in parentheses after the error is the number of determinations.



sodium chloride to rubidium chloride to crown  $\text{2}_{\text{N}}$  show that rubidium complexes 50 to 60 times better with crown  $\text{2}_{\text{N}}$  than does sodium. The results from the 10:2:1 case are less reliable due to the small difference in intensity between it and the rubidium chloride/crown  $\text{2}_{\text{N}}$  standard.

The initial experiments on the sodium complex of crown  $\text{2}_{\text{N}}$  were only done using a five-fold excess of sodium chloride ( $2.00 \times 10^{-4}$  M crown). The above results indicate that this would not be a sufficient excess for complete complexation of crown. Assuming an equilibrium constant of  $10^6$  for the rubidium complex of crown  $\text{2}_{\text{N}}$  (based on the essentially complete complexation with a two-fold excess of salt indicated by Figures 56 and 57), an equilibrium constant of approximately  $2 \times 10^4$  is indicated for the sodium complex. Thus, complexation would be only about 94% complete with a five-fold excess of salt. Quantum yield, energy, and emission spectra were redetermined with a hundred-fold excess of sodium chloride and the results were essentially the same as those for a five-fold excess. The overall changes are small, however, so this isn't surprising.

The results of a similar competition study between barium bromide and rubidium chloride/crown  $\text{2}_{\text{N}}$  are given in Table 19. The results are somewhat rougher than for the sodium competition study, probably because of the smaller differences, but indicate that rubidium and barium have about the same complexing affinity for crown  $\text{2}_{\text{N}}$ .

The third type of quantum yield determination is similar in nature to the first. The fluorescence and phosphorescence quantum yields of fully complexed crowns were determined relative to those

Table 19. Competition for  $1.00 \times 10^{-4}$  M 1,8-Naphtho-21-Crown-6 (2) in Uncracked 95% Ethanol Glass at 77 K by Barium Bromide and Rubidium Chloride Followed by Monitoring Arbitrary Relative Integrated Intensity.

System	Arbitrary Rel. Integrated Intensity	Rel/ Equil. Constant $K_{Rb+}/K_{Ba++}$
BaBr <sub>2</sub> /2 = 10/1	1.00	
1,8-Cr-6 (2)	0.96	
RbCl/2 = 2.5/1	0.68 ± .01 (2)	
BaBr <sub>2</sub> /RbCl/2 = 1/1/1	0.87 ± .01 (1)	0.5
BaBr <sub>2</sub> /RbCl/2 = 12.5/2.5/1	0.92 ± .01 (2)	1.7

<sup>a</sup>Errors are given in terms of the standard deviation. The number in parentheses after the error is the number of determinations.

of the parent free crown, which, in turn, were determined relative to naphthalene (vide infra). Sufficient salt, as determined from the titrations described above, was added so that the crown would be essentially completely complexed. Emission quantum yields of the alkali metal chloride, barium bromide, and silver triflate complexes of crowns 1, 2, and 3 are given in Tables 20, 21, and 22, respectively; those of the ammonium and alkyl ammonium complexes of crowns 1, 2, and 3 in Tables 23, 24 and 25, respectively; and those of the haloalkylammonium chloride complexes of crowns 1, 2, and 3 in Tables 26, 27, and 28, respectively.

The values given in Tables 20 through 28 are the result of at least four determinations made using only one set of excitation wavelengths. (See experimental for wavelengths at which determinations were made.) The errors given are standard deviations and indicate the precision of the comparison of the quantum yield of the complex to that of the free crown. In many cases, they are better than the standard deviation indicated for the quantum yield of the parent crown. The absolute accuracy of the quantum yields of the complexes obviously can't be any better than the accuracy of the quantum yield to which they are referred (naphthalene, ultimately). But quantum yield comparisons between free crown and complexed crown can probably be made more accurately than quantum yield comparisons between free crown and naphthalene, since the 77 K UV spectra of the complexes are more similar to free crown than are the 77 K UV spectra of free crown to naphthalene.

The fourth type of quantum yield experiment involved comparison

Table 20. Emission Quantum Yields ( $\phi_f$  and  $\phi_p$ ) and Lifetimes ( $\tau_f$  and  $\tau_p$ ) for 2,3-Naphtho-20-Crown-6 ( $\lambda_c$ ) and Alkali Metal Chloride, Barium Bromide, and Silver Triflate Complexes of Crown  $\lambda_c$  in Alcohol Glass at 77 K.

System	$\phi_f^{b,c}$	$\tau_f$ (ns) <sup>d,e</sup>	$\phi_p^{b,c}$	$\tau_p$ (s) <sup>c,e</sup>
2,3-Cr-6 ( $\lambda_c$ )	$0.26 \pm 0.01^a$	94	$0.049 \pm 0.002^a$	2.8
$\lambda_c$ + NaCl	$0.189 \pm 0.003$	112	$0.072 \pm 0.004$	3.4
$\lambda_c$ + KCl	$0.154 \pm 0.002$	94	$0.081 \pm 0.003$	3.1
$\lambda_c$ + RbCl	$0.117 \pm 0.003$	80	$0.092 \pm 0.002$	2.7
$\lambda_c$ + CsCl	$0.048 \pm 0.001$	86	$0.137 \pm 0.002$	2.2
$\lambda_c$ + BaBr <sub>2</sub>	$0.048 \pm 0.002$	52	$0.138 \pm 0.002$	2.7
$\lambda_c$ + AgOSO <sub>2</sub> CF <sub>3</sub>	$0.123 \pm 0.004$	---	$0.068 \pm 0.002$	3.2

<sup>a</sup>Quantum yields of crown  $\lambda_c$  were determined relative to naphthalene (see Table 8). <sup>b</sup>Quantum yields of complexes were determined relative to free crown  $\lambda_c$ . The indicated errors are standard deviations for averages of at least four quantum yield comparisons at a single wavelength. <sup>c</sup>In uncracked 95% ethanol glass. <sup>d</sup>All  $\tau_f$  values are from 95% ethanol glass except that for the barium bromide complex, which is from ethanol-methanol (4:1, v/v) glass. <sup>e</sup>Estimated relative errors are  $\pm 5\%$ ;  $\pm 10\%$  for barium bromide complex.<sup>π</sup>

Table 21. Emission Quantum Yields ( $\phi_f$  and  $\phi_p$ ) and Lifetimes ( $\tau_f$  and  $\tau_p$ ) for 1,8-Naphtho-21-Crown-6 ( $\lambda$ ) and Alkali Metal Chloride, Barium Bromide, and Silver Triflate Complexes of Crown  $\lambda$  in Alcohol Glass at 77 K.

System	$\phi_f^{b,c}$	$\tau_f$ (ns) <sup>d,e</sup>	$\phi_p^{b,c}$	$\tau_p$ (s) <sup>c,e</sup>
1,8-Cr-6 ( $\lambda$ )	$0.106 \pm 0.006^a$	44	$0.075 \pm 0.006^a$	2.4
$\lambda$ + NaCl	$0.107 \pm 0.003$	46	$0.073 \pm 0.001$	2.3
$\lambda$ + KCl	$0.176 \pm 0.006$	56	$0.046 \pm 0.002$	1.37
$\lambda$ + RbCl	$0.176 \pm 0.005$	51	$0.046 \pm 0.002$	1.31
$\lambda$ + CsCl	$0.140 \pm 0.004$	46	$0.062 \pm 0.002$	1.23
$\lambda$ + BaBr <sub>2</sub>	$0.123 \pm 0.001$	--	$0.064 \pm 0.001$	1.14
$\lambda$ + AgOSO <sub>2</sub> CF <sub>3</sub>	$0.153 \pm 0.002$	--	$0.064 \pm 0.001$	2.16

<sup>a</sup>Quantum yields of crown  $\lambda$  were determined relative to naphthalene (see Table 8). <sup>b</sup>Quantum yields of complexes were determined relative to free crown  $\lambda$ . The indicated errors are standard deviations for averages from at least four quantum yield comparisons at a single wavelength. <sup>c</sup>In uncracked 95% ethanol glass. <sup>d</sup>In 95% ethanol glasses, most glasses cracked. <sup>e</sup>Estimated relative errors are  $\pm 5\%$ .

Table 22. Emission Quantum Yields ( $\phi_f$  and  $\phi_p$ ) and Lifetimes ( $\tau_f$  and  $\tau_p$ ) for 1,5-Naphtho-22-Crown-6 and Alkali Metal Chloride, Barium Bromide, and Silver Triflate Complexes of Crown  $\beta$  in Alcohol Glass at 77 K.

System	$\phi_f^{b,c}$	$\tau_f$ (ns) <sup>d,e</sup>	$\phi_p^{b,c}$	$\tau_p$ (s) <sup>e</sup>
1,5-Cr-6 ( $\beta$ )	$0.114 \pm 0.006^a$	35	$0.16 \pm 0.02^a$	2.2
$\beta$ + NaCl	$0.076 \pm 0.002$	29	$0.126 \pm 0.002$	2.4
$\beta$ + KCl	$0.061 \pm 0.002$	27	$0.119 \pm 0.004$	2.0
$\beta$ + RbCl	$0.0185 \pm 0.0006$	--	$0.181 \pm 0.003$	1.7
$\beta$ + CsCl	$0.00152 \pm 0.00004$	--	$0.333 \pm 0.002$	0.36
$\beta$ + BaBr <sub>2</sub>	$0.096 \pm 0.001$	--	$0.198 \pm 0.002$	2.1
$\beta$ + AgOSO <sub>2</sub> CF <sub>3</sub>	$0.0060 \pm 0.0006$	--	$0.84 \pm 0.002$	0.19

<sup>a</sup>Quantum yields of crown  $\beta$  were determined relative to naphthalene (see Table 8). <sup>b</sup>Quantum yields of complexes were determined relative to free crown  $\beta$ . The indicated errors are standard deviations for averages from at least four quantum yield comparisons at a single wavelength. <sup>c</sup>In uncracked 95% ethanol glass. <sup>d</sup>In 95% ethanol-methanol (4:1, v/v) glass. <sup>e</sup>Estimated relative errors are  $\pm 5\%$ .

Table 23. Emission Quantum Yields ( $\phi_f$  and  $\phi_p$ ) and Lifetimes ( $\tau_f$  and  $\tau_p$ ) for 2,3-Naphtho-20-Crown-6 ( $\lambda_c$ ) and Ammonium and Alkylammonium Chloride Complexes of Crown  $\lambda_c$  in Alcohol Glass at 77 K.

System	$\phi_f^{b,c}$	$\tau_f$ (nd) <sup>d,e</sup>	$\phi_p^{b,c}$	$\tau_p$ (s) <sup>c,e</sup>
2,3-Cr-6 ( $\lambda_c$ )	$0.26 \pm 0.01^a$	94	$0.049 \pm 0.002^a$	2.8
$\lambda_c + \text{NH}_4\text{Cl}$	$0.154 \pm 0.001$	87	$0.084 \pm 0.004$	2.8
$\lambda_c + \underline{n}\text{-PrNH}_3\text{Cl}$	$0.112 \pm 0.003$	58	$0.079 \pm 0.003$	2.4
$\lambda_c + \underline{i}\text{-PrNH}_3\text{Cl}$	$0.181 \pm 0.007$	97	$0.074 \pm 0.001$	3.0
$\lambda_c + \underline{t}\text{-BuNH}_3\text{Cl}$	$0.23 \pm 0.01$	106	$0.068 \pm 0.002$	3.1

<sup>a</sup>Quantum yields of crown  $\lambda_c$  were determined relative to naphthalene (see Table 8). <sup>b</sup>Quantum yields of complexes were determined relative to free crown  $\lambda_c$ . The indicated errors are standard deviations for averages from at least four quantum yield comparisons at a single wavelength. <sup>c</sup>In uncracked 95% ethanol glass. <sup>d</sup>In 95% ethanol-methanol (4:1, v/v) glass. <sup>e</sup>Estimated relative errors are  $\pm 5\%$ .

Table 24. Emission Quantum Yields ( $\phi_f$  and  $\phi_p$ ) and Lifetimes ( $\tau_f$  and  $\tau_p$ ) for 1,8-Naphtho-21-Crown-6 ( $\mathcal{Z}$ ) and Ammonium and Alkylammonium Chloride Complexes of Crown  $\mathcal{Z}$  in Alcohol Glass at 77 K.

System	$\phi_f^{b,c}$	$\tau_f$ (ns) <sup>d,e</sup>	$\phi_p^{b,c}$	$\tau_p$ (s) <sup>c</sup>
1,8-Cr-6 ( $\mathcal{Z}$ )	$0.106 \pm 0.006^a$	44	$0.075 \pm 0.006^a$	2.4
$\mathcal{Z} + \text{NH}_4\text{Cl}$	$0.175 \pm 0.008$	54	$0.049 \pm 0.003$	1.7
$\mathcal{Z} + \text{n-PrNH}_3\text{Cl}$	$0.181 \pm 0.004$	52	$0.046 \pm 0.002$	1.7
$\mathcal{Z} + \text{i-PrNH}_3\text{Cl}$	$0.174 \pm 0.008$	54	$0.053 \pm 0.002$	1.9
$\mathcal{Z} + \text{t-BuNH}_3\text{Cl}$	$0.112 \pm 0.002$	52	$0.071 \pm 0.001$	2.4

<sup>a</sup>Quantum yields of crown  $\mathcal{Z}$  were determined relative to naphthelene (see Table 8). <sup>b</sup>Quantum yields of complexes were determined relative to free crown  $\mathcal{Z}$ . The indicated errors are standard deviations for averages from at least four quantum yield comparisons at a single wavelength. <sup>c</sup>In uncracked 95% ethanol glass. <sup>d</sup>In 95% ethanol-methanol (4:1, v/v) glass. <sup>e</sup>Estimated relative errors are  $\pm 5\%$ .



Table 25. Emission Quantum Yields ( $\phi_f$  and  $\phi_p$ ) and Lifetimes ( $\tau_f$  and  $\tau_p$ ) for 1,5-Naphtho-22-Crown-6 ( $\lambda_c$ ) and Ammonium and n-Propylammonium Complexes of Crown  $\lambda_c$  in 95% Ethanol Glass at 77 K.

System	$\phi_f^{b,c}$	$\tau_f$ (ns) <sup>d</sup>	$\phi_p^{b,c}$	$\tau_p$ (s) <sup>c,e</sup>
1,5-Cr-6 ( $\lambda_c$ )	$0.114 \pm 0.006^a$	35	$0.16 \pm 0.02^a$	2.2
$\lambda_c + \text{NH}_4\text{Cl}$	$0.104 \pm 0.002$	--	$0.169 \pm 0.003$	2.2
$\lambda_c + \text{n-PrNH}_3\text{Cl}$	$0.111 \pm 0.001$	--	$0.190 \pm 0.005$	2.1

<sup>a</sup>Quantum yields of crown  $\lambda_c$  were determined relative to naphthalene (see Table 8). <sup>b</sup>Quantum yields of complexes were determined relative to free crown  $\lambda_c$ . The indicated errors are standard deviations for averages from at least four quantum yield comparisons at a single wavelength. <sup>c</sup>In uncracked 95% ethanol glass. <sup>d</sup>In cracked 95% ethanol glass. <sup>e</sup>Estimated relative errors are  $\pm 5\%$ .

Table 26. Emission Quantum Yields ( $\phi_f$  and  $\phi_p$ ) for 2,3-Naphtho-20-Crown-6 ( $\lambda$ ) and Haloalkylammonium Chloride Complexes of Crown  $\lambda$  in Uncracked 95% Ethanol Glass at 77 K.

System	$\phi_f^{a,b}$	$\phi_p^{a,b}$
2,3-Cr-6 ( $\lambda$ )	$0.26 \pm 0.01$	$0.049 \pm 0.002$
$\lambda + \text{Br}(\text{CH}_2)_2\text{NH}_3\text{Cl}$	$0.165 \pm 0.004$	$0.083 \pm 0.002$
$\lambda + \text{Br}(\text{CH}_2)_3\text{NH}_3\text{Cl}$	$0.108 \pm 0.003$	$0.107 \pm 0.001$
$\lambda + \text{I}(\text{CH}_2)_2\text{NH}_3\text{Cl}$	$0.030 \pm 0.003$	$0.104 \pm 0.004$
$\lambda + \text{I}(\text{CH}_2)_3\text{NH}_3\text{Cl}$	$0.056 \pm 0.006$	$0.073 \pm 0.002$

<sup>a</sup>Quantum yields of crown  $\lambda$  were determined relative to naphthalene.

<sup>b</sup>Quantum yields of complexes were determined relative to free crown  $\lambda$ . The indicated errors are standard deviations for averages from at least four quantum yield comparisons at a single wavelength.

Table 27. Emission Quantum Yields ( $\phi_f$  and  $\phi_p$ ) for 1,8-Naphtho-21-Crown-6 ( $\lambda$ ) and Haloalkylammonium Chloride Complexes of Crown  $\lambda$  in Uncracked 95% Ethanol Glass at 77 K.

System	$\phi_f$ <sup>a,b</sup>	$\phi_p$ <sup>a,b</sup>
1,8-Cr-6 ( $\lambda$ )	$0.106 \pm 0.006$	$0.075 \pm .006$
$\lambda$ + Br(CH <sub>2</sub> ) <sub>2</sub> NH <sub>3</sub> Cl	$0.189 \pm 0.004$	$0.049 \pm 0.002$
$\lambda$ + Br(CH <sub>2</sub> ) <sub>3</sub> NH <sub>3</sub> Cl	$0.186 \pm 0.005$	$0.046 \pm 0.001$
$\lambda$ + I(CH <sub>2</sub> ) <sub>2</sub> NH <sub>3</sub> Cl	$0.153 \pm 0.005$	$0.060 \pm 0.003$
$\lambda$ + I(CH <sub>2</sub> ) <sub>3</sub> NH <sub>3</sub> Cl	$0.165 \pm 0.004$	$0.046 \pm 0.001$

<sup>a</sup>Quantum yields of crown  $\lambda$  were determined relative to naphthalene.

<sup>b</sup>Quantum yields of complexes were determined relative to free crown  $\lambda$ . The indicated errors are standard deviations for averages from at least four quantum yield comparisons at a single wavelength.

Table 28. Emission Quantum Yields ( $\phi_f$  and  $\phi_p$ ) for 1,5-Naphtho-22-Crown-6 ( $\mathfrak{3}$ ) and Haloalkylammonium Chloride Complexes of Crown  $\mathfrak{3}$  in Uncracked 95% Ethanol Glass at 77 K.

System	$\phi_f^{a,b}$	$\phi_p^{a,b}$
1,5-Cr-6 ( $\mathfrak{3}$ )	$0.114 \pm 0.006$	$0.16 \pm 0.02$
$\mathfrak{3} + \text{Br}(\text{CH}_2)_2\text{NH}_3\text{Cl}$	$0.063 \pm 0.001$	$0.170 \pm 0.004$
$\mathfrak{3} + \text{Br}(\text{CH}_2)_3\text{NH}_3\text{Cl}$	$0.073 \pm 0.001$	$0.25 \pm 0.01$
$\mathfrak{3} + \text{I}(\text{CH}_2)_2\text{NH}_3\text{Cl}$	$0.0113 \pm 0.0003$	$0.146 \pm 0.002$
$\mathfrak{3} + \text{I}(\text{CH}_2)_3\text{NH}_3\text{Cl}$	$0.0148 \pm 0.0005$	$0.164 \pm 0.002$

<sup>a</sup>Quantum yields of crown  $\mathfrak{3}$  were determined relative to naphthalene.

<sup>b</sup>Quantum yields of complexes were determined relative to free crown  $\mathfrak{3}$ . The indicated errors are standard deviations for averages from at least four quantum yield comparisons at a single wavelength.

of the fluorescence and phosphorescence quantum yields of a compound or complex in ethyl bromide-ethanol-methanol (1:4:1, v/v) glass to the same compound or complex in ethanol-methanol (4:1, v/v) glass. Table 29 gives the results of this type of comparison for naphthalene (10), crowns 1, 2, and 3, potassium and cesium chloride complexes of crowns 1, 2, and 3, and the rubidium chloride complex of crown 3. Since the presence of ethyl bromide in the glass is not expected to change the 77 K UV absorption spectra (shapes of emission spectra are unchanged), the main source of inaccuracy in these comparisons should be the effect of refractive index differences between the two glasses. The errors given in Table 29 are standard deviations. The numbers in parentheses after the errors give the number of determinations made in each case. These errors should probably be regarded as indicators of precision rather than of accuracy, though it is not thought that the refractive index differences will affect the accuracy that much. Note that ethyl bromide doesn't start absorbing until 300 nm (the absorbance of a 1 cm pathlength at 270 nm is approximately one), so none of the emitted light is absorbed. The same experiments couldn't be done using ethyl iodide, since ethyl iodide starts absorbing at 400 nm and a 1 cm pathlength has an absorbance of approximately two at 350 nm.

#### Fluorescence and Phosphorescence Lifetimes at 77 K

The following general comments apply as indicated to reported lifetimes. All lifetimes are from determinations at 77 K. All

Table 29. Emission Quantum Yields ( $\phi_f$  and  $\phi_p$ ) for Naphthalene, 2,3-Naphtho-20-Crown-6 (1), 1,8-Naphtho-21-Crown-6 (2), 1,5-Naphtho-22-Crown-6 (3), and Alkali Metal Complexes of Crowns 1, 2, and 3 in Uncracked Ethyl Bromide-Ethanol-Methanol (4:1:1, v/v) Glass and in Ethanol-Methanol (4:1, v/v) Glass at 77 K. Numbers in Parentheses are for Results in Ethanol-Methanol (4:1, v/v) Glass at 77 K.

System	$\phi_f^b$	$\phi_p^b$
Naphthalene	0.74±0.01 <sup>c</sup> (0.30)	0.38±.02 (0.030)
2,3-Cr-6 (1)	0.70±.007 (0.26)	0.188±.005 (0.26)
1 + KCl	0.084±.003 (0.154)	0.282±.004 (0.084)
1 + CsCl	0.032±.003 (0.048)	0.326±.006 (0.137)
1,8-Cr-6 (2)	0.052±0.001 (0.106)	0.17±.01 (0.075)
1 + KCl	0.105±.002 (0.176)	0.129±.003 (0.046)
1 + CsCl	0.080±.005 (0.140)	0.136±.001 (0.062)
1,5-Cr-6 (3)	0.068±.003 (0.114)	0.31±.03 (0.16)
3 + KCl	0.044±.001 (0.061)	0.22±.01 (0.126)
3 + RbCl	0.0150±.003 (0.018)	0.241±.004 (0.181)
3 + CsCl	0.0015±.0001 (0.0015)	0.336±.002 (0.333)

<sup>a</sup> concentrations (room temperature) for naphthalene and crowns are  $1.00 \times 10^{-4}$  M.

<sup>b</sup> All quantum yields in the ethyl bromide containing glass were determined relative to the same compound or complex in ethanol-methanol (4:1, v/v) glass. Quantum yields in ethanol-methanol glass are assumed to be the same as those determined in 95% ethanol glass (see Tables 8 and 20 through 22).

<sup>c</sup> Errors given are standard deviations for the average of at least four quantum yield comparisons.

phosphorescence lifetimes ( $\tau_p$ ) are from determinations made in 95% ethanol glass, with the exception of the special set of experiments done in ethyl bromide-ethanol-methanol (1:4:1, v/v) glass. Fluorescence lifetimes ( $\tau_f$ ) are from determinations in either 95% ethanol glass, 95% ethanol-methanol (4:1, v/v) glass, or ethanol-methanol (4:1, v/v) glass. The methanol was added with the hope that it would prevent the glasses from cracking (see experimental). The footnotes to the tables indicate which glass composition was used in each case. Data for substances with phosphorescence lifetimes longer than one second were obtained using a mechanical recorder to record the spectrophotofluorimeter out-put as a function of time. Data for shorter phosphorescence lifetimes were obtained by photographing an oscilloscope presentation of the decay curve. Data for fluorescence lifetimes were obtained using the single photon counting method.<sup>71</sup>

Phosphorescence and fluorescence lifetimes are generally listed in the same tables as the corresponding quantum yields. Lifetimes of naphthalene derivatives 1 through 9 as well as those of naphthalene are given in Table 8. Lifetimes of the alkali metal chloride, barium bromide, and silver triflate complexes of crowns  $1$ ,  $2$ , and  $3$  are listed in Tables 20, 21, and 22, of the ammonium and alkylammonium complexes of crowns  $1$ ,  $2$ , and  $3$  in Tables 23, 24, and 25. Fluorescence lifetimes of bromoalkylammonium complexes of crowns  $1$  and  $2$  are given in Table 30. Phosphorescence lifetimes of bromo- and iodoalkylammonium chloride complexes of crowns  $1$ ,  $2$ , and  $3$  are given in Table 31. Phosphorescence lifetimes of naphthalene, crowns  $1$ ,

Table 30. Fluorescent Lifetimes (Double and Single Exponential Analysis) for Bromoalkylammonium Chloride Complexes of 2,3-Naphtho-20-Crown-6 (1) and 1,8-Naphtho-21-Crown-6 (2) in 95% Ethanol-Methanol (4:1, v/v) Glass at 77 K.

System	Single Exponential Analysis $\tau_1$ (ns)	Double Exponential Analysis		
		$\tau_1$ (ns)	$\tau_2$ (ns)	Fraction With Faster Decay
1 + Br(CH <sub>2</sub> ) <sub>2</sub> NH <sub>3</sub> Cl <sup>d</sup>	92 ± 1 <sup>a,b</sup>	53 ± 6 <sup>a,c</sup>	170 ± 30	0.7 ± 0.1
1 + Br(CH <sub>2</sub> ) <sub>3</sub> NH <sub>3</sub> Cl	52.5 ± .5	42 ± 16	170 ± 30	0.90 ± 0.04
2 + Br(CH <sub>2</sub> ) <sub>2</sub> NH <sub>3</sub> Cl <sup>d</sup>	53.2 ± .5	48 ± 2	91 ± 40	0.9 ± .1
2 + Br(CH <sub>2</sub> ) <sub>3</sub> NH <sub>3</sub> Cl	52.9 ± .5	50 ± 13	(1±1)×10 <sup>3</sup>	0.85

<sup>a</sup>Errors given are linear estimates of the standard deviation given by program KINFIT.

<sup>b</sup>Typical multiple correlation coefficients for single exponential analyses were approximately 0.80. See results, discussion, and experimental sections.

<sup>c</sup>Typical multiple correlation coefficients for these double exponential analyses were in the 0.98 to 0.99 range.

<sup>d</sup>Molar crown concentrations (room temperature) are 2.00 × 10<sup>-4</sup> M.



Table 31. Triplet Lifetimes (Double and Single Exponential Analysis) for Haloalkylammonium Chloride Complexes of 2,3-Naphtho-20-Crown-6 (1), 1,8-Naphtho-21-Crown-6 (2), and 1,5-Naphtho-22-Crown-6 (3) in Uncracked 95% Ethanol Glass at 77 K.<sup>a</sup>

System	Single Exponential Analysis	Double Exponential Analysis		
	$\tau_1$ (sec)	$\tau_1$ (sec)	$\tau_2$	Fraction With Faster Decay
1 + Br(CH <sub>2</sub> ) <sub>2</sub> NH <sub>3</sub> Cl <sup>b</sup>	2.0±.2	0.69±.03	2.90±.06	0.50±.01
1 + Br(CH <sub>2</sub> ) <sub>3</sub> NH <sub>3</sub> Cl <sup>b</sup>	1.8±.2	1.0±.1	2.4 ±.1	0.48±.04
1 + I(CH <sub>2</sub> ) <sub>2</sub> NH <sub>3</sub> Cl <sup>c</sup>	1.0± .1	0.21±.02	3.0±.1	0.64±.01
1 + I(CH <sub>2</sub> ) <sub>3</sub> NH <sub>3</sub> Cl <sup>c</sup>	0.82±.05	0.33±.02	2.3±.3	0.71±.03
2 + Br(CH <sub>2</sub> ) <sub>2</sub> NH <sub>3</sub> Cl <sup>b</sup>	1.6±.2	1.15±.06	2.8±.5	0.8±.1
2 + Br(CH <sub>2</sub> ) <sub>3</sub> NH <sub>3</sub> Cl <sup>b</sup>	1.5±.1	1.15±.06	2.3±.4	0.8±.1
2 + I(CH <sub>2</sub> ) <sub>2</sub> NH <sub>3</sub> Cl <sup>c</sup>	2.0±.3	1.00±.06	2.6±.1	0.46±.03
2 + I(CH <sub>2</sub> ) <sub>3</sub> NH <sub>3</sub> Cl <sup>c</sup>	1.7±.2	1.2±.1	2.3±.1	0.48±.03
3 + Br(CH <sub>2</sub> ) <sub>2</sub> NH <sub>3</sub> Cl <sup>c</sup>	1.28±.02	0.83±.05	2.0±.1	0.7±.1
3 + Br(CH <sub>2</sub> ) <sub>3</sub> NH <sub>3</sub> Cl <sup>c</sup>	1.48±.02	1.0±.1	2.3±.3	0.7±0.1
3 + I(CH <sub>2</sub> ) <sub>2</sub> NH <sub>3</sub> Cl <sup>c</sup>	1.6±.1	0.18±.02	1.7±.2	0.65±.02
3 + I(CH <sub>2</sub> ) <sub>3</sub> NH <sub>3</sub> Cl <sup>c</sup>	1.27±.03	0.30±.02	1.20±.04	0.47±.03

<sup>a</sup>See notes a and b for Table 30.

<sup>b</sup>Molar crown concentration (room temperature) is  $2.00 \times 10^{-4}$  M.

<sup>c</sup>Molar crown concentration (room temperature) is  $1.00 \times 10^{-4}$  M.

2, and 3, potassium and cesium chloride complexes of crowns 1, 2, and 3, and the rubidium chloride complex of crown 3 in ethyl bromide-ethanol-methanol (1:4:1, v/v) glass are given in Table 32.

Phosphorescence lifetimes are available for all reported compounds and complexes. Fluorescence lifetimes are available for all naphthalene derivatives and many but not all complexes. Fluorescence lifetimes could not be obtained for complexes with quantum yields much smaller than 0.04. Other lifetimes were not obtained because their determination was not judged to be worthwhile in light of previously obtained results (see discussion section on rate constants for excited state processes). Still other fluorescence lifetimes were not obtained for practical reasons, i.e., they are significantly more difficult to determine than phosphorescence lifetimes. As will be seen, however, these are not serious deficiencies. Also, where fluorescence lifetimes are not available, estimates of the rate constant for fluorescence can be made from the 77 K UV absorption spectra (see discussion).

All fluorescence and phosphorescence decay curves were analyzed using the KINFIT curve fitting program developed by Professor Dye and coworkers.<sup>72</sup> In all cases, except for the haloalkylammonium chloride complexes and the results in ethyl bromide containing glass, it was possible to obtain a good fit of the observed decay curve to a curve generated by a function containing a single exponential term. We will refer to such decay as "single exponential decay".

For most of the haloalkylammonium chloride complexes and for the compounds and complexes in ethyl bromide containing glass, however,

Table 32. Triplet Lifetimes (Single and Double Exponential Analysis) for Naphthalene, 2,3-Naphtho-20-Crown-6, 1,8-Naphtho-21-Crown-6 (2), 1,5-Naphtho-22-Crown-6 (3), and Alkali Metal Chloride Complexes of Crowns 1, 2, and 3 in Uncracked Ethyl Bromide-Ethanol-Methanol (1:4:1, v/v) Glass at 77 K.

System	Single Exponential Analysis	Double Exponential Analysis <sup>b</sup>		
	$\tau_1(\text{sec})$	$\tau_1(\text{sec})$	$\tau_2(\text{sec})$	Fraction With Faster Decay
Naphthalene	0.64±.02	0.042±.004	0.72±.01	0.264±.004
2,3-Cr-6 (1)	0.89±.03	0.14±.01	1.11±.01	0.32±.01
1 + KCl	1.00±.03	0.21±.01	1.32±.02	0.33±.01
1 + CsCl	0.81±.02	0.16±.01	1.00±.01	0.28±.01
1,8-Cr-6 (2)	0.71±.04	0.053±.006	1.03±.01	0.43±.06
2 + KCl	0.45±.01	0.012±.001	0.54±.01	0.28±.03
2 + CsCl	0.50±.01	0.027±.004	0.55±.03	0.23±.04
1,5-Cr-6 (3)	0.78±.01	0.16±.01	1.04±.01	0.28±.01
3 + KCl	0.81±.02	0.16±.01	1.00±.01	0.25±0.04
3 + RbCl	0.79±.01	0.26±.02	1.14±.03	0.40±.01
3 + CsCl	0.300±.002	0.03±.02	0.305±.003	0.04±.01

<sup>a</sup>Errors given are linear estimates of the standard deviation given by program KINFIT.

<sup>b</sup>Typical multiple correlation coefficients for single exponential analyses are in the 0.60 range. See results, discussion, and experimental sections.

<sup>c</sup>Typical multiple correlation coefficients for double exponential analyses are in the 0.90 to 0.98 range. Formal concentrations (room temperature) for naphthalene and for crowns is  $1.00 \times 10^{-4}$  M. Salts are present in 5:1 molar excesses.

it was not possible to get good single exponential fits. The results of attempts to fit decays from these systems to a function containing a single exponential term and to a function containing a sum of two exponential terms (double exponential) are given in Table 30 for fluorescence decays from the bromoalkylammonium chloride complexes of crowns  $1_{\lambda}$  and  $2_{\lambda}$  and in Table 31 for the triplet decays from the bromo- and iodoalkylammonium complexes of crowns  $1_{\lambda}$ ,  $2_{\lambda}$ , and  $3_{\lambda}$ . (See experimental section for the forms of the equations used to do these fits.) For the double exponential fits, an estimate of the fraction of the total decay due to each of the parallel decays is available. The fraction of the total decay due to the faster decay (shorter lifetime) is the one that is tabulated. It is recognized that more than two parallel decays could be present, but, with the available data, results of attempted fits with more parameters would not be meaningful. Also given in Tables 30 and 31 are error estimates provided by the KINFIT program. These error estimates are linear estimates of the standard deviation. Roughly put, this error estimate for a given parameter indicates how much the value of this parameter could change without requiring an adjustment of the values of the other parameters. It indicates the extent of the reliability of a given parameter, in spite of possible correlations among the parameters, provided that the "correct" equation has been used to do the fit. KINFIT also supplies multiple correlation coefficients ( $R_1$ ) for each parameter. It gives a measure of the mathematical coupling of the parameters (for  $R_1 = 0$ , errors are completely uncorrelated; for  $R_1 = 1$ , errors are completely correlated). The

notes in Tables 31, 32 and 33 give typical multiple correlation coefficients for parameters from single and double exponential fits.

For what we have called good single exponential fits, linear estimates of the standard deviation for phosphorescence decays are 0.3%, for naphthalene and naphthalene derivatives, and 0.5 to 1% for crown complexes. Error estimates for fluorescence decays of both naphthalene derivatives and for crown complexes are typically about 1%. Attempts to fit what appears to be single exponential decay to a sum of two exponentials gives one decay rate constant with a relatively small error and one decay rate constant, much smaller or larger than the first, with a much larger error. Conversely, attempts to fit what appears to be mixed exponential decay to a single exponential function gives a decay rate constant with an error which is much larger than for what has been called good single exponential decay.

Good double exponential fits give decay rate constants which have reasonable errors of the same magnitude. The linear estimates of the standard deviation are larger than those for good single exponential fits, since the larger number of parameters gives each parameter a larger range in which it can change without requiring the values of other parameters to change. Another indicator which has been relied upon for distinction between single exponential and mixed (double or more) exponential decay is comparison between the observed and calculated decay curves provided by program KINFIT. For what has been called good single exponential phosphorescence decay, the majority of calculated and observed points are the same within

the allowed error limits, and the rest of the observed points cluster closely about the calculated curve. For what has been called good double exponential phosphorescence decay, however, comparison of the observed and calculated single exponential decay curves generated by KINFIT shows that there is both faster and slower decays present in the observed decay curve. Calculated and observed points are only the same in the region in which the two curves cross. Furthermore, while plots of the logarithm of the intensity versus time give good conformity to a straight line for what has been called good single exponential decay, the same kind of plot gives linear behavior for the first and last part of the decay, the slopes being different and the middle section curved, for what we have called good double exponential decay. For fluorescence decay curves, due to their statistical nature (see experimental), there are fewer points which fall exactly on the calculated single exponential decay curve (i.e., are the same as the calculated values within the allowed errors), but observed points cluster closely about the calculated curve throughout the entire decay.

The results of single and double exponential analyses of the triplet decay from the haloalkylammonium chloride complexes of crowns  $\lambda$ ,  $\lambda$ , and  $\lambda$  provide useful illustrations of what has been described as good or poor fits of either the single or double exponential variety. Single exponential analyses of the triplet decay of the haloalkylammonium chloride complexes of crowns  $\lambda$  and  $\lambda$  give error estimates for the lifetimes, in relative terms, of about 6 to 15%. These errors are much larger than the 1% error typical for good

single exponential decay from complexed crowns. Double exponential analysis of the same decays give error estimates for the two lifetimes which are large (2 to 10%) but of about the same magnitude. The error estimates for the fraction of each decay present are also reasonable (approximately 2 to 10% error). Comparison of the observed decay curves to calculated single exponential decay curves clearly shows that faster and slower decay than that calculated for single exponential decay is present. Thus, for these cases, the double exponential analysis provides a better analysis of the observed decay.

Double exponential analysis of the haloalkylammonium complexes of crown  $\mathfrak{3}$  give lifetime estimates with errors similar to those for the haloalkylammonium complexes of crowns  $\mathfrak{1}$  and  $\mathfrak{2}$ , but, with the exception of the  $\beta$ -iodoammonium chloride complex, the error estimates for the lifetimes from single exponential analyses are fairly small. For these cases, comparison of the observed decay curve to that calculated for single exponential decay shows that the difference between the two curves is less, but the two curves still cross each other, which indicates both a slower and faster decay than that calculated for the single exponential decay. Thus, a double exponential fit provides a better analysis of the data in these cases as well.

Analysis of the triplet decay of the cesium chloride complex of crown  $\mathfrak{3}$  in ethyl bromide containing glass (Table 32) provides a clear cut example of good single exponential analysis versus poor double exponential analysis. Single exponential analysis gives a

lifetime with small error estimate (about 1.5%), whereas double exponential analysis gives one lifetime (about the same as from single exponential analysis) with a small error estimate (about 1.5%) and one lifetime (much shorter) with a much larger error estimate (about 60%). Also, the estimated fraction of the shorter lifetime is very small ( $0.04 \pm 0.01$ ). Furthermore, there is good agreement between the observed decay curve and that calculated for single exponential decay.

The results of single and double exponential analyses of the triplet decay observed for other compounds and complexes in ethyl bromide containing glass are similar to those for the haloalkylammonium chloride complexes of crown  $\text{3}$ . The error estimates for the lifetimes from single exponential analyses range from about 2 to 5%. The error estimates for the longer lifetime from double exponential analyses range from about 1 to 3%, those for the shorter lifetime from about 5 to 10%, and those for the fraction of the shorter lifetime from about 3 to 15%. The smaller error for the longer lifetime is understandable in view of the estimate that most of the decay is due to the slower decay. Comparison of the observed decay curve to that calculated for single exponential decay makes the presence of both slower and faster decay evident. Given the somewhat larger errors for single exponential analysis, reasonable errors for double exponential analysis, and the graphical comparisons, the double exponential analyses provide better analyses of the observed decays.

Single exponential analyses of the fluorescence decay from the bromoalkylammonium chloride complexes of crown  $\text{1}$  (Table 30) give



lifetimes with error estimates of only approximately 1%. For the  $\beta$ -bromoethylammonium complex of crown  $\lambda$ , however, double exponential analysis gives lifetimes with error estimates of about 15% ( $53 \pm 6$  and  $170 \pm 30$  ns), which are still reasonable errors for a double exponential fit. For the  $\gamma$ -bromopropylammonium complex of crown  $\lambda$ , double exponential analysis gives a shorter lifetime with a relatively large error estimate ( $42 \pm 16$  ns, about 40% relative error) and a longer lifetime with a smaller error estimate ( $170 \pm 30$  ns, about 20% relative error). The fraction of the total decay estimated to be due to the shorter decay, however, is  $0.90 \pm 0.04$ . The ability to get good single exponential fits in these cases may be due to the small amount of slow decay present. For the  $\beta$ -bromoethylammonium complex, the estimated fraction of long decay is  $0.3 \pm 0.1$  and the error estimates for the two lifetimes are smaller than for the  $\gamma$ -bromopropylammonium complex for which the fraction of the slower decay is estimated to be only  $0.06 \pm 0.04$ . Comparison of observed decay curves to calculated single exponential decay curves for both complexes indicates the presence of faster decay than that calculated for single exponential decay.

For the bromoalkylammonium complexes of crown  $\lambda$  (see Table 30), single exponential analysis gives lifetimes with small error estimates ( $\pm 1\%$ ). Double exponential analysis gives, for both complexes, a short lifetime with relatively small error and a long lifetime with larger error. In both cases, the faster decay (shorter lifetime) is estimated to account for most of the decay. Comparison of the observed decay curves to the calculated single exponential decay

curves to the calculated single exponential decay curves indicates close agreement throughout the entire decay. Single exponential analysis provides a better analysis of the data for these two cases.

The experimental section should be consulted for experimental factors that are involved in determination of these decay curves which may affect their analysis. Also, note that while the linear estimate of the standard deviation for any given good single exponential decay is about 0.3 to 1.0%, the error indicated by the reproducibility from different decay curves is larger. Phosphorescence lifetime estimates for crowns obtained from determinations made over a period of three years show a variation of about 5%. Multiple estimates for crown complexes are also in good agreement (1 to 5%). Fewer multiple fluorescence lifetime times determinations are available and some of these are from different solvent systems (see experimental section). In many cases, however, the results are the same within 1 to 2%. In two cases, the difference is about 10%. Due to the statistical nature of single photon counting (see experimental), lifetimes obtained are known to be somewhat subject to variation. An estimate of at least  $\pm 5\%$  is placed on their accuracy. Thus, the error estimates given in Tables 8 and 2 through 25 are from the variation indicated by multiple determinations, not from KINFIT error estimates.

### Tests for Anion Effects on Emission Properties at 77 K

Emission properties (shapes, intensities, and decay curves) at 77 K in 95% ethanol glass are the same regardless of whether 5:1 molar excesses of sodium fluoride, sodium chloride, or sodium bromide are added to crown  $\text{1}$  ( $2.00 \times 10^{-4}$  M). The same is also true for addition of 5:1 molar excesses of these same salts to crown  $\text{2}$  ( $2.00 \times 10^{-4}$  M). The effects of a 5:1 molar excess of sodium iodide on the emission properties of crown  $\text{1}$  are substantially different from those of the other sodium halide salts. Differences are also noted between the effects due to addition of a 5:1 molar excess of sodium iodide to crown  $\text{2}$  and the effects due to addition of 5:1 molar excesses of the other sodium halides. The differences are less than the corresponding differences for crown  $\text{1}$ , however. The effects of cesium nitrate on the emission properties of crown  $\text{1}$  appear to be somewhat different from those with cesium chloride, but the differences are small enough to be within experimental error. Sodium fluoride, chloride, bromide, and iodide have the same effect on the fluorescence quantum yield of crown  $\text{3}$ ; and cesium chloride and bromide results agree with each other.

Effects of 5:1 molar excesses of bromoalkylammonium chlorides and bromides on the emission properties of crown  $\text{1}$  are the same. The same is also true for the effects of these salts on the emission properties of crown  $\text{2}$ .

## DISCUSSION

### Preamble

The discussion will proceed in the following fashion. The first section will deal with a few preliminary matters which are necessary to the remaining discussion (complexation and the identity of highest energy emission or lowest energy absorption bands). After the preliminaries, the crucial issue of the validity of the proposed perturbational method will be addressed. The limits of the proposed method having been established, the remainder of the discussion will be structured around the following questions suggested in the introduction:

1. Is there a directional dependence for the external heavy atom effect (HAE), and, if so, which direction(s) of approach is (are) most effective?
2. How sensitive is the external HAE to variation in the distance between the perturber and the perturbed species?
3. Do effects observed for cationic perturbers depend upon the positively charged nature of the perturber?
4. Does the mechanism of the external HAE necessarily involve charge transfer states?
5. How does the effectiveness of a second external perturber vary as a function of perturbation already present in a chromophore (due to a complexed perturber, for example)?
6. Is there any difference in the relative susceptibilities

of rate constants for excited state processes? If so, are the relative susceptibilities the same or different for perturbors with the same relative orientation to the chromophore, or are relative susceptibilities also a function of relative orientation?

### Preliminaries

It is essential to establish before discussion of the results that the observed changes in spectra, quantum yields, and lifetimes are due to essentially fully complexed crown and that the observed changes depend only on the cation and not on the anion. The molar excess of salt required for essentially complete complexation of the crown was established in most cases by titrations followed by monitoring either relative integrated intensities or relative peak intensities as a function of added salt. The results of these and other related experiments are given in Figures 55 through 60 and in Tables 9 through 19 in the quantum yield section of the results. These results are sufficient to establish the molar excess of salt needed for essentially complete complexation. The results section on anion independence shows that the results are independent of the anion (chloride, in most cases), since, for a given cation, similar results were observed for different anions (fluoride, bromide, nitrate). Sodium iodide gave different results than the other sodium halides when complexed by crowns 1 or 2. The titrations also show that there is no further effect due to added salt after

sufficient salt for essentially complete complexation has been added. This indicates that there is no effect due to salt in the bulk solution. The fact that a 150-fold excess of cesium chloride has no effect on  $\phi_f$  or  $\phi_p$  of methoxymethyl derivatives  $\mathcal{A}$  and  $\mathcal{B}$ , whereas a 2-fold excess is sufficient to produce maximum changes for crowns  $\mathcal{1}$ ,  $\mathcal{2}$ , and  $\mathcal{3}$ , shows that the crown ether is responsible for most of the observed association. Also, note that silver (I), which is known to form complexes with  $\pi$ -donors,<sup>73</sup> apparently does not under, the given experimental conditions, associate strongly with the naphthalene  $\pi$ -system, since it complexes less strongly with crown  $\mathcal{3}$  than with crown  $\mathcal{1}$  or  $\mathcal{2}$  (100-fold versus 25-fold excesses of salt required). This is to be expected in part because silver (I) is a small cation (approximately the same size as the potassium cation) and crown  $\mathcal{3}$  has a larger cavity than  $\mathcal{1}$  or  $\mathcal{2}$ . Apparently interaction with the  $\pi$ -system (there is evidence for some, vide infra) does not contribute much to stabilization of the complex. Note that in all cases, the concentration of salt required is much lower than concentrations that are required for traditional external perturbation studies.

Another indication that the crowns are fully complexed by the molar excess of salt used and that essentially only one complex is present is that good single exponential decay (see results section on lifetimes) was observed for all metal cation and alkylammonium complexes. The degree of the single exponential decay character, however, was less pronounced than for pure crowns. This may be the result of the presence of residual uncomplexed crown or more likely

the result of the existence of several different conformations of the same complex which have slightly different lifetimes (or greatly different lifetimes but with the majority of the total decay related to one lifetime).

Comparisons of spectral energy shifts due to substitution of naphthalene or complexation of crowns have been based on the highest energy emission bands ( $S_1$  and  $T_1$ ) or the lowest energy absorption bands ( $S_1$  and  $S_2$ ) that are apparent. The energies of these bands (in  $\text{cm}^{-1}$ ) and some energy shifts of interest are tabulated in Tables 1 through 8. Since the rest of a spectrum generally shifts in the same direction as these bands do, these numbers generally provide a useful indication of redistribution of spectral energy due to substitution or complexation. These bands were referred to as "0-0 bands" (bands due to transitions between the lowest vibrational states of different electronic states) in the results section as a matter of convenience and justification for the appellation delayed. For fluorescence and absorption ( $S_1$ ), a good indication that these are 0-0 bands is the small energy difference between them (from approximately 20 to 200  $\text{cm}^{-1}$ ). The large difference in intensity between the  $S_2$  and  $S_1$  absorption bands of naphthalene and its derivatives makes it reasonable to assume that the lowest energy peak in the higher intensity band corresponds to the energy for the  $S_{0,0} \rightarrow S_{2,0}$  transition.<sup>67</sup> The shapes of the phosphorescence spectra are sufficiently similar to naphthalene (vide infra) that it is reasonable to assume that the highest energy peak corresponds to the  $T_{1,0} \rightarrow S_{0,0}$  transition. As noted in the results section, the

highest energy band in the phosphorescence spectrum of crown 1 is a broad rounded hump. Comparisons to other spectra (see results) suggests that this band is composed of two peaks of roughly equal intensity. The experimental section on energy shifts gives details for the method used to estimate the position of the higher energy band.

#### Validity of the Perturbational Method Used

An attempt to establish the validity of the perturbational method used (see introduction for problems) will be made. This attempt will involve making comparisons of spectral shapes and rate constants between 1) naphthalene and naphthalene derivatives (1 through 9), 2) free crown and complexes of the same crown, and 3) complexes of one crown and those of another crown.

The object of the spectral comparisons is to determine the degree of similarity between the states of different complexes. The assumption underlying spectral comparisons is that if the spectral shapes are similar, the states giving rise to them will be similar. When spectral shapes are different, there is less that will be able to be said here about how similar or dissimilar the states are. Whether or not states are similar to naphthalene is not as important as whether or not they are similar for complexes of the same crown or whether or not they are similar for complexes of different crowns. If the states for different crown complexes are similar, then differences in rate constants for excited state processes for these complexes should be a function of the difference in the



properties of the complexed perturber and/or of the difference in the relative orientation of the perturber relative to the chromophore. It should be pointed out that while spectra obtained at 77 K are much better resolved than at room temperature, they are poorly resolved compared to resolution obtainable at 4.2 K. Thus, spectra which appear to be similar at 77 K may show different vibronic activity at 4.2 K.<sup>40</sup>

The purpose of the rate constant comparisons is 1) to see how substituents change naphthalene's excited state behavior, and 2) to see whether changes due to complexed cations can in some way be separated from those due to substituents. For the 2,3-, the 1,8-, and 1,5- series of naphthalene derivatives and alkali metal cation complexes, rate constants will be analyzed in terms of the effect of replacing H by CH<sub>3</sub>, CH<sub>3</sub> by CH<sub>2</sub>OCH<sub>3</sub> (oxygen effect), CH<sub>2</sub>OCH<sub>3</sub> by crown ring (ring effect), and empty crown ring with perturber (cation effect). For the haloalkylammonium work, an attempt to separate the effect of the alkyl halide from the effect due to complexation of the ammonium group will be made by comparing the effects of complexed alkylammonium to those of haloalkylammonium complexes. The ethyl bromide work is exactly similar in method to traditional external HAE studies<sup>15a</sup> except that the perturbed species will be a complex, not a compound.

The basis for making comparisons of spectral shapes was laid in the results section. Generalizations resulting from observations made there will now be summarized. The broadest generalizations and conclusions from them will be given first. Having taken care of

these, the more difficult comparisons will be taken up.

The broadest generalization proposed is that all phosphorescence spectra (Figures 20 through 54, even numbered) are naphthalene-like. This is most obviously the case for the 1,5-series naphthalene derivatives and complexes, but there are five sets of bands evident for all complexes and all naphthalene derivatives ( $\lambda$  through  $\rho$ ) that appear to be similar to the bands of naphthalene at approximately 469, 480, 502, 540, and 590 nm. As noted in the results section, the relative intensity of the two highest energy bands is quite variable for the 2,3- and 1,8-series of derivatives and complexes. The two highest energy bands are distinct for crown  $\lambda$ , apparently merged for crown  $\mu$ , and of greatly different relative intensities for complexes of these crowns. As also noted in the results section, the haloalkylammonium complexes of crown  $\mu$  have an additional prominent peak in the 480 to 495 nm region. These peaks may correspond to less prominent peaks or shoulders in similar regions of other phosphorescence spectra. Thus, it appears that neither substitution of naphthalene by  $\text{CH}_3$ ,  $\text{CH}_2\text{OCH}_3$ , or crown, nor complexation of crowns drastically changes the nature of naphthalene's  $T_1$  triplet state. It might be expected, then, that  $k_p$  and  $k_{dt}$  for different complexed perturbors and different crowns can validly be compared.

Another broad generalization is that the fluorescence spectra of all complexes have the same shape as other complexes of the same crown. The only exceptions to this are for the  $\text{Na}^+$ ,  $\text{Ag}^+$ , and  $t$ -butylammonium complexes of crown  $\lambda$ , which are more similar to free crown  $\lambda$  than fluorescence spectra of other complexes of crown  $\lambda$ .

The fluorescence spectra of complexes of crown  $\mathfrak{3}$  have essentially the same shape as free crown  $\mathfrak{3}$ . It is somewhat difficult to determine how similar the fluorescence spectra of complexes of crown  $\mathfrak{2}$  are relative to free crown  $\mathfrak{2}$ . As noted in the results section, there is a general increase of fluorescence intensity accompanied by a general muddling of fine structure for complexes of crown  $\mathfrak{2}$  relative to free crown  $\mathfrak{2}$ . The tops of the peaks for the spectra of the complexes, however, seem to correspond to the peaks of crown  $\mathfrak{2}$  at approximately 330, 335, and 340 nm. The fine structure of complexes of crown  $\mathfrak{1}$  is somewhat different from that of the free crown  $\mathfrak{1}$ . The 0-0 bands are blue shifted, but some lower energy transitions are red shifted relative to what appear to be the corresponding transitions for the free crown. This appears to be somewhat characteristic of the effects of substitution at the 2,3-positions of naphthalene, since the same trend is noted in going from H to  $\text{CH}_3$  to  $\text{CH}_2\text{OCH}_3$  to crown (see Figure 61 below and accompanying discussion). The great degree of similarity between the shapes of fluorescence spectra for complexes of the same crown suggests that the  $S_1$  state for all complexes of that crown are similar. Thus, the effects of various perturbors on the rates of excited state processes involving  $S_1$ ,  $k_f$  and  $k_{isc}$ , should be comparable for complexes of a given crown. Since  $k_{isc}$  is sensitive to the energy difference between  $S_1$  and the triplet state to which crossing occurs ( $T_1$  is not necessarily the triplet state involved),<sup>74</sup> changes in  $k_{isc}$  may also reflect energy level changes induced by complexation.

Turning now to 77 K UV spectra, the following generalization

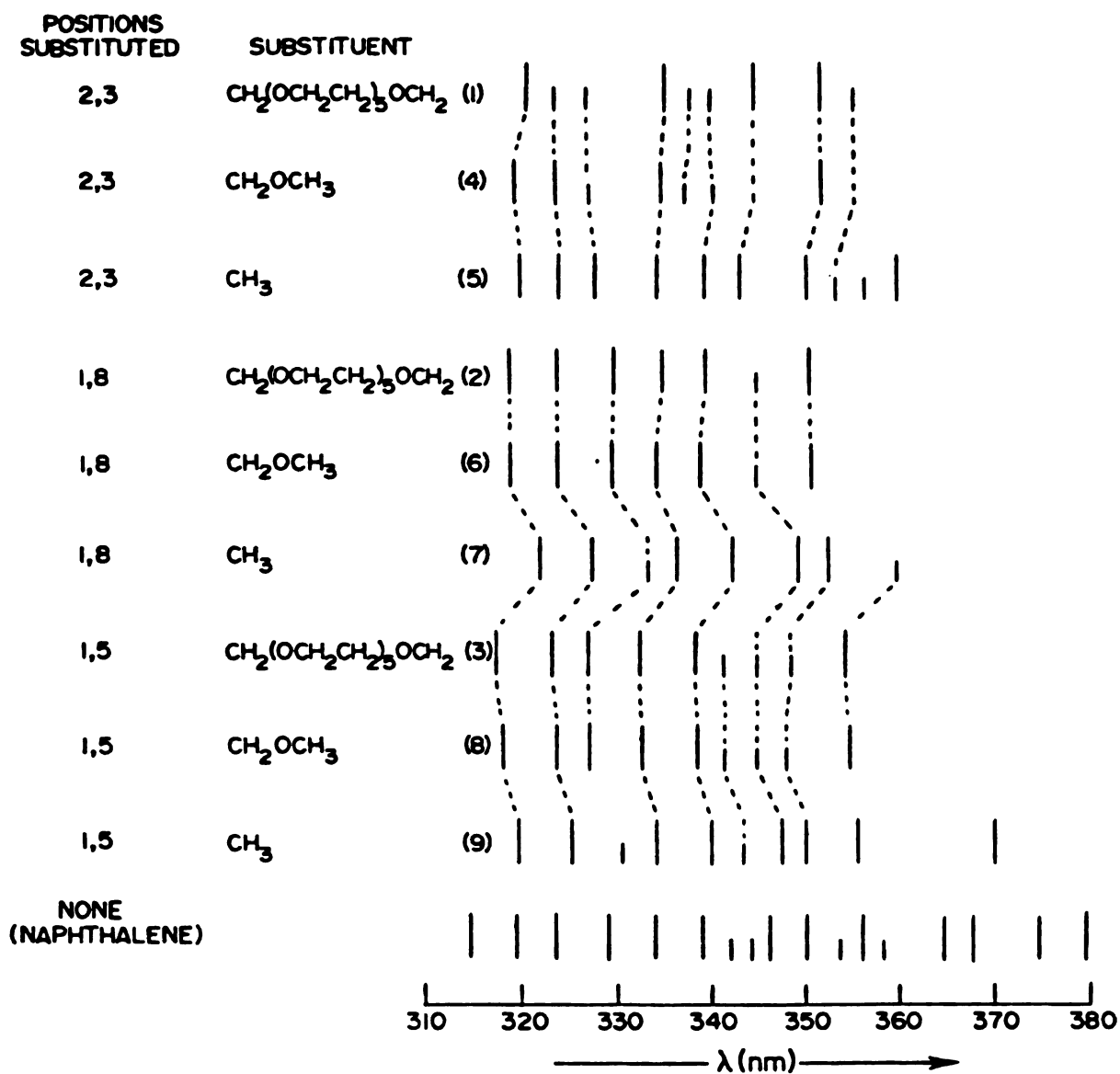


Figure 61. Wavelength positions of peaks and shoulders (half-height lines) for fluorescence spectra of naphthalene and 2,3-, 1,8-, and 1,5-disubstituted naphthalenes in 95% ethanol glass at 77 K.

emerges for  $S_2$  absorption bands. The  $S_2$  absorption bands of all crown complexes and naphthalene derivatives are similar in shape to the  $S_2$  band of naphthalene.  $S_2$  bands for the 1,8- and 1,5-series of naphthalene derivatives are red shifted by about  $1000\text{ cm}^{-1}$ . Complexation of crowns 2 and 3 generally induces further red shifts, but these are generally much smaller ( $100\text{ cm}^{-1}$ ) than those induced by substitution. The energies of the  $S_2$  bands for the 2,3-series of naphthalene derivatives are not as affected by substitution as for the 1,8- and 1,5-series. The intensity of the  $S_2$  absorption bands of complexes are not of greatly different intensity relative to free crown except for the alkali metal complexes of crown 3, which show a 50 to 100% increase in intensity relative to free crown. The above generalization suggests that the  $S_2$  states of naphthalene, naphthalene derivatives 1 through 9, and complexes of crowns 1, 2, and 3 are all similar but of somewhat lower energy relative to naphthalene for complexes and derivatives in the 1,8- and 1,5-series and of similar energy relative to naphthalene for the 2,3-series. Since  $S_2$  is not directly involved with any of the observed decay rates (it is  $S_3$  that is thought to be vibronically coupled to  $S_1$  for naphthalene),<sup>74,75</sup> this conclusion does not have any direct bearing on whether rates involving decay from  $S_1$  and  $T_1$  ought to be comparable for different crown complexes.

Considering now the  $S_1$  absorption bands, it turns out that complexes of the same crown have  $S_1$  absorption bands which are very similar to each other. This again suggests that results for different complexes of the same crown ought to be comparable. Also,

for crowns  $\mathcal{L}$  and  $\mathcal{J}$ , the shape of the  $S_1$  band of the free crown is similar to those of its complexes. The  $S_1$  absorption band of crown  $\mathcal{I}$  is also similar to those of its complexes, but the latter show three additional small peaks not evident for the former. The fact, however, that the intensities of peaks in the  $S_1$  bands of complexes of crown  $\mathcal{I}$  are generally of roughly the same or lower intensities than those for free crown  $\mathcal{I}$  suggests that complexation does not promote vibronic coupling with higher excited singlets, since this would be expected to further increase the intensity of this band<sup>76</sup> (see introduction section on proposed perturbational method). These results suggest that results associated with the singlet manifold should be comparable for complexes of a given crown.

The only comparisons which remain to be made are between the fluorescence spectra and  $S_1$  absorption bands of naphthalene derivatives  $\mathcal{I}$  through  $\mathcal{J}$  to each other and to naphthalene. To aid comparison of these spectra, stick spectra (only peak positions indicated as a function of wavelength) for fluorescence are given in Figure 61 and for  $S_1$  absorption bands in Figure 62. It is difficult to discern peaks in the fluorescence tails for many of these compounds, so comparisons will be based on roughly the same portion of the higher energy region for all compounds. Positions of shoulders are indicated by lines one-half the height of those for well-defined peaks. Suggested correlations between different spectra are indicated by dashed lines. These correlations are based on the similarity of spacings between sets of sticks in both spectra. (The spacings are linear in wavelength, not  $\text{cm}^{-1}$ , but over a small range of



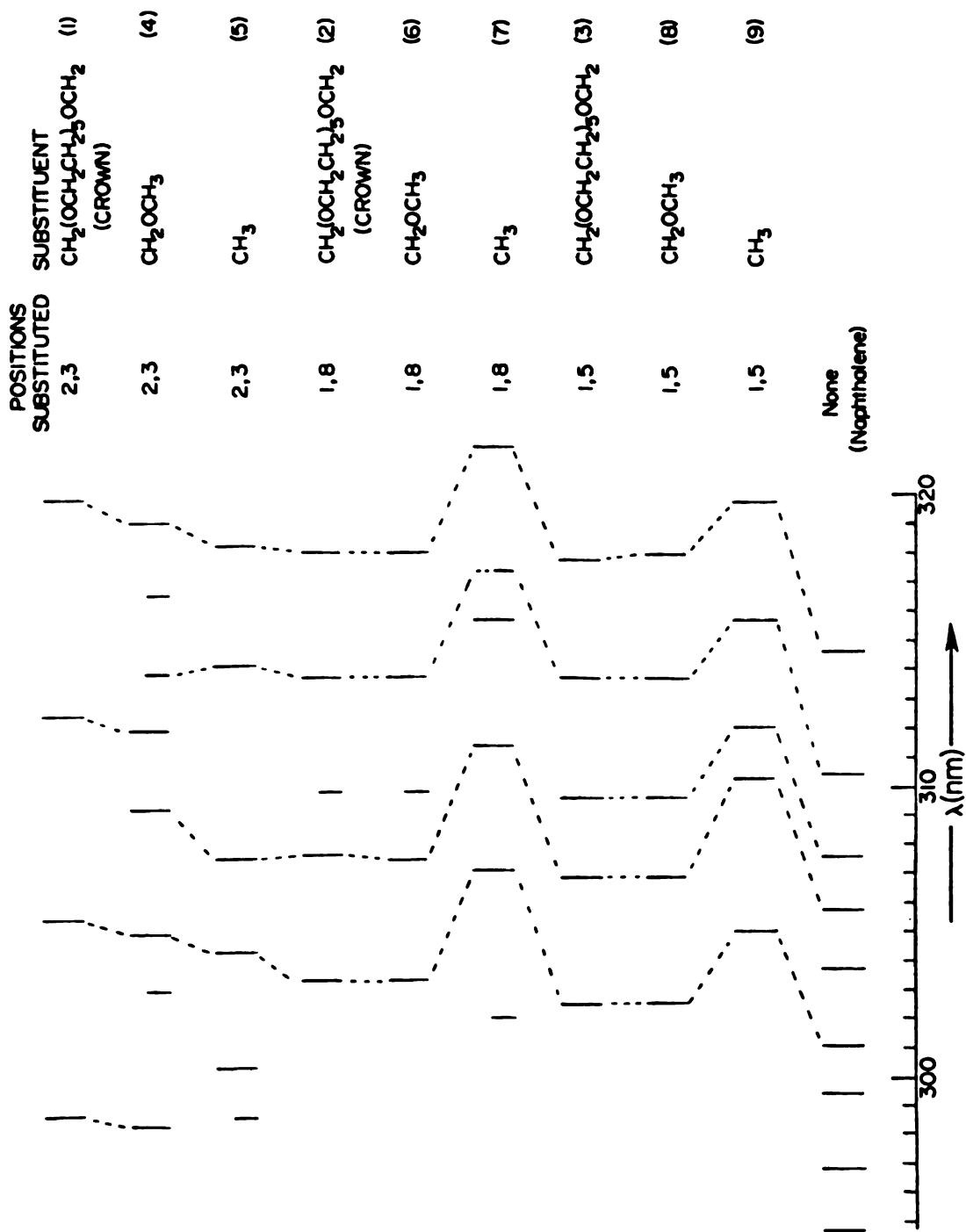


Figure 62. Wavelength positions of peaks and shoulders (half-height lines) for UV absorption spectra of naphthalene and 2,3-, 1,8- and 1,5-disubstituted naphthalenes in 95% ethanol glass at 77 K.



wavelengths energy differences will be roughly proportional to wavelength differences.) The object of these comparisons is to see whether or not these spectra differ only by being displaced to lower or higher energy and to see how similar or dissimilar their vibrational structure is. If the vibrational structures are the same, it will be assumed that the states are the same.

Inspection of the stick representations of the fluorescence spectra given in Figure 61 bears out observations made in the results section without the aid of this figure: 1) the vibrational spacings for crown and methoxymethyl derivatives are similar within the 2,3-, 1,8-, or 1,5-series; 2) the fluorescence spectrum of 2,3-dimethylnaphthalene has more peaks than the 2,3-crown or methoxymethyl derivatives but includes all of the peaks and nearly the same vibrational spacings seen for the latter two; and 3) the fluorescence spectrum of the 1,5-dimethyl derivative has most of the same vibrational spacings and peaks as the 1,5-crown and methoxymethyl derivatives. A generalization suggested by Figure 61 is that the vibrational structure of all 1,8- and 1,5-crown, methoxymethyl, and dimethyl derivatives are the same (only the position of one shoulder for the 1,5-dimethyl derivative does not quite correlate). Note for the 2,3-series that in going from methyl to methoxymethyl to crown the higher energy peaks shift to higher energy and the lower energy peaks to lower energy. A similar trend was noted above for complexes of the 2,3-crown relative to free crown. No correlations have been suggested between the 2,3- and the 1,8-series, since the vibrational spacings are different. Also, no correlations between

naphthalene and any of its derivatives have been suggested. Since vibronic coupling with higher singlets affects which vibrational levels of  $S_0$  are populated by fluorescence,<sup>76</sup> the fact that these spacings are the same for the 1,8- and 1,5- series suggests that vibronic coupling is the same throughout both series. Since complexes of the 1,8- and the 1,5-crowns have the same vibrational spacings as the free crowns, this conclusion applies to them as well. The differences in vibrational spacings for the 2,3-series do not necessarily mean that  $S_1$  for the 2,3-series is coupled differently. The differences may instead be due to differences in molecular symmetry, which also affects the allowedness of vibrational modes.<sup>77</sup> This point will be discussed further in the discussion of intensities of absorption spectra.

Inspection of Figure 62 bears out observations made in the results section for  $S_1$  absorption bands of naphthalene derivatives: 1) the vibrational spacings are similar within the 2,3-, 1,8-, or 1,5-series for methoxymethyl and crown derivatives; 2) many of the same vibrational spacings are observed throughout the 1,8- and the 1,5-series (there are a few shoulders apparent in some cases but not in others); and 3) vibrational spacings for the 1,8- and 1,5-series are similar to those observed for naphthalene. Only one further correlation is suggested by Figure 62 that was not suggested in the results section and that is that some of the vibrational spacings for the 2,3-series are the same as those observed to be constant throughout the 1,8- and 1,5-series. The similarity of vibrational spacings throughout the 1,5- and 1,8-series indicates that vibronic

coupling is the same throughout both series. Vibrational spacings within the 2,3-series are similar but correlations with the 1,8- or 1,5-series is tenuous. Thus, essentially the same conclusion is reached based on similarity of vibrational spacings in absorption spectra as was reached based on vibrational spacings in fluorescence spectra.

The preceding arguments have been based on similarities of vibrational spacings. But changes in molecular symmetry can also affect vibrational structure<sup>67</sup> so differences in vibrational structure does not necessarily imply a difference in vibronic coupling. The following arguments will be based on relative peak intensities in an attempt to determine whether the difference in vibrational structure between the 2,3- and the 1,8- or 1,5-series is due to a difference in the way electronic states are vibronically coupled thus giving rise to peaks associated with nontotally symmetric vibrations, or due to a difference in molecular symmetry, which might be expected to change the intensity of the 0-0 band. 0-0 electronic transitions are not greatly affected by vibronic coupling, changes in the intensities of 0-0 peaks due to chemical substitution are likely to be due to changes in molecular symmetry, not to substituent induced vibronic coupling.<sup>78</sup> Thus, a naphthalene's 0-0 absorption peak is 10 to 20 times less intense than the rest of the  $S_1$  absorption band and its 0-0 emission peak is 6 times smaller than the most intense emission peak. For all the 2,3-disubstituted naphthalene derivatives (Figure 1), the intensity of the entire  $S_1$  absorption band is increased relative to naphthalene but the

intensity of the 0-0 peak is increased the most. The same situation obtains for the fluorescence spectra (Figure 19): the 0-0 peak is the most intense peak for each member of the 2,3-series. For the 1,8- (Figures 2 and 21) and the 1,5-series (Figures 3 and 22), the 0-0 band is not the most intense peak in either the absorption or in the fluorescence spectra for crown or methoxymethyl derivatives. But for the 1,8-crown and methoxymethyl derivatives, the  $S_0$  0-0 absorption peak is about two times more intense than for naphthalene, whereas the second peak is two times less intense than the corresponding peak for naphthalene. For the fluorescence spectra of these two 1,8-derivatives, the 0-0 peak is about three times more intense than for naphthalene, whereas the second peaks are about of the same intensity as for naphthalene. For the 1,5-crown and methoxymethyl derivatives, the  $S_1$  0-0 absorption peaks are about five times more intense than naphthalene, whereas the second highest energy peaks are only about two times more intense than for naphthalene. The fluorescence spectra for the 1,5-crown and methoxymethyl derivatives have about the same relative peak intensities as for naphthalene throughout their spectra. The  $S_1$  0-0 absorption peaks and 0-0 fluorescence peaks for the 1,8- and 1,5-dimethyl derivatives are the most intense peaks in their spectra. Therefore, the main effect of 2,3-, 1,8-, and 1,5- disubstitution appears to be to change molecular symmetry without enhancing vibronic coupling between electronic states. Since, as noted in the previous comparisons (vide supra), complexation does not greatly alter fluorescence or absorption spectra of complexes relative to parent free crown, this

Table 33. Estimates for Rate Constants of Excited State Processes of Naphthalene and 2,3-, 1,8-, and 1,5-Disubstituted-naphthalenes in Alcohol Glass at 77 K.<sup>a</sup>

Naphthalene Substitution	$k_f \times 10^{-6}$	$k_{nr} \times 10^{-6}$	$k_p \times 10^2$	$k_{dt}$
None (10)	1.4	3.3	1.7	0.38
2,3-Dimethyl (4)	2.4	4.6	1.2	0.36
2,3-Bis(methoxymethyl) (5)	2.5	8.5	1.4	0.35
2,3-Crown-6 (1)	2.8	7.9	2.4	0.33
1,8-Dimethyl (6)	4.8	7.5	1.1	0.53
1,8-Bis(methoxymethyl) (7)	2.0	19	3.3	0.39
1,8-Crown-6 (2)	2.4	20	3.5	0.38
1,5-Dimethyl (8)	4.1	5.1	1.5	0.37
1,5-Bis(methoxymethyl) (9)	1.7	11	3.7	0.36
1,5-Crown-6 (3)	3.3	25	8.2	0.37

<sup>a</sup>All rate constants in terms of  $\text{sec}^{-1}$ .



Table 34. Estimates for Rate Constants of Excited State Processes for 2,3-Naphtho-20-Crown-6 ( $\text{1}$ ) and Alkali Metal Chloride, Barium Bromide, and Silver Triflate Complexes of Crown  $\text{1}$  in Alcohol Glass at 77 K.<sup>a</sup>

System	$k_f \times 10^{-6}$	$k_{nr} \times 10^{-6}$	$k_p \times 10^2$	$k_{dt}$
2,3-Cr-6 ( $\text{1}$ )	2.8	7.9	2.4	0.33
$\text{1} + \text{NaCl}$	1.7	7.2	2.6	0.27
$\text{1} + \text{KCl}$	1.7	9.1	3.1	0.29
$\text{1} + \text{RbCl}$	1.5	11	3.9	0.33
$\text{1} + \text{CsCl}$	0.56	11	6.5	0.39
$\text{1} + \text{BaBr}_2$	0.92	18	5.4	0.32
$\text{1} + \text{AgOSO}_2\text{CF}_3$	----	$20^b$	2.4	0.29

<sup>a</sup>All rate constants in terms of  $\text{sec}^{-1}$ .

<sup>b</sup>Calculated assuming that  $k_f = 2.8 \times 10^6$ . Assumption based on 77 K UV absorption spectra (see text for rate constant calculations for alkali metal chloride complexes of crown  $\text{3}$  and Figure 16).

Table 35. Estimates for Rate Constants of Excited State Processes for 1,8-Naphtho-21-Crown-6 ( $\lambda$ ) and Alkali Metal Chloride, Barium Bromide, and Silver Triflate Complexes of Crown  $\lambda$  in Alcohol Glass at 77 K.<sup>a</sup>

System	$k_f \times 10^{-6}$	$k_{nr} \times 10^{-6}$	$k_p \times 10^2$	$k_{dt}$
1,8-Cr-6 ( $\lambda$ )	2.4	20	3.4	0.38
$\lambda$ + NaCl	2.3	19	3.6	0.40
$\lambda$ + KCl	3.2	15	4.0	0.67
$\lambda$ + RbCl	3.4	16	4.3	0.73
$\lambda$ + CsCl	3.0	19	6.0	0.77
$\lambda$ + BaBr <sub>2</sub>	---	21 <sup>b</sup>	6.4	0.81
$\lambda$ + AgOSO <sub>2</sub> CF <sub>3</sub>	---	17 <sup>b</sup>	3.2	0.43

<sup>a</sup>All rate constants in terms of sec<sup>-1</sup>.

<sup>b</sup>Calculated assuming  $k_f = 3.0 \times 10^6$ . Assumption is based on 77 K UV absorption spectra (compare Figures 14 and 17 to Figure 5 and see text for calculation of rate constants for alkali metal chloride complexes of crown  $\lambda$ ).



Table 36. Estimates for Rate Constants of Excited State Processes for 1,5-Naphtho-22-Crown-6 ( $\lambda$ ) and Alkali Metal Chloride, Barium Bromide, and Silver Triflate Complexes of Crown  $\lambda$  in Alcohol Glass at 77 K.<sup>a</sup>

System	$k_f \times 10^{-6}$	$k_{nr} \times 10^{-6}$	$k_p \times 10^2$	$k_{dt}$
1,5-Cr-6 ( $\lambda$ )	3.3	25	8.2	0.37
$\lambda$ + NaCl	2.6	32	5.7	0.36
$\lambda$ + KCl	2.3	35	6.3	0.44
$\lambda$ + RbCl	---	52 <sup>b</sup>	11	0.48
$\lambda$ + CsCl	---	670 <sup>b</sup>	93	1.85
$\lambda$ + BaBr <sub>2</sub>	---	31	10	0.37
$\lambda$ + AgOSO <sub>2</sub> CF <sub>3</sub>	---	500	450	0.82

<sup>a</sup>All rate constants in terms of sec<sup>-1</sup>.

<sup>b</sup>Calculated assuming  $k_f = 1.0 \times 10^6$  (see text).

<sup>c</sup>Calculated assuming  $k_f = 3.3 \times 10^6$ . Assumption is based on 77 K UV spectra (compare Figure 15 and 18 to Figure 6 and see text for calculation of rate constants for alkali metal chloride complexes of crown  $\lambda$ ).



conclusion applies to the effects of complexation as well. This conclusion suggests that effects due to perturbers complexed by 2,3-, 1,8-, or 1,5-crown derivatives should reflect properties of the perturber and the position of the perturber relative to the chromophore without overpowering effects due to substituent or perturber induced vibronic coupling.

The discussion will turn now to a consideration of the validity of the proposed perturbational method based on a consideration of changes in rate constants as a function of type of substitution and as a function of the type of alkali metal cation.

Rate constants ( $k_f$ ,  $k_{nr}$ ,  $k_p$ , and  $k_{dt}$ ) for naphthalene and naphthalene derivatives ( $\mathcal{1}$  through  $\mathcal{9}$ ) and for the alkali metal chloride complexes of crowns  $\mathcal{1}$ ,  $\mathcal{2}$ , and  $\mathcal{3}$  are given in Tables 33 through 36, respectively. These rate constants have been calculated from quantum yield ( $\phi_f$  and  $\phi_p$ ) and lifetime ( $\tau_f$  and  $\tau_p$ ) data given in Tables 8 and 20 through 22 according to the equations given in the introduction section on excited state processes. These calculations assume (see introduction) that  $k_{ds}$  is negligible compared to  $k_f + k_{isc}$  which can be expressed by assuming that  $1 - \phi_f = \phi_{isc}$ .<sup>6</sup> Since, if this assumption is wrong, the value of  $k_{isc}$  will be affected, the rate constants tabulated will be referred to as nonradiative decay from the singlet,  $k_{nr}$  ( $k_{nr} = k_{ds} + k_{isc}$ ). Thus, even if the assumption is wrong, the tabulated values of  $k_{nr}$  would still be correctly labelled, although they would be a composite of two rates, the ratio of which would be unknown.  $k_{nr}$  will be thought of and discussed, however, as dominated by  $k_{isc}$ .

$\tau_f$  for the  $\text{Rb}^+$  and  $\text{Cs}^+$  complexes of crown  $\text{3}$  could not be determined due to experimental constraints (see results section on lifetime determinations), either because  $\phi_f$  was too low or because  $\tau_f$  was too short. So a value of  $k_f$  based on 77 K UV spectra was guessed to allow calculation of  $k_{nr} = (1 - \phi_f)k_f\phi_f^{-1}$ . There is a general relationship between  $k_f$  and the oscillator strength of the  $S_1$  absorption band, i.e.,  $k_f$  is expected to increase as the intensity of the  $S_1$  absorption band increases.<sup>79</sup> Generally, good absorbers are good emitters.<sup>79</sup> Put somewhat more exactly, the inherent radiative lifetime,  $\tau^0$  ( $\tau^0 = k_f^{-1}$ ), is inversely proportional to the integrated intensity of the  $S_1$  absorption band. This relationship doesn't always hold, however.<sup>79</sup> From the results of this investigation, a rough correlation is found between  $k_f$  and the intensity of the 0-0 absorption peak; i.e.,  $k_f$  increases as the intensity of the 0-0 absorption peak increases. Unfortunately, this correlation doesn't hold up very well for the  $\text{Na}^+$  and  $\text{K}^+$  complexes of crown  $\text{3}$ ,  $k_f$  decreases slightly as the intensity of the 0-0 absorption peak increases. (Compare Table 36 to Figure 6.) The rest of the  $S_1$  bands for these complexes are increased in intensity as well. This being the case, it is difficult to do anything else but guess at what  $k_f$  might be. The 0-0 absorption peaks for the  $\text{Rb}^+$  and  $\text{Cs}^+$  complexes are about half as intense as that for the free crown, but the rest of the  $S_1$  bands of these complexes are of about the same intensity as for the  $\text{Na}^+$  and  $\text{K}^+$  complexes. It is expected that  $k_f$  is about the same for the  $\text{Rb}^+$  and  $\text{Cs}^+$  complexes as for the  $\text{Na}^+$  and  $\text{K}^+$  complexes, so it is thought that a value of  $1 \times 10^6$  is

sufficiently low so that increases in  $k_{nr}$  are underestimated rather than overestimated. If this assumption is correct, then  $\tau_f = \phi_f/k_f = 2$  nsec for the  $Cs^+$  complex of crown 3, which would be too short to measure given the experimental problems discussed in the results section. ( $\phi_f = 0.0015$  would also make determination of a longer lifetime difficult.)

Relative errors for  $k_f$ ,  $k_{nr}$ , and  $k_p$  are estimated to be about 10% and, for  $k_{dt}$ , about 5%.  $k_{dt}$  is determined mainly by  $\tau_p$  in most cases and  $\tau_p$  estimates are thought to be good to about 5% (see results). The absolute errors may be larger if the estimates used for  $\phi_f$  and  $\phi_p$  of naphthalene are in error. This investigation puts limits at least on how large  $\phi_p$  for naphthalene can be, since  $\phi_p$  for the  $Ag^+$  complex of crown 3 was found to be  $0.84 \pm 0.08$ .

Rate constants as a function of naphthalene substitution and complexed alkali metal ion perturbers have been presented graphically in Figures 63 through 65 for the 2,3-, the 1,8-, and the 1,5-series, respectively, to facilitate comparisons. Tables 33 through 36 can be referred to for numerical values if desired. Of interest will be: comparison of the effect that each kind of substituent ( $CH_3$ ,  $CH_3OCH_2$ , or crown) in a given series has on changing a given rate constant; comparison of substituent induced changes of rate constants to changes induced by complexation of alkali metal cations; and comparisons of substituent and complexation induced changes of rate constants between the 2,3-, 1,8-, and 1,5-series.

Considering changes in  $k_f$  for the 2,3-series, it is seen that  $CH_3$ ,  $CH_3OCH_2$ , and crown substitution all increase  $k_f$  by roughly

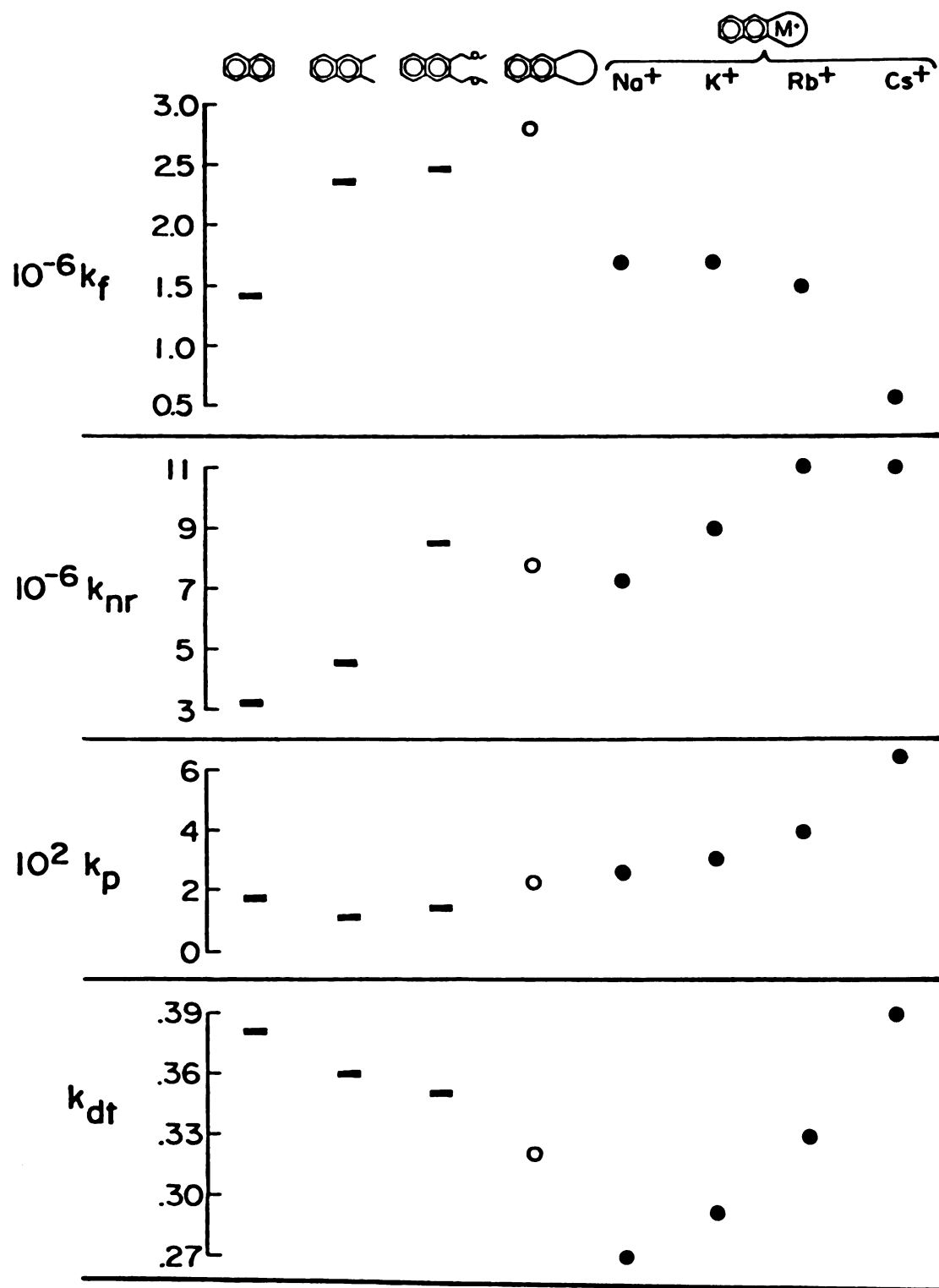


Figure 63. Changes in estimated rate constants caused by 2,3-disubstitution of naphthalene and by alkali metal cation perturbation of the 2,3-crown (1).

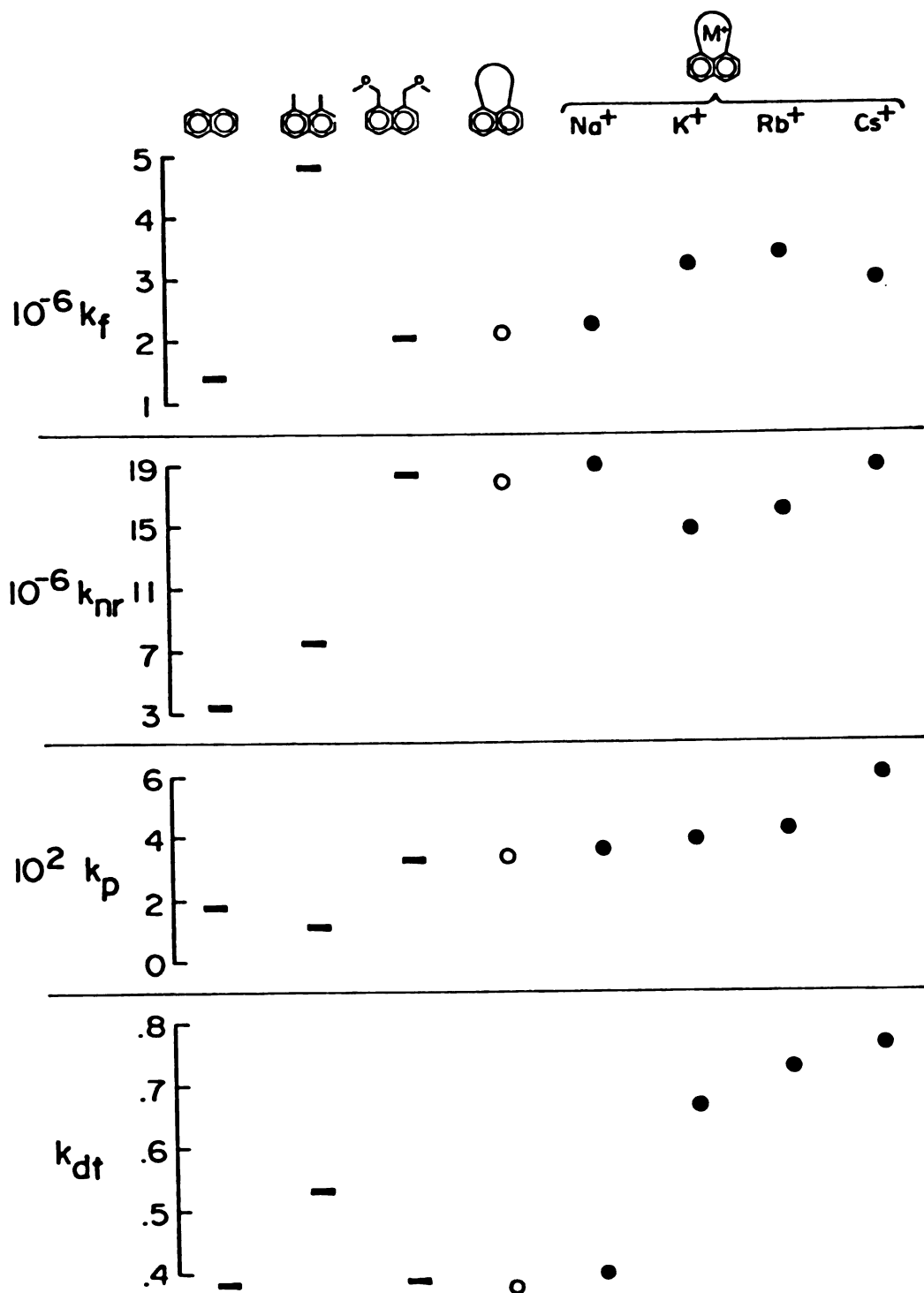


Figure 64. Changes in estimated rate constants caused by 1,8-disubstitution of naphthalene and by alkali metal cation perturbation of the 1,8-crown ( $\lambda$ ).

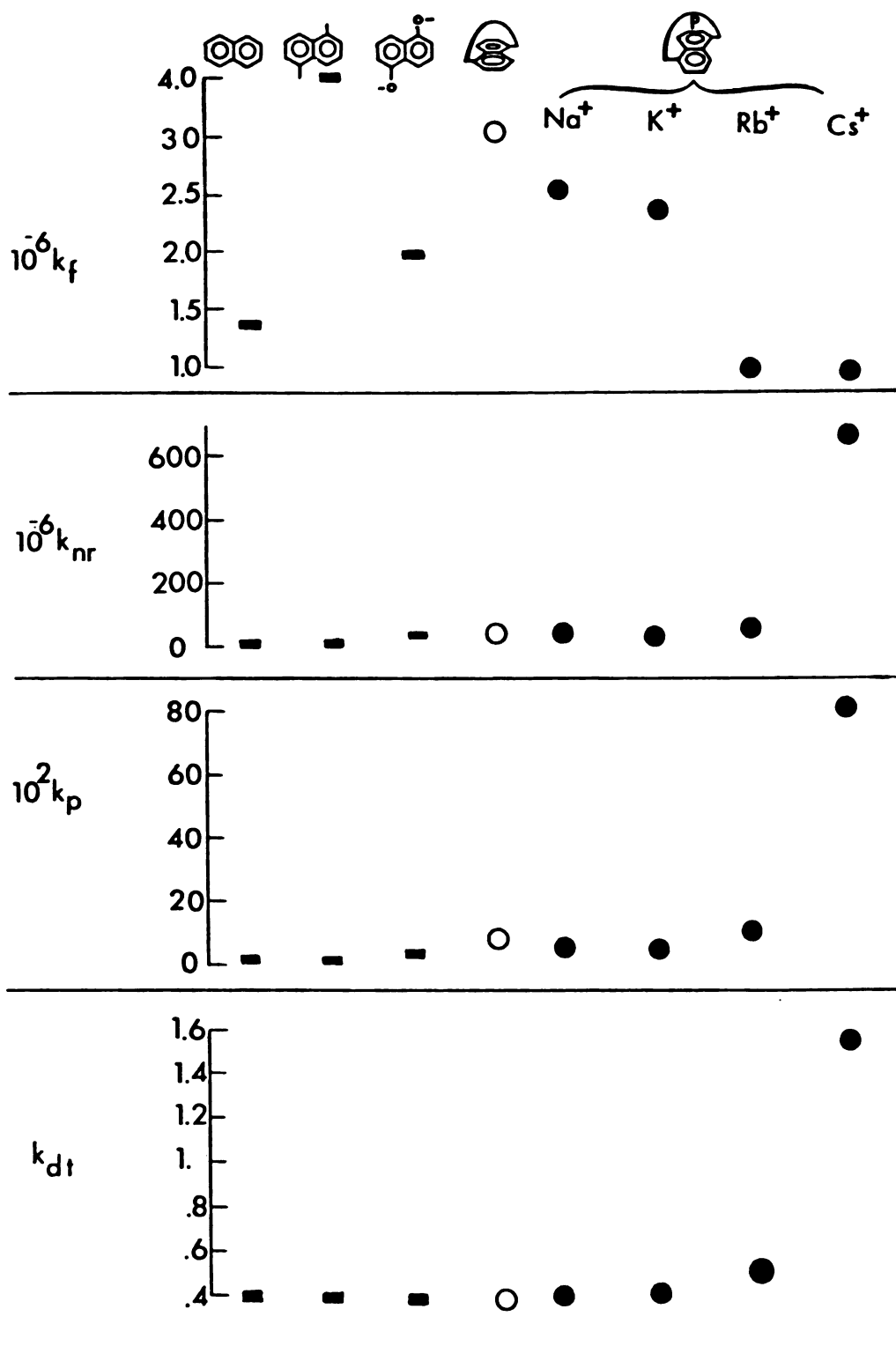


Figure 65. Changes in estimates of rate constants caused by 1,5-disubstitution of naphthalene and by alkali metal cation perturbation of the 1,5-crown (3).



the same amount. Complexation of cations, however, decreases  $k_f$  relative to free crown 1. There is about a 5-fold decrease relative to free crown induced by  $\text{Cs}^+$  complexation, whereas the increase due to substituents is only a 2-fold increase. For  $k_{nr}$ ,  $\text{CH}_3$  causes a slight increase relative to naphthalene;  $\text{CH}_3\text{OCH}_2$  and crown both cause about a 3-fold increase (oxygen effect). Complexation of  $\text{Na}^+$  causes little change relative to free crown, of  $\text{K}^+$  a small increase, and of  $\text{Rb}^+$  and  $\text{Cs}^+$  larger increases of the same magnitude. These increases in  $k_{nr}$  caused by complexation appear to be in addition to whatever change is induced by crown substitution itself. Note that the relative increase in  $k_{nr}$  due to complexation is less than the relative decrease in  $k_f$ , so the observed decrease in  $\phi_f$  is mostly due to the decrease in  $k_f$ , not to the increase in  $k_{nr}$ . For  $k_p$ , substituents cause only small changes relative to naphthalene in comparison to the increase in  $k_p$  relative to crown caused by complexation of alkali metal cations. Note the increase in  $k_p$  due to complexation of  $\text{Rb}^+$  and  $\text{Cs}^+$ , for example, the increases become progressively larger as  $\text{Na}^+$ ,  $\text{K}^+$ ,  $\text{Rb}^+$ , and  $\text{Cs}^+$  are successively complexed. For  $k_{dt}$ , there is a decrease introduced by each substituent in going from H to  $\text{CH}_3$  to  $\text{CH}_2\text{OCH}_3$  (oxygen effect) to crown (crown effect). Complexation of  $\text{Na}^+$  causes a further decrease in  $k_{dt}$  relative to crown, but  $k_{dt}$  then progressively increases relative to  $k_{dt}$  for the  $\text{Na}^+$  complex as  $\text{K}^+$ ,  $\text{Rb}^+$ , and  $\text{Cs}^+$  are successively complexed. The decrease of  $k_{dt}$  relative to free crown followed by an increase suggests the operation of competing factors (see discussion below on correlations of rate constants with energy differences). Note

that  $\text{CH}_3\text{OCH}_2$  and crown substitution have about the same effect on each rate constant (except  $k_{dt}$ ), indicating that there is little crown effect - little effect due to joining the  $\text{CH}_3\text{OCH}_2$  oxygens in a crown cycle.

Turning now to the 1,8-series (Figure 64), it is seen that  $\text{CH}_3$  causes the largest change in  $k_f$  relative to naphthalene. Note that a similar large increase in  $k_f$  is caused by 1,5-dimethyl substitution (Figure 65), so it is doubtful that peri interactions are responsible. Note also that there is a corresponding large increase in the intensity of the  $S_1$  absorption band (Figure 2) complexation of  $\text{Na}^+$  causes little change in  $k_f$  relative to free crown; complexation of  $\text{K}^+$ ,  $\text{Rb}^+$ , and  $\text{Cs}^+$  causes changes in  $k_f$  relative to free crown which are as large as those caused by  $\text{CH}_3\text{OCH}_2$  and crown substitution relative to naphthalene. For  $k_{nr}$ ,  $\text{CH}_3$  substitution causes a 3-fold increase relative to naphthalene;  $\text{CH}_3\text{OCH}_2$  and crown substitution both produce about a 6-fold increase in  $k_{nr}$ . The changes in  $k_{nr}$  induced by complexation of cations relative to free crown is smaller than the change induced by  $\text{CH}_3\text{OCH}_2$  or crown substitution relative to naphthalene. Complexation of  $\text{Na}^+$  causes little change in  $k_{nr}$  relative to free crown, but complexation of  $\text{K}^+$  causes about a 25% decrease which is followed by progressive increases in  $k_{nr}$  for successive complexation of  $\text{Rb}^+$  and  $\text{Cs}^+$ . As for  $k_{dt}$  in the 2,3-series, this suggests the operation of competing effects.  $k_p$  for the 1,8-series is not affected very much for  $\text{CH}_3$  substitution but is increased about 2-fold by  $\text{CH}_3\text{OCH}_2$  and crown substitution. Successive complexation of  $\text{Na}^+$ ,  $\text{K}^+$ ,  $\text{Rb}^+$ , and  $\text{Cs}^+$  results in progressively larger

increases in  $k_p$  relative to free crown. Except for a larger oxygen effect on  $k_p$  for the 1,8-series, the effects of substitution and complexation are similar to those for the 2,3-series. For  $k_{dt}$ , only  $\text{CH}_3$  substitution causes a marked increase, but successive complexation of  $\text{Na}^+$ ,  $\text{K}^+$ ,  $\text{Rb}^+$ , and  $\text{Cs}^+$  results in progressively larger increases in  $k_{dt}$  relative to free crown.

Figure 65 for the 1,5-series, graphically shows that, for this series, substituent induced changes in rate constants are negligible compared to the effects due to complexation of  $\text{Cs}^+$ . Note that if  $k_f$  was plotted on the same scales used for  $k_{nr}$  or  $k_p$ , that there would appear to be essentially no variation in  $k_f$ . Note that the value of  $k_f$  for the  $\text{Rb}^+$  and  $\text{Cs}^+$  complexes is an assumed value (vide supra). For this series, inspection of tabulated values is necessary to put  $k_{nr}$ ,  $k_p$ , and  $k_{dt}$  in perspective to those in the 2,3- and 1,8- series. Inspection of Table 33 shows that there is a significantly larger difference between the effects of  $\text{CH}_3\text{OCH}_2$  and crown substitution in the 1,5-series than in the 2,3- or in the 1,8-series. For the 1,5-series,  $k_f$ ,  $k_{nr}$ , and  $k_p$  for crown substitution are each about twice as large as the corresponding rate constants for  $\text{CH}_3\text{OCH}_2$  substitution (crown effect). That there is such a difference in the 1,5- and not in the 2,3- or 1,8-series is not surprising in view of the fact that the crown ring passes over the face of the naphthalene  $\pi$ -system for the 1,5-series.  $k_{dt}$  is essentially the same as for naphthalene throughout the 2,3-, 1,8-, and 1,5-series for  $\text{CH}_3\text{CH}_2\text{OCH}_2$ , and crown substitution except for  $\text{CH}_3$  substitution in the 1,8-series.

Figure 65 also makes the effects of complexation of other cations appear to be negligible relative to the effects due to complexation of  $\text{Cs}^+$ . Inspection of Table 36, however, shows that  $k_{\text{nr}}$  progressively increases relative to free crown as  $\text{Na}^+$ ,  $\text{K}^+$ ,  $\text{Rb}^+$ , and  $\text{Cs}^+$  are successively complexed.  $k_{\text{p}}$  and  $k_{\text{dt}}$  first decrease and then increase relative to free crown as complexation successively proceeds from  $\text{Na}^+$  through  $\text{Cs}^+$ . It might be argued that tying the  $\text{CH}_3\text{OCH}_2$  oxygens into a crown cycle changes the naphthyl carbon-methylene carbon-oxygen angles in such a way that the oxygens nonbonded electrons do interact more with the  $\pi$ -system. If this interpretation is correct, then it might be supposed that this kind of interaction or inductive effect would be modified by complexation of cations. Changes in  $k_{\text{nr}}$  and  $k_{\text{p}}$  due to cation complexation might then be a function of how this interaction is modified by complexed cations. The fact, however, that  $k_{\text{nr}}$ ,  $k_{\text{p}}$ , and  $k_{\text{dt}}$  (for which there is no oxygen effect) generally tend to increase relative to free crown in the 2,3-, 1,8-, and 1,5-series as  $\text{Na}^+$ ,  $\text{K}^+$ ,  $\text{Rb}^+$ , and  $\text{Cs}^+$  are successively complexed, indicates the likelihood of some common interaction. The three crowns involved, however, are sufficiently different that it is likely that possible interactions of their naphthylic oxygens with the  $\pi$ -system would produce the same common effect in each case. For instance, for crown 3 there may be one kind of interaction between the naphthylic oxygens and the  $\pi$ -system enforced by the polyether chain which passes over the  $\pi$ -face (activation energy of about 6 kcal per mole for rotation of crown ring around naphthalene substrate),<sup>80</sup> another kind of interaction enforced by

peri interactions for crown  $\mathcal{L}$  (vide infra), and, perhaps, only conformationally enforced interactions for crown  $\mathcal{L}_1$ . The suggested enforced interaction for crown  $\mathcal{L}_3$  is evidenced by a much larger crown effect for crown substitution in the 1,5-series than in the 2,3-series (some crown effect) or in the 1,8-series (little crown effect), as noted previously. The peri interactions suggested for crown  $\mathcal{L}_2$  would restrict conformational freedom and, perhaps, result in a more or less restricted range of possible interactions. The absence of an oxygen effect in the 2,3-series for  $k_p$  but the presence of a crown effect ( $k_p$  is increased by a factor of two for crown substitution relative to  $\text{CH}_3\text{OCH}_2$  substitution) suggests a set of somewhat different kinds of interactions.

The increases in  $k_p$  observed for complexation of alkali metal cations by the 2,3-, 1,8-, and 1,5-crowns, except for complexation of  $\text{Na}^+$  and  $\text{K}^+$  by the 1,5-crown, are more significant than the increases in  $k_{nr}$  and  $k_{dt}$ , since, in general, radiative transitions are less dependent on energy differences than nonradiative transitions.<sup>81</sup> Indeed, it turns out that there is a good linear correlation (correlation coefficient ( $R$ ) = 0.998) between  $\log k_{dt}$  and the change in triplet energy relative to crown,  $(E_{T_1} - S_0)$ , for alkali metal complexes of crown  $\mathcal{L}$ , as shown in Figure 66. Note that Figure 66 includes points for metals not discussed yet,  $\text{Ba}^{++}$  and  $\text{Ag}^+$ . The correlation appears to be less good for the alkali metal complexes of crown  $\mathcal{L}_1$ . There appears to be a correlation for three of the points ( $R = 0.992$ ), but the point for the  $\text{Cs}^+$  complex definitely does not fit the correlation ( $R = 0.466$  if this point is included).

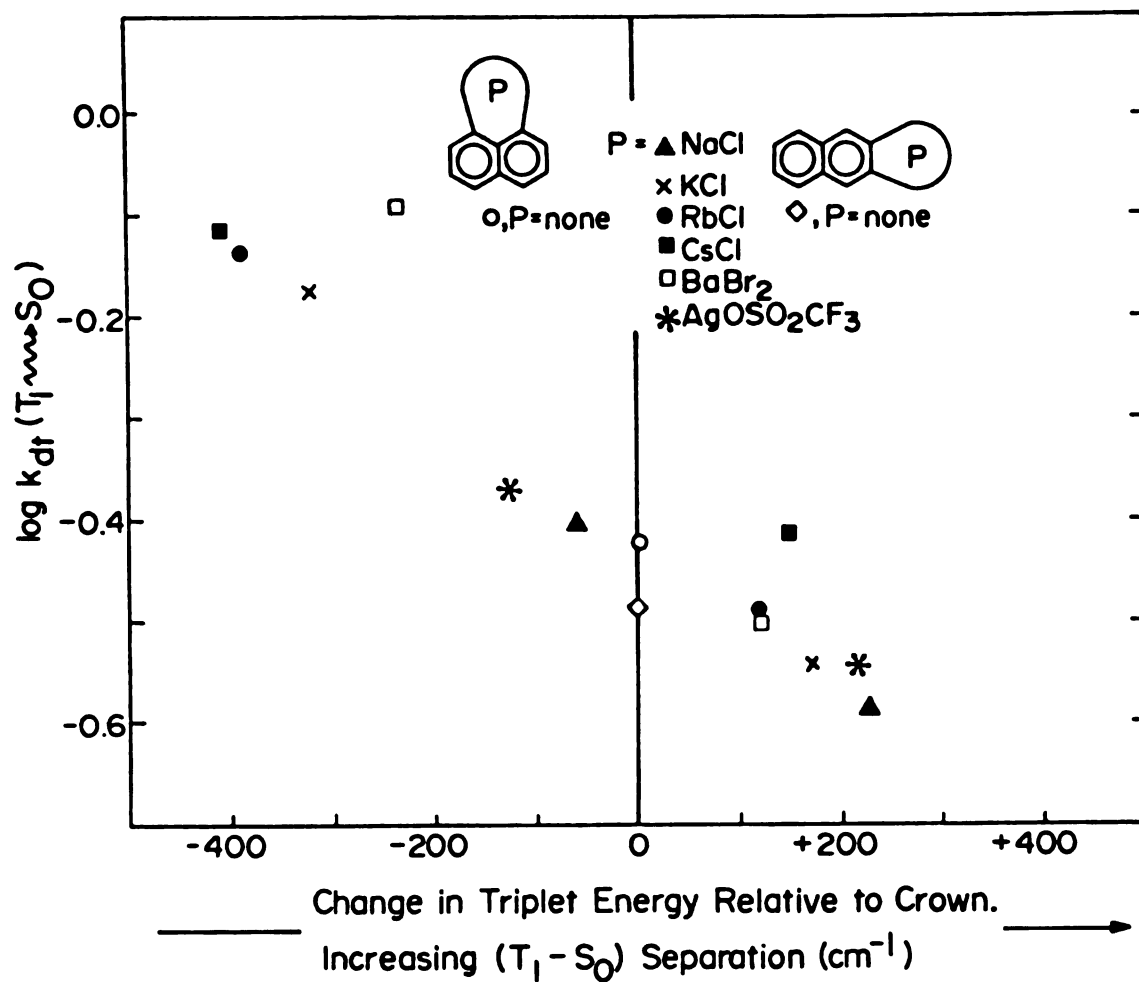


Figure 66. Plot of  $\log k_{dt}$  versus the change in the  $T_1 - S_0$  energy separation in  $\text{cm}^{-1}$  caused by alkali metal, barium, and silver cation perturbation of crowns  $\lambda_1$  and  $\lambda_2$ .

Note that it may be fortuitous that points for the free crowns appear to fit with the correlation for the complexes. Also, it may be fortuitous that points for complexes of both the 2,3- and the 1,8-crown appear to fall on roughly the same line. Note that  $\Delta(E_{T_1} - S_0)$  is estimated to be good to  $\pm 20 \text{ cm}^{-1}$  and  $k_{dt}$  to be accurate within  $\pm 5\%$ , so the position of the point for the  $\text{Cs}^+$  complex of the 2,3-crown is not merely due to experimental scatter. The larger value of  $k_{dt}$  observed with  $\text{Cs}^+$  complexation by 1 can be rationalized by enhanced spin-orbital coupling which may not depend on the  $T_1 - S_0$  energy separation. Note that the point for the  $\text{Ag}^+$  complex of the 1,8-crown appears to correlate with the points for the alkali metal complexes, whereas the point for the  $\text{Ba}^{++}$  complex definitely does not. The points for the  $\text{Ag}^+$  and  $\text{Ba}^{++}$  complexes of crown 1 appear to correlate with the points for the  $\text{Na}^+$ ,  $\text{K}^+$ , and  $\text{Rb}^+$  complexes. There is, however, no apparent correlation between  $\log k_p$  versus  $\Delta(E_{T_1} - S_0)$  or between  $\log k_{nr}$  versus  $\Delta(E_{T_1} - S_0)$ . One would not necessarily expect a correlation between  $\log k_p$  and  $\Delta(E_{T_1} - S_0)$ .<sup>81</sup>  $k_{isc}$ , however, is known to depend on the energy separation between the coupled states. The lack of correlation between  $\log k_{nr}$  and  $\Delta(E_{S_1} - T_1)$  may be because intersystem crossing does not necessarily occur directly to  $T_1$ .  $T_2$  for naphthalene is energetically very close to  $S_1$ .<sup>74</sup> Thus, the decrease relative to the 1,8-crown in  $k_{nr}$  for complexation of  $\text{K}^+$  and the decrease in  $k_{nr}$  relative to the 2,3-crown due to complexation of  $\text{Na}^+$  may be due to an increase in the energy separation between the coupled states. The subsequent increase in  $k_{nr}$  as other alkali metal cations are successively complexed may be

due in part, anyway, to a subsequent decrease in the energy separation between the states that are coupled. For the 1,5-crown, energy shifts induced by complexed metal cations are much smaller than those induced by complexed metal cations for the 2,3- and the 1,8-crown (compare Table 4 to Tables 2 and 3), and no correlations between logarithms of rate constants and energy differences are found.

Therefore, the larger increases in  $k_{nr}$  and  $k_{dt}$  for alkali metal complexes of crown  $\text{\textcircled{3}}$  are more meaningful than those for the 2,3- or 1,8-crown, since  $k_{dt}$ , anyway, for the latter cases shows a marked correlation with  $\Delta(E_{T_1} - S_1)$  for most complexes.

For the 2,3- and the 1,8-crown, it appears that there are correlations between  $\Delta(E_{S_1} - T_1)$  and  $\Delta(E_T - S_0)$  with the polarizing strength of the alkali metal cations. "Polarizing strength" is defined to be the absolute charge of an ion divided by the square of its ionic radius ( $1/r^2$  for monovalent ions).<sup>83</sup> Plots of  $\Delta(E_{S_1} - T_1)$  versus  $1/r^2$  are shown in Figure 67 for the alkali metal cation for complexes of the 2,3-crown ( $R = 0.93$ ) and of the 1,8-crown ( $R = 0.97$ ). Plots of  $\Delta(E_{T_1} - S_0)$  versus  $1/r^2$  are shown in Figure 68 for alkali metal complexes of the 2,3-crown ( $R = 0.91$ ) and of the 1,8-crown ( $R = 0.993$ ). Thus, changes in  $k_{dt}$  relative to free crown due to complexation of alkali metals by the 2,3-crown and by the 1,8-crown may be a function of the properties of the complexed cations but partially, anyway, vis-a-vis energy shifts induced by the complexed cation. Note (see Figure ) that only the  $\text{Ba}^{++}$  complex of the 1,8-crown and the  $\text{Cs}^+$  complex of the 2,3-crown would not fit a linear correlation between  $\log k_{dt}$  and  $\Delta(E_{T_1} - S_0)$ . Energy differences



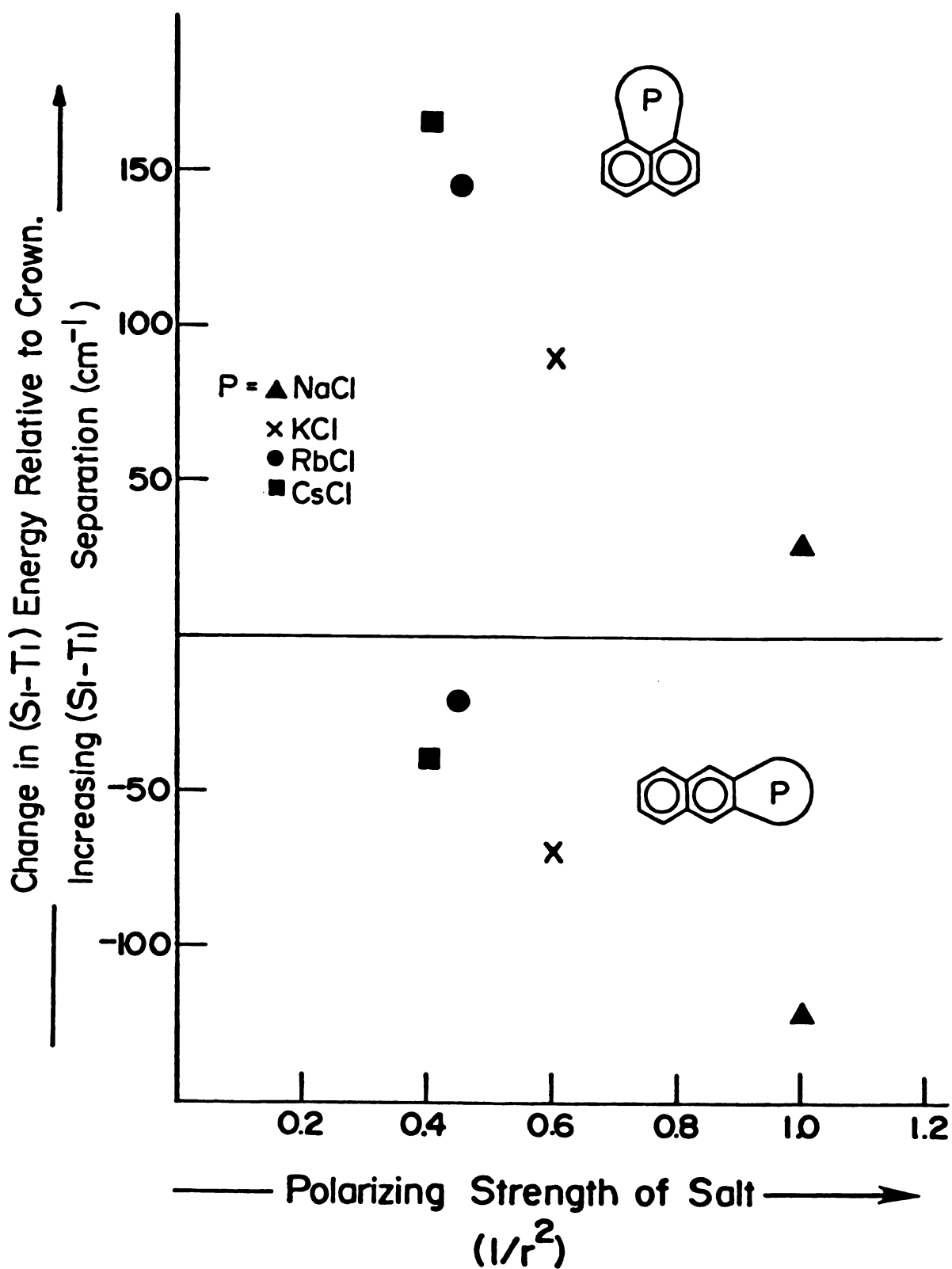


Figure 67. Plot of the change in the  $S_1 - T_1$  energy separation caused by alkali metal cation perturbation of crowns  $\mathbf{1}$  and  $\mathbf{2}$  versus the polarizing strength of the alkali metal cations.

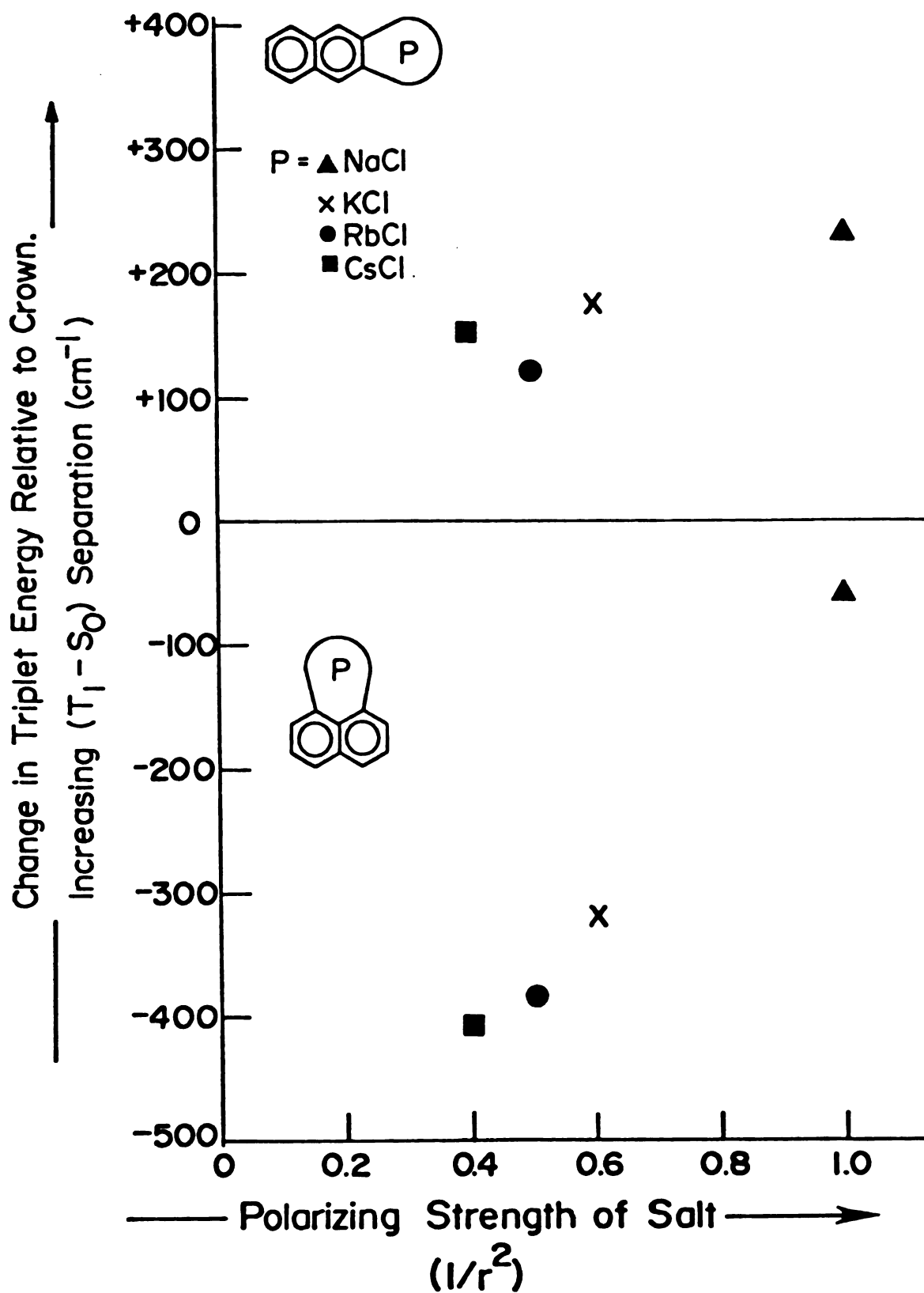


Figure 68. Plot of the change in the  $T_1 - S_0$  energy separation caused by alkali metal cation perturbation of crowns 1 and 2 versus the polarizing strength of the alkali metal cations.

and the polarizing strength of  $\text{Ba}^{++}$  and  $\text{Ag}^+$  do not fit with the apparent correlations of energy differences with polarizing strength for complexes of the 2,3-crown and the 1,8-crown. This is perhaps because  $\text{Ba}^{++}$  and  $\text{Ag}^+$  are members of different periodic series and because there is difficulty in deciding what the actual polarizing strength of  $\text{Ag}^+$  should be.<sup>82</sup>

It is not surprising that complexation of metal ions induces energy shifts. What is perhaps surprising is that energy shifts are not larger (see below under question about the effects of the positive charge of the perturber). It is not clear what factors are responsible for energy shifts due to complexation of metal cations. The above correlations suggest that differences in solvation may be responsible since solvation energies are also related to the radius of the cation and of the anion. Alternatively, energy shifts may be due to field induced  $\pi$ -polarization due to complexed cations. The results of  $^{13}\text{C}$  nuclear magnetic resonance (CMR) studies<sup>83</sup> at room temperature showed that changes in the chemical shifts of the naphthalene carbons which occur upon complexation of alkali metal cations could be explained in terms of field induced  $\pi$ -polarization. While there were shifts in  $\pi$  electron densities due to complexed cations (as indicated by chemical shifts for the naphthalene carbons of the 2,3- and of the 1,8-crown) there was little shift in  $\pi$  electron densities due to complexed metal cations for the naphthalene carbons of the 1,5-crown, as indicated by absence of chemical shifts for the naphthalene carbons. Chemical shifts of the ipso carbons for the 2,3- and the 1,8-crown were consistent with an

increase of  $\pi$  electron density, which is as would be predicted by field induced  $\pi$ -polarization. Thus, the fact that larger energy shifts are produced by complexation of metal cations by the 2,3- or the 1,8-crown than by complexation of metal cations by the 1,5-crown is consistent with an explanation of these energy shifts in terms of greater shifts of  $\pi$  electron density for the former cases than for the latter. However, the  $\pi$  electron polarizations (as evidenced by  $^{13}\text{C}$  chemical shift changes) were similar with  $\text{Na}^+$ ,  $\text{K}^+$ ,  $\text{Rb}^+$ , and  $\text{Cs}^+$  and not a function of  $1/r^2$ . This argues against a direct dependence of energy shifts and  $\pi$ -polarization.

In addition to the general increase of  $k_p$  (and, to a lesser extent,  $k_{nr}$  and  $k_{dt}$  except for the 1,5-series) by complexation of alkali metal cations, results from the CMR work cited above<sup>83</sup> together with results from this investigation suggest that the changes in excited state rate constants due to complexation of metal cations don't merely reflect modified interactions of non-bonded oxygen electrons with the naphthalene  $\pi$ -system. The observations which suggest this conclusion are: 1) that changes in  $k_{nr}$  and  $k_p$  relative to free crown for complexation of alkali metal cations are smaller for the 1,8-crown (2) than for the 2,3-crown; while 2), the CMR results suggest a much larger adjustment of the C(2): C(1): C(11): O(12) dihedral angle for the former case (2) than the C(1): C(2): C(11): O(12) dihedral angle for the latter case (1). The larger change in dihedral angle postulated for the former case is reasonable in view of possible peri interactions. Provided that ground state and  $S_1$  geometries are not too different, these observations from room

temperature CMR studies may validly be applied in this argument.

Also, it does not seem possible to account for changes in rate constants due to complexation of cations in terms of variation of the inductive effect of the naphthyl oxygens by different metal cations, since, if this was the major mode of interaction, one would expect similar results regardless of which crown the metal cation is complexed. (The effects of substituents on carbons 1 and 2 of naphthalene are expected to be of the same sign, but perhaps of different magnitude).<sup>83</sup> But there are large differences (in size and often sign) in changes produced by complexation of  $\text{Cs}^+$  by the 1,5-crown and changes produced by complexation of  $\text{Cs}^+$  by either the 2,3- or the 1,8-crown.

There seems to be evidence for the effects of peri-interactions on  $k_{nr}$  for 1,8- and for 1,5-dimethylnaphthalene. There also has been precedence for this in the literature.<sup>84</sup> For a series of mono and dimethylated naphthalenes and 1,4,5,8-tetramethylnaphthalenes, it was noted that two compounds had exceptionally high  $k_{isc}$  values, 1,8-dimethylnaphthalene and 1,4,5,8-tetramethylnaphthalene. These exceptionally high values of  $k_{isc}$  were thought to be the result of enhanced spin-orbital (SO) coupling brought about by steric distortion of the planarity of the naphthalene nucleus. This distortion from planarity was thought to induce rehybridization of the skeletal naphthalene carbons to include more  $\sigma^*$  character and less  $\pi$  character. The increase in  $k_{isc}$ , then, was viewed as being due to enhanced mixing of  $n\pi^*$  and  $\pi\pi^*$  states. The results of this investigation are consistent with the results of this previous investigation.

The order of increase of  $k_{nr}$  (Table 33) relative to naphthalene for dimethylnaphthalenes is  $2,3 < 1,5 < 1,8$ . It is not unreasonable in the 1,5-case that there may still be significant peri-interactions between the  $\alpha$ -methyl and  $\alpha$ -hydrogen. Thus, the decrease in  $k_{nr}$  relative to crown observed for complexation of  $K^+$  by the 1,8-crown and the subsequent increases relative to the  $K^+$  complex for complexation of  $Rb^+$  and  $Cs^+$  could be explained in terms of variations in the amount of distortion produced by complexation of various cations. This view would be supported by the CMR evidence cited above,<sup>83</sup> which suggests that there are larger changes in dihedral angles for the 1,8-crown than for the 2,3-crown. But these changes in  $k_{nr}$  could just as well be explained in terms of shifts in energies for the states involved in intersystem crossing. Other decreases in rate constants due to complexation followed by increases for complexation of other metal cations have been previously noted.

The preceding discussion of effects due to complexation of cations by crowns  $\lambda$ ,  $\mu$ , and  $\nu$  is summarized in Figure 69. The effects relative to free crown for complexation of  $K^+$  and  $Cs^+$  by crowns  $\lambda$ ,  $\mu$ , and  $\nu$  are indicated by arrows, the length of which indicates (to scale) how the ratio of the rate constants for perturbed and unperturbed crown differ from unity (the larger rate constant was taken as the numerator in each case). An arrow pointing up indicates that the rate constant for perturbed crown increases. For perturbation by  $K^+$ , a light cation, real but not overpowering changes in all rate constants occurs. Each crown and each rate constant responds differently; i.e., no two rows and no two columns agree even as to

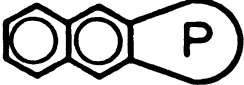


Cation Induced Changes in Rate Constants				
				
light atom (K <sup>+</sup> )	$k_f$	↓	↑	↓
	$k_{nr}$	▲	↓	↑
	$k_p$	↑	▲	↓
	$k_{dt}$	↓	↑	▲
heavy atom (Cs <sup>+</sup> )	$k_f$	↓ <sup>x4</sup>	↑	↓ <sup>x2</sup>
	$k_{nr}$	↑	▲	↑ <sup>x26</sup>
	$k_p$	↑ <sup>x2</sup>	↑	↑ <sup>x9</sup>
	$k_{dt}$	▲	↑	↑ <sup>x4</sup>

Figure 69. Changes in rate constants of excited state processes of crowns  $\bar{1}$ ,  $\bar{2}$ , and  $\bar{3}$  caused by K<sup>+</sup> (a light cation) and Cs<sup>+</sup> (a heavy cation).

the direction of the cation induced changes. However, for perturbation by  $\text{Cs}^+$ , a heavy cation, each of the rate constants involving intersystem crossing,  $k_{nr}$ ,  $k_p$ , and  $k_{dt}$  are increased by cation perturbation for each crown. The magnitudes of the increases are much larger for  $\text{Cs}^+$  perturbation of the 1,5-crown than for the 1,8- or 2,3-crown. The results for  $\text{Cs}^+$  perturbation warrant several important conclusions. First, it can be concluded that there is a HAE for  $\text{Cs}^+$  perturbation of all three crowns, since each of the rate constants for a spin-forbidden process are increased in each case, although by different amounts. The fact that there is a large difference for  $\text{Cs}^+$  perturbation of the 1,5-crown and the 2,3- or 1,8-crown implies that the magnitude of the change is not a function of substituent induced changes which obfuscate HAE's but are a function of where and how the cation is held relative to the naphthalene chromophore. This difference in magnitude of the effect, however, does not establish that there is a directional dependence for the external HAE, since the distance and position of the complexed cation may vary from cation to cation (see below). Also, as prefaced in the introduction, the methylene units inserted between the naphthalene nucleus and the crown ether oxygen for the purpose of electronic insulation prevent the perturber from approaching the edge of the chromophore as closely as it could if there were hydrogen substituents instead. It can be concluded, however, that approach of a heavy atom perturber to the edge of a substituted naphthalene chromophore results in much less effective perturbation than if the perturber approaches the  $\pi$ -face.



### Conclusions for Validity of Studying Excited State Perturbation via Complexed Perturbers

General conclusions concerning the validity of the proposed method for studying excited state perturbation via complexed metal ions are summarized below. These conclusions are drawn from both rate constant and from spectral comparisons.

Spectral comparisons suggest that perturber induced changes in rate constants for all three crowns might be comparable, since 1) all phosphorescence spectra were seen to be similar; 2) the  $S_1$  absorption bands and fluorescence spectra for 1,8- and 1,5-disubstituted naphthalenes were found to be very similar; and 3) comparison of the intensities of 0-0 absorption and 0-0 fluorescence peaks to those of vibronically induced peaks suggest that the main effect of substitution is to change molecular symmetry without enhancing vibronic coupling. Spectral comparisons also suggested that even if perturber induced changes in rate constants aren't comparable for different crowns, that at least all results for a given crown should be comparable, since all spectra of a given type are very similar for a given crown regardless of the perturber.

Rate constant comparisons within and between the 2,3-, 1,8-, and 1,5- series of naphthalene derivatives and complexes suggest that changes due to cation perturbation are not merely the result of modification of substituent effects, since 1) changes introduced by cation perturbers are as large or larger than those due to substituents; 2) there is a general tendency for most alkali metal cations to increase  $k_{nr}$ ,  $k_p$ , and  $k_{dt}$  for all three crowns; although 4) the

changes in  $k_{dt}$  for cation perturbation for the 2,3- and 1,8-crown were shown to correlate with  $\Delta(E_{T_1} - S_0)$  except for  $Cs^+$  perturbation of the 2,3-crown (and  $Ba^{++}$  perturbation of the 1,8-crown); 5) changes in  $k_{nr}$  for the 2,3- and 1,8-crown may also depend on  $\Delta(E_{S_1} - T_1)$ , although no correlation of  $\Delta(E_{S_1} - T_1)$  was found; 6) changes in  $k_{nr}$  for cation perturbation of the 1,8-crown may reflect variable peri-interactions; 7) energy shifts are smaller for cation perturbation of the 1,5-crown, and no correlation of  $k_{dt}$  or any other rate constant with energy differences were found; 8)  $\Delta(E_{S_1} - T_1)$  and  $\Delta(E_{T_1} - S_0)$  were found to correlate with the polarizing strength of alkali metal cation perturbers; 9) although an oxygen substituent effect is observed for  $k_{nr}$  and  $k_p$  of all three crowns (except  $k_p$  for the 2,3-crown), the importance of non-bonded oxygen interaction with the naphthalene  $\pi$ -system is discounted on the basis of common trends for cation perturbation on rate constants for all three crowns and on the basis of indications from room temperature CMR studies; 9) there is an increase in  $k_{nr}$ ,  $k_p$ , and  $k_{dt}$  for  $Cs^+$  perturbation of all three crowns; and 10) the difference in magnitude between  $Cs^+$  perturbation of the 1,5-crown and the 2,3- and 1,8-crown implies that the effectiveness of the perturbation depends on where and how the cation is held.

#### Validity of Method Used for Study of Perturbation Due to Alkyl Halides via Complexed Haloalkylammonium Chloride Salts

The discussion now turns to a consideration of the perturbing effects of complexed haloalkylammonium chlorides in terms of the

perturbing effects due to complexation of the ammonium function. The effects of these two different kinds of perturbations have to in some way be separable in order for any conclusions about the perturbation due to the alkyl halide portion of the molecule to be drawn. The proposed procedure is to compare the effects due to alkylammonium perturbation to those due to haloalkylammonium perturbation. Effects due to alkylammonium perturbation are of interest in themselves but will assume here only an ancillary role in considering the effects due haloalkylammonium perturbation.

Estimates of  $k_f$ ,  $k_{nr}$ ,  $k_p$ , and  $k_{dt}$  for alkylammonium and haloalkylammonium complexes of crowns  $1$ ,  $2$ , and  $3$  are presented in Tables 37, 38, and 39, respectively.  $\tau_f$  estimates are available (Tables 37 and 38) for all alkylammonium complexes of crowns  $1$  and  $2$ , so calculation of rate constants for these complexes requires no assumptions other than  $k_{ds}$  is negligible (see introduction section on excited state processes).  $\tau_f$  is not known for the  $\text{NH}_4\text{Cl}$  and  $n$ -propylammonium complexes of crown  $3$ , but changes in the intensities of the  $S_1$  bands of the complexes relative to free crown  $3$  are small, so it is not likely that  $k_f$  for the complexes is much different than  $k_f$  for the free crown (vide infra). This assumption is also reasonable in view of the fact that  $\phi_f$ ,  $\phi_p$ , and  $\tau_p$  of these complexes are not very different from those of free crown (see Table 25). Therefore,  $k_{nr}$  for these complexes was calculated assuming that  $k_f = 3.3 \times 10^6$  (same estimate as for free crown). Comparison of Table 39 with Tables 37 and 38 will show that crown  $3$  is the crown that is least perturbed by complexation with  $\text{NH}_4\text{Cl}$  or  $n\text{-PrNH}_3\text{Cl}$ , a surprising result.

Table 37. Estimates for Rate Constants of Excited State Processes of 2,3-Naphtho-22-Crown-6 ( $\lambda$ ) and Ammonium, Alkylammonium, and Haloalkylammonium Chloride Complexes of Crown  $\lambda$  in Alcohol Glass at 77 K.<sup>a</sup>

System	$k_f \times 10^{-6}$	$k_{nr} \times 10^{-6}$	$k_p \times 10^2$	$k_{dt}$
2,3-Cr-6 ( $\lambda$ )	2.8	7.9	2.4	0.33
$\lambda$ + $\text{NH}_4\text{Cl}$	1.8	9.7	3.6	0.32
$\lambda$ + n-PrNH <sub>3</sub> Cl	1.9	15	3.7	0.38
$\lambda$ + i-PrNH <sub>3</sub> Cl	1.9	8.4	3.0	0.30
$\lambda$ + t-BuNH <sub>3</sub> Cl	2.2	7.3	2.9	0.29
$\lambda$ + Br(CH <sub>2</sub> ) <sub>2</sub> NH <sub>3</sub> Cl	---	10 <sup>b</sup>	14 <sup>c</sup>	1.3 <sup>c</sup>
$\lambda$ + Br(CH <sub>2</sub> ) <sub>3</sub> NH <sub>3</sub> Cl	---	17	12	0.88
$\lambda$ + I(CH <sub>2</sub> ) <sub>2</sub> NH <sub>3</sub> Cl	---	65	51	4.3
$\lambda$ + I(CH <sub>2</sub> ) <sub>3</sub> NH <sub>3</sub> Cl	---	34	23	2.8

<sup>a</sup>All rate constants in terms of sec<sup>-1</sup>.

<sup>b</sup> $k_{nr}$  for haloalkylammonium chloride complexes calculated assuming  $k_f = 2.0 \times 10^{-6}$  (see text).

<sup>c</sup> $k_p$  and  $k_{dt}$  for haloalkylammonium chloride complexes calculated using shorter phosphorescence lifetime from double exponential analysis.

Table 38. Estimates for Rate Constants of Excited State Processes of 1,8-Naphtho-21-Crown-6 ( $\mathcal{Z}$ ) and Ammonium, Alkylammonium, and Haloalkylammonium Chloride Complexes of Crown  $\mathcal{Z}$  in Alcohol Glass at 77 K.<sup>a</sup>

System	$k_f \times 10^{-6}$	$k_{nr} \times 10^{-6}$	$k_p \times 10^2$	$k_{dt}$
1,8-Cr-6 ( $\mathcal{Z}$ )	2.4	20	3.5	0.38
$\mathcal{Z} + \text{NH}_4\text{Cl}$	3.2	15	3.5	0.55
$\mathcal{Z} + n\text{-PrNH}_3\text{Cl}$	3.5	16	3.3	0.56
$\mathcal{Z} + i\text{-PrNH}_3\text{Cl}$	3.2	15	3.4	0.49
$\mathcal{Z} + t\text{-BuNH}_3\text{Cl}$	2.2	17	3.3	0.38
$\mathcal{Z} + \text{Br}(\text{CH}_2)_2\text{NH}_3\text{Cl}$	3.6	15 <sup>b</sup>	5.3 <sup>c</sup>	0.82 <sup>c</sup>
$\mathcal{Z} + \text{Br}(\text{CH}_2)_3\text{NH}_3\text{Cl}$	3.5	15	4.9	0.82
$\mathcal{Z} + \text{I}(\text{CH}_2)_2\text{NH}_3\text{Cl}$	---	19	7.1	0.93
$\mathcal{Z} + \text{I}(\text{CH}_2)_3\text{NH}_3\text{Cl}$	---	18	4.6	0.79

<sup>a</sup>All rate constants in terms of  $\text{sec}^{-1}$ .

<sup>b</sup> $k_{nr}$  for haloalkylammonium chloride complexes calculated assuming  $k_f = 3.5 \times 10^6$  (see text).

<sup>c</sup> $k_p$  and  $k_{dt}$  for haloalkylammonium chloride complexes calculated using shorter phosphorescence lifetime from double exponential analysis.

Table 39. Estimates for Rate Constants of Excited State Processes of 1,5-Naphtho-22-Crown-6 ( $\lambda$ ) and Ammonium, Alkylammonium, and Haloalkylammonium Chloride Complexes of Crown  $\lambda$  in Alcohol Glass at 77 K.<sup>a</sup>

System	$k_f \times 10^{-6}$	$k_{nr} \times 10^{-6}$	$k_p \times 10^2$	$k_{dt}$
1,5-Cr-6 ( $\lambda$ )	3.3	25	8.2	0.37
$\lambda + \text{NH}_4\text{Cl}$	---	28 <sup>b</sup>	8.6	0.37
$\lambda + n\text{-PrNH}_3\text{Cl}$	---	26	10	0.37
$\lambda + \text{Br}(\text{CH}_2)_2\text{NH}_3\text{Cl}$	---	50	22 <sup>c</sup>	1.00 <sup>c</sup>
$\lambda + \text{Br}(\text{CH}_2)_3\text{NH}_3\text{Cl}$	---	42	27	0.73
$\lambda + \text{I}(\text{CH}_2)_2\text{NH}_3\text{Cl}$	---	290	82	4.7
$\lambda + \text{I}(\text{CH}_2)_3\text{NH}_3\text{Cl}$	---	220	56	2.9

<sup>a</sup>All rate constants in terms of  $\text{sec}^{-1}$ .

<sup>b</sup> $k_{nr}$  for all complexes calculated assuming  $k_f = 3.3 \times 10^6$  (see text).

<sup>c</sup> $k_p$  and  $k_{dt}$  for haloalkylammonium chloride complexes calculated using shorter phosphorescence lifetime from double exponential analysis.

The assumptions used to arrive at the rate constant estimates given for the haloalkylammonium complexes requires somewhat more comment. As noted in the results section on lifetimes, none of the fluorescence or phosphorescence decay curves for haloalkylammonium complexes (with the possible exception of the fluorescence decay from the bromoalkylammonium complexes of crown 2) are of good single exponential decay character. This is not surprising, since one would expect single exponential decay only if one kind of perturbed species were present. Given the conformational freedom of the alkyl chain, one would not expect the halogen of the alkyl halide portion of the salt to always be in the same position relative to the chromophore unless there were sufficient attractive interaction between the halogen and the naphthalene  $\pi$ -system to compensate for loss of entropy. Thus, one would expect that the observed decay to be a composite of several decays, since each position of the halogen relative to the chromophore might give a different decay, unless there were no directional or distance dependence for the external HAE.

Given the limitations of multi-parameter fits and the quality of the data, no more than double exponential decay fits were possible (see results section). But the estimates from such fits for the decay curves from haloalkylammonium complexes are reasonable. Comparisons of triplet lifetimes for alkylammonium complexes (all from good single exponential fits, Tables 23, 24, 25) to the longer lifetime estimates from the double exponential fits for the haloalkylammonium complexes (Table 31) shows that the latter are about what

one would expect for an alkylammonium complex. For crown  $\bar{1}$ ,  $\tau_p$  for alkylammonium complexes ranges from 2.4 to 3.1 sec.; the longer  $\tau_p$  estimate for the haloalkylammonium complexes range from 2.3 to 3.0 sec. For crown  $\bar{2}$ ,  $\tau_p$  for alkylammonium complexes ranges from 1.7 to 2.4 sec.; the longer  $\tau_p$  estimates for the haloalkylammonium complexes range from 2.3 to 2.8 sec. For crown  $\bar{3}$ ,  $\tau_p$  is 2.1 and 2.4 sec for the  $\text{NH}_4\text{Cl}$  and  $n\text{-PrNH}_3\text{Cl}$  complexes, respectively; the longer  $\tau_p$  estimates for haloalkylammonium chloride complexes range from 1.2 to 2.3 sec. Therefore, a reasonable interpretation of the data is that the halogen atom is sometimes too far away and/or in the wrong position relative to the chromophore for effective perturbation. Thus, it appears reasonable to assume that the species responsible for the long  $\tau_p$  is similar to an alkylammonium complex.

It does not seem possible, however, to put a reasonable limit on the number of short decays present. However, the shorter  $\tau_p$  estimates given by the double exponential analyses are reasonable, however. For haloalkylammonium complexes of crowns  $\bar{1}$  and  $\bar{3}$ , the shorter  $\tau_p$  estimates for the iodoalkylammonium complexes are three to five times shorter than for the bromoalkylammonium complexes. This is as should be, since alkyl iodides are better heavy atom perturbers than alkyl bromides. Also, the estimates for the bromo- and iodoalkylammonium complexes (1.0 and 0.2 sec., respectively) are similar to the first "half-life" estimates for perturbation of naphthalene by propyl bromide and iodide glasses at 77 K (0.14 and 0.076 sec., respectively).<sup>13</sup> (First "half-life" is defined as the time required for the intensity to drop to one-half its



initial intensity). While this method of analysis neglects the multi-exponential character of the decay, it was found that the lifetimes obtained were in good agreement with estimates from the initial slope of a plot of the logarithm of intensity versus time.) The estimates from this investigation may be somewhat longer because there is essentially only one heavy atom in the vicinity of the chromophore, whereas in a heavy atom glass the chromophore is surrounded by heavy atom containing molecules.

The estimates for the shorter lifetimes for the haloalkylammonium complexes of crown  $\lambda$  are about the same for both bromo and iodo analogs and for both chain lengths. This must mean that the halogen is oriented in such a way relative to the chromophore such that its interaction is less effective. This result does not mean that 1,8-disubstitution interferes with the effect of the heavy atom, since ethyl bromide is found to perturb both crown  $\lambda$  and alkali metal complexes of crown  $\lambda$ .

If the decay curves could accurately be analyzed accurately for several decay rate constants and for the fraction of the total decay associated with each constant, quantum yields for each decay could be found assuming that all species have the same extinction coefficient. The estimated fraction of the total decay due to the faster decays ranges from 0.5 to 0.8. These estimates are probably good enough to warrant the conclusion that most of the decay is from species perturbed by the alkyl halide portion of the haloalkylammonium cations but probably not good enough to warrant adjustment of quantum yields before rate constant calculations. The proposed

procedure for calculation of rate constants is to use the shorter lifetime estimates and quantum yields uncorrected for contributions from the longer decay. This procedure will tend to underestimate rather than overestimate changes in rate constants relative to unperturbed crown.

This approximation will be best for the haloalkylammonium complexes of crown  $\mathcal{L}$ , since  $\phi_f$  and  $\phi_p$  don't change very much relative to what they are for the alkylammonium complexes (compare Tables 24 and 27), yet the shorter decay is estimated to account for most of the decay. In general, but especially applicable to crowns  $\mathcal{L}$  and  $\mathcal{J}$ , decreases in  $\phi_f$  due to heavy atom perturbation will be underestimated, so (assuming  $k_f$  doesn't change much, see below) increases in  $k_{nr}$  will be underestimated. Increases in  $\phi_p$  will be underestimated, so increases in  $k_p$  will be underestimated.  $k_{dt}$  is generally about  $10^2$  larger than  $k_p$ , so  $k_{dt}$  won't be affected very much ( $k_{dt} = \tau_p^{-1} - k_p$ ).

Under the usual assumption that the HAE affects the rate constants of spin forbidden processes the most, it will be assumed that  $k_f$  is not affected very much by the external heavy atom. (Note, however, that  $k_f$  is the rate constant most affected by  $\text{Cs}^+$  perturbation of crown  $\mathcal{L}$ ). For crown  $\mathcal{L}$  and  $\mathcal{J}$ , however, it is known that  $k_f$  is changed by complexation of alkylammonium cations. Tables 37 and 38 show that  $k_f$  is practically invariant for  $\text{NH}_4\text{Cl}$ ,  $n\text{-PrNH}_3\text{Cl}$ , and  $i\text{-PrNH}_3\text{Cl}$  complexes of crown 1 ( $k_f$  about  $2.0 \times 10^6$ ). The fluorescence decays of the haloalkylammonium complexes of crown  $\mathcal{L}$  appears to be double exponential, but the estimates are rough (see results section).

It was preferred to calculate  $k_{nr}$  for this series of complexes using the same value of  $k_f$  in all cases rather than to have the values for the bromo analogs reflect experimental and analytical uncertainty and to have the values for the iodo complexes reflect the uncertainty of a guess. So  $k_{nr}$  for these complexes was calculated assuming  $k_f = 2.0 \times 10^6$ , a typical value for an alkylammonium complex.

$k_f$  is also practically constant for the alkylammonium complexes of crown  $\lambda$  ( $k_f$  ranges from  $3.2 \times 10^6$  to  $3.5 \times 10^6$ ; see Table 38). The fluorescence decay for the  $\beta$ - and  $\gamma$ -bromo analogs gave a better single exponential analysis than double exponential analysis (see results).  $k_f$  calculated using the  $\tau_f$  estimate from single exponential analysis gives an estimate in either case of about  $3.5 \times 10^6 \text{ sec}^{-1}$ , which is about the same as  $k_f$  for an alkylammonium complex. So  $k_{isc}$  for the iodoalkylammonium complexes of crown  $\lambda$  was calculated assuming  $k_f = 3.5 \times 10^6$ . Note that it is possible that fluorescence and phosphorescence decay might not both be multi-exponential in character, depending upon how  $k_{nr}$  vis-a-vis  $k_p$  or  $k_{dt}$  is affected by the perturbation. The results for the bromoalkylammonium complexes of crown  $\lambda$  suggests that  $k_{nr}$  is not greatly affected by the external heavy atom but  $k_p$  and/or  $k_{dt}$  are, since the fluorescence decay appears to be single exponential but the phosphorescence decay multi-exponential.

Haloalkylammonium cations complexed by crown  $\lambda$  do seem to have some effect (perhaps due to the presence of the external heavy atom) which is different than would be predicted on the basis of changes in  $(E_{T_1} - S_0)$ . It appears that there is a good linear correlation

( $R = 0.97$ ) between  $\log k_{dt}$  and  $\Delta(E_{T_1} - S_0)$  for alkylammonium complexes, but that  $\log k_{dt}$  is either independent of  $\Delta(E_{T_1} - S_0)$  for the haloalkylammonium complexes or that two of the points for the haloalkylammonium complexes fit the same correlation as for the alkylammonium complexes but that two of the points don't (see Figure 70).

For the alkylammonium complexes of crown 1,  $k_{dt}$  appears to decrease as the energy separation  $\Delta(E_{T_1} - S_0)$  increases. The exception in the case of  $n\text{-PrNH}_3\text{Cl}$  may be explained by noting that, although the 0-0 phosphorescence band is blue shifted, that all other peaks are red shifted (Figure 32). Thus, the larger value of  $k_{dt}$  than would be expected based on  $\Delta(E_{T_1} - S_0)$  estimated from the 0-0 band may be because higher vibrational states of  $S_0$  are brought closer to  $T_1$  by red shifts. For the haloalkylammonium complexes of crown 1,  $\log k_{dt}$  is either independent of  $\Delta(E_{T_1} - S_0)$  or decreases much more rapidly as a function of increasing  $\Delta(E_{T_1} - S_0)$  than for other plots of  $\log k_{dt}$  versus  $\Delta(E_{T_1} - S_0)$  ( $R = 0.97$ ; see Figure 66 and 70). Note that the 0-0 peak (used to determine  $\Delta E(T_1 - S_0)$  in Figure 70) is blue shifted by haloalkylammonium perturbation but that the rest of the peaks are red shifted (Figure 38). Since this is also true for  $n\text{-PrNH}_3\text{Cl}$  perturbation, the halogen itself does not appear to be the cause of the shifts.

#### Method for Consideration of Perturbation by Ethyl Bromide Containing Glass

Calculation of rate constants from observed values of  $\phi_f$ ,  $\phi_p$ , and  $\tau_p$  for perturbation by ethyl bromide-ethanolmethanol (1:4:1, v/v)

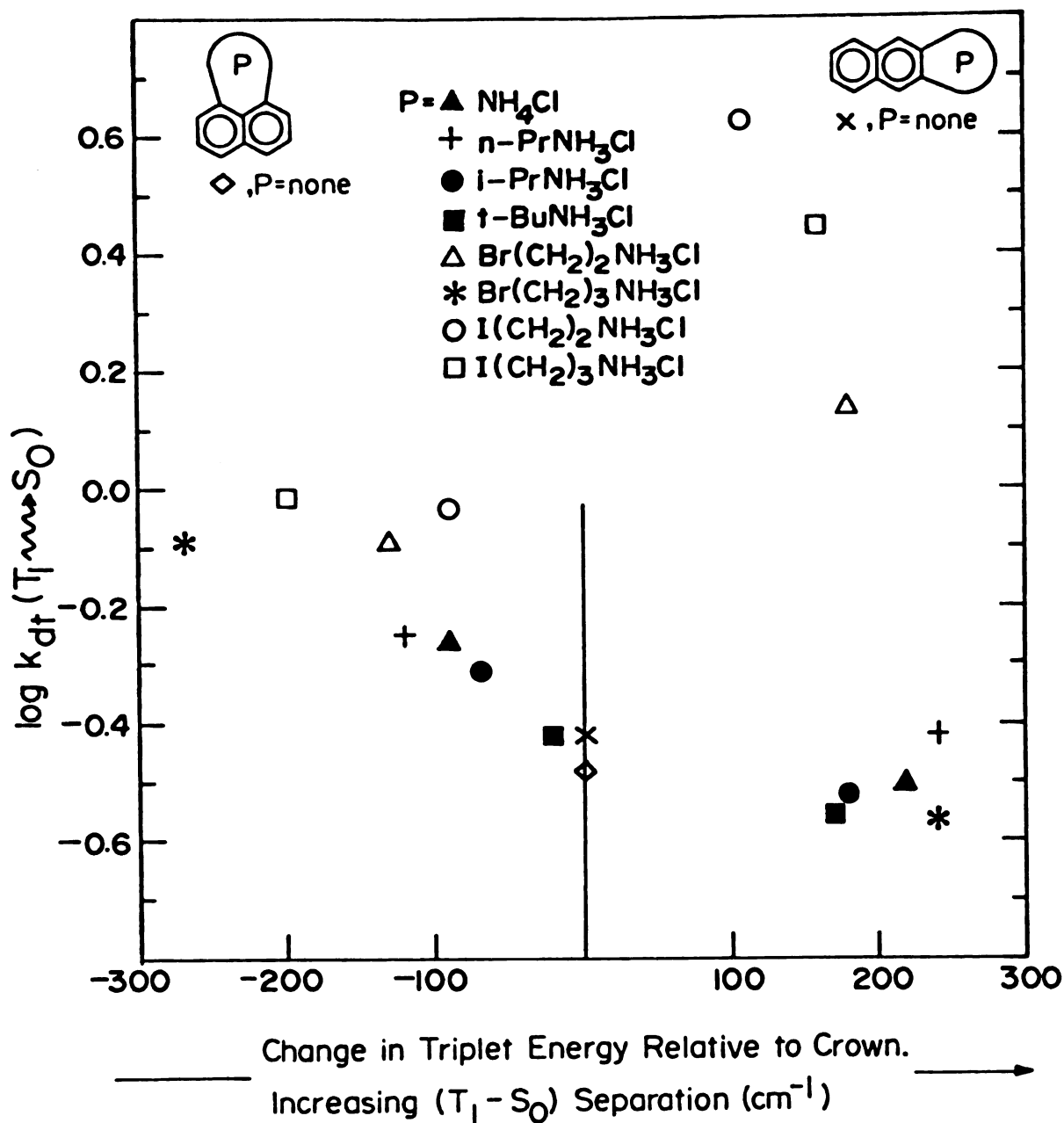


Figure 70. Plot of  $\log k_{dt}$  versus the change in the  $T_1 - S_0$  energy separation in  $\text{cm}^{-1}$  caused by ammonium, alkylammonium, and haloalkylammonium cation perturbation of crowns 1 and 2.

glass would not be meaningful, since the observed quantities are probably complicated composites arising from different values due to different relative orientations and distances between the perturber and the perturbed chromophore. As is usually done for this kind of study, conclusions will be drawn based on the way in which ratios of quantum yields and ratios of lifetimes ( $\tau_p$ ) change. Ratios in Table 40 are given so that all ratios increase as a function of perturbation in order to make comparisons of relative decreases and increases easier. The ratio of  $\phi_f$  in alcohol glass to  $\phi_f$  in ethyl bromide (EtBr) containing glass ( $\phi_{f,o}/\phi_{f,EtBr}$ ),  $\phi_p$  in EtBr containing glass to  $\phi_p$  in alcohol glass ( $\phi_{p,EtBr}/\phi_{p,o}$ ) and  $\tau_p$  in alcohol glass to  $\tau_p$  in EtBr containing glass ( $\tau_{p,o}/\tau_{p,EtBr}$ ) are tabulated in Table 40 for naphthalene, crowns 1, 2, and 3, and alkali metal complexes of these crowns.

The  $\tau_{p,EtBr}$  values used are the shorter lifetime estimates from a double exponential analysis (see Table 32). Longer lifetime estimates are in the neighborhood of 1 sec except for complexes of crown 2 and the  $Cs^+$  complex of crown 3. In the latter case, the decay is better represented by a single exponential analysis than double. The longer lifetime estimate for naphthalene perturbed by EtBr (0.72 sec) is similar to a literature estimate for naphthalene (1.14 sec) in ethanol-ethyl bromide (4:1, v/v) glass at 77 K which was based on the "first half-life" of the decay (vide infra).<sup>53</sup> The shorter lifetime estimate for naphthalene (0.042 sec) is similar to a literature<sup>13</sup> estimate (0.14 sec) in propyl bromide glass at 77 K which was also based on the "first half-life". Thus the analytically

Table 40. Estimates for Ratios of Fluorescence ( $\phi_{f,o}$ ) and Phosphorescence ( $\phi_{p,o}$ ) Quantum Yields and Phosphorescence Lifetimes ( $\tau_{p,o}$ ) in Alcohol Glass to the Corresponding Quantum Yields ( $\phi_{f,EtBr}$  and  $\phi_{p,EtBr}$ ) and Lifetimes ( $\tau_{p,EtBr}$ ) in Ethyl Bromide-Ethanol-Methanol (1:4:1, v/v) Glass at 77 K.

System	$\phi_{f,o}$ $\phi_{f,EtBr}$	$\phi_{p,EtBr}$ $\phi_{p,o}$	$\tau_{p,o}^a$ $\tau_{p,EtBr}$
Naphthalene	4.0	12.7	60
2,3-Cr-6 ( $\lambda$ )	1.5	3.8	20
$\lambda$ + KCl	1.8	3.4	15
$\lambda$ + CsCl	1.5	2.4	14
$\lambda$ ,8-Cr-6 (2)	2.0	2.3	46
$\lambda$ + KCl	1.7	2.8	110
$\lambda$ + CsCl	1.8	2.2	46
1,5-Cr-6 ( $\lambda$ )	1.6	1.9	14
$\lambda$ + KCl	1.4	1.8	13
$\lambda$ + RbCl	1.2	1.33	7
$\lambda$ + CsCl	1.0	1.00	1.3

$\tau_{p,EtBr}^a$  is shorter lifetime estimate from double exponential analysis.

obtained estimates of lifetimes for naphthalene as perturbed by EtBr are in good agreement with literature precedent.

The discussion now turns to a consideration of the questions posed in the preamble to the discussion.

#### Directional Dependence of External Heavy Atom Effect

It had initially been hoped that differences in metal cation perturbation of crowns  $\lambda$ ,  $\lambda$ , and  $\lambda$  would provide an experimental demonstration of the directional dependence or lack thereof for external perturbation. As pointed out above, there are at least two factors which cloud such a demonstration by these model systems: 1) the steric blocking due to the naphthyl methylene units in crowns 1 and 2, and 2) the indeterminacy of the position of cations complexed by crowns  $\lambda$ ,  $\lambda$ , or  $\lambda$ . The results of perturbation by  $\text{Cs}^+$  and  $\text{Ag}^+$ , however, shows that there is either a strong directional and/or distance dependence for external perturbation by metal cations, since the effects of perturbation by  $\text{Cs}^+$  or  $\text{Ag}^+$  on crown  $\lambda$  are much larger than those for crowns  $\lambda$  or  $\lambda$ .

The strongest piece of evidence for a directional dependence for the external HAE comes from perturbation of naphthalene and crowns  $\lambda$ ,  $\lambda$ , and  $\lambda$  by ethyl bromide containing glass (ethyl bromide-ethanol-methanol (1:4:1)) at 77 K. Table 40 shows that naphthalene is more perturbed (i.e., quantum yield and lifetime ratios are changed the most) by EtBr than any of the crown substituted naphthalenes. Crowns  $\lambda$  and  $\lambda$  are perturbed by EtBr to roughly the same extent, but crown 3, for which the crown ring passes over the  $\pi$ -face, is least



perturbed. This is the best direct experimental demonstration to date to this writer's knowledge that an aromatic hydrocarbon like naphthalene is most susceptible to external perturbation in the vicinity of the  $\pi$ -face. As indicated in the background section on the HAE (see introduction), other authors have thought this to be the case, based on various experimental indications, but have not been able to directly demonstrate it.

The results of perturbation of crown  $\mathfrak{3}$  by complexed haloalkylammonium salts also provides evidence that the  $\pi$ -face is most susceptible to a heavy atom perturber. Table 39 shows that  $k_{nr}$ ,  $k_p$ , and  $k_{dt}$  are larger in each case for the  $\beta$ -haloalkylammonium complexes than for the  $\gamma$ -haloalkylammonium complexes ( $k_p$  is approximately the same for the  $\gamma$ - and  $\beta$ -bromoalkylammonium complexes. This difference in behavior is consistent with the conclusion that the  $\pi$ -face is most susceptible to the external HAE, since, given the geometric constraints imposed by crown  $\mathfrak{3}$ , the halogen on the three carbon chain can't attain the same degree of proximity to the  $\pi$ -face as can the halogen on the two carbon chain without the alkyl chain assuming a much more strained conformation.

For the haloalkylammonium complexes of crown  $\mathfrak{1}$ ,  $k_{nr}$ ,  $k_p$ , and  $k_{dt}$  are generally larger for the  $\beta$ -haloalkylammonium complexes than for the  $\gamma$ -haloalkylammonium complexes ( $k_p$  is about the same for the  $\beta$ - and  $\gamma$ -bromo cases and  $k_{nr}$  is larger for the  $\gamma$ -bromo than for the  $\beta$ -bromo). This is not what one might expect for this crown, since in this case the halogen on the longer chain should be able to reach out over the  $\pi$ -face better than the halogen on the shorter chain.

Corey-Pauling-Katum (CPK) models show that for crown  $1_{\text{c}}$ , the halogen on the two carbon chain can just reach the edge of the  $\pi$ -system, whereas the halogen on the longer chain can reach out further over the  $\pi$ -face. The fact that larger effects are not observed for the  $\pi$ -halo analogs does not contradict the conclusion reached for the haloalkylammonium complexes of crown  $3_{\text{c}}$ . The spatial constraints imposed by crown  $3_{\text{c}}$  for a complexed haloalkylammonium salt are different from those imposed by crown  $1_{\text{c}}$ . For crown  $3_{\text{c}}$ , the halogen is more likely to be in the vicinity of the  $\pi$ -face for either the long or the short chain, since the site of complexation of the ammonium group is over the face, although the longer chain tends to keep the halogen closer to the outer edge of the  $\pi$ -system. An indication of this greater likelihood is that  $k_{\text{p}}$  and  $k_{\text{nr}}$  for a haloalkylammonium complex of crown  $3_{\text{c}}$  are larger than for the corresponding complex of crown  $1_{\text{c}}$ . For crown  $1_{\text{c}}$ , the site of complexation of the ammonium group is on the side of the naphthalene nucleus. Barring attractive interactions between the halogen and the  $\pi$ -system, the likelihood of the halogen being in the vicinity of the  $\pi$ -face will be governed mainly by statistics. As the chain length increases, the number of conformational degrees of freedom increase, and the probability of the halogen being in the vicinity of the  $\pi$ -face decreases. In fact, the smaller effects observed for the  $\pi$ -halo analogs suggests that any enthalpy gain due to attractive interactions between the halogen and the  $\pi$  system has to be less than the entropy loss which would be required.

For haloalkylammonium complexes of crown  $2_{\text{c}}$ ,  $k_{\text{nr}}$ ,  $k_{\text{p}}$ , and  $k_{\text{dt}}$

are not much larger than for the alkylammonium complexes (Table 38). This is an indication of either a strong distance or directional dependence for the external HAE. (This also suggests that there is very little tendency for the halogen atoms of the haloalkylammonium salts to be near the naphthalene nucleus.)

#### Distance Dependence of the External Heavy Atom Effect

Both exchange and CT mechanisms for the external HAE are predicted to show an  $S^4$  distance dependence (where  $S$  is an inter-molecular molecular orbital overlap<sup>62</sup>). Therefore, one would expect the external HAE to be subject to a very sensitive distance dependence. Other studies have experimentally indicated that there is a distance dependence (see background section of introduction) but weren't able to specify the degree of sensitivity. Results from this investigation also indicate a distance dependence. Although no precise formulation for how the magnitude of the effects vary as a function of the distance between the perturber and perturbed chromophore will be possible, the fact that relative spatial orientations are better known than for other investigations will allow some qualitative observations on the sensitivity of the effect as a function of distance to be made.

Results from the CMR work previously referred to<sup>83</sup> indicate that, for a given crown, the position of the center of positive charge is about the same for all alkali metal complexes. The evidence for this is that all alkali metal cations induce very nearly the same change in the chemical shifts of the naphthalene carbons for a given

crown (the shifts are somewhat more variable for 1,8-Cr-6 (2)). The same is true for the alkaline earth metal cations, but the magnitudes of the changes in CMR shifts are larger than those induced by the alkali metal cations. Also, for 2,3-naphtho-17-crown-5 (2,3-Cr-5) and for 1,8-naphtho-18-crown-5 (1,8-Cr-5), the magnitude of the changes induced by alkali metal cations are larger than for 2,3-Cr-6 (1) or 1,8-Cr-6 (2). These results show that the chemical shifts of the naphthalene carbons are a function of the magnitude and position of the center of positive charge. Changes in the chemical shifts of the ether carbons induced by complexation of metal ions are consistent with either small conformational changes or with small adjustments of the center of positive charge. On the basis of the evidence from the changes in the chemical shifts of the naphthalene carbons, it is thought that the former interpretation is correct. Thus, if the center of positive charge is in roughly the same place for all alkali metal complexes of a given crown, then the smaller cations will be further away from the chromophore. The smaller effects due to perturbation of a given crown by light cations, then, might in part be because the higher cations ( $\text{Na}^+$  and  $\text{K}^+$ ) are smaller than the heavier cations ( $\text{Rb}^+$  and  $\text{Cs}^+$ ).

Perhaps the best indication that the less effective perturbation by light cations is due in part to having their regions of electron density (but perhaps not their nuclei) further away from the chromophore comes from alkali metal cation perturbation of crown 3. For typical internal or external HAE for a series of heavy atom perturbers, it has been found that there is a linear relationship between the

logarithm of the perturbed rate constant and the logarithm of the square of the spin-orbital coupling parameter ( $\xi$ ).<sup>85</sup> It was thought that the rate constants for alkali metal cation perturbation might show such a correlation. But no such linear relationship was observed for  $\log k_{nr}$  or  $\log k_p$  versus  $\log \xi^2$ . The plots show a disproportionately large increase in  $\log k$  as function of  $\log \xi^2$  for  $\text{Cs}^+$  perturbation of crown  $\text{3}$ . This suggests that the other alkali metal cations are less effective perturbers than would be expected. The most reasonable explanation for this seems to be that smaller cations are held with their van der Waals radius further away from the chromophore.

If this explanation is correct, then one would expect, say,  $\text{Rb}^+$  to be a more effective perturber of 1,5-naphtho-19-crown-5 than 1,5-naphtho-22-crown-6 ( $\text{3}$ ). This smaller 1,5-crown has been synthesized, but the effects of alkali metal cation perturbation have not yet been investigated. Alkali metal cation perturbation of smaller 2,3- and 1,8-crowns (2,3-naphtho-17-crown-5 and 1,8-naphtho-18-crown-5) has been investigated.  $\text{Cs}^+$  was found to be a more effective perturber of 2,3-Cr-5 than of 2,3-Cr-6 ( $\text{1}$ ) (i.e.,  $k_{nr}$ ,  $k_p$ , and  $k_{dt}$  all increased more in former case than in latter). (Note, however, that  $\text{Cs}^+$  forms complexes with  $\text{Cs}^+:\text{crown} = 1:2$  stoichiometry, since the break in the titration curve is at the  $\text{Cs}^+:\text{crown} = 1:2$  point. It is not known whether or not a 1:1 complex is formed at higher  $\text{Cs}^+:\text{crown}$  ratios, since no further break in the titration curve is observed. The more effective perturbation of the smaller 2,3-crown may be because the  $\text{Cs}^+$  cation might be complexed in such a way that it is positioned

above the plane of the naphthalene nucleus and in closer proximity to the  $\pi$ -system.)  $\text{Cs}^+$ , however, is a less effective perturber of 1,8-Cr-5 than of 1,8-Cr-6 (2). Given what has been learned, one would expect different size 1,5-crowns to be more useful in discerning distance effects than different size 2,3- or 1,8-crowns, since the latter have the steric interference due to the naphthyl methylene groups.

A rough estimate of the degree of sensitivity of external heavy atom perturbation as a function of distance can be made from the deviation from linearity of the  $\log k$  versus  $\log \xi^2$  plots for  $k$ ,  $k_p$ , and  $k_{dt}$  of crown 3 as perturbed by complexed alkali metal cations. Assuming that the center of charge is in the same place (which could be the case based on CMR work with crowns 1 and 2), then  $\text{Rb}^+$  would be  $0.21 \text{ \AA}$  further from the  $\pi$ -system than  $\text{Cs}^+$ . (Because of the rigidly and widely spaced naphthalic oxygens of the 1,5-crown, it is also possible that the cations would tend to associate with the oxygens in the more flexible part of the ring.) Assuming that the perturbation due to  $\text{Na}^+$  would be small in any case (like an alkyl fluoride) and connecting the points for  $\text{Na}^+$  and  $\text{Cs}^+$  on the log-log plot by a straight line, then  $k_{nr}$  and  $k_p$  for  $\text{K}^+$  ( $0.36 \text{ \AA}$  smaller than  $\text{Cs}^+$ ) and  $\text{Rb}^+$  perturbation are three to five times smaller than would be predicted by the straight line. This suggests that even a few tenths of an angstrom difference in distance can greatly decrease the effectiveness of an external heavy atom perturber.

### Effects of the Positive Charge of the Perturber

As has already been indicated, CMR studies<sup>83</sup> show that all alkali metal cations complexed by 2,3-Cr-6 or 1,8-Cr-6 cause shifts in  $\pi$ -electron density that are similar for a given crown, but that cations complexed by 1,5-Cr-6 cause smaller shift in electron density. This shows that the positive charge, independent of any other properties of the cation, can perturb the chromophore, but that these shifts in electron density are unrelated to the observed changes in rate constants, since different cations have different effects on rate constants of excited state processes, but all ions of the same charge cause similar shifts in  $\pi$ -electron density (in the ground electronic state, anyway).

The fact that light cations ( $\text{Na}^+$  and  $\text{K}^+$ ) induce only small changes in rate constants argues against any large perturbation due to the charge itself. The results of alkylammonium perturbation provide another indication that the mere presence of a center of positive charge has little perturbing effect on the rates of excited state processes. What is perhaps most surprising is that complexation of positively charged species in the vicinity of the  $\pi$ -face via crown  $\beta$  has little perturbing effect.

It had initially been thought that a comparison of perturbation by  $\text{Cs}^+$  and  $\text{Ba}^{++}$  might provide an indication of the role (if any) of the positive charge of the perturber.  $\text{Cs}^+$  and  $\text{Ba}^{++}$  have similar nuclear charges, so it is thought that they might both be capable of inducing similar enhancements of spin-orbital coupling. All other things being equal, any differences in their perturbations

would be ascribable to their difference in ionic charge. Unfortunately, other things are not equal, since  $\text{Ba}^{++}$  is smaller than and less polarizable than  $\text{Cs}^+$ . The fact that  $\text{Ba}^{++}$  is a much less effective perturber of crown  $\mathfrak{3}$  than  $\text{Cs}^+$  is a striking result (see Table 36). But this may be due to the fact that  $\text{Ba}^{++}$  is smaller than  $\text{Cs}^+$  (more similar in size to  $\text{K}^+$ ) and, therefore, it may be complexed in such a way that it is much further away from the  $\pi$ -face than is  $\text{Cs}^+$  (see above under distance effects). Alternatively,  $\text{Ba}^{++}$  is not as polarizable as  $\text{Cs}^+$ , and it is possible that the degree of polarizability as well as the magnitude of the nuclear charge determine an atom's effectiveness as an external heavy atom perturber. Thus, it is thought that HAE due to rare gas matrices are a function of their physical polarizability, since chemical interaction is thought to be unlikely.<sup>86</sup> Perturbation of a smaller 1,5-crown by  $\text{Ba}^{++}$  would perhaps indicate whether its ineffective perturbation of crown  $\mathfrak{3}$  is a function of its smaller size vis-a-vis distance or of its lower polarizability.

Comparison of perturbation of crown  $\mathfrak{1}$  by  $\text{Cs}^+$  and by  $\text{Ba}^{++}$  (Table 34) shows that, for this crown,  $\text{Ba}^{++}$  is as effective as  $\text{Cs}^+$ .  $k_f$  is perturbed somewhat less by  $\text{Ba}^{++}$  than by  $\text{Cs}^+$  (3-fold decrease versus 5-fold decrease),  $k_{nr}$  is perturbed more by  $\text{Ba}^{++}$  than by  $\text{Cs}^+$  (2-fold increase versus 0.5-fold increase), and  $k_p$  and  $k_{dt}$  are perturbed to approximately the same extent.  $\text{Ba}^{++}$  has about the same effect on crown  $\mathfrak{2}$  as does  $\text{Cs}^+$ , but note that (vide supra)  $k_{dt}$  as perturbed by  $\text{Ba}^{++}$  does not correlate with  $\Delta(E_{T_1} - S_0)$ , whereas  $k_{dt}$  as perturbed by  $\text{Cs}^+$  does (see Figure 66). These results for crowns



$\lambda_1$  and  $\lambda_2$  show that  $Ba^{++}$  and  $Cs^+$  are similar and yet different perturbors, but it is not possible to say from these results which differences in properties of  $Ba^{++}$  and  $Cs^+$  account for the differences in perturbation. The greater similarity between  $Ba^{++}$  and  $Cs^+$  perturbation of either crowns  $\lambda_1$  or  $\lambda_2$  as compared to the great dissimilarity between  $Ba^{++}$  and  $Cs^+$  perturbation of crown 3 may be a function of the fact that the effects of  $Cs^+$  perturbation in the former cases is much smaller than in the latter case.

#### Necessity of Charge Transfer States for the External Heavy Atom Effect

As indicated in the background section on the heavy atom effect (HAE), McGlynn<sup>58</sup> concludes that it is theoretically difficult to choose between an exchange and a charge transfer (CT) mechanism for the external HAE. He prefers a CT mechanism based on various experimental indications; however, his interpretations and arguments were criticized in the background section both on the basis of observations by other investigators and on logical grounds. The results of this investigation show no spectral evidence for charge transfer character except perhaps in the case of the  $Ag^+$  complex of crown  $\lambda_2$  (vide infra).

One of McGlynn's arguments for the involvement of CT character in the interaction between perturbing alkyl halide and the naphthalene chromophore was based on red shifts of naphthalene's 0-0 phosphorescence peak induced by propyl halide glasses at 77 K (see background

section of introduction for fuller description of observations and arguments made from them). While the observed red shifts cannot be disputed, the observations of this investigation show that perturbation of crowns  $1$ ,  $2$ , and  $3$  by haloalkylammonium chlorides do not induce similar red shifts but do enhance spin-orbital coupling, as evidenced by increases in  $k_{nr}$ ,  $k_p$ , and  $k_{dt}$ . This shows that CT, as evidenced by red shifts anyway, is not necessarily involved in SO enhancement by external alkyl halides.

For crown  $1$ , complexation of  $\gamma$ -haloalkylammonium salts induces blue shifts of the  $T_1$  0-0 peak relative to free crown similar in magnitude to those induced by alkali metal and alkylammonium cations. Also, note that the magnitude of the blue shift for  $\gamma$ -bromopropylammonium perturbation is very similar to that due to n-propylammonium perturbation. This indicates that the properties of the bromine have nothing to do with the shift. It might be argued that the failure to observe a red shift in the  $T_1$  0-0 peak is because the blue shift induced by complexation obscures a red shift due to CT interaction with the  $\pi$ -system by the halogen. Indeed, smaller blue shifts are observed for perturbation of crown  $1$  by  $\beta$ -haloalkylammonium perturbation, which are more effective perturbers of crown  $1$  than the  $\gamma$ -analogs, as has been previously noted. But the blue shifts are smaller by about the same amount (about  $60\text{ cm}^{-1}$ ) for perturbation by the  $\beta$ -bromo and the  $\beta$ -iodo isomers. A smaller blue shift should have been observed for perturbation by the  $\beta$ -iodo isomer if CT was involved. McGlynn<sup>88</sup> noted a red shift of  $325\text{ cm}^{-1}$  for propyl iodide perturbation and of  $155\text{ cm}^{-1}$  for propyl bromide

perturbation of naphthalene. Also, as has already been noted, while haloalkylammonium perturbation of crown  $\lambda$  red shifts other peaks in the phosphorescence spectra, so also does  $n\text{-PrNH}_3\text{Cl}$  perturbation. In a similar vein,  $\beta$ -halo perturbation of crown  $\lambda$  red shifts the  $S_2$  0-0 absorption peaks by  $500\text{ cm}^{-1}$ , so also does  $n\text{-PrNH}_3\text{Cl}$  perturbation.

For crown  $\lambda$ , complexation of all perturbers induces red shifts. The  $\gamma$ -haloalkylammonium are somewhat more effective perturbers of crown 2 than the  $\gamma$ -halo analogs (see Table 38), but they induce smaller red shifts. It might be argued that this is because the halogen is not in the right position to form a CT complex with the  $\pi$ -system, which may be true, but these perturbers do increase  $k_{nr}$ ,  $k_p$ , and  $k_{dt}$ , though less so than for perturbation of crowns  $\lambda$  or  $\lambda$ . But this is another indication that SO coupling does not require a CT complex.

For crown  $\lambda$ , which is the crown most effectively perturbed by complexed haloalkylammonium cations  $\lambda$  (compare Table 39 to Table 37 and 38), only small blue shifts of the  $T_1$  0-0 peaks are induced by complexation of these perturbers, except for a small red shift ( $30\text{ cm}^{-1}$ ) induced by perturbation by the  $\beta$ -bromo analog. But perturbation by  $\text{NH}_4\text{Cl}$  also produces a small red shift ( $10\text{ cm}^{-1}$ ). Most perturbers induce only small blue shifts (10 to  $40\text{ cm}^{-1}$ ). These blue shifts are small enough so that they wouldn't obscure red shifts of the magnitude observed by McGlynn.

It might be argued that the failure to observe red shifts due to the interaction of the halogen and the  $\pi$ -system is because the

emission spectra are composites of emission from perturbed and unperturbed species. But the results of double exponential analysis of the phosphorescence decay curves (Table 31) indicate that shorter decay accounts for 50 to 80% of the total decay. Furthermore, for crown 3, for which energies change least and perturbation is most effective, spectral shapes are unchanged by haloalkylammonium cation perturbation. It is for this case that observation of a red shift due to CT interaction of the halogen would be least likely to be obscured by opposing energy shifts due to perturbation due to complexation or changes in spectral shapes. But red shifts aren't observed. Therefore, it is concluded that there is no evidence for CT involvement in mediating the eternal HAE due to complexed haloalkylammonium perturbers.

There is a general tendency for complexation of crown 3 to induce small blue shifts, but in the case of  $\text{Ag}^+$  complex of crown 3 every spectral 0-0 peak is red shifted relative to free crown (see Table 4). This might be taken as an indication that  $\pi$ -molecular orbitals of naphthalene interact rather strongly, and with net stabilization, with atomic orbitals of  $\text{Ag}^+$ . This is not unreasonable, since  $\text{Ag}^+$  is known to form  $\pi$ -complexes.<sup>73</sup> Note that  $\text{Ag}^+$  perturbs  $k_{\text{nr}}$ ,  $k_{\text{p}}$ , and  $k_{\text{dt}}$  of crown 3 differently than  $\text{Cs}^+$ .  $k_{\text{nr}}$  appears to be perturbed to about the same extent by both  $\text{Ag}^+$  and  $\text{Cs}^+$ ,  $k_{\text{p}}$  is increased about 60-fold relative to crown versus a 10-fold increase due to  $\text{Cs}^+$ , and  $k_{\text{dt}}$  is increased about 2-fold by  $\text{Ag}^+$  but about 5-fold by  $\text{Cs}^+$  (see Table 36). Evidently, depending upon the kind of interaction, different rate constants may be affected differently. Thus, while

some external perturbers may form weak CT complexes, it does not appear that CT character is necessary to the external HAE, since  $\text{Ag}^+$  and  $\text{Cs}^+$  both have external HAE and it is doubtful that much CT occurs to  $\text{Cs}^+$  (unfortunately, the reduction potential of  $\text{Cs}^+$  in 95% ethanol is not known).

#### Effectiveness of External Perturbation as Function of Perturbation Already Present

The results of EtBr perturbation (EtBr-ethanol-methanol (1:4:1, v/v) glass) of alkali metal complexes of crowns 1, 2, and 3 nicely fit with McGlynn's observations for the effectiveness of a given external heavy atom perturber as a function of the spin-orbital perturbation already present due to an internal heavy atom. McGlynn<sup>13</sup> observed (see background section in introduction for more complete description) that as the internal spin-orbital coupling increased, that the ratio of the external effect to internal effect decreases. Table 40 shows that for alkali metal complexes of crowns 1 and 3,  $\phi_{\text{p,EtBr}}/\phi_{\text{p,o}}$  or  $\tau_{\text{p,o}}/\tau_{\text{p,EtBr}}$  both decrease as the spin-orbital coupling parameter of the complexed alkali metal cation increases. Also, note that the ratio of the external to the internal effect is smallest for the "internally" most perturbed crown, the  $\text{Cs}^+$  complex of crown 3.  $\phi_{\text{f,o}}/\phi_{\text{f,EtBr}}$  (all ratios are given so as to be greater than 1) decreases less than  $\phi_{\text{p,EtBr}}/\phi_{\text{p,o}}$ . This indicates that most of the change in  $\phi_{\text{p,EtBr}}/\phi_{\text{p,o}}$  is due to changes in  $k_{\text{p}}$ , not to increases in  $\phi_{\text{isc}}$  (assuming that  $k_{\text{f}}$  isn't affected and that  $k_{\text{ds}}$  is negligible; see introduction). Note that the only apparent anomaly is for the

$K^+$  complex of crown  $\mathcal{Z}$ . It is perturbed more by EtBr than are free crown  $\mathcal{Z}$  or the  $Cs^+$  complex of  $\mathcal{Z}$ . This anomaly may in some way relate to the decrease in  $k_{nr}$  caused by  $K^+$  perturbation of crown  $\mathcal{Z}$  (see Table 35). McGlynn's observations were for covalently bonded perturbers. A complexed perturber is most like an external perturber, but as long as the observations are thought of in terms of the effectiveness of the external perturber (i.e., EtBr) as a function of the spin-orbital perturbation already present, be it due to a covalently bonded perturber, a complexed perturber, or another external perturber, there is really not much difference between the present study and McGlynn's.

The results in Table 40 (especially the results for crown  $\mathcal{Z}$ ) are not rationalized by McGlynn's suggestion that external heavy atom perturbers (EtBr in this case) are more effective when a substantial amount of SO coupling is already present. If it is assumed that external SO coupling, like that caused by  $Cs^+$  complexation by crown  $\mathcal{Z}$ , is similar in effect to internal SO coupling, the effect of EtBr on  $\mathcal{Z}$  plus complexed  $Cs^+$  should be larger than the effect of EtBr on  $\mathcal{Z}$  plus complexed  $Rb^+$ . The opposite is observed. There may be a sharp difference between internally and externally promoted SO coupling, or the suggested synergistic effect of internal SO coupling may not be general.

### Relative Susceptibility of Rate Constants for Excited State Processes

As indicated in the introduction, various investigators have been interested in the relative susceptibility of rate constants for excited state processes and different conclusions about which rate constants are most susceptible have been drawn,<sup>89</sup> This isn't surprising, since this writer sees no reason to expect that conclusions drawn from CT complexes containing heavy atoms,<sup>13</sup> for instance, should have anything to do with alkyl halide perturbation. Indeed, a major conclusion of this investigation is that the relative susceptibility of rate constants is a function of where the perturber is and the nature of the perturber. Since the only chromophores studied are based on naphthalene, any conclusions reached will not be assumed to be true for other aromatic hydrocarbons.

Tables 41 and 42 give relative rate constant susceptibilities as a function of crown and of perturber type. These orders of relative susceptibilities were derived from Tables 34 through 39 by selecting the rate constant which was changed most by a perturber of a given type.  $\text{Cs}^+$  was the most effective perturber in all cases for the alkali metal cations except for  $k_f$  ( $\text{Rb}^+$ ) and  $k_{nr}$  ( $\text{K}^+$ ) of crown  $\mathcal{L}$ .  $n\text{-PrNH}_3\text{Cl}$  was usually the most effective alkylammonium perturber. The most effective haloalkylammonium perturber depends upon the crown perturbed. Their relative effectiveness was discussed for each crown in the preceding discussion. Note that when the value of  $k_f$  isn't derived from  $\tau_f$  measurements, that  $k_{nr}$  is not included unless it is thought that the relative value of  $k_{nr}$  would not be much in error relative to the other rate constants due to the error in the

Table 41. Relative Susceptibility of Rate Constants of Excited State Processes of 2,3-Naphtho-20-Crown-6 (1), 1,8-Naphtho-21-Crown-6 (2), and 1,5-Naphtho-22-Crown-6 (3) to Perturbation by Complexed Alkali Metal, Barium and Silver Cations in Alcohol Glass at 77 K.

Crown	Perturber Type	Relative Susceptibility of Rate Constants
2,3-Cr-6 (1)	Alkali Metal	$k_f > k_p > k_{nr} > k_{dt}$
1,8-Cr-6 (2)	Alkali Metal	$k_{dt} > k_p > k_f > k_{nr}$
1,5-Cr-6 (3)	Alkali Metal	$k_{nr} > k_p > k_{dt}$
2,3-Cr-6 (1)	$Ba^{++}$	$k_f \approx k_p \approx k_{nr} > k_{dt}$
1,8-Cr-6 (2)	$Ba^{++}$	$k_p \approx k_{dt}$
1,5-Cr-6 (3)	$Ba^{++}$	$k_p \approx k_{dt}$
2,3-Cr-6 (1)	$Ag^+$	$k_p \approx k_{dt}$
1,8-Cr-6 (2)	$Ag^+$	$k_p \approx k_{dt}$
1,5-Cr-6 (3)	$Ag^+$	$k_p > k_{nr} \gg k_{dt}$



Table 42. Relative Susceptibility of Rate Constants of Excited State Processes of 2,3-Naphtho-20-Crown-6 (1), 1,8-Naphtho-21-Crown-6 (2), and 1,5-Naphtho-22-Crown-6 (3) to Perturbation by Complexed Alkyl and Haloalkylammonium Cations in Alcohol Glass at 77 K.

Crown	Perturber Type	Relative Susceptibility of Rate Constants
2,3-Cr-6 (1)	Alkylammonium	$k_{nr} > k_f \approx k_p > k_{dt}$
1,8-Cr-6 (2)	Alkylammonium	$k_f \approx k_{dt} > k_{nr} > k_p$
1,5-Cr-6 (3)	Alkylammonium	$k_{nr} \approx k_p \approx k_{dt}$
2,3-Cr-6 (1)	Haloalkylammonium	$k_p > k_{dt} > k_{nr}$
1,8-Cr-6 (2)	Haloalkylammonium	$k_{dt} > k_p > k_{nr}$
1,5-Cr-6 (3)	Haloalkylammonium	$k_{nr} \approx k_{dt} > k_p$

"guess" for  $k_f$ .

While one's initial impression from inspection of Tables 41 and 42 might be that there are no regularities, there are perhaps some generalities which can be extracted. For the alkali metals, note that  $k_p$  is the second most affected rate constant in each case.  $k_{dt}$  is usually least affected, except for perturbed crown  $\lambda$ . Inspection of the rest of Tables 41 and 42 will show that, for crown  $\lambda$ ,  $k_{dt}$  is generally either the most affected rate constant, next to it, or, when only  $k_p$  and  $k_{dt}$  are known well, affected to approximately the same extent as  $k_p$ . Perhaps it is the out of plane distortions due to peri-interactions in 1,8-disubstituted naphthalene which are responsible for this enhancement of radiationless decay ( $k_p$  is usually thought to be affected more by the HAE).<sup>55</sup>

Not enough is known about perturbation by  $Ba^{++}$  to allow much to be said about its effects relative to  $Cs^+$ . For crown  $\lambda$ , the curious result that emerges is that  $k_f \approx k_p \approx k_{nr}$ . Also, it is curious that  $k_p \approx k_{dt}$  for  $Ba^{++}$  perturbation of both crown  $\lambda$  and  $\lambda$ . Perturbation of crowns  $\lambda$  and  $\lambda$  by  $Ag^+$  also affects  $k_p$  and  $k_{dt}$  to approximately the same extent.

For haloalkylammonium perturbation of crowns  $\lambda$ ,  $\lambda$ , and  $\lambda$ , it is curious that the relative order of  $k_{nr}$ ,  $k_p$ , and  $k_{dt}$  is different for each crown. For crown  $\lambda$ , the crown that is most affected by haloalkylammonium cation perturbation, the nonradiative modes,  $k_{nr}$  and  $k_{dt}$ , are enhanced more than the radiative modes,  $k_p$ . For crown  $\lambda$   $k_{dt}$  is observed to be perturbed most, as was also noted to be the case with alkali metal perturbation. For crown  $\lambda$ ,  $k_p$  (radiative

mode) is affected more than either of the nonradiative modes by halo-alkylammonium perturbation.

## EXPERIMENTAL

### General Procedures

Melting points were determined using a Thomas-Hoover apparatus (capillary tube) and are uncorrected. Mass determinations were done on a Mettler H20T analytical balance ( $\pm 0.01$  mg). Infrared spectra were recorded on a Perkin-Elmer 237B infrared grating spectrophotometer.  $^1\text{H}$  NMR spectra were determined on a Varian T-60 spectrometer using tetramethylsilane as an internal standard. Ultraviolet absorption spectra at room temperature and at 77 K were recorded on a Cary 17 spectrophotometer. Mass spectra were determined on a Perkin-Elmer Model RMU 6 mass spectrometer. Elemental analyses were performed by Instranal Laboratory, Inc., Rensselaer, NY; or by Chemalytics, Tempe, Arizona.

### 77 K UV Spectra

Ultraviolet absorption spectra at 77 K were determined using a Cary Model 17 spectrophotometer. A round commercial grade quartz dewar and a round commercial grade quartz sample tube ( $\sim 14$  mm, i.d.) were used. The dewar was centered in the light path by means of a tip on its bottom and a hole in a plate which fitted on top of the sample compartment. The sample tube was centered in the dewar by means of a collar at the top of the tube and a notched teflon ring which fitted about the sample tube and into the dewar. Absorbancies from duplicate runs were reproducible to within  $\pm 1\%$ . The glassy solution

at 77 K was compared to a nitrogen atmosphere at room temperature. The base line obtained was relatively flat up to about 260 nm, where the alcoholic solvent and quartz used start absorbing. Relative extinction coefficients at a given wavelength can be determined quite well by this method, but the relative extinction coefficients for different wavelengths in a given spectrum are somewhat distorted due to the fact that the change in refractive index with wavelength of the liquid nitrogen, the quartz, and the glassy solvent are not compensated for by comparison to a similar blank. The results are quite adequate for our purposes, however, since 1) only relative extinction coefficients are necessary for quantum yield determinations and 2) the spectral shapes are qualitatively correct and the spectral intensities semi-quantitatively correct. Comparison of the extinction coefficients ( $\epsilon$ ) of 2,3-naphtho-20-crown-6 (1) at room temperature given by 1.000 cm cells with those given by the round low temperature apparatus at room temperature (calculated assuming a 1 cm path ( $V$  77 K/ $V$  298 K  $\approx$  0.8) length and neglecting increased concentration due to contraction of the glass; actual tube diameter was approximately 1.4 cm) showed the latter to be larger by a factor of approximately 1.5 for the  $S_1$  band (approximately 6% variation within this band) and larger by a factor of approximately 1.2 for the  $S_2$  band (approximately 5% variation within this band). (See Table 43.) These factors should be  $>1$ , due to the longer path length, but they should all be the same if there weren't any other factors involved. This precludes the possibility of calculating an effective path length for the low temperature apparatus. But extinction

Table 43. Comparison of Room Temperature UV Absorption Spectra of 2,3-Naphtho-20-Crown-6 ( $\lambda$ ) in Square Cells and in Round Dewar.

In Square Cells				In Round Dewar <sup>a</sup>				
$\lambda$ (nm)	A <sup>c</sup>	$\epsilon$	$\epsilon_{320.5}$ $\epsilon_x$	$\lambda$ (nm)	A <sup>c</sup>	$\epsilon^b$	$\epsilon_{320.5}$ $\epsilon_x$	$\epsilon_{\text{round}}$ $\epsilon_{\text{square}}$
320.5	0.0462	274	1.00	320.5	0.0490	408.3	1.00	1.49
313.5	0.0463	274	1.00	313.5	0.0515	429.2	1.05	1.57
306.5	0.0612	363	1.33	306.5	0.0670	558.3	1.37	1.54
285(sh	0.54	3205	11.7	285(sh)	0.465	3875	9.49	1.21
275.5	0.842	4997	18.2	295.5	0.685	5708	13.98	1.14
266.5	0.823	4884	17.8	266.5	0.680	5667	13.88	1.16

<sup>a</sup>Dewar filled with water to cut down on scattered light.

<sup>b</sup>Calculated assuming a 1.4 cm path length.

<sup>c</sup>Absorbance (A).

coefficients roughly indicating the strength of an absorption band can be calculated from the data in the figures using either the effective path lengths indicated by the above comparisons (1.5 for the  $S_1$  band, 1.2 for the  $S_2$  band) or the actual diameter of the tube, 1.4 cm. Finally, it should be pointed out that in order to obtain a room temperature spectrum in the low temperature apparatus it was necessary to fill the dewar with some liquid to minimize changes in refractive indices at interfaces. Water ( $n_D^{25} = 1.33287$  versus  $n_D^{-190}$  for liquid nitrogen) was used, but it is recognized that the above comparison may not be valid if the refractive indices of water and liquid nitrogen are greatly different or change differently in the wavelength region with which we are dealing.

All UV absorption spectra at 77 K were determined on solutions prepared from 95% ethanol-methanol (4:1, v/v) or from ethanol-methanol (4:1, v/v) solvent mixtures. With the exception of the determinations made in ethyl bromide containing solutions, all emission, phosphorescence lifetimes, and many of the fluorescence lifetime determinations were made on solutions in 95% ethanol glass. It was necessary to add at least 20% by volume of methanol to obtain uncracked glasses in the larger sample tubes used for determination of 77 K UV absorption spectra. Addition of 20% by volume of methanol to 95% ethanol did not always result in uncracked glasses for fluorescence lifetime determinations, however. It did seem that addition of 20% by volume of methanol to absolute alcohol (200 Proof Gold Shield Alcohol) did result in fewer cracked glasses (see section on fluorescence lifetime determinations below). It is not thought

that addition of a small amount of another hydroxylic solvent or removal of most of a small amount of water (ethanol and methanol were dry but not serupously so) should affect spectral or photophysical properties.<sup>9</sup> UV absorption spectra of 2,3-naphtho-20-crown-6 (1) were the same for solutions in 95% ethanol-methanol (4:1, v/v) and in 95% ethanol-methanol (3:2, v/v), and UV spectra of 1,5-naphtho-22-crown-6 (3) were the same for solutions in 95% ethanol/methanol (4:1, v/v) and in ethanol-methanol (4:1, v/v).

### Reagent Purity

Sodium, potassium, rubidium, and cesium chlorides were all ultra-pure salts from Ventron, as were cesium bromide and ammonium chloride. Sodium fluoride (Baker), sodium bromide (Matheson-Coleman-Bell), sodium iodide (Baker), barium bromide (Fisher), and cesium nitrate (Fisher) were all reagent grade salts. All of the above salts were used without further purification. Solutions of silver triflate (from Ventron, 99%) were filtered through medium sintered glass before use to remove particulate matter. Solutions of this salt remained clear and colorless for several months provided that they were stored in the dark. All solutions of the above salts showed neither UV absorption nor fluorescent or phosphorescent emission.

The alkylammonium chloride salts (prepared by passing technical grade gaseous hydrochloric acid (Matheson) through a solution of the liquid amine in diethyl ether) were all purified by recrystallization. n-Propylammonium chloride (somewhat hygroscopic) was recrystallized four times from certified A.C.S. spectranalyzed acetone



(Fisher), mp (162-163<sup>o</sup>, and was dried for 6 h at 120<sup>o</sup>C and 0.1 mm.

i-Propylammonium chloride (very hygroscopic) was recrystallized twice from acetone, m.p. 157-159<sup>o</sup>C, and dried for 18 h at 78<sup>o</sup>C and 0.1 mm. t-Butylammonium chloride (not very hygroscopic) was recrystallized four times from acetone and ethanol (200 Proof Gold Shield Alcohol), m.p. > 300<sup>o</sup>C and was dried for 12 h at 120<sup>o</sup>C and 0.1 mm.

$\beta$ -Bromoethylammonium chloride (not very hygroscopic, see below for preparation) was purified by recrystallization (three times) from benzene-ethanol (reagent grade benzene, 200 Proof Gold Shield Alcohol), m.p. 130-132<sup>o</sup>C, and was dried for 12 h at 78<sup>o</sup>C and 0.05 mm.  $\gamma$ -Bromoethylammonium chloride (not very hygroscopic, see below for preparation) was purified by recrystallization from benzene-ethanol), m.p. 152-153<sup>o</sup>C, and was dried for 12 h at 80<sup>o</sup>C and 0.1 mm. The stability of these salts in 95% ethanol was investigated by monitoring the nuclear magnetic resonance (NMR) spectra as a function of time. The NMR spectrum of salt that had been dissolved in 95% ethanol at room temperature for one week was unchanged compared to that of the pure salt. Also, the NMR of salt that had been dissolved in refluxing 95% ethanol was unchanged. At the concentrations used for emission and absorption experiments, these salts showed neither fluorescent nor phosphorescent emission, nor did they show absorption discernibly different from that of the alcoholic solvent in which they were dissolved.

$\beta$ -Iodoethylammonium chloride (not very hygroscopic, see below for preparation) was purified by recrystallization (twice) from

chloroform-ethanol, m.p. 151.5-154.0.  $\gamma$ -Iodopropylammonium chloride (not very hygroscopic, see below for preparation) was also purified by recrystallization from chloroform-ethanol, m.p. 100-101°C. 95% ethanol solutions of these salts which were left exposed to room light gradually turned yellow. Solutions of these salts stored in the dark, however, remained colorless for several weeks. The stability of the  $\beta$ -iodoethylammonium chloride in 95% ethanol was checked by monitoring its NMR spectrum (vide infra) as a function of time. The NMR spectrum of salt that had been dissolved in 95% ethanol in the dark at room temperature for 6 days was the same as that for the pure salt. After 24 h at reflux, however, the NMR spectrum of recovered material was different. Neither of these salts showed any emission under the same conditions used for emission determinations of their crown complexes. These salts do absorb in the UV spectral region, as shown in Figures 10, 11, and 12, but, at the concentrations used, absorption by the salts is negligible in the region in which the complexed crowns were excited (296 nm or longer).

Ethyl bromide (Aldrich) was purified by first stirring with 3A molecular sieves for 24 h and then distilling through a 1/2" x 15" column packed with stainless steel Heli Pak (vide infra). A large middle fraction (approximately 80%) with a constant boiling point of 37°C was collected. This sample showed no UV absorption at wavelengths longer than 300 nm (absorbance at 290 nm for 1 cm path-length was, 0.03; at 280 nm, 0.62; and at 268 nm, 0.90). Under the conditions of the emission experiments in which ethyl bromide was used, no emission from the ethyl bromide containing glass was observed. 95% ethanol was purified by first refluxing for 24 hours

and then distilling from 100 ml of 12 N sulfuric acid, followed by distillation from excess distilled water to remove diethyl ether formed in the first distillation and to produce the 95% azeotrope. 18 mm by 100 cm vacuum jacketed columns were used for these distillations. The column used for the distillation from sulfuric acid was packed with 1/16" glass helicies (estimated 15-20 theoretical plates); the column used for the second distillation was packed with 100 x 100 mm stainless steel Heli-Pak (Podbielniak, estimated 90-100 theoretical plates). The take-off rate for both distillations was approximately 1 l per 24 hours. The alcohol before purification showed a maximum in its UV spectrum at 275 nm (absorbance of 0.020 in a 1 cm cell path length). The alcohol after purification showed no absorbance (0.1 A slidewire, 1 cm path length) at wavelengths longer than 265 nm in the UV region. Furthermore, no emission from the alcohol was observed under conditions used to determine spectra or quantum yields. At very high sensitivities (approximately 100 times those used for naphthalene phosphorescence measurements), a phosphorescent impurity with a lifetime of approximately 0.1 sec was observed. Methanol (Fisher, reagent grade) was purified in the same manner, with the exceptions that the distillations were done under a nitrogen atmosphere and that the second distillation was used to remove water. A 95% ethanol-methanol (4:1, v/v) glass gave a fluorescence decay with a lifetime of about 8 nsec, but this decay is probably due to scattered light from the decay of the lamp flash (vide infra).

Pentane used for recrystallizations was purified by stirring

practical grade pentane (Matheson-Coleman-Bell) with concentrated sulfuric acid for four hours, washing with 10% sodium carbonate, then with water, drying over calcium chloride and distilling from sodium through the column packed with Heli-Pak described above.

Naphthalene (Mallinckrodt) was recrystallized eight times from ethanol/water (200 Proof Gold Shield Alcohol). The emission spectra for the stock naphthalene and naphthalene at various stages of purification showed no change in fine structure or relative intensity. Both fluorescent and phosphorescent decay curves gave good single exponential fits (see experimental and results sections lifetime discussion) and were close to literature values.<sup>90</sup> These same criteria (unchanged emission fine structure and relative intensities and good single exponential fluorescent and phosphorescent decay) were used to establish the purity of all compounds investigated. 2,3-Naphtho-20-crown-6 (**1**), already recrystallized to constant m.p., was recrystallized eight times from diethyl ether-pentane (ether, Matheson-Coleman-Bell; pentane, purified as indicated above). No difference was found between the purity of the crown after recrystallization to a constant m.p. (58.5-59.0°) and after the eight additional recrystallizations. In general, compounds were recrystallized four additional times after a constant m.p. had been achieved. 2,3-Bis-methoxymethyl)naphthalene (**4**) (vide infra) was obtained as an oil. It was purified by chromatography on neutral silica gel with dichloromethane elution, followed by molecular distillation at 55° and 0.05 mm. Its fluorescent and phosphorescent decay gave good single exponential fits and no emission outside the emission range for other naphthalene derivatives was observed. The oil quickly

becomes colored if left standing exposed to air, but remains a clear, colorless oil if stored under nitrogen in the dark and in the refrigerator. 2,3-Dimethylnaphthalene (5) (Aldrich, 99% +, m.p. 102-103°) was recrystallized from ethanol/water (200 Proof Gold Shield Alcohol) to a constant m.p. of 104-105° and sublimed (0.04 mm, 40°). There was evidence of a small amount of phosphorescent impurity in the stock sample. Its phosphorescence occurred at shorter wavelengths and overlapped the main phosphorescence spectrum. Its intensity decreased as the number of times the sample was recrystallized increased, while the shape of the main phosphorescence spectrum was unchanged. There was a residual amount of this impurity in the final sample used for determinations (as indicated by the slightly higher baseline before the onset of the phosphorescence), but this residual amount would have been too weak to significantly affect the determinations, since 1) the fluorescence was much more intense (no change in fluorescence was observed as a function of purification), 2) the overlap with the phosphorescence spectrum in the final sample was negligible and, as noted above, the shape of the phosphorescence spectrum did not change as the impurity phosphorescence decreased with the extent of purification, and 3) both fluorescent and phosphorescent decay gave good single exponential decay (though the lifetime of one species can be obtained independently of that of another provided that they don't emit in the same region).

All of the 1,8-disubstituted naphthalene derivatives were crystalline and satisfied the above criteria for purity. 1,8-Naphtho-

21-crown-6 (2) was recrystallized four times from ether-pentane, m.p. 54.0-55.0°. 1,8-Bis-(methoxymethyl)naphthalene (6) was recrystallized from purified pentane four times. 1,8-Dimethylnaphthalene (7) was recrystallized four times from alcohol/water (200 Proof Gold Shield Alcohol), followed by sublimation (m.p. 63.4-64.0°).

All of the 1,5-disubstituted naphthalene derivatives were crystalline and satisfied the above criteria for purity. 1,5-Naphtho-22-crown-6 (3) was recrystallized several times from ether-pentane followed by two recrystallizations from spectrograde cyclohexane (Matheson-Coleman-Bell), m.p. 55.5-57.0°C. 1,5-Bis-(methoxymethyl)naphthalene (8) was recrystallized three times from purified pentane (vide supra), m.p. 62-63°C. 1,5-Dimethylnaphthalene (9) (Pfaltz and Bauer) was recrystallized four times from ethanol-water (200 Proof Gold Shield Alcohol), m.p. 80.0-81.5

#### Preparation of Samples for Emission Spectroscopy and Quantum Yield Determinations

All emission spectra were from 95% EtOH solutions. Pyrex NMR tubes (Willmad, 505 PS, 4.26±.13 mm i.d., 5 mm o.d., highly polished) were used for samples excited at wavelengths longer than 296 nm (the pyrex in these tubes starts absorbing at about 310 nm). Quartz NMR tubes (Willmad, 701 PQ, 3.43±.013 mm i.d., 5 mm o.d., highly polished) were used for all samples excited at wavelengths shorter than 296 nm. These tubes were joined to 10/30 male joints to allow for degassing and sealing under vacuum.

Due to the large number of compounds and complexes investigated

and due to the fact that, in general, aromatic hydrocarbons are susceptible to oxygen quenching, all samples were routinely subjected to six freeze-thaw degassing cycles on a system capable of obtaining a vacuum of less than  $10^{-6}$  mm. In the course of degassing, the pressure in the system dropped to  $10^{-5}$  mm by the last cycle. Furthermore, removal of oxygen should improve sample stability. For all cases checked, spectral shapes from samples stored at  $0^{\circ}$  in the dark remained unchanged even after several months. Spectra and lifetimes were generally determined within a week after preparation. Solutions containing crown and salt were prepared by diluting the appropriate volumes of stock solutions.

#### Emission Spectra

The corrected emission spectra shown in Figures 1 through 54 were determined using a Hitachi/Perkin-Elmer Spectrophotofluorometer Model MPF-44A with computerized corrected spectra accessory. The spectra show the full resolution obtainable at 77 K in 95% EtOH uncracked glass. A 1 nm emission bandpass was sufficient to resolve the fluorescence spectra and a 2 nm bandpass was sufficient for the phosphorescence spectra. An excitation bandpass sufficiently large so as to be consistent with good resolution and low noise level was used. The excitation bandpasses used to obtain well-resolved spectra were too large to allow for accurate quantum yield determinations from the same spectra. The relative spectral intensities qualitatively correlate with relative quantum yields, however. The phosphorescence spectra were determined without use of a phosphoroscope, since use

of the phosphoroscope introduced roughly a ten-fold attenuation of the signal and tailing fluorescence did not interfere. Concentrations were in the  $10^{-4}$  M range.

### Spectral Energy Levels

In order to obtain precise frequencies for emission bands it was necessary to use a greatly expanded wavelength scale, usually either 1 nm/16 mm or 1 nm/8 mm. For symmetrical bands, the position of the maximum was located using the symmetry of the band to locate the center. For unsymmetrical bands, the maximum was either visually sighted and/or located making use of the symmetry at the top of the band. The probable error in the band positions reported are  $\pm 20$   $\text{cm}^{-1}$  for the highest energy fluorescent band, and  $\pm 10$   $\text{cm}^{-1}$  for the highest energy phosphorescent band. The accuracy of these values should be within  $\pm 0.2$  nm (  $20$   $\text{cm}^{-1}$  at 320.0 nm and  $\pm 10$   $\text{cm}^{-1}$  at 470.0 nm). Both the emission and excitation monochrometers were calibrated against the 450.1 and 467.1 nm bands in the emission spectrum of the xenon lamp. Also, the emission monochrometer calibration was checked by determining the absorption spectrum of holmium oxide. All band positions were within  $\pm 0.2$  nm of the well known holmium oxide absorption spectrum.

The triplet energy for 2,3-naphtho-20-crown-6 (**1**) requires some comment as to how the value used was derived. It is almost certain that the highest energy band in the phosphorescence spectrum of **1** (472.3 nm) is unresolved (see Figures 20 and 26), as indicated by its width and by comparison to other naphthalene derivatives



and salt/crown complexes. Therefore, using the center of this band would give a low estimate of the triplet energy of this compound. The following scheme was used to get a higher and hopefully more correct estimate of the triplet energy. The unresolved band in the crown spectrum and the "doublet" in the salt/crown spectra were assumed to have the same bandwidth in  $\text{cm}^{-1}$ . The centers of the broad band in the crown spectrum and center of the "doublet" were found making use of their symmetry. The difference, in  $\text{cm}^{-1}$ , between the center of the "doublet" and the position of the higher energy band in the "doublet" was found to be relatively constant for all alkali metal chloride/crown complexes ( $226 \pm 18 \text{ cm}^{-1}$ ). This average energy difference (in  $\text{cm}^{-1}$ ) was added to the position of the center of the broad band in the crown spectrum to obtain an estimate of the position of the "true" 0-0 band.

77 K UV absorption spectra were also determined using a sufficiently expanded wavelength scale (either 3 nm/inch or 6 nm/inch) so that precise frequencies of absorption bands could be obtained. The calibration of the Cary 17 monochrometer was checked by Cary personnel before the beginning and after the end of this investigation and was found to have been unchanged.

#### Quantum Yields

The preparation of samples for quantum yields was the same as for emission spectra. The concentrations were sufficiently low so that the optical density of the solution at the depth at which it

is viewed was  $\leq 0.02$  A, or so that  $\epsilon_1 C_1 = \epsilon_2 C_2$  (where  $\epsilon_1$  is the relative extinction coefficient of solution one and  $C_1$  is its concentration). 77 K UV spectra were the basis for selecting appropriate excitation wavelengths, and the relative extinction coefficients from them were used to either adjust concentrations before making quantum yield comparisons or to correct the apparent relative quantum yields.

There is some difference of opinion as to how low the optical densities should be for the emission output to be a linear function of concentration. One source<sup>91</sup> indicates that it should be 0.02 or less, otherwise a 4% error is incurred, while another source<sup>92</sup> indicates it should be 0.1 or less, otherwise a 1% error is incurred. Except for the quantum yield determinations for the alkali metal complexes of crown  $\lambda$  relative to free crown  $\lambda$  (vide infra), all of the quantum yield determinations reported here satisfy the lower estimate. The optical density for these complexes in the region in which they were excited (approximately 297 nm) is estimated to have been 0.2. The relative emission outputs were corrected making use of the relative extinction coefficients, but these only differ by about 10%, so the difference in optical gradients was probably not very large. Furthermore, a check set of experiments done subsequently in which the complexes and free crown  $\lambda$  were excited in the 313 nm region (the optical density was approximately 0.02 A, and the relative emission outputs were corrected making use of relative extinction coefficients) gave quantum yield estimates which were the same within 3 to 5% to those obtained using higher optical densities.

Quantum yields of naphthalene derivatives  $\lambda$  through  $\eta$  were

determined relative to naphthalene ( $\phi_f = 0.30$ ,  $\phi_p = 0.030$ ). Excitation bandpasses of 1.5 to 2.0 nm were used. The agreement between quantum yields obtained from determinations at different wavelengths (see results section and Table 8) shows that the exciting light was sufficiently monochromatic. Table 44 shows the wavelengths at which the comparisons were made and, in the first set of parentheses, the number of fluorescent quantum yield determinations, and, in the second set of parentheses, the number of phosphorescent quantum yield determinations. Since tailing fluorescence did not interfere, phosphorescent quantum yields were determined without use of a phosphoroscope, since the phosphoroscope introduces approximately a 10-fold attenuation of the signal.

Quantum yields for the crowns in the presence of salts were determined by comparison to the free crown. Table 44 gives the excitation wavelengths used to make quantum yield comparisons between "fully" complexed crowns and the parent free crown. To show that the excitation bandpass was sufficiently monochromatic, comparisons were made using progressively smaller excitation bandpasses until the quantum yields became constant. A 2 nm bandpass was sufficiently monochromatic.

The quantum yields for all naphthalene derivatives and the salt/crown = 5/1 cases were determined using a Hitachi/Perkin-Elmer MPF 44A spectrophotofluorometer with computerized corrected spectra accessory, which was interfaced to a Digital PDP-8 computer. A 1 V corrected signal from the corrected spectrum accessory was collected as a function of time and stored. The monochromator speeds of the

Table 44. Wavelengths (nm) at which Quantum Yield Comparisons Relative to Naphthalene Were Made and Number of Determinations Made for Disubstituted Naphthalenes.

System	$\lambda$ (nm) # of $\phi_f$ det.) (# of $\phi_p$ det.)	
Naphthalene	297.0	285.0 267.3
2,3-Naphtho-20-crown-6 ( $\lambda$ )	298.2 (2) <sup>a</sup> (0) <sup>b</sup>	287.5 (9) (2) 266.0 (4) (2)
2,3-Dimethylnaphthalene ( $\lambda$ )		287.4 (5) (2) 269.1 (4) (3)
2,3-Bis(methoxymethyl)naphthalene ( $\lambda$ )	299.5 (4) (0)	287.5 (4) (2) 266.0 (4) (2)
Naphthalene	297.0	285.0 274.0
1,8-Naphtho-21-Crown-6 ( $\lambda$ )	296.8 (4) (0)	284.5 (2) (4) 274.0 (2) (2)
1,8-Dimethylnaphthalene ( $\lambda$ )	298.2 (4) (6)	286.3 (2) (5) 275.3 (2) (3)
1,8-Bis(methoxymethyl)naphthalene ( $\lambda$ )	296.8 (4) (0)	284.3 (2) (4) 273.6 (2) (2)
Naphthalene	297.0	285.0 276.9
1,5-Naphtho-22-Crown-6 ( $\lambda$ )	296.9 (5) (4)	284.8 (6) (7) 274.0 (5) (6)
1,5-Dimethylnaphthalene ( $\lambda$ )	303.8 <sup>c</sup> (5) (8)	287.0 (9) (8) 275.7 (6) (10)
1,5-Bis(methoxymethyl)naphthalene ( $\lambda$ )	306.9 <sup>d</sup> (4) (4)	285.0 (6) (8) 274. (6) (6)

<sup>a</sup>Number of  $\phi_f$  determinations. <sup>b</sup>Number of  $\phi_p$  determinations. <sup>c</sup>Relative to naphthalene excited at 303.8 nm. <sup>d</sup>Relative to naphthalene excited at 305.9 nm.

Table 45. Wavelengths at Which Quantum Yield Comparisons Relative to Free Crowns Were Made.

Salt	2,3-Cr-6 (1)	1,8-Cr-6 (2)	1,5-Cr-6 (3)
None	305.6	296.9	296.9
NaCl	304.5	297.3	296.7
KCl	304.6	297.1	296.6
RbCl	305.0	297.1	296.4
CsCl	304.9	297.3	296.3
NH <sub>4</sub> Cl	305.2	297.2	296.9
n-PrNH <sub>3</sub> Cl	305.6	297.3	296.9
i-PrNH <sub>3</sub> Cl	305.3	297.2	-----
t-BuNH <sub>3</sub> Cl	305.2	297.3	-----
Br(CH <sub>2</sub> ) <sub>2</sub> NH <sub>3</sub> Cl	305.3	297.2	296.9
Br(CH <sub>2</sub> ) <sub>3</sub> NH <sub>3</sub> Cl	305.6	297.3	296.9
I(CH <sub>2</sub> ) <sub>2</sub> NH <sub>3</sub> Cl	305.6	297.3	296.9
I(CH <sub>2</sub> ) <sub>3</sub> NH <sub>3</sub> Cl	305.6	297.3	296.9
BaBr <sub>2</sub>	304.4	297.3	296.9
AgOSO <sub>2</sub> CF <sub>3</sub>	304.4	297.3	296.9

instrument and the clock in the PDP-8 were well synchronized. Data was sampled 60 times over a 0.5 nm interval, averaged, and placed in an array at a position corresponding to the beginning of the interval. The program provided for control over position of the baseline by allowing one to draw a straight line at any level desired. Wavelength was converted to wavenumber and the area under the curve of spectral intensity versus wavenumber calculated and stored. Areas from different runs could be compared and quantum yields calculated.

#### Titration Monitored by Following Relative Integrated Emission Intensity

The comments made in this section apply to data reported in Figures 55 through 60 and in Tables 9 through 16. Titrations of crowns with salts were monitored by following the relative integrated emission intensities as a function of the mole ratio of added salts. The purpose of these experiments was to establish the mole ratio of salt required for essentially complete complexation of the crown. Emission spectra obtained from these experiments were integrated by the three methods outlined below. As indicated in the results section, some of the integrated intensities obtained from one of the methods were not sufficiently precise to be useful. In these cases, relative peak intensities were used to establish the mole ratio of salt required.

The titration curves shown in Figures 55 through 58 were derived from data obtained using an Aminco-Bowman spectrophotofluorometer. These titrations were followed by comparing emission from free crown

and from crown plus various mole ratios of salt to the emission from naphthalene. The emission curves obtained were corrected for instrument response by applying a set of correction factors derived from a comparison of the observed naphthalene spectrum to a corrected spectrum from the literature. Intensity was converted to a function of frequency ( $\text{cm}^{-1}$ ) rather than of wavelength and the resulting curve integrated. All computations were done by computer.

The remainder of the titrations were done using a Hitachi/Perkin-Elmer MPF-44A spectrophotofluorometer with computerized corrected spectrum accessory. Emission spectra obtained from this instrument can automatically be corrected for instrument response and can be integrated directly after converting the intensity to a function of  $\text{cm}^{-1}$ . One method of doing this involved digitizing the curves as a function of wavelength and submitting the digitized data to a computer to change intensity to a function of  $\text{cm}^{-1}$  and to integrate the resulting curve. This was a time consuming and tedious process, and there was a significant time lag between the time the curves were digitized and when the computational results were available. The results turned out not to be as precise in most cases as the results from the Aminco-Bowman. This does not reflect the difference in instrumentation, but probably the difference in the way in which the curves were digitized. Emission curves from the Aminco-Bowman were digitized by reading intensities at a standard set of wavelengths. This was done so that the intensity matrix would always match the correction factor matrix. This had the disadvantage that maxima did not always fall at one of the wavelengths in the set, but it

had the advantage that each digitized curve had the same number of points. The intensity of the curves from the Hitachi/Perkin-Elmer did not require correction, so it was decided to digitize them by reading intensities and wavelengths at convenient places, i.e., maxima and minima and a sufficient number of other places so that connecting the points by straight lines would reasonably well reproduce the shape of the spectrum. This had the advantage of allowing one to take fewer points to digitize broad characterless spectra. In retrospect, however, this may have been a disadvantage. Thus, for titrations of crowns 1 and 2 with ammonium, alkylammonium, and, for crown 1, that bromoalkylammonium chlorides, relative peak heights as a function of the mole ratio of added salt are reported instead (see results section). This type of data is certainly adequate to establish the mole ratio of salt to crown required for essentially complete complexation, but differences in relative peak heights are not necessarily a linear function (vide infra) of the fraction of complexed crown present.

The second method of digitizing emission spectra from the Hitachi/Perkin-Elmer was via an interfaced Digital PDP-8 computer (vide supra). This is by far the most accurate way to digitize, replot, and integrate these emission curves. It also allows one to obtain good precision, since 1) the results are obtained immediately, and 2) a great many more determinations can be integrated than if the digitizing were to be done manually.

As pointed out in the results section, the integrated intensities obtained from these titration experiments are not true quantum



yields. Provided, however, that 1) the absorbancies are directly proportional to concentrations (Beer's Law); that 2) the optical density is sufficiently low (see note under quantum yield section above) so that the emittancies are directly proportional to concentrations; and that 3) free and 1:1 complexed crown are the only two absorbing and emitting species, then the observed integrated intensities can be reexpressed as a linear combination of the observed intensities of free crown ( $I_{\text{exp,cr}}$ ) and of complexed crown ( $I_{\text{exp,com}}$ ):

$$I_{\text{obs}} = I_{\text{exp,cr}}(\chi_1) + I_{\text{exp,com}}(\chi_2)$$

where  $\chi_1$  is the mole fraction of free crown and  $\chi_2$  is the mole fraction of complexed crown. Then, since  $\chi_1 + \chi_2$  is assumed to be equal to one,

$$I_{\text{obs}} = I_{\text{exp,cr}}(\chi_1) + I_{\text{exp,com}}(1-\chi_1)$$

Thus, for any given value of  $I_{\text{obs}}$ , the fraction of free and of complexed crown can be calculated. If the correct quantum yields of free crown ( $\phi_{\text{cor,cr}}$ ) and of complexed crown ( $\phi_{\text{cor,com}}$ ) are known, then observed integrated intensity can be reexpressed in terms of them:

$$\phi_{\text{cor}} = \phi_{\text{cr,cor}}(\chi_1) + \phi_{\text{com,cor}}(\chi_2).$$

This reexpression of  $I_{\text{obs}}$  in terms of  $\phi_{\text{cor}}$  can be accomplished by

applying the following calculation to each experimental point:

$$\phi_{\text{cor}} = \phi_{\text{ap}} \left[ \chi_1 \frac{\phi_{\text{cr,cor}}}{\phi_{\text{cr,un}}} + (1-\chi_1) \frac{\phi_{\text{com,cor}}}{\phi_{\text{com,un}}} \right]$$

$$\chi_1 = \frac{\phi_{\text{ap}} - \phi_{\text{com,un}}}{\phi_{\text{cr,un}} - \phi_{\text{com,un}}}$$

$$\phi_{\text{ap}} = \frac{I_{\text{obs}}}{I_{\text{exp,cr}}} \cdot \phi_{\text{cr,cor}}$$

$$\phi_{\text{com,un}} = \frac{I_{\text{exp,com}}}{I_{\text{exp,cr}}} \phi_{\text{cr,cor}}$$

The term  $\chi_1(\phi_{\text{cr,cor}}/\phi_{\text{cr,un}})$  allows correction of  $\phi_p$  for a change in the estimate for the correct quantum yield of free crown ( $\phi_{\text{cr,cor}}$ ).  $\phi_{\text{cr,un}}$  is the "uncorrected" or previous estimate of the quantum yield of free crown.  $\phi_{\text{com,cr}}$  is the correct quantum yield for the complexed crown. Its value is determined in a separate set of experiments (vide infra).

This has been done for the titrations of crowns 1, 2, and 3 with alkali metal cations (Figures 55 through 60). As noted in the results section, the only distortion introduced by this manipulation is to make the relative change between the plotted quantum yields of the complex and of the free crown larger or smaller than the relative change in integrated intensities. Qualitatively, however, the relative differences are about the same (within a factor of two).

The remainder of the titration data are presented in Tables 9 through 16. The numbers given in these tables are relative integrated intensities modified only by making them proportional to the quantum yield of free crown. All titrations of crown 1 were done using an excitation wavelength in the 306 nm region. Optical densities of  $1.00 \times 10^{-4}$  M to  $2.00 \times 10^{-4}$  M solutions excited in this region are estimated to be  $\leq 0.02$  A. Most titrations of crowns 2 and 3 were done using an excitation wavelength in the 297 nm region. The optical densities of  $1.00 \times 10^{-4}$  to  $2.00 \times 10^{-4}$  M solutions excited in this region are estimated to be 0.1 to 0.2 A. An optical density of 0.2 A may be too high for a linear dependence of the emittance upon concentration, but see note in the quantum yield section above.

#### Complexation Competition Studies

The analysis of integrated intensities for complexation studies is essentially the same as and makes the same assumptions as the above treatment for titrations. The integrated intensity for a crown complex which has a much different emittance than the free crown is determined ( $I_A$ ). The integrated intensity of a solution with sufficient excess of the salt which causes little change such that the crown is assumed to be fully complexed is also determined ( $I_B$ ). These determinations can be made with somewhat arbitrary choices of instrumental settings (slit widths and excitation wavelengths) provided that they are kept the same for the entire experiment. The salt which causes little change in emittance is used to titrate the complex for which there is a large change. If the species which

causes little change does not complex too much more weakly, then the integrated intensity should change as its concentration is increased. The observed integrated intensity with both salts present should be a linear combination of  $I_A$  and  $I_B$ , given the assumptions made previously and, in this case, assuming that the two complexes are the only absorbing and emitting species present:

$$I_{\text{obs}} = \chi_A I_A + \chi_B I_B$$

where  $\chi_A$  is the mole fraction of complex A and  $\chi_B$  is the mole fraction of complex B. Given that  $\chi_A + \chi_B = 1$ , the fraction of each complex can be calculated. Knowing these and the formal concentrations of crown and salts used, relative equilibrium constants can be calculated. By making an estimate of the equilibrium constant for the complex which shows a large change in emittance based upon its titration curve, one can make an estimate of the equilibrium constant for the other complex and check ones initial guess as to the amount of salt necessary for complete complexation.

#### Variables Affecting Quantum Yield and Integrated Intensity Determinations

The following factors affect values obtained for integrated intensities, and, therefore, quantum yields as well: 1) variations in the mechanical dimensions and in the glass composition of the tubes used; 2) tube positioning in the dewar; 3) concentration errors; 4) lamp stability; 5) errors in the correction factors applied;

6) digitizing procedure used; and 7) emitting impurities. The following factors affect quantum yields but not the relative values of integrated intensities: 1) monochromaticity of exciting light can effect relative intensities if species with different UV absorption curves are compared; and 2) errors in relative extinction coefficients from 77 K UV spectra. Some of these factors have already been discussed. They are listed here for the sake of completeness and will only be alluded to briefly and note given of the location of the previous discussion. There are obviously too many potential sources of error to be able to estimate the precise contribution of each to the total error, but an estimate of the relative importance of each source of error will be made.

The uniformity of the composition of the quartz and pyrex NMR tubes used (see preparation of samples for emission spectra and quantum yield determinations) is not known, since they are not manufactured for their optical properties. The glass used in their manufacture, however, comes from a continuous flow operation, so the composition of a given lot of tubes is not likely to be too different. A large number of NMR tubes were purchased at the same time and reused throughout the project. Variation in the dimensions of the tubes (manufacturer's specifications given previously) are another source of error. In many cases, different tubes of the same solution gave very similar results (1% or less). The largest difference noted which was thought to be due to tube differences was about 5%. All quantum yield determinations, however, involved comparison of at least two tubes of standard to two tubes of unknown, so differences

due to tubes are averaged. Since multiple determinations on the same tube of sample (i.e., thawing and recooling) gave integrated intensities which were very similar, it is not thought that observed variations are very dependent upon either tube positioning in the dewar or to effects of glass inhomogeneity. The finger of the dewar of the Hitachi/Perkin-Elmer is designed to accept a 5 mm tube. With this size tube, there is minimal clearance between the walls of the finger and the sample tube (about 0.5 mm), so the position of the tube is fairly well fixed.

Perhaps the most serious source of error in making quantum yield determinations by the relative method is failure to satisfy the requirement that the solutions compared either absorb the same amount of light or that the difference in the relative amounts of light absorbed be correctable. Errors in concentrations, relative extinction coefficients, or insufficiently monochromatic exciting light can cause this requirement not to be satisfied. Concentration errors alone could account for 1 to 2% relative error. Reasonably concentrated stock solutions were made but, after dilutions, concentrations are estimated to be good to only  $\pm 1\%$ . Relative extinction coefficients are estimated to be good to about 2%. The real problem, though, for compounds which have a lot of fine structure in their absorption spectra, is to excite a compound only in a given absorption peak. While the Hitachi/Perkin-Elmer has continuously adjustable slits, there is a trade off between monochromaticity of exciting light and emission intensity. Furthermore, there is a minimum excitation slit width which can be used when this instrument is used in its ratio mode,

since the sample photomultiplier tube dynode voltage increases as the size of the excitation slits decrease. The minimum slit size is a function of lamp intensity, how well the lamp is focused, and the excitation wavelength used. Usually, 1.5 to 2.0 nm bandpasses can be obtained in the 300 nm region and 2.0 to 2.5 nm bandpasses in the 275 nm region. It is desirable to operate the instrument in its ratio mode for two reasons: 1) better instrument stability and 2) it allows excitation of standard and unknown at somewhat different wavelengths, since, when the excitation monochromator is also calibrated, variation in the intensity of exciting light as a function of wavelength is compensated. While the position of absorption peaks of standard and unknown are similar (see Tables 43 and 44), they are seldom identical. The problem of selectively exciting both unknown and standard is why one attempts to pick out regions of the absorption spectra where both compounds have similar spectral shapes and intensities, with similarity of shape being more important than similarity of intensity. As indicated in the results section, the precision of the quantum yield comparisons between naphthalene and disubstituted naphthalenes is sufficiently good (2 to 10%) to indicate that these determinations satisfy the above requirement. The quantum yield comparisons between free and complexed crowns were made using only one set of excitation wavelengths. To show that the excitation bandpass was sufficiently monochromatic, comparisons were made using progressively smaller excitation bandpasses until the quantum yields became constant. A 2 nm bandpass was found to be sufficiently monochromatic in all cases. As remarked in the results section, quantum

yield comparisons between complexed and free crowns are probably more accurate in general than those between naphthalene and naphthalene derivatives because the 77 K UV absorption spectra are more similar in the former comparison.

Variation in lamp intensity is another source of error, since relative quantum yield determinations require that both standard and unknown receive the same light flux. This assumption is checked experimentally by always making at least two quantum yield comparisons. If the results of both comparisons are the same, it can reasonably be assumed that both standard and unknown received the same light flux. When the Hitachi/Perkin-Elmer is used in its ratio mode, there is about a 2% drift in overall instrument stability per hour. This drift is about 2% per 10 min in its energy mode. In either mode, however, there can be occasional sudden jumps of 10 to 20% in relative emission intensity due to shifting of the position of the lamp arc. Since all quantum yield comparisons were made in the instruments ratio mode and required only about 10 min per comparison, normal drift should not be a serious contributor to the overall error. Sudden large changes in lamp intensity are not a source of error, since they are safeguarded against by multiple determinations.

Errors in the correction factors applied to emission curves can affect the accuracy of the relative quantum yields. This will be the case if the compounds compared have different spectral distributions. If the standard, say, has much more intensity in one region than the unknown, and if the correction factors are also larger than they should be in this region, then the quantum yield of the unknown



will be smaller than it should be. The difference in spectral distribution between compounds whose emission quantum yields have been compared are not great, and errors in correction factors generated by the Hitachi/Perkin-Elmer are not thought to be large (perhaps  $\pm 2\%$ ). So this is not thought to be an appreciable source of error. Note that relative quantum yields can be obtained from relative peak heights if spectral shapes are the same.

The accuracy of quantum yield comparisons obviously depends upon the accuracy with which emission curves are digitized, corrected, and integrated. See the discussion under the section on titrations above.

Impurities which emit in the same spectral region are another source of error. See sections on reagent purity and sample preparation. Absorbing impurities which do not interact with the compounds investigated will not interfere unless they are present in sufficient concentrations to compete for exciting light. Impurities which quench excited states can be another source of error, but these determinations are all made in alcoholic glasses, which have very high viscosities ( $1 \times 10^{13}$  poise for 95% ethanol glass),<sup>93</sup> so this is probably not a source of error.

### Fluorescent and Phosphorescent Lifetimes

Fluorescent lifetimes at 77 K were determined using the single photon counting technique. The decay curves were determined on an instrument similar to that developed and described by Ware.<sup>71</sup>

Sample preparation, including degassing, was the same as for emission

spectra and quantum yield determinations. It was initially thought to be necessary to use square cells to minimize scattered light. The glasses formed frequently crack, however, and cracked glasses act as excellent scatterers. It appears that in many cases determinations may be done in round cells (the same lifetime estimate,  $\pm 1\%$ , was obtained for crown 1 in round and square cells). The square cells ( $1.0 \text{ cm}^2$ ) were made from fluorescence free suprasil quartz fused to a tee which had a round ball for degassing purposes on one side and a 10/30 male joint on the other side.

The fluorescence lifetimes of all alkali metal complexes of crowns 1 and 2 were determined in square cells. Most of the other lifetimes were determined in round (approximately 1 to 1.4 cm internal diameter) commercial grade quartz tubes. Aside from being cheaper and simpler to fabricate, solutions could be degassed directly in these cells and were less prone to breakage when the solvent glass cracked (square cells frequently break when the solvent glass cracks). It was hoped that uncracked glasses could be obtained in the round cells, since scattered light does turn out to be a problem. It was known that uncracked glasses could consistently be obtained in the large diameter tubes used for determination 77 K UV absorption spectra (vide supra) provided that at least 20% by volume of methanol was added. Note that the reason for using large diameter sample cells had to do with 1) the large amount of scattered light obtained from smaller tubes and 2) the problem of positioning the sample tube in the paths of the exciting light and of the emission monochromator (located at  $90^\circ$  to each other), since the instrument used

did not provide for a means of doing this reproducibly.

A quartz dewar which had flat faces oriented at  $180^\circ$  to each other was used. Excitation was through the flat side. The exciting light was filtered using a 275 nm interference filter. The emission monochromator was set at whichever wavelength which minimized scattered light and maximized fluorescence decay (usually 350 nm). The side of the cell facing the exciting light was covered with a piece of cardboard with a 2 to 3 cm slit cut in the center and which extended past the edges of the cell to eliminate scattering of exciting light from the face and corners of the cell.

Concentrations were in the  $10^{-4}$  M range. See Tables 8, 20 through 25, 30, 31 and 32 in the results section for the formal concentration and glass composition used in each case. Different solvent systems were tried with the hope of finding one which would consistently give uncracked glasses under the experimental conditions. For determination of 77 K UV absorption spectra, uncracked glasses could be consistently obtained using 95% ethanol-methanol (4:1, v/v) in a 1.4 cm round quartz tube. It is somewhat puzzling why the same solvent system did not consistently give uncracked glasses in the similar size tubes used for the lifetime determinations. Cracking is not a function of the sample, since the same sample may form a cracked glass in one cell and an uncracked glass in another. Apparently, surface imperfections in the quartz or a particle of dust can cause these glasses to crack. Later experiments did seem to indicate that ethanol-methanol (4:1, v/v) gave fewer cracked glasses. This glass is known to be especially stable compared to other alcohol glasses.<sup>94</sup> It is not thought that these different

glass compositions should affect photophysical processes in a significantly different fashion.<sup>9</sup> The same estimate ( $\pm 1\%$ ) for the fluorescence lifetime of crown  $\lambda$  was obtained from both 95% ethanol and 95% ethanol-methanol (4:1, v/v) glasses. Also, the same estimate ( $\pm 1\%$ ) was obtained for crown  $\lambda$  plus a 5-fold excess of sodium chloride in these two glasses. Estimates of  $43.9 \pm 0.2$  and  $49.5 \pm 0.4$  were obtained for the fluorescence lifetime of crown  $\lambda$  in 95% ethanol and in 95% ethanol-methanol glasses, respectively. Estimates of  $93.6 \pm 0.1$  and  $85.6 \pm 0.1$  nsec were obtained for crown  $\lambda$  in 95% ethanol and in ethanol-methanol (4:1, v/v) glasses, respectively. The differences in these later two comparisons are larger than those for the first two comparisons, but the differences are still small enough to be considered within experimental error (vide infra).

Cracked glasses are a problem because they scatter light. Scattered light is a problem because, when scattered light from the lamp decay is present in the decay curve, the decay curve cannot be deconvoluted for the effects of the buildup (about 1 to 2 nsec) and decay (lifetime of 2 to 3 nsec) of the lamp flash. Given a better monochromator, scattered light from the lamp decay could be eliminated, but the intensity of the fluorescence decay would also be diminished. Lifetimes whose determinations were attempted were sufficiently long that the problem could be dealt with by ignoring the first part of the decay curve (30 channels spanning 71.34 nsec which contained the lamp buildup and decay) and analyzing the remainder of the decay curve (98 channels spanning 321.24 nsec). The lamp flash occurred at about channel 13 so about 40 nsec of

actual decay were neglected. (See results section and below for methods of analysis.) Cracked and uncracked glasses of crown 1 analyzed by neglecting the first 30 channels gave the same fluorescence lifetime estimate ( $\pm 2\%$ ).

Although several lifetimes were included in the analyses, lack of knowledge about the first part of the decay places limitations on detection of fast decay and constraints on interpretation of slower decays which appear to give good single exponential analyses. It could always be argued that species with lifetimes short enough to have already decayed to a large extent in 40 nsec would be completely missed by a double exponential analysis and a single exponential analysis would appear to give a good analysis of the decay. It is not thought that this is very much of a problem for compounds and complexes which give good fluorescence and phosphorescence single exponential decay, though it is not necessarily the case that fluorescent and phosphorescent states should be affected by perturbing species in the same way. The bromoalkylammonium complexes of crown 1 appear to give at least double exponential phosphorescence decay and, probably, at least double exponential fluorescence decay. For crown 2, however, the bromoalkylammonium complexes give at least double exponential phosphorescence decay, but the best analysis of the fluorescence decays is from a single exponential treatment (see results section and Tables 30 and 31). This difference in the character of the fluorescence and phosphorescence decays of these complexes, unfortunately, is open to either experimental or theoretical interpretation.

Phosphorescence lifetimes at 77 K in uncracked 95% ethanol glass were determined using an Aminco-Bowman spectrophotofluorometer equipped with phosphorescope and solenoid operated shutter (1 msec closing time) positioned in the path of the exciting light inside the sample compartment. For long lifetimes (longer than about 1 sec) the unfiltered amplified signal was recorded on a Linear Instrument Model 261 recorder running at the rate of 16.00 inches/min (rate calibration checked). Shorter lifetimes were obtained using a Techtronics Model storage type oscilloscope. 3-1/4" x 4-1/4" polaroid photographs of the oscilloscope trace were photographically enlarged to about 5" x 6-1/2" before they were digitized (vide infra). The determinations were made using the same sample tubes as used for quantum yield and spectral determinations. In general, decay was observed at whatever wavelength maximum emission occurred, generally around 500 to 515 nm. The emission was very poorly resolved, since close to maximum slit widths had to be used to get a sufficiently strong, relatively noise free signal at low amplifications. One study for the potassium and cesium chloride complexes of crown  $\lambda$  in which the decay was observed at three widely spaced wavelengths (470, 500, and 550 nm) gave essentially identical decay rates at all wavelengths.

Both fluorescence and phosphorescence decays were analyzed using a curve fitting program called KINFIT (see results section and below). The single exponential fits used the two parameter equation  $I = I_0 e^{-kt}$  where  $I$  is the intensity at time  $t$ ,  $I_0$ , the initial intensity, and  $k$ , the decay rate constant, are the two parameters

which the program attempts to fit to the experimental time versus intensity measurements. The value of  $I_0$ , although experimentally known, is allowed to float, otherwise its experimental error could bias the way the rest of the curve is fitted. For good single exponential fits, there was good agreement between the calculated and observed values of  $I_0$ . For decays which gave good double exponential fits (vide infra), however, single exponential analyses of the same decays gave calculated values of  $I_0$  which were much lower than the observed values.

Double exponential fits for phosphorescence decays used the four parameter equation

$$I = u_1 e^{-k_1(u_2+t)} + (I_0 - u_1) e^{-k_2(u_2+t)}$$

$I$  is the intensity at time  $t$ . The parameters fitted are  $u_1$ ,  $u_2$ ,  $k_1$ , and  $k_2$ .  $k_1$  is the decay rate constant for the faster decay and  $k_2$  that for the slower decay.  $I_0$ , in this case, is treated as a constant, and is the intensity before the shutter is closed.  $u_1$  is the preexponential weighting factor for the faster decay, and  $(I_0 - u_1)$  that for the slower decay.  $u_2$  is the time elapsed between the time the shutter is closed and when the first data point is taken. The form of this equation is partially a function of the way the decay curves were digitized. For decay curves obtained using a recorder, approximately the first 20 to 25% of the decay was ignored. The reason for doing so was that there were frequently bumps in this part of the decay curve due to disturbance of the liquid nitrogen

and of the sample tube by the closing of the solenoid operated shutter, which closes with considerable force. The reason for using the intensity before closing the shutter for  $I_0$  is so that the fit gives proper recognition to the contribution of a faster decay to the total decay. Thus, even if, say, 30% of the species with shorter lifetime has decayed by the time the first data is taken, the fit will recognize that this point is lower in intensity than it should be compared to an essentially single exponential curve for the later decay. The curve, then, is fit as though the entire curve from  $t = 0$  is represented. Since the first data point is not taken at  $t = 0$ , either an experimental estimate of the time at which the first point is taken,  $u_2$  has to be made or it has to be treated as a parameter. It was decided to treat  $u_2$  as a parameter so that an error in an experimental estimate would not prejudice the rest of the fit. Calculated estimates of  $u_2$  were close to experimental estimates and the values of  $u_2$  correlated with the value of the faster decay rate constant: the faster the decay, the smaller  $u_2$ . Error estimates (linear estimates of the standard deviation; see results) for  $u_2$  for good double exponential fits were reasonable (5 to 10%).

All decay curves obtained using a recorder were digitized in the same fashion. A standard set of 40 points were taken, 30 (at equally spaced intensity intervals) over the first 85% of the decay and 10 (at equally spaced intensity intervals) over the last 15% of the decay. The number of points taken and where they are taken has some influence on the fit, since KINFIT tends to weight values more heavily in regions in which a function is changing slowly than in



regions where the function is changing rapidly, unless the error estimates for the region in which the function is changing rapidly are small.

The photographed decay curves from the oscilloscope were not all of the same size, and, therefore, couldn't all be digitized using the same standard set of points. They were digitized taking from 28 to 52 points at intensity intervals roughly similar to those of the standard set of 40; i.e., proportionately the same number of points were taken over the initial and later parts of the decay. The initial intensity was lower in some cases for some of the later obtained data (decays for the iodoalkylammonium complexes of crowns 1 and 3 and silver triflate complex of crown 3), since the storage function on the oscilloscope wasn't working and the intensity of light seen by the film was a function of how fast the signal was changing. This is unfortunate, since information about the early part of the decay is lost. The analyses based on fewer points didn't appear to be significantly inferior to those based on a larger number. Decay curves for crown 3 obtained using a recorded (40 points) and using an oscilloscope (52 points) gave very similar lifetime estimates (2.23 versus 2.20 sec, respectively). Better results could be obtained by determining several decay curves spanning different portions of the decay instead of just one curve spanning the entire decay. The data available, however, is believed to be sufficiently good for the purpose of identifying trends in a large body of data.

Double exponential analysis of fluorescence decay used a somewhat

different equation than that used for phosphorescence decays, since the initial intensity without the effect of the lamp decay is not known:

$$I = u_1 e^{-k_1 t} + u_2 e^{-k_2 t}$$

$I$  is the intensity (number of counts) in time interval including  $t$ .  $u_1$ ,  $u_2$ ,  $k_1$ , and  $k_2$  are the parameters.  $u_1$  and  $u_2$  are preexponential weighting factors and  $k_1$  and  $k_2$  are the rate constants.

Single photon counting, as the name suggests, is statistical in nature. The number of photons counted in a given time interval is placed in a given channel corresponding to this time interval. Thus, the error in the time is one-half the channel width. In most cases, 2.378 n/channel were used. The number of counts in a given channel is also a matter of statistics. The estimated error, from observed scatter, is about 10% of the counts recorded. Initial counts of  $1 \times 10^4$  to  $1 \times 10^5$  at channel 30, the channel at which data analysis was begun, were typical. Counts of  $1 \times 10^2$  to  $1 \times 10^3$  at channel 128 were typical. The quality of the decay curve is affected both by how strongly the sample emits and by how long counts are collected. For highly emissive samples (quantum yield of 0.2 to 0.3), 20 to 30 min was sufficient to build up a well defined decay curve, as determined by inspection of the oscilloscope logarithmic plot of the number of counts versus time. Less highly emissive samples required one to two hours. Decay curves could not be obtained for complexes with fluorescence quantum yields much less than 0.04

( $\tau_f$  couldn't be obtained for rubidium chloride complex of crown 3,  $\phi_f \approx 0.02$ ).

Due to their statistical nature, decay curves obtained from the single photon counting method are not as smooth as the decay curves obtained using a recorder or an oscilloscope. Thus, while error estimates for phosphorescence lifetimes (single exponential analysis) of naphthalene derivatives and crown complexes are about 0.3 and 1%, respectively, a 1% error estimate is typical for fluorescence lifetimes (single exponential analysis) of both naphthalene derivatives and complexes.

## Synthesis

### Synthesis of 2,3-Naphtho-20-crown-6 (1)

2,3-Bis-(hydroxymethyl)naphthalene (4.00 g, 21.28 mmol) was dissolved in 600 mL of dry tetrahydrofuran and 60 mL of sieve dried dimethylformamide and stirred at room temperature under a nitrogen flow for 45 min before the addition of 4.87 g (43.4 mmol) of potassium t-butoxide. The resulting white slurry was stirred for 20 min before the addition (all at once) of 100 mL of dry tetrahydrofuran containing 11.52 g (21.28 mmol) of pentaethylene glycol ditosylate (the solution of ditosylate had been under flowing nitrogen for one h before its addition). The reaction slurry was stirred 12 h (over night) and then suction filtered through celite. The celite and potassium tosylate on the filter were washed with dichloromethane. The filtrate was concentrated on a rotary evaporator using an

aspirator and finally an oil pump to remove dimethylformamide. The 9.5 g of light orange-brown oil was chromatographed on a column containing 600 g of 80-200 mesh alumina (Fisher). After initial elution with 0.5 L of dichloromethane, 0.5% methanol in dichloromethane was used. Fractions (21 mL) 183 through 233 contained a yellow oil which gave, after repeated recrystallization from ether-pentane, 0.96 g (11.5%) of 1 with mp 58-59.5°C. Spectral data were: NMR (CDCl<sub>3</sub>)  $\delta$  3.63 (9 H, s), 3.70 (11 H, s), 4.78 (4 H, s), 7.2-7.7 (6 H, m); IR (CHCl<sub>3</sub>) 3010 (m), 1600 (w), 1250 (m), 1120 (s), 1035 (w), 963 (w), and 900 cm<sup>-1</sup> (s); UV (95% EtOH)  $\lambda(\epsilon)$ , 321.0 (273), 313.5 (273), 306.5 (366), 285 sh (33226), 275.5 (5012), 266.5 (4900), 260 sh (4048), 228 (192876), and 223 sh (8604) nm; mass spectrum (70 eV) m/e (rel intensity) 390 (3), 170 (24), 169 (24), 168 (22), 155 (66), 154 (94), 153 (39), 152 (17), 133 (46), 128 (12), 89 (100), 77 (43), 59 (22), 45 (65). This product was further purified by repeated recrystallization to give material (58.5-59.0) suitable for spectral work.

Anal. Calcd for C<sub>22</sub>H<sub>30</sub>O<sub>6</sub>: C, 67.67; H, 7.74. Found: C, 67.67; H, 7.89.

#### Synthesis of 1,8-Naphtho-21-crown-6 (2)

In a procedure like that described for the synthesis of 1, 1,8-bis-(hydroxymethyl)naphthalene (2.00 g, 10.64 mmol), plus 2.44 g (21.7 mmol) of potassium t-butoxide was reacted with 5.82 g (10.64 mmol) of pentaethylene glycol ditosylate to give 0.345 g (8.3%) of 2 (mp 53-54.5°C) after alumina chromatography and repeated

recrystallization. Spectral data were: NMR ( $\text{CDCl}_3$ )  $\delta$  3.62 (12 H, s), 3.70 (8 H, s), 5.07 (4 H, s), 7.15–7.8 (6 H, m); IR ( $\text{CHCl}_3$ ) 3050 (w), 1125 (s), 1909 (s), 840 (m), and  $820\text{ cm}^{-1}$  (m); UV (95% EtOH)  $\lambda(\epsilon)$ , 318 sh (235), 315 (466), 295.4 (5393), 824.2 (7746), 275.3 (6397), 265 sh (3998), 255 sh (1936), 227.0 (75587), 223 sh (57471), and 213 sh (24988) nm; mass spectrum (70 eV) m/e (rel intensity) 390 (.5), 182 (.7), 169 (13), 154 (10), 153 (47), 152 (100), 141 (11), 133 (3), 115 (3), 89 (14), 77 (6), 59 (4).

Anal. Calcd for  $\text{C}_{22}\text{H}_{30}\text{O}_6$ : C, 67.67; H, 7.74. Found: C, 67.77; H, 7.79.

#### Synthesis of 2,3-Bis-(methoxymethyl)naphthalene (5)

2,3-Bis-(hydroxymethyl)naphthalene (2.00 g, 10.6 mmol) in 80 mL of dry tetrahydrofuran was added all at once to 100 mL of a tetrahydrofuran suspension of 22.4 mmol of sodium hydride which had been washed free of oil (1.03 g of 50% dispersion used) by pentane and tetrahydrofuran and stirred under a nitrogen flow for ten min. The resulting white suspension was stirred for 0.5 h before the addition of methyl iodide (14.4 g, 100 mmol) in 100 mL tetrahydrofuran. The mixture was stirred for 12 h at a room temperature under a nitrogen atmosphere. After distillation to remove excess methyl iodide ( $\sim$ 50 mL of distillate), the reaction mixture was cooled to room temperature and absolute ethanol added under a nitrogen flow. This mixture was rotary evaporated at reduced pressure and the residue taken up in 200 mL of dichloromethane. The dichloromethane solution was washed with water (3 x 100 mL) and saturated sodium chloride

(1 x 100 mL), dried ( $\text{MgSO}_4$ ), filtered, and rotary evaporated at reduced pressure to give 2.27 g (99% yield) of 5 as a yellow oil which was pure by NMR analysis. This oil was chromatographed on 100 g of neutral alumina (Fisher), and a center cut (1.75 g) of the only band eluted by dichloromethane rechromatographed. The later fractions of this second chromatography gave colorless 5. Molecular distillation ( $55^\circ\text{C}$ , 0.05 mm) produced a clear, colorless oil which gave the following spectral data: NMR ( $\text{CDCl}_3$ )  $\delta$  3.24 (6 H, s), 4.43 (4 H, s), 7.2-7.8 (6 H, m); IR (neat) 3069 (m), 1603 (m), 1196 (vs), 1107 (s), 1074 (s), 887 (s), and  $755\text{ cm}^{-1}$  (s); UV (95% EtOH)  $\lambda(\epsilon)$ , 320.8 (260), 313.8 (261), 306.5 (340), 284.8 sh (3097), 275.3 (4745), 265.9 (4583), 260 sh (3746), 252.3 sh (3746), 227.1 (132000), and 221.8 sh (89910) nm; mass spectrum (70 eV) m/e (rel intensity) 216 (11), 185 (18), 184 (100), 183 (23), 169 (76), 155 (78), 141 (88), 128 (16), 115 (45).

Anal. Calcd for  $\text{C}_{14}\text{H}_{16}\text{O}_2$ : C, 77.45; H, 7.46. Found: C, 77.23; H, 7.42.

#### Synthesis of 1,8-Bis-(methoxymethyl)naphthalene (6)

In a procedure like that used for 5, a suspension of 1,8-bis-(hydroxymethyl)naphthalene (2.00 g, 10.6 mmol) and sodium hydride (1.03 g of 50% oil dispersion, 22.4 mmol) was reacted with methyl iodide (14.4 g, 100 mmol). Crystallization proceeded spontaneously upon removal of the dichloromethane during the workup to give 2.4 g of yellow crystals. This crude product was recrystallized once from

pentane to give 1.95 g of 6 (86%, crude yield). This material was recrystallized four additional times to give material suitable for spectral work, mp 59.5–60.0°C. Spectral data were: NMR (CCl<sub>4</sub>)  $\delta$  3.21 (6 H, s), 4.81 (4 H, s), 7.1–7.7 (6 H, m); IR (nujol, fluorolube mulls) 3055 (w), 1175 (s), 1120 (m), 1075 (s), 893 (m), 842 (m), 805 (s), 775 (s), and 687 (m) cm<sup>-1</sup>; UV (95% EtOH)  $\lambda(\epsilon)$ , 318.2 (230), 314.6 (430), 294.8 (5463), 283.9 (7850), 274.4 (6538), 266 sh (4288), 226.3 (83500), 222 sh (63750), and 211 sh (25000) nm; mass spectrum (70 eV) m/e (rel intensity) 216 (9.2), 185 (18).

#### 1,5-Naphtho-22-Crown-6 (3)

A solution of pentaethylene glycol (2.39 g, 10 mmol) and 1,5-bis-(bromomethyl)naphthalene (3.14 g, 10 mmol) in 150 mL dry tetrahydrofuran was added dropwise to a refluxing tetrahydrofuran slurry (500 mL) of potassium t-butoxide (2.36 g, 21 mmol) over a 6 h period under a dry nitrogen atmosphere. The slurry was stirred at reflux another 4 h before filtration and subsequent washing of the filter cake with tetrahydrofuran. Solvent was removed from the filtrate under vacuum, and the resulting yellow oil chromatographed on alumina in a quartz column (400 g Fisher alumina with LUMILUX added) and eluted with dichloromethane-methanol (200:1). The first band which was observable on the column using a 375 nm lamp gave a yellow-brown oil. Some fractions of this band crystallized from ether-pentane. After repeated recrystallizations from ether-pentane, 0.54 g (14.2%) of 3 were obtained, mp 55.5–57.0°C. Spectral data were: NMR (CDCl<sub>3</sub>)  $\delta$  3.10 (4 H, s), 3.25 (8 H, s), 3.53 (8 H, s), 4.92 (4 H, s), 7.37

(4 H, m), 8.00 (2 H, m); IR ( $\text{CHCl}_3$ ) 2975 (m), 2942 (s), 2898 (s), 2865 (s), 1502 (m), 1407 (m), 1291 (m), 1176 (s), 1110 (m), 1036 (m), 826 (m); UV (95% EtOH)  $\lambda(\epsilon)$ , 318.1 (275), 314.6 (475), 296.3 (6030), 284.4 (8300), 274.7 (6680), 266.7 sh (4300) 259 sh (2250), 228.1 (78500) 210.6 sh (26000); mass spectrum (70 eV) m/e (rel. intensity) 390 (53), 174 (4), 169 (19), 155 (43), 154 (100), 153 (35), 141 (23), 133 (36), 105 (15), 89 (71).

Anal. Calcd for  $\text{C}_{22}\text{H}_{30}\text{O}_6$ : C, 67.67; H, 7.74. Found: C, 67.77; H, 7.79.

1,5-Bis-(methoxymethyl)naphthalene (8)

1,5-Bis-(bromomethyl)naphthalene (1.38 g, 4.39 mmol) was added in one portion to 250 mL of a methanol solution of sodium methoxide (2.85 g, 52.7 mmol) which had been prepared under a nitrogen flow. The resulting mixture was stirred under a nitrogen flow for another 15 min before heating was commenced. After 24 h at reflux, the mixture was allowed to cool to room temperature before pouring into 500 mL of ice-water, followed by careful neutralization with concentrated hydrochloric acid. The white precipitate which formed upon pouring into the ice water was removed by vacuum filtration and washed carefully with water. After prolonged air drying, 0.33 g (35%), mp  $60-61^\circ\text{C}$ , of white solid was obtained. After repeated recrystallization from pentane, white crystals of 8, mp  $62-63^\circ\text{C}$ , were obtained. Spectral data were: NMR ( $\text{CDCl}_3$ )  $\delta$  3.37 (6 H, s), 4.80 (4 H, s), 7.33 (4 H, m), 7.90 (2 H, m); IR ( $\text{CHCl}_3$ ) 3025 (m), 2900 (s), 2925 (s), 2875 (s), 2825 (s), 1500 (w), 1450 (m), 1375 (m), 1175 (m), 1085 (vs),



950 (m), 920 (m); UV (95% EtOH)  $\lambda(\epsilon)$  318.6 (285), 314.8 (500), 295.5 (6250), 284.7 (8650), 274.6 (6888), 268 sh (4225), 227.1 (78880), 223.1 (62130); mass spectrum (70 eV) m/e (rel. intensity) 216 (100.0), 201 (4), 185 (35), 184 (30), 171 (24), 169 (48), 156 (76), 155 (26), 154 (30), 141 (49), 128 (14), 115 (22).

Anal. Calcd for  $C_{14}H_{16}O_2$ : C, 77.45; H, 7.46. Found: C, 77.60; H, 7.40.

#### Preparation of Haloalkylammonium Chlorides

Haloalkylammonium chloride salts, except for 3-iodopropylammonium chloride, were prepared from either the bromide or iodide salt via ion exchange according to the following general procedure.

New Dowex 21 K resin was conditioned by first washing with water, then with methanol-water (1:1), then methanol, then methanol-water (1:1), then water, then 10% hydrochloric acid, and finally with water until neutral.

An aqueous solution of the bromide or iodide salt (25 mmol) was passed through 200 g of conditioned Dowex 21 K resin (estimated 5 mequiv. chloride per gram resin) packed in water in a 1-1/2" column. Development of the column was followed by checking the eluate for chloride by treating with 5% aqueous silver nitrate. Water was removed under reduced pressure at less than 40°C using a rotary evaporator. Absolute alcohol was added after most of the water had been removed to facilitate removal of the remaining water. The solid which precipitated as the solvent was removed was purified by

recrystallization as indicated in the reagent purification section. Spectral properties of the prepared salts are given below.

2-Bromoethylammonium Chloride - Prepared by above procedure from the bromide (from Aldrich, mp 172-174°C). Mp of chloride salt is 130-132°C. NMR (DMSO-d<sub>6</sub>): δ 3.2 (2 H, t), 3.7 (2 H, t), 8.2 (3 H, br s).

Anal. Calcd for C<sub>2</sub>H<sub>7</sub>NBrCl: C, 14.97; H, 4.40; Cl, 22.10; Br, 49.80. Found: C, 14.84, H, 4.13; Cl, 20.37; Br, 53.11.

NMR (DMSO-d<sub>6</sub>) of 2-chloroethylammonium chloride (from Aldrich, mp 143-146°C): δ 3.2 (2 H, t), 3.9 (2 H, t), 8.5 (3 H, br s).

3-Bromopropylammonium Chloride - Prepared by the above procedure from the bromide (from Aldrich, mp, 171-172°C). Mp of chloride salt is 152-153°C. NMR (DMSO-d<sub>6</sub>): δ 2.2 (2 H, qt), 3.1 (2 H, br t), 3.6 (2 H, t), 8.0 (3 H, br s).

2-Iodoethylammonium Chloride - Prepared from the iodide by the above procedure. The iodide salt was prepared from 2-ethanolamine according to the procedure of Billimoria and Lewis. Mp of the chloride salt is 151.5-154.0°C. Spectral data were: NMR (DMSO-d<sub>6</sub>) δ 3.2 (3 H, m), 3.9 (1 H, br t), 8.1 (3 H, br s); mass spectrum (70 eV), highest m/e at 171, M-HCl.

3-Iodopropylammonium Chloride - 3-Bromopropylammonium bromide (5.00 g, 24.4 mmol) was added to sodium iodide (40 g, 266 mmol) dissolved in 100 mL of acetone. The resulting suspension was stirred

at room temperature for three days, after which the mixture was poured into 500 mL ice/water in contact with 500 mL dichloromethane. The aqueous layer was neutralized with 15% sodium hydroxide and extracted several additional times with dichloromethane. The dichloromethane extract was washed, first with water, then with saturated sodium chloride, and dried by gravity filtration through anhydrous sodium sulfate. Dry hydrochloric acid (Matheson, technical grade) was passed through the dried dichloromethane extract, and the white solid which precipitated removed by vacuum filtration and washed thoroughly with dichloromethane. The mp after recrystallization (see reagent purity section) was 100-101°C. Spectral data were: NMR (DMSO- $d_6$ )  $\delta$  2.0 (2 H, br t), 3.2 (2 H, br s), 3.7 (2 H, t), 7.9 (3 H, br s); mass spectrum (70 e/v), highest m/e at 185, M-HCl.

## REFERENCES

## REFERENCES

1. The following texts may be consulted for general considerations of excited state processes: (a) J. G. Calvert and J. N. Pitts, "Photochemistry", John Wiley and Sons, New York, NY, 1966; (b) J. A. Barltrop and J. D. Coyle, "Excited States in Organic Chemistry", John Wiley and Sons, New York, NY, 1975; (c). S. P. McGlynn, T. Azumi, and M. Kinoshita, "Molecular Spectroscopy of the Triplet State", Prentice-Hall, Englewood Cliffs, NJ, 1969; (d) N. J. Turro, "Molecular Photochemistry", W. A. Benjamin, New York, NY, 1967.
2. A. R. Horrocks and F. Wilkinson, Proc. Roy. Soc. A, 306, 257 (1968).
3. M. Kasha, Discussions Faraday Soc., 9, 14 (1950).
4. A. A. Lamola and G. S. Hammond, J. Chem. Phys., 43, 2129 (1965).
5. V. L. Ermolaev, Soviet Phys. Doklady (Engl. Transl.), 6, 600 (1962).
6. T. D. Gierke, R. J. Watts, and S. J. Strickler, J. Chem. Phys., 50, 5425 (1969).
7. J. C. Miller, J. S. Meek, and S. J. Strickler, J. Am. Chem. Soc., 99, 8175 (1977).
8. R. P. Frosch and G. W. Robinson, J. Chem. Phys., 33, 934 (1960).
9. D. S. McClure, J. Chem. Phys., 17, 905 (1948).
10. (a) S. F. Fischer, A. L. Stanford and E. C. Lim, J. Chem. Phys., 61, 582 (1974);  
(b) H. Gatterman and M. Stockburger, J. Chem. Phys., 63, 4541 (1975).
11. For papers on differences between gas phase and solution spectra see: (a) N. S. Bayliss and L. Hulme, Austr. J. Chem., 6, 257 (1953); (b) N. S. Bayliss and E. G. McRae, J. Phys. Chem., 58, 1002 (1954); (c) E. G. McRae, J. Phys. Chem., 61, 562 (1956); and (d) H. C. Longuett-Higgins and J. A. Pople, J. Chem. Phys., 27, 192 (1957).
12. For a review of environmental effects on fluorescence of organic compounds in solution see B. L. Van Duuren, Chem. Rev., 63, 325 (1963).

13. S. P. McGlynn, M. J. Reynolds, G. W. Daigre, and N. D. Christodoyeas, J. Phys. Chem., 66, 2499 (1962).
14. G. G. Giachino and D. R. Kearns, J. Chem. Phys., 52, 2964 (1970).
15. (a) S. P. McGlynn, J. Daigre, and F. J. Smith, J. Chem. Phys., 39, 675 (1963); (b) S. Siegel and H. S. Judeikis, J. Chem. Phys., 43, 3060 (1965).
16. (a) G. W. Robinson, J. Mol. Spectroscopy, 6, 58 (1961); (b) E. C. Lim, J. Chem. Phys., 36, 3497 (1962); (c) A. Grabowska, Spectrochim. Acta., 19, 307 (1963).
17. Y-P Hsu and P. M. Johnson, J. Chem. Phys., 59, 136 (1971).
18. R. Sahai, R. H. Hofeldt, S. H. Lin, Trans. Faraday Soc., 67, 1690 (1971).
19. L. K. Patterson and S. J. Rzad, Chem. Phys. Lett., 31, 254 (1975).
20. C. Steel and H. Linschitz, J. Phys. Chem., 66, 2577 (1962).
21. (a) S. J. Formosinho, Mol. Photochem., 7, 13 (1976); (b) G. Porter and M. R. Wright, Discuss. Faraday Soc., 27, 18 (1959); (c) J. Nag-Chaudhuri, L. Stoessell, and S. P. McGlynn, J. Chem. Phys., 38, 2027 (1963).
22. (a) H. Tsubomura and R. S. Mulliken, J. Am. Chem. Soc., 82, 5966 (1960); (b) G. J. Hoijtink, Mol. Phys., 3, 67 (1960); (c) D. F. Evans, Nature (London), 178, 534 (1956); (d) D. F. Evans, J. Chem. Soc., 1351 and 3885 (1957).
23. P. Yuster and S. I. Weissman, J. Chem. Phys., 17, 1182 (1949).
24. C. J. Marzzacco, J. Phys. Chem., 79, 1706 (1975).
25. P-S. Song, Q. Chae, M. Fujita, and H. Baba, J. Am. Chem. Soc., 98, 819 (1976).
26. (a) F. R. Hopf and D. G. Whitten, "Photochemistry of Porphyrins and Metalloporphyrins", in "Porphyrins and Metalloporphyrins", ed. by K. M. Smith, Elsevier Scientific Publishing Company, New York, NY, 1975; (b) M. Gouterman, "Volume III. Physical Chemistry Part A, Chapter 1", in "The Porphyrins", ed. by D. Dolphin, Academic Press, New York, NY, 1978.
27. F. E. Lytle and D. M. Hercules, J. Am. Chem. Soc., 91, 253 (1969).

28. (a) G. Kavarnos, T. Cole, P. Scribe, J. C. Dalton, and N. J. Turro, J. Am. Chem. Soc., 93, 1032 (1971); (b) G. Kavarnos, V. Fung, A. L. Lyons, Jr., T. Cole, Jr., and N. J. Turro, J. Am. Chem. Soc., 94, 1392 (1972).
29. For some reviews of crown ether chemistry see (a) C. J. Pedersen and H. K. Frensdorff, Angew. Chem. Int. Ed. Engl., 11, 16 (1972); (b) J. J. Christensen, D. J. Eatough, and R. M. Izatt, Chem. Rev., 74, 351 (1974); (c) D. J. Cram and J. M. Cram, Science, 183, 83 (1974).
30. (a) J.-M. Lehn, Struct. Bonding (Berlin), 16 (1973); (e) G. W. Gokel and H. D. Durst, Synthesis, 168 (1976)
31. (a) J. M. Timko, R. C. Helgeson, M. Newcomb, G. W. Gokel, and D. J. Cram, J. Am. Chem. Soc., 96, 7097 (1974); (b) See Reference 30(c).
32. G. W. Gokel, R. J. Petcavitch, S. Kotzeniowski, M. M. Coleman, Tetrahedron Lett., 2647 (1977).
33. R. E. Terry, B. L. Haymore, L. D. Hansen, N. K. Dalley, A. G. Avondet, J. J. Christensen, and R. M. Izatt, J. Am. Chem. Soc., 98, 7620 (1976).
34. M. E. Farago, Inorg. Chim. Acta, 25, 71 (1977).
35. J. D. Lamb, J. J. Christensen, B. L. Haymore, and R. M. Izatt, J. Am. Chem. Soc., 99, 8344 (1977).
36. E. P. Kyba, personal communication, 1972.
37. N. Nae and J. Jagur-Grodzinski, J. Am. Chem. Soc., 99, 489 (1977).
38. M. Stockburger, H. Gatterman, and W. Klusmann, J. Chem. Phys., 63, 4519 (1975).
39. See Reference 1(c), p. 240.
40. B. W. Gash and Steven D. Colson, J. Chem. Phys., 59, 3528 (1973).
41. A. R. Watkins, J. Phys. Chem., 78, 2555 (1974).
42. I. B. Berlman, J. Phys. Chem., 77, 562 (1973).
43. I. N. Levine, "Quantum Chemistry; Volume I: Quantum Mechanics and Molecular Electronic Structure", Allyn and Bacon, Boston, MA, 1970, p. 308.
44. Reference 1(d), page 29.

45. A. N. Zaiken and A. M. Zhabotinskii, Nature (London), 225, 535 (1970).
46. Reference 1(c), page 199.
47. M. asha, J. Chem. Phys., 20, 71 (1952).
48. Ref. 1(c), p. 261 and p. 315.
49. S. P. McGlynn and T. Azumi, J. Chem. Phys., 40, 507 (1963).
50. Ref. 1(c), p. 315.
51. Ref. 1(c), p. 279.
52. J. C. Miller, K. U. Breakstone, J. S. Meek, and S. J. Strickler, J. Am. Chem. Soc., 99, 1142 (1977).
53. S. Siegel and H. S. Judeikis, J. Chem. Phys., 42, 3060 (1965).
54. S. E. Webber, Chem. Phys. Lett., 5, 466 (1970).
55. Greater susceptibility of  $k_p$  compared with  $k_{dt}$  was seen in work by the following authors: (a) reference 15(b); (b) reference 61; and (c) K. B. Eisenthal and M. A. El-Sayed, J. Chem. Phys., 42, 794 (1965). Work by McGlynn (see references 14 and 15(b)), however, suggests that  $k_{dt}$  is more susceptible to external heavy atom perturbers.
56. H. Dreeskamp, E. Koch, and M. Zander, Chem. Phys. Lett., 31, 251 (1975).
57. C. C. Ladwig and R. S. H. Liu, J. Am. Chem. Soc., 96, 6210 (1974).
58. Ref. 1(c), p. 311.
59. C. Dijkgraaf and G. J. Hoijtink, Tetrahedron, Suppl. 2, p. 179 (1963).
60. S. P. McGlynn, V. Ramakrishnan, and R. Sunseri, J. Chem. Phys., 45, 1365 (1966).
61. Ref. 13 and references cited therein.
62. Ref. 1(c), p. 320.
63. Ref. 1(c), p. 321.
64. Ref. 13, p. 262.
65. T. Pavlopoulos and M. A. El-Sayed, J. Chem. Phys., 41, 1082 (1964).



66. The results of this investigation have been published in part:  
(a) L. R. Sousa and J. M. Larson, J. Am. Chem. Soc., 99, 307 (1977); (b) L. R. Sousa and J. M. Larson, J. Am. Chem. Soc., 100, 1943 (1978).
67. For a discussion of the band structure of the UV absorption spectra of polycyclic hydrocarbons see H. H. Jaffe and M. Orchin, "Theory and Applications of Ultraviolet Spectroscopy", John Wiley and Sons, New York, NY, 1962, p. 287.
68. Ref. 67, p. 294.
69. (a) See reference 1(a), p. 799; (b) J. W. Longworth, "Luminescence Spectroscopy", in "Creation and Detection of the Excited State", ed. by A. A. Lamola, Marcel Dekker, New York, NY, 1971, p. 353.
70. V. L. Ermolaev, Sov. Phys.-Usp. (Engl. Trans.), 333 (1963).
71. W. R. Ware, "Transient Luminescence Measurements", in "Creation and Detection of the Excited State", ed. by A. A. Lamola, Marcel Dekker, New York, NY, 1970.
72. J. L. Dye and V. A. Nicely, J. Chem. Educ., 48, 443 (1971).
73. For a review of transition metal complexes with  $\pi$ -bonded systems see S. P. McGlynn, Chem. Rev., 58, 1113 (1958).
74. M. J. S. Dewar and H. C. Longuet-Higgins, Proc. Phys. Soc. (London), A67, 795 (1954).
75. R. Pariser, J. Chem. Phys., 24, 250 (1956).
76. Ref. 38 and Ref. 63, p. 129.
77. Ref. 94, p. 111.
78. (a) D. P. Craig, J. M. Hollas, M. F. Redies, and S. C. Wait, Jr., Proc. Chem. Soc., 361 (1959); (b) D. S. McClure, J. Chem. Phys., 22, 1668 (1954).
79. R. T. Ross, Photochem. Photobio., 21, 401 (1975).
80. Unpublished results by Houston S. Brown, Michigan State University.
81. Ref. 1(a), p. 300.
32. R. Rice, "Periodic Correlations", W. A. Benjamin, New York, NY, 1965, p. 64.
83. Mark R. Johnson, "Part 1: Heterocyclic Photochemistry: The Photochemical Synthesis of  $\beta$ -Lactams; Part 2: The  $^{13}\text{C}$  Spectra of Naphthalene Crown Ether Complexes: Field Induced  $\pi$ -Polarization and Crown Ether Conformational Changes", Ph.D. Dissertation, Michigan State University, 1978.

84. A. Reiser and T. R. Wright, J. Chem. Phys., 59, 3433 (1973).
85. Ref. 1(c), p. 265.
86. (a) G. W. Robinson, J. Mol. Spectroscopy, 6, 58 (1961); (b) E. C. Lim, J. Chem. Phys., 36, 3497 (1962).
87. Ref. 1(c), p. 314.
88. Ref. 1(c), p. 315.
89. See Reference 63. Also, note that according to McGlynn (References 14 and 16(a)),  $k_{nr}$  is the rate constant for naphthalene which is most susceptible to external heavy atom perturbers. This is not consistent, however, with the work of Siegel (Reference 61).
90. (a)  $\tau_f$  for naphthalene at room temperature in degassed 95% ethanol (98 nsec) is in good agreement with literature values (100 nsec). See R. Bonneau, J. Faure, and J. Jousot-Dubien, Chem. Phys. Lett., 2, 65 (1968); (b)  $\tau_p$  for naphthalene in degassed 95% ethanol glass at 77 K (2.5 sec) is in good agreement with literature values. See reference 10, 2.6 sec in EPA glass at 77 K; D. S. McClure, E. H. Gilmore, G. E. Gibson, J. Chem. Phys., 20, 829 (1952), 2.6 sec in EPA glass at 77 K; R. J. Watts and S. J. Strickler, J. Chem. Phys., 49, 3867 (1968), 2.6 sec in ethanol glass at 77 K; R. Li and E. C. Lim, J. Chem. Phys., 57, 605 (1972), 2.3 sec in EPA glass at 77 K.
91. Ref. 1(a), p. 799.
92. Ref. 96(b).
93. W. G. Herkstroeter, "Special Methods in Absorption Spectrophotometry", in "Creation and Detection of the Excited State", ed. A. A. Lamola, Marcel Dekker, NY, New York, 1971, p. 43.
94. I. J. Bryce, Nature, 186, 965 (1960).